

This document was produced
by scanning the original publication.

Ce document est le produit d'une
numérisation par balayage
de la publication originale.

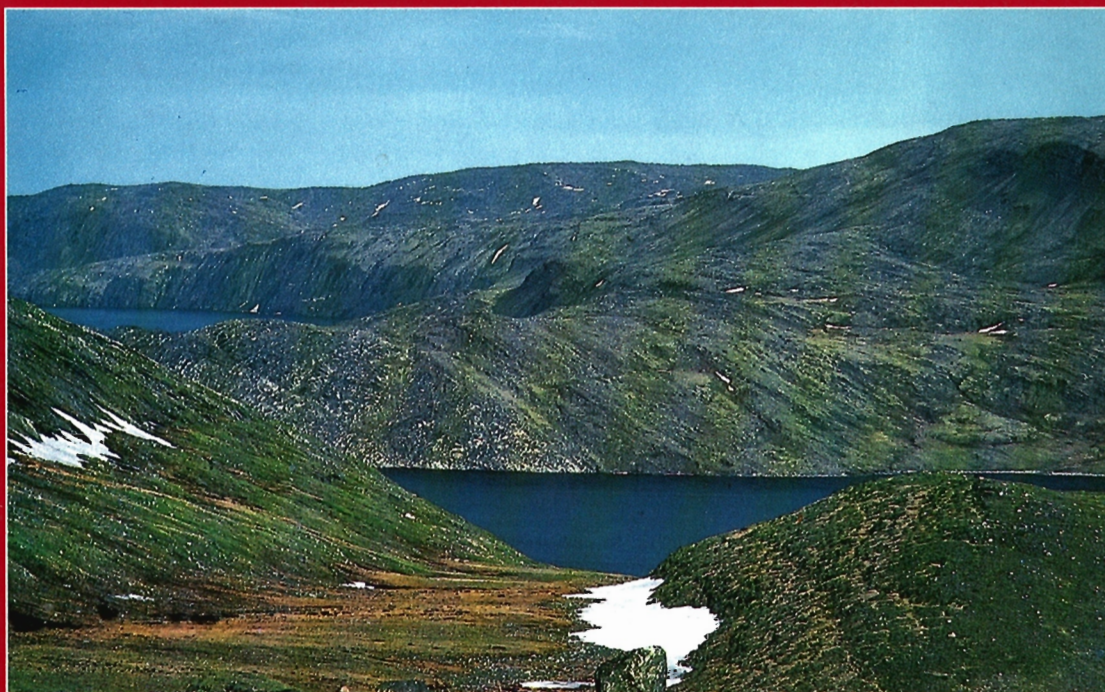


**GEOLOGICAL SURVEY OF CANADA
MEMOIR 438**

**GEOLOGY OF THE EASTERN CAPE SMITH BELT:
PARTS OF THE KANGIQSUJUAQ,
CRATÈRE DU NOUVEAU-QUÉBEC,
AND LACS NUVILIK MAP AREAS, QUEBEC**

M.R. St-Onge and S.B. Lucas

1993



Energy, Mines and
Resources Canada

Energie, Mines et
Ressources Canada

Canada

THE ENERGY OF OUR RESOURCES

THE POWER OF OUR IDEAS

GEOLOGICAL SURVEY OF CANADA
MEMOIR 438

**GEOLOGY OF THE EASTERN CAPE SMITH BELT:
PARTS OF THE KANGIQSUJUAQ,
CRATÈRE DU NOUVEAU-QUÉBEC,
AND LACS NUVILIK MAP AREAS, QUEBEC**

M.R. St-Onge and S.B. Lucas

Quaternary section by
R.-A. Daigneault

1993

© Minister of Supply and Services Canada 1993

Available in Canada through
authorized bookstore agents and other bookstores
or by mail from

Canada Communications Group - Publishing
Ottawa, Canada K1A 0S9

and from

Geological Survey of Canada offices:

601 Booth Street
Ottawa, Canada K1A 0E8

3303-33rd Street N.W.
Calgary, Alberta T2L 2A7

A deposit copy of this publication is also available for reference
in public libraries across Canada

Cat. No. M46-438E
ISBN 0-660-14993-1

Price subject to change without notice

Critical Readers

K.D. Card
D.A. St-Onge
D.J. Scott
M. Parent

Authors' addresses

M.R. St-Onge
S.B. Lucas
Geological Survey of Canada
Continental Geoscience Division
601 Booth Street
Ottawa, Ontario K1A 0E9

R.-A. Daigneault
Geological Survey of Canada
Centre géoscientifique de Québec
2700, rue Einstein
Ste-Foy (Québec) G1V 4C7

Cover Description

South shore of Wakeham Bay, looking east. Exposed along the shore and on the cliff faces, are the sedimentary and volcanic rocks of the Early Proterozoic Povungnituk Group (right side of photograph, brown and black outcrops) and the Archean basement of the Superior Province (left side of photograph, pink outcrops). As in most of the map area, the cover rocks of the Cape Smith Belt are separated from the basement gneisses by the basal décollement (centre of photograph) of the Early Proterozoic thrust belt.

Original manuscript received: June 1992

Final version approved for publication: September 1992

Preface

The Cape Smith Belt is one of the most geologically interesting and well mapped parts of the Canadian Shield. Despite its remote setting in the northern Ungava Peninsula, it has experienced a long history of geological mapping, geophysical surveying, and mineral exploration by the Geological Survey of Canada (GSC), the Ministère de l'Énergie et des Ressources du Québec (MERQ), and private industry starting with the pioneering work of A.P. Low in 1897 and intensified with the discovery of major Ni-Cu deposits in 1955. This memoir and the companion 1:50 000-scale maps, already published by the GSC, document the geology of the eastern portion of the Cape Smith Belt which was mapped during a series of three-month field seasons from 1985 to 1987. The maps of the eastern portion of the belt complement 1:50 000-scale maps produced by the MERQ (1982-1988) for the western portion of the belt, and highlight the successful, co-operative relationship that was struck between the GSC and MERQ in this most northerly part of Quebec.

The tectonostratigraphy of the eastern portion of the Cape Smith Belt is characterized by sedimentary and volcanic units associated with continental rift, oceanic, and fore-arc basin settings. An important result of GSC mapping was the discovery of a fragment of ancient oceanic crust, the Purtuniq ophiolite, in the northern part of the belt which has yielded a U-Pb zircon age of 1998 ± 2 Ma, making it one of the oldest ophiolites in the world and supporting the notion of Early Proterozoic plate tectonics. The eastern portion of the Cape Smith Belt is marked by a complex history of faulting, folding, and metamorphism associated with development of a collisional thrust belt during ca. 1.9-1.8 Ga growth of the Laurentian (proto-North American) continent. The memoir provides detailed documentation of the structure of the thrust belt, its metamorphic (pressure-temperature-time) history, the relationship between the thrust belt and the continental basement of the Superior Province craton, and the stratigraphic and structural setting of Ni-Cu-PGE deposits. The memoir and maps illustrate the importance of multidisciplinary field and laboratory studies and interagency co-operation in effective mapping the Canadian Shield.

Elkanak A. Babcock
Assistant Deputy Minister
Geological Survey of Canada

Préface

La ceinture de Cape Smith est une des parties les mieux cartographiées et les plus intéressantes géologiquement du Bouclier canadien. Malgré l'isolement de la ceinture dans le nord de la péninsule d'Ungava, la Commission géologique du Canada (CGC), le ministère de l'Énergie et des Ressources du Québec (MERQ) et le secteur privé y entreprennent depuis longtemps des études géophysiques et des travaux de cartographie et de prospection minérale, et ce depuis les premiers travaux menés par A.P. Low en 1897 et notamment depuis la découverte, en 1955, de gisements majeurs de Ni-Cu. Le mémoire et les cartes à l'échelle de 1/50 000 qui l'accompagnent et qui ont déjà été publiées par la CGC, décrivent la géologie de la partie est de la ceinture de Cape Smith. Cette région a été cartographiée entre 1985 et 1987 au cours d'une série de saisons de trois mois de travaux sur le terrain. Les cartes de la partie est de la ceinture viennent compléter les cartes à l'échelle de 1/50 000 de la partie ouest produites par le MERQ (1982-1988). Elles soulignent aussi l'esprit de collaboration qui a régné entre la CGC et le MERQ dans cet extrême nord du Québec.

La tectonostratigraphie de la partie est de la ceinture de Cape Smith se caractérise par la présence d'unités sédimentaires et volcaniques qui sont associées à des milieux de rift continental, d'océan et de bassin d'avant-arc. Les travaux de cartographie de la CGC ont donné un résultat important, soit la découverte d'un fragment de croûte océanique ancienne, l'ophiolite de Purtuniq, dans le nord de la ceinture. La datation à l'U-Pb du zircon donne un âge de 1998 ± 2 Ma pour cette ophiolite, ce qui en fait une des plus anciennes ophiolites connues au monde; cette datation appuie l'hypothèse de la tectonique de plaques au Protérozoïque précoce. La partie est de la ceinture de Cape Smith possède une histoire complexe de fracturation, de plissement et de métamorphisme associés au développement d'une zone de cisaillement de collision au cours de l'évolution, vers 1,9-1,9 Ga, du continent laurentien (proto-continent nord-américain). Le mémoire décrit en détail la structure de la zone de chevauchement de collision, son évolution métamorphique (pression-température-temps), le lien entre la zone de chevauchement et le socle continental du craton de la Province du Supérieur, et le milieu stratigraphique et structural des gisements de nickel, de cuivre et de métaux du groupe du platine. Le mémoire et les cartes montrent l'importance qu'ont les études multidisciplinaires menées sur le terrain et en laboratoire et la coopération interorganisation pour la cartographie efficace du Bouclier canadien.

Elkanak A. Babcock
sous-ministre adjoint
Commission géologique du Canada

CONTENTS

1	Abstract / Résumé
2	Summary / Sommaire
5	Introduction
5	Location and access
7	Settlements
7	Climate and vegetation
7	Physiography
7	Previous and recent work
11	Field methods and extent of mapping
12	Acknowledgments
13	General geology: Tectonic domains of the Ungava orogen
17	Domain 1: Plutonic units of the Superior Province
17	Plutonic units (Agn)
17	Domain 2: Autochthonous to allochthonous tectonostratigraphic units of the Cape Smith Belt
19	Lower Povungnituk Group (PPs - PPms)
19	Autochthonous sedimentary rocks (PPs)
21	Allochthonous sedimentary and volcanic rocks (PPi - PPms)
21	Ironstone (PPi)
21	Semipelite, arkosic quartzite, dolomite (PPse)
22	Basalt, volcanoclastic rock (PPv)
22	Micaceous quartzite (PPms)
23	Northward change in tectonostratigraphic facies
23	Gabbro sills (ga)
23	Tectonostratigraphic interpretation and parentage of the lower Povungnituk Group
25	Upper Povungnituk Group (PPb)
25	Tectonostratigraphic interpretation and parentage of the upper Povungnituk Group
26	Chukotat Group (PCol - PCpl)
27	Olivine-phyric basalt (PCol)
27	Pyroxene-phyric basalt (PCpy)
27	Plagioclase-phyric basalt (PCpl)
27	Layered mafic-ultramafic sills (pe, ga)
28	Tectonostratigraphic interpretation and parentage of the Chukotat Group
29	Domain 3: 'Suspect' tectonostratigraphic units of the Cape Smith Belt
30	Watts Group (PWp - PWb)
30	Layered peridotite (PWp)
31	Layered gabbro (PWg)
32	Pyroxenite (PWpy)
32	Basalt, gabbro sills, sheeted dykes and plagiogranite (PWb)
34	Tectonostratigraphic interpretation and parentage of the Watts Group
34	Spartan Group (PSpe)
35	Tectonostratigraphic interpretation and parentage of the Spartan Group
35	Tonalite intrusions (Pt)
36	Late diabase dykes
36	Structural history of the Cape Smith Belt: Overview
37	Structural sections of the Cape Smith Belt

41	Archean basement (domain 1) deformation history
41	D ₁ structures
44	D ₂ structures
47	D ₃ structures
48	Povungnituk and Chukotat groups (domain 2) deformation history
48	D ₁ structures
48	Basal décollement
50	Piggyback-sequence thrust system
56	Basal shear zone
60	D ₂ structures
64	Watts and Spartan groups (domain 3) deformation history
64	D ₁ structures
64	D ₂ structures
64	Thermal peak fault system
67	Post-thermal peak fault system
72	Correlation of deformation histories between tectonostratigraphic domains
73	Post-thrusting, thick-skinned deformation episodes
74	West-trending folds
74	Eastern outliers
75	Eastern end of the belt
75	Northern margin
77	Outcrop- and grain-scale folding
78	Cross-folds
78	Mechanics of thick-skinned folding
79	Metamorphic history of the Cape Smith Belt: Overview
79	Early D ₁ thermal conditions in the Povungnituk and Chukotat groups
80	Metamorphic mineral zones in mafic rocks of the Povungnituk, Chukotat, and Watts groups
81	External domain
83	Internal domain
84	Relations between mineral growth and deformation
84	External domain
84	Internal domain
85	Relative timing of thermal peak metamorphism between domains
85	Analytically-derived P-T paths in pelites
87	Analytical procedure
87	Microstructure and mineral chemistry
90	Temperature and pressure determinations
91	Thermochemical modeling of garnet zoning
92	P-T paths for external domain samples
92	P-T paths for internal domain samples
92	Tectonothermal evolution of the Cape Smith Belt
93	Metamorphic conditions associated with basement-involved folding
94	Regional tectonic setting of the Cape Smith Belt
96	Quaternary geology
96	General statement
96	Previous work
98	Glacial features
98	Deglaciation features
99	Modern geological processes

99	Economic geology
99	History of mineral exploration
99	Asbestos deposits
100	Ni-Cu-PGE deposits

103	References
-----	------------

Tables

16	1. Tectonostratigraphic table for the Wakeham Bay - lac Watts area
37	2. Correlation of structural-metamorphic histories between principal tectonostratigraphic domains
86	3. Representative garnet analyses
86	4. Representative biotite analyses
88	5. Representative plagioclase analyses

Illustrations

6	1. Map illustrating the tectonic elements of the Ungava Peninsula north of 60°N
6	2. Index to the fifteen published Geological Survey of Canada maps for the eastern Cape Smith Belt
8	3. Previous and recent mapping in the Cape Smith Belt
13	4. Space and time relationships for the tectonostratigraphic assemblages in the Ungava orogen
14	5. Geological compilation map for the eastern Cape Smith Belt
17	6. Biotite-hornblende tonalite of the Superior Province
18	7. Location and U-Pb age determination for samples in the western portion of the map area (1721A-1726A)
19	8. Summary of U/Pb (zircon and baddeleyite) data
19	9. Autochthonous arkosic quartzites of the lower Povungnituk Group
19	10. Basal conglomerate of the lower Povungnituk Group
20	11. Quartz pebble-bearing arkosic grit of the lower Povungnituk Group
20	12. Crossbedded ironstone unit of the lower Povungnituk Group
20	13. Arkosic quartzite bed showing trough crossbeds in the lower Povungnituk Group
20	14. Interbedded magnetite and grunerite schist of the lower Povungnituk Group
21	15. Thinly bedded semipelite from the lower Povungnituk Group
21	16. Arkosic quartzite beds of the lower Povungnituk Group
21	17. Channel structure in a quartzite of the lower Povungnituk Group
22	18. Dolomite from the lower Povungnituk Group
22	19. Polymitic conglomerate from the lower Povungnituk Group
22	20. Micaceous quartzite unit of the lower Povungnituk Group
23	21. Semipelite and quartzite beds of the lower Povungnituk Group
23	22. Semipelite and pelite from the lower Povungnituk Group
24	23. Quartzite beds from the lower Povungnituk Group
24	24. Pillowed basalt from the upper Povungnituk Group
24	25. Irregular pillows in the upper Povungnituk Group
24	26. Vesicular basalt flow in the upper Povungnituk Group
24	27. Flow top breccia in the upper Povungnituk Group
24	28. Mafic conglomerate from the upper Povungnituk Group
25	29. Massive gabbroic sill emplaced in the upper Povungnituk Group
25	30. Olivine-phyric basalt flow of the Chukotat Group
26	31. Ropey lava surface in the Chukotat Group
26	32. Lava withdrawal shelves in the Chukotat Group
26	33. Pillow tubes in the Chukotat Group
26	34. Layered peridotite-gabbro sill emplaced in the Chukotat Group
27	35. Peridotite at the base of a layered peridotite-gabbro sill

- 27 36. Plagioclase cumulate layering in the gabbroic portion of a layered sill
- 28 37. Quartz ferrogabbro portion of a layered sill
- 28 38. Upper contact of a layered sill with sedimentary rocks of the lower Povungnituk Group
- 28 39. Enclave of quartzite in granophyre of a layered sill
- 29 40. Simplified geological map for the Watts Group in the lac Watts (1721A) and Purtunig (1722A) area
- 30 41. Reconstructed composite section through the rocks of the Watts Group
- 30 42. Layered peridotite from the Watts Group
- 30 43. Layered gabbro from the Watts Group
- 31 44. Metre-scale layering in a gabbro of the Watts Group
- 31 45. Centimetre-scale layering in a gabbro of the Watts Group
- 31 46. Deformed anorthositic layer in a gabbro of the Watts Group
- 32 47. Xenoliths of layered anorthositic gabbro in pyroxenite
- 32 48. Sheeted dykes from the Watts Group
- 32 49. Basalt intruded by discrete gabbroic dykes, Watts Group
- 32 50. Pillowed basalt of the Watts Group
- 33 51. Plagiogranite sill intruding basalts of the Watts Group
- 33 52. Schematic block diagram for the Cape Smith Belt units at 1.9 Ga
- 34 53. Interbedded graphitic pelite and semipelite of the Spartan Group
- 34 54. Fine grained quartzite from the Spartan Group
- 35 55. Schematic block diagram for the Ungava orogen units at 1.87 Ga
- 36 56. Medium grained Early Proterozoic biotite tonalite
- 38 57. Strike-parallel sections of the eastern Cape Smith Belt
- 39 58. Downplunge constrained strike-perpendicular cross-section of the eastern portion of the Cape Smith Belt
- 40 59. Archean tonalite gneiss
- 40 60. Tectonic contact between the Archean basement and the Early Proterozoic cover
- 40 61. Detail of the basement/cover contact
- 40 62. Reworked Archean basement in the shear zone underneath the basement/cover contact
- 41 63. Detail of ultramylonite zone derived from Archean basement gneiss
- 41 64. Reworked Archean basement gneiss and ultramylonite zone
- 42 65. Reworked mylonitic basement and overlying sheared cover units
- 42 66. Transverse stretching lineation defined by rodding of quartz and feldspar
- 42 67. Transverse lineation defined by rodding of quartz and feldspar and growth of garnet
- 42 68. Asymmetric fold of reworked basement
- 43 69. Photomicrograph of a shear zone in reworked Archean tonalite
- 43 70. Photomicrograph of a plagioclase porphyroclast in protomylonite derived from an Archean tonalite
- 43 71. Photomicrograph showing detail of a plagioclase porphyroclast in protomylonite derived from an Archean tonalite
- 43 72. Photomicrograph of garnet, biotite, and muscovite in reworked Archean tonalite
- 44 73. Photomicrograph of reworked Archean tonalite
- 44 74. Photomicrograph of reworked Archean tonalite
- 44 75. Photomicrograph of reworked Archean tonalite
- 44 76. Photomicrograph of reworked Archean tonalite
- 45 77. Simplified geological map of the northern margin of the Cape Smith Belt (1722A, 1723A)
- 46 78. Imbricate of Archean tonalite gneiss
- 46 79. Contact between basement imbricate and cover units
- 47 80. Detailed downplunge constrained cross-section of northern margin
- 48 81. Early D₁ thrust fault
- 48 82. Regional extent of ductile shear zones in map area
- 49 83. Strike-parallel and strike-perpendicular cross-sections of outliers (1734A, 1735A)
- 50 84. Geological map of a boudined mafic-ultramafic sill (1727A, 1728A)
- 51 85. Compilation of D₁ and D₂ thrust faults and associated folds
- 52 86. Siliciclastic sedimentary rocks of the lower Povungnituk Group with early D₁ cleavages

- 52 87. Photomicrograph of pressure solution cleavage in a quartzite of the lower Povungnituk Group
- 53 88. Photomicrograph of a semipelite of the lower Povungnituk Group from the footwall fault zone of a folded early D₁ thrust fault
- 53 89. Slaty cleavage developed in a semipelite from the lower Povungnituk Group
- 54 90. Photomicrograph of slaty cleavage in a semipelite of the lower Povungnituk Group
- 54 91. Photomicrograph of an arkosic quartzite from the lower Povungnituk Group
- 54 92. Photomicrograph of a quartzite from the lower Povungnituk Group
- 55 93. Photomicrograph of dilatant fractures in a basalt of the Povungnituk Group
- 55 94. D₁ basal shear zone
- 55 95. Micaceous quartzite of the lower Povungnituk Group with deformed quartz veins
- 55 96. Quartz-plagioclase "smears" defining a transverse stretching lineation
- 56 97. Plagioclase "smears" defining a transverse stretching lineation
- 56 98. Tight fold of micaceous quartzite, lower Povungnituk Group
- 56 99. Deformed pillowed basalt of the upper Povungnituk Group
- 57 100. Photomicrograph of an arkosic quartzite of the lower Povungnituk Group
- 57 101. Photomicrograph of a shear band in micaceous quartzite of the lower Povungnituk Group
- 57 102. Photomicrograph of a garnet porphyroblast in a pelitic schist of the lower Povungnituk Group
- 58 103. Compilation of the mean orientations of stretching lineations in the map area
- 58 104. Photomicrograph of an arkosic quartzite of the lower Povungnituk Group
- 58 105. Photomicrograph of a quartzite from the lower Povungnituk Group
- 59 106. Photomicrograph of a quartzite from the lower Povungnituk Group
- 60 107. Photomicrograph of the basal shear zone fabric in a mafic volcanoclastic unit of the upper Povungnituk Group
- 60 108. Photomicrograph of the basal shear zone fabric in a metabasalt from the upper Povungnituk Group
- 61 109. Simplified geological map and down-plunge constrained cross-section of the lac Cross area (1724A)
- 62 110. Photomicrograph of a syntectonic garnet in a prograde D₂ shear zone
- 62 111. Posttectonic kyanite, garnet, and staurolite in a pelitic schist of the lower Povungnituk Group
- 62 112. Photomicrograph of a thermal peak garnet in a metabasalt of the upper Povungnituk Group
- 63 113. Deformed pyroxene-phyric pillowed basalt of the Chukotat Group
- 63 114. Photomicrograph of the mafic schist along thrust fault S
- 63 115. Photomicrograph of deformed Chukotat Group basalt in the footwall of thrust V
- 64 116. Straight gneiss derived from a Watts Group layered gabbro
- 65 117. Sheath fold of Povungnituk Group quartzite
- 65 118. D₂ stretching lineation in a quartzite of the lower Povungnituk Group
- 65 119. Shear band fabric in a deformed gabbro of the Watts Group
- 66 120. Photomicrograph of a metamorphosed layered gabbro from the Watts Group
- 66 121. Photomicrograph of a deformed quartz vein in a pelite of the Spartan Group
- 67 122. Heterogeneous deformation of a layered gabbro from the Watts Group
- 67 123. Photomicrograph of the D₂ shear zone foliation in a gabbro of the Watts Group
- 67 124. Sheared and boudined layered gabbro from the Watts Group
- 68 125. Post-thermal peak fault BB
- 68 126. Shear bands deforming thermal peak foliation in a deformed gabbro of the Watts Group
- 68 127. Photomicrograph of late D₂ shear bands in a layered gabbro of the Watts Group
- 69 128. Photomicrograph of a late D₂ ultramylonite
- 69 129. Greenschist grade mylonite derived from layered gabbro of the Watts Group
- 69 130. Sheared and boudined layered gabbro from the Watts Group
- 69 131. Zone of transition from heterogeneously deformed layered gabbro to chlorite-actinolite-plagioclase schist
- 70 132. Ultramylonite derived principally from layered gabbro of the Watts Group

- 70 133. Boudins of anorthosite and pyroxenite in ultramylonite
70 134. Anorthositic boudin
71 135. Hanging wall (within <5 m) of fault Y
71 136. Hornblende porphyroclasts reacting to actinolite tails
73 137. Compilation of axial traces for D₃ and D₄ macroscopic folds
74 138. Compilation of mesoscopic and macroscopic D₃ fold axial traces in
the Wakeham Bay area (1727A, 1728A, 1729A, 1733A, 1734A)
75 139. Mesoscopic D₃ folds of quartzite from the lower Povungnituk Group
75 140. Mesoscopic D₃ folds of well-foliated upper Povungnituk Group basalt
76 141. Simplified geological map for the area northwest of lac St-Germain (1731A)
77 142. Asymmetric D₃ folds of Archean tonalite
77 143. Photomicrograph of crenulated semipelite from the lower Povungnituk Group
77 144. Photomicrograph of crenulated muscovite pelite from the lower Povungnituk Group
80 145. Metamorphic map of the eastern portion of the Cape Smith Belt
81 146. Down-plunge constrained cross-section illustrating the metamorphic mineral zones
and isograds
82 147. Detailed metamorphic map of the northern portion of the Cape Smith Belt (1721A)
83 148. Schematic P-T diagram showing mafic reaction curves
84 149. Photomicrograph of a garnet-kyanite-staurolite pelite of the lower Povungnituk Group
85 150. Photomicrograph of a hornblende porphyroblast reacting to actinolite and epidote in a
layered gabbro of the Watts Group
85 151. Photomicrograph of a retrograde mineral assemblage in a gabbro of the Watts Group
89 152. Garnet zoning profiles for pelite sample #4
91 153. Analytically derived P-T paths for pelite samples from the external domain
91 154. Analytically derived P-T paths for pelite samples from the internal domain
94 155. Photomicrograph of garnet porphyroblast overgrowing D₃ microfolds of
the basal shear zone fabric
96 156. Schematic block diagram for the Ungava orogen units at 1.83 Ga
97 157. Ice flow directions and A-axis fabric of pebbles contained in till
98 158. Roche moutonnée
101 159. Simplified geological map for the lac Cross (1724A) - Kattiniq (1725A) -
Donaldson (Raglan) (1726A) area

The following 1:50 000 A-series geological maps collectively cover
the study area and are available separately.

1721A	Lac Watts, Quebec
1722A	Purtunig, Quebec
1723A	Lac Lecorré, Quebec
1724A	Lac des Deux-îles, Quebec
1725A	Lac Fleury, Quebec
1726A	Lac Rinfret, Quebec
1727A	Lac Wakeham, Quebec
1728A	Mont Albert-Low, Quebec
1729A	Wakeham Bay, Quebec
1730A	Lac Forcier, Quebec
1731A	Cratère du Nouveau Québec, Quebec
1732A	Lac Cournoyer, Quebec
1733A	Lac Vicenza, Quebec
1734A	Lac Samandré-Lac Charlery, Quebec
1735A	Joy Bay-Burgoyne Bay, Quebec

GEOLOGY OF THE EASTERN CAPE SMITH BELT: PARTS OF THE KANGIQSUJUAQ, CRATÈRE DU NOUVEAU-QUÉBEC, AND LACS NUVILIK MAP AREAS, QUEBEC

Abstract

The tectonostratigraphic units of the eastern Cape Smith Belt comprise sedimentary and volcanic units associated with rifting of the Superior Province (Povungnituk and Chukotat groups) and crustal components of an ophiolite (Watts Group) and fore-arc basin (Spartan Group).

The deformation associated with a collision between the Superior Province and the Watts and Spartan groups is characterized by an interplay among thrusting, penetrative bulk shear, and metamorphism. Both the Povungnituk and Chukotat groups record the development of a thrust belt characterized by south-verging faults. Following the accretion of the 'tectonically suspect' Watts and Spartan groups to the thrust belt, both the allochthons and the footwall basement were deformed into regional-scale folds during two folding episodes.

Metamorphic mineral assemblages were mapped in mafic extrusive and intrusive rocks. Field and petrological work constrained four isograds: hornblende-in, oligoclase-in, actinolite-out, and garnet/clinopyroxene-in.

Pressure-temperature (P-T) estimates in pelitic rocks indicate progressively higher temperatures (430°C to 590°C) from south to north in the external domain of the thrust belt. An increase in the recorded maximum pressures is documented from 6.5 kbar to over 9 kbar. Internal domain samples are characterized by steeper prograde P-T path segments than those for the external domain.

The record of ice-flow indicators shows regional flow directions toward the northeast. There is also field evidence for an older Quaternary ice flow (east-southeast).

Ni-Cu-PGE mineralization is associated with mafic-ultramafic bodies which have been interpreted as co-magmatic with the komatiitic basalts of the Chukotat Group. The most important deposits of the Cape Smith Belt occur in the Raglan horizon, located at the tectonic boundary between the Povungnituk and Chukotat groups.

Résumé

Les unités tectonostratigraphiques de la portion est de la ceinture du Cap Smith incluent les unités sédimentaires et volcaniques associées avec le rifting de la province du Supérieur (groupes de Povungnituk et Chukotat) et les composantes crustales d'une ophiolite (groupe de Watts) et d'un avant arc (groupe de Spartan).

La déformation associée avec la collision entre la province du Supérieur et les groupes de Watts et Spartan est caractérisée par une interaction entre les chevauchements, la déformation pénétrante et le métamorphisme. Les groupes de Povungnituk et Chukotat documentent la formation d'une ceinture de chevauchement caractérisée par des failles à transport vers le sud. Suite à l'accrétion des groupes 'suspects' de Watts et Spartan à la ceinture de chevauchement, les nappes allochtones et le socle furent repris par des plis d'échelle régionale pendant deux épisodes de plissement.

Les assemblages de minéraux métamorphiques furent cartographiés dans les roches mafiques intrusives et extrusives. Les travaux de terrain et de pétrologie ont précisés la localisation de quatre isogrades: apparition de la hornblende, apparition de l'oligoclase, disparition de l'actinote et apparition du grenat ou du clinopyroxène.

Des estimés pression-température (P-T) dans des roches pélitiques indiquent des températures de plus en plus élevées (430°C à 590°C) du sud vers le nord dans le domaine externe de la ceinture de chevauchement. Une augmentation dans les pressions maximales est documentée de 6.5 kbar à plus de 9 kbar. Les échantillons du domaine interne sont caractérisés par des segments prograde de trajectoire P-T plus raides que ceux du domaine externe.

Des traces d'écoulement ancien de glace vers l'est-sud-est au cours du Quaternaire se retrouvent dans la région cartographiée. De nombreux indices associés au dernier mouvement de glace existent dans la partie est de la ceinture du Cap Smith et documentent une direction nord-est.

Une minéralisation en Ni-Cu-EGP est associée avec des unités mafiques-ultramafiques qui sont interprétés comme co-magmatique avec les basaltes komatiitiques du groupe de Chukotat. Les dépôts les plus importants de la ceinture du Cap Smith se retrouvent dans l'horizon Raglan localisé au contact tectonique entre les goupes de Povungnituk et Chukotat.

SUMMARY

The Wakeham Bay-lac Watts area occupies the eastern portion of the Cape Smith Belt in northern Quebec, from longitude 74°30'W to the western coast of Ungava Bay and underlies an area of about 8000 km².

The Cape Smith Belt is the foreland thrust belt of the Early Proterozoic Ungava orogen. The orogen is interpreted as an arc-continent collisional belt which comprises tectonostratigraphic elements accumulated on or accreted to the northern margin of the Superior Province during >0.2 Ga of divergent and convergent margin tectonic activity. The tectonostratigraphic units of the eastern Cape Smith Belt comprise: (1) autochthonous and allochthonous sedimentary and volcanic units inferred to be associated with rifting of the Superior Province craton (Povungnituk and Chukotat groups) and (2) allochthonous crustal components of assemblages interpreted as an ophiolite (Watts Group) and as fore-arc basin deposits (Spartan Group).

Units of the Povungnituk and Chukotat groups are Early Proterozoic in age and outcrop as predominantly allochthonous cover in the southern portion of the Cape Smith Belt. The Povungnituk Group contains a lower sequence of clastic sedimentary rocks (conglomerate, quartzite, ironstone, semipelite, pelite) and minor carbonate (dolomite) which are overlain by a bimodal suite of basalt and rhyolite. Fault-scarp conglomerates and the distribution of tectonostratigraphic units indicate accumulation of the Povungnituk Group in a tectonically-active basin. The Chukotat Group includes pillowed and massive basalt flows. Both the Povungnituk Group and the lower Chukotat Group are host to numerous layered peridotite-gabbro sills.

The Watts and Spartan groups are also Early Proterozoic but they occur solely as allochthonous packages in the northern portion of the Cape Smith Belt. The Watts Group comprises a distinctive assemblage of layered mafic and ultramafic rocks, massive and pillowed basalt flows, mafic sills and sheeted dykes, and plagiogranite intrusions. The Spartan Group comprises mostly pelite interbedded with semipelite and fine grained quartzite. The Watts Group is intruded by a number of plutons of quartz diorite, tonalite, and monzogranite. These plutons may be associated with regional Early Proterozoic magmatic suites preserved in crystalline thrust imbricates north of the Cape Smith Belt.

SOMMAIRE

La région de Wakeham Bay - lac Watts se trouve dans la partie est de la ceinture du Cap Smith (Québec septentrional). Cette région qui s'étend de 74° 30' W à la côte ouest de la baie d'Ungava couvre à-peu-près 8 000 km².

La ceinture du Cap Smith est la ceinture de chevauchement d'avant-pays de l'orogène de l'Ungava. L'orogène peut être interprétée en terme d'une collision entre un continent et un arc magmatique. L'orogène comprend les éléments tectonostratigraphiques accumulés sur ou accrétés à la marge nord de la province du Supérieur durant plus de 0.2 Ga d'activité tectonique de marge divergente et convergente. Les unités tectonostratigraphiques de la portion est de la ceinture du Cap Smith incluent: (1) les unités sédimentaires autochtones et allochtones et les unités volcaniques autochtones associées avec le rifting du craton de la province du Supérieur (groupes de Povungnituk et Chukotat) et (2) les composantes crustales allochtones d'ensembles tectonostratigraphiques interprétés comme ophiolite (groupe de Watts) et dépôts d'avant arc (groupe de Spartan).

Les unités des groupes de Povungnituk et Chukotat sont d'âge Protérozoïque inférieur et affleurent surtout comme unités de couverture allochthone dans la partie sud de la ceinture du Cap Smith. Le groupe de Povungnituk contient une séquence inférieure de roches sédimentaires clastiques (conglomérat, quartzite, roche ferrugineuse, aleurolite, phyllade) et quelques carbonates (dolomie) sur laquelle repose une suite bimodale de basalte et rhyolite. Des conglomérats d'escarpement de faille et la distribution des unités tectonostratigraphiques indiquent que l'accumulation des unités du groupe de Povungnituk s'est faite dans un bassin tectonique actif. Le groupe de Chukotat comprend des laves coussinées et massives. Les groupes de Povungnituk et Chukotat sont tous deux recoupés par de nombreux filons-couches stratifiés de peridotite et gabbro.

Les groupes de Watts et Spartan sont aussi d'âge protérozoïque inférieur mais ces derniers affleurent seulement comme entités allochtones dans la portion septentrionale de la ceinture du Cap Smith. Le groupe de Watts comprend un assemblage distinct de roches mafiques et ultramafiques stratifiées, de basaltes massifs et coussinés, de filons-couches mafiques, de dykes en feuillets et d'intrusions de plagiogranites. Le groupe de Spartan comprend surtout des pélites interlitées avec des aleurolite et des quartzites fines. Le groupe de Watts est recoupé par une série de plutons de diorite à quartz, tonalite et monzogranite. Ces plutons sont peut-être associés avec des suites magmatiques régionales qui sont préservées dans une série de nappes chevauchantes au nord de la ceinture du Cap Smith.

The deformation history of the map area can be subdivided into distinct structural-metamorphic episodes for each of three principal tectonostratigraphic domains: (1) Archean basement, (2) Povungnituk and Chukotat groups, and (3) Watts and Spartan groups. The principal correlation tool between domains is the relationship between deformation and metamorphism, as observed at map- to thin section-scale and related to the timing of the thermal peak of metamorphism.

The deformation leading up to and including the collision between the Superior Province continental margin and the Watts and Spartan groups is characterized by a complex interplay between thrusting, penetrative bulk shear, and metamorphism. The tectonostratigraphic units of the Povungnituk and Chukotat groups record the development of a foreland thrust belt characterized by south-verging faults ramping up from a basal décollement located at the Archean basement-Early Proterozoic cover contact. The 'tectonically suspect' Watts and Spartan groups were accreted to the thrust belt along south-verging faults which re-imbricated the foreland thrust belt, and which resulted in at least 100 km of displacement with respect to the underlying autochthonous basement.

Following the accretion of the Watts and Spartan groups to the thrust belt, both the allochthons and the autochthonous footwall basement of the Ungava orogen were deformed into regional-scale folds during two post-thrusting folding episodes (east-trending and northwest-trending). As a result of the folding episodes, the eastern portion of the Cape Smith Belt is characterized by a large, west-plunging synform which exposes an oblique crustal cross-section allowing direct geological examination of more than 18 km of structural relief at the present erosion surface.

The geometry of the thermal peak metamorphic culmination was established at the regional scale by systematic mapping of metamorphic mineral assemblages in mafic extrusive and intrusive rocks. Field work constrained the locations of three mineral isograds: hornblende-in, actinolite-out, and garnet/clinopyroxene-in. This was followed by a detailed petrological study of the metamorphic mineral assemblages in the mafic units which refined the position of the mapped mineral isograds and defined the position of an oligoclase-in isograd with petrographic and microprobe work.

The sequences of mineral isograds document an increase in metamorphic grade from lower greenschist facies to middle amphibolite facies conditions within the thrust belt. Two contrasting metamorphic field gradients can be defined in the thrust belt. In a southern external domain a higher-temperature gradient, characterized by hornblende-oligoclase and garnet-oligoclase assemblages, is exposed by the present erosion surface. In contrast, an internal domain displays a lower-temperature metamorphic field gradient, characterized by hornblende-albite (without actinolite) and garnet-albite mineral assemblages.

L'histoire de la déformation dans la région cartographiée peut être subdivisée en épisodes structuraux-métamorphiques pour chacun de trois principaux domaines tectonostratigraphiques: (1) le socle archéen, (2) les groupes de Povungnituk et Chukotat, et (3) les groupes de Watts et Spartan. L'outil de corrélation principal entre les domaines est la relation entre la déformation et le métamorphisme, tel qu' observée à l'échelle des lames minces et de la carte et considérée par rapport à l'apogée thermique du métamorphisme.

La déformation menant à et incluant la collision entre la marge continentale de la province du Supérieur et les groupes de Watts et Spartan est caractérisée par une interaction complexe entre les chevauchements, la déformation pénétrante et le métamorphisme. Les unités tectonostratigraphiques des groupes de Povungnituk et Chukotat documentent la formation d'une ceinture de chevauchement d'avant-pays caractérisée par des failles à transport vers le sud et se rattachant à un décollement de base localisé au contact entre le socle archéen et la couverture d'âge protérozoïque inférieur. Les groupes Watts et Spartan qui sont tectoniquement 'suspects' furent accrétés à la ceinture de chevauchement le long de failles à direction sud qui ont donné lieu à plus de 100 km de déplacement par rapport au socle autochtone sous-jacent.

Suite à l'accrétion des groupes de Watts et Spartan à la ceinture de chevauchement, les nappes allochtones et le socle autochtone de l'orogène de l'Ungava furent tous deux repris par des plis d'échelle régionale pendant deux épisodes de plissement (à direction est et à direction nord-ouest). Dû aux épisodes de plissement, la partie est de la ceinture du Cap Smith est caractérisée par un grand synforme à plongement vers l'ouest de sorte que la surface d'érosion actuelle met en évidence une section crustale oblique de plus de 18 km.

La cartographie systématique des assemblages de minéraux métamorphiques dans les roches mafiques intrusives et extrusives a permis de déterminer la géométrie de l'apogée thermique à l'échelle régionale. Le travail de terrain a précisé la localisation de trois isogrades: apparition de la hornblende, disparition de l'actinote et apparition du grenat ou du clinopyroxène. Ce travail fut suivi d'une étude pétrologique détaillée des assemblages de minéraux métamorphiques dans les unités mafiques ce qui a raffiné la position des isogrades cartographiés ainsi que défini la position d'un isograde caractérisé par l'apparition de l'oligoclase.

La séquence des isogrades cartographiés documente une augmentation du grade métamorphique à partir du faciès des schistes verts inférieur jusqu'au faciès des amphibolites moyen dans la ceinture de chevauchement. Deux séquences métamorphiques de terrain peuvent être définies dans la ceinture de chevauchement. Dans un domaine externe, la surface d'érosion expose un gradient de haute température relative, caractérisé par des assemblages de hornblende-oligoclase et grenat-oligoclase. En contrast, un domaine interne est caractérisé par un gradient de basse température relative et par des assemblages de hornblende-albite (sans actinote) et grenat-albite.

Pelitic layers of the lower Povungnituk Group with mineral assemblages appropriate for thermobarometric work were studied in both the external and internal tectonothermal domains of the Cape Smith Belt. Pressure-temperature (P-T) estimates based on the compositions of garnet rims and matrix minerals indicate a progressive change in P-T conditions from south to north in the external domain. Progressively higher rim temperatures (430°C to 590°C) are recorded from southern (external) to more northern (internal) sample locations. In addition, thermochemical modelling of the garnet zoning profiles indicates an increase in the recorded maximum pressures, from 6.5 kbar for the most external sample along the southern margin of the belt to over 9 kbar for the most internal sample of the external domain west of Wakeham Bay.

Internal domain metamorphic samples are characterized by steeper prograde P-T path segments than those for the external domain. The steeper dP/dT segments may reflect intervals of more rapid exhumation in the internal part of the thrust belt as compared to the external part. Potential explanations for the differences in P-T paths between the two domains include the thermal peak thrusting and post-thermal peak normal faulting which are unique to the internal domain.

The record of ice-flow indicators, including glacial striae and boulder trains of distinctive rock-types, shows regional flow directions toward the northeast in the eastern portion of the Cape Smith Belt. Numerous features are associated with this episode of ice flow in the region. These include erosional microforms, mainly striae, that are better preserved on the mafic rocks of the Cape Smith Belt than on the granitic rocks of the Archean basement, as well as mesoforms such as 'roches moutonnées'. There is also field evidence for an older Quaternary ice flow (east-southeast) in the southern portion of the map area. It includes glacial grooves oriented east-southeast and boulders and granules of rocks derived from the Cape Smith Belt.

The presence of raised deltas composed of sandy, stratified, locally fossiliferous sediments in the fiords indicates that deglaciation was followed by marine submergence. In the rivière Wakeham valley, marine deposits reach a thickness of 45 m. Along the Hudson Strait, the upper limits of 'wave-washing' lie at 148 m near Cape Prince of Wales and at 130 m west of pointe Akulivik. Inland, a series of eskers, meltwater channels, and outwash plains indicate that the ice front retreated towards the southwest.

Chrysotile asbestos occurs in ultramafic cumulate rocks of the Watts Group at Purtuniqu. The paragenesis of the alteration assemblages appears to include an early episode of serpentinization prior to regional metamorphism and deformation.

Numerous Ni-Cu-PGE sulphide deposits have been discovered in the eastern part of the Cape Smith Belt since the 1950s. The mineralization is associated with differentiated mafic-ultramafic and more homogeneous

Des horizons pélitiques dans le groupe de Povungnituk inférieur avec des assemblages de minéraux appropriés à des analyses thermobarométriques furent étudiés dans les domaines tectonothermiques externe et interne de la ceinture du Cap Smith. Des estimés pression-température (P-T) basés sur les compositions de cernes de grenat et celles des minéraux de la matrice indiquent un changement graduel des conditions P-T dans le domaine externe. Des températures de plus en plus élevées (430°C à 590°C) sont documentées du sud (zone plus externe) vers le nord (zone plus interne). En plus la modélisation thermochimique de la zonation compositionnelle des grenats indique une augmentation dans les pressions maximales de 6.5 kbar pour l'échantillon le plus externe le long de la marge sud de la ceinture à plus de 9 kbar pour l'échantillon le plus interne du domaine externe à l'ouest de Wakeham Bay.

Les échantillons du domaine métamorphique interne sont caractérisés par des segments prograde de trajectoire P-T plus raides que ceux du domaine externe. Les segments dP/dT plus raides indiquent peut-être des intervalles d'exhumation plus rapide de la portion interne de la ceinture de chevauchement. Les failles de chevauchement syn-apogée thermique et/ou les failles normales post-apogée thermique, qui toutes deux caractérisent la zone interne, sont peut-être responsables pour la différence entre les trajectoires P-T des deux domaines.

Des traces d'écoulement ancien de glace vers l'est-sud-est au cours du Quaternaire se retrouvent dans la partie sud de la région cartographiée: cannelures glaciaires orientées est-sud-est et des blocs et granules de roches dérivées de la ceinture du Cap Smith. De nombreux indices associés au dernier mouvement de glace existent dans la région. Ceux-ci incluent des microformes d'érosion, surtout des stries, qui sont mieux préservées sur les roches mafique de la ceinture du Cap Smith que sur les roches granitiques du socle archéen, ainsi que des mésoformes tel que des roches moutonnées. Ces indications d'écoulement glaciaire documentent une direction nord-est dans la partie est de la ceinture du Cap Smith.

Dans les fjords, la présence de deltas soulevés composés de sédiments sableux stratifiés, localement fossilifères, indique que la déglaciation fut suivie d'une invasion marine. Dans la vallée de la rivière Wakeham, les dépôts marins atteignent une épaisseur de 45 m. Le long du détroit d'Hudson, la limite supérieure du délavage par les vagues se situe à 148 m près du Cape Prince of Wales et à 130 m à l'ouest de la pointe Akulivik. A l'intérieur de la péninsule, une série d'eskers, de chenaux d'eau de fonte et de plaines d'épandage fluvio-glaciaire indique que le front glaciaire se retirait vers le sud-ouest.

La minéralisation d'asbestos (chrysotile) est localisée dans les roches à cumulats ultramafiques du groupe de Watts à Purtuniqu. La formation des assemblages d'altération comprenant l'asbestos sont associé en partie à une période de serpentinisation précoce qui prédate le métamorphisme et la déformation régionale.

De nombreux dépôts de sulphures avec Ni-Cu-EGP furent découverts dans la partie est de la ceinture du Cap Smith depuis les années 50. La minéralisation est associée surtout avec des filons-couches différenciés mafiques-ultramafiques et des filons-couches ultramafiques plus homogènes qui sont interprétés

ultramafic bodies (principally sills) which have been interpreted as co-magmatic with the MgO-rich komatiitic basalts of the lower part of the Chukotat Group. The sills intrude all volcanic and sedimentary units of the Povungnituk Group and the predominantly olivine-phyric basalt sequence of the Chukotat Group. The Ni-Cu-PGE mineralization occurs in two principal horizons in the map area. The most important deposits (subeconomic to economic) of the Cape Smith Belt occur in the Raglan horizon (lac Cross, Kattiniq, Donaldson), located at the tectonic boundary between the Povungnituk and Chukotat groups. The second mineralized zone, termed the Delta horizon, occurs within the Povungnituk Group and is host to relatively small (sub- to noneconomic) Ni-Cu-PGE sulphide deposits.

The Raglan horizon is situated in relatively deep-water (distal) sedimentary units of the Povungnituk Group. The sedimentary rocks are characterized by black, graphitic and sulphidic pelites interlayered with minor semipelite and quartzite which are interpreted as the most outboard (distal) deposits of the Povungnituk Group preserved in the Cape Smith Belt. Mapping has shown that the along-strike extent of the Raglan horizon is controlled by the structural geometry of a D₂ (out-of-sequence) thrust fault, which truncates both hanging wall Chukotat Group basalts and the entire Raglan horizon.

INTRODUCTION

Within the borders of the Wakeham Bay-lac Watts area, northern Quebec, a natural oblique cross-section is exposed through the Early Proterozoic Cape Smith Thrust Belt (Fig. 1). The south-verging thrust belt contains tectonostratigraphic assemblages which record rifting of the northern Superior Province, accumulation of sedimentary and volcanic units on a north-facing continental-margin, and the formation of transitional and oceanic crust ca. at 2.0 to 1.9 Ga. As well, map-scale structures, tectonic fabrics, and metamorphic mineral assemblages document a mountain building episode at ca. 1.9-1.8 Ga. The area contains a number of Cu-Ni-PGE mineralized zones which are localized at the contacts between layered gabbro-peridotite sills and sulphidic clastic sedimentary rocks. This memoir is our final report on the geology of the eastern portion of the Cape Smith Belt and it is intended as a companion document to the fifteen published Geological Survey of Canada maps (1721A-1735A; St-Onge and Lucas, 1989a-c, 1990a-l) for that area (Fig. 2).

Location and access

The map area covered by this study occupies the eastern portion of the Cape Smith Belt in northern Quebec, from longitude 74°30'W to the western coast of Ungava Bay (Fig. 1). The region includes portions of NTS map sheets 25E (Kangiqsujaq), 35H (Cratère du Nouveau-Québec), and 35G (Lacs Nuvilik) and covers about 8000 km² (Fig. 2). Access to the area is possible with Air Inuit on scheduled

comme co-magmatique avec les basaltes komatiitiques riches en MgO de la partie inférieure du groupe de Chukotat. Les filons-couches sont mis en place dans les unités volcaniques et sédimentaires du groupe de Povungnituk et dans la séquence de basalte à olivine du groupe de Chukotat. La minéralisation en Ni-Cu-EGP se retrouve dans deux horizons principaux dans la région cartographiée. Les dépôts les plus importants (sub-économique à économique) de toute la ceinture du Cap Smith se retrouvent dans l'horizon Raglan (lac Cross, Kattiniq, Donaldson), localisé au contact tectonique entre les goupes de Povungnituk et Chukotat. Le deuxième horizon minéralisé, appelé l'horizon Delta, se retrouve dans le groupe de Povungnituk et contient des dépôts relativement petits (sub- à non-économique) de sulphures avec Ni-Cu-EGP.

L'horizon Raglan est situé dans des unités sédimentaires distales d'eau relativement profonde du groupe de Povungnituk. Les roches sédimentaires sont caractérisées par des pélites noires contenant de la graphite et des sulphures. Les pélites sont interlitées avec des quartzites qui sont interprétées comme les dépôts les plus distaux dans la stratigraphie de la ceinture du Cap Smith. La cartographie a démontré que l'extension latérale de l'horizon Raglan est contrôlée par la géométrie d'un chevauchement D₂ (hors-série) qui recoupe le groupe de Chukotat dans la lèvre supérieure et l'ensemble de l'horizon Raglan dans la lèvre inférieure.

Twin Otter flights to the village of Kangiqsujaq (1729A) three times a week. As well, chartered fixed-wing aircraft can be arranged out of Kujjuaq (Quebec) or Iqaluit (N.W.T.) with landings either at Kangiqsujaq, or at the Purtuniq (Asbestos Corp.) (1722A) or Raglan mine site (Falconbridge Ltd.) (1726A) airstrips. Equipment, fuel, and heavy freight can be shipped to Kangiqsujaq by boat (Sealift) with arrivals generally in August or September.

In the summer, travel within the map area is possible by boat along the Ungava coast or on the larger lakes (lac Watts, lac François-Malherbe; 1721A). All other lakes and all rivers in the area are too small, shallow, or bouldery to be navigable. Inland, the generally rolling topography which is treeless, lends itself perfectly to foot-traverses. As well, rapid travel within the area is possible by helicopter (Bell 206) equipped with skis. In the winter the local Inuit travel over land and ice with snowmobiles and dog-teams.

Roads are limited to areas of mine development and exploration. An abandoned 65 km gravel road joins Purtuniq (1722A) and Deception Bay (Fig. 2) and was still in excellent condition during the summer of 1987. A cleared path or pseudo-road extends east from lac Cross (1724A) to Kattiniq (1725A) and the Raglan mine site (1726A). In 1987, it was in very bad shape and usable only with a four-wheel drive vehicle. Northeast from the Raglan mine site, a recently upgraded (1991) 38 km gravel road joins the mine to the southwest arm of Douglas Harbour (Fig. 2). Short side roads to drill sites or sources of gravel used for road construction occur erratically.

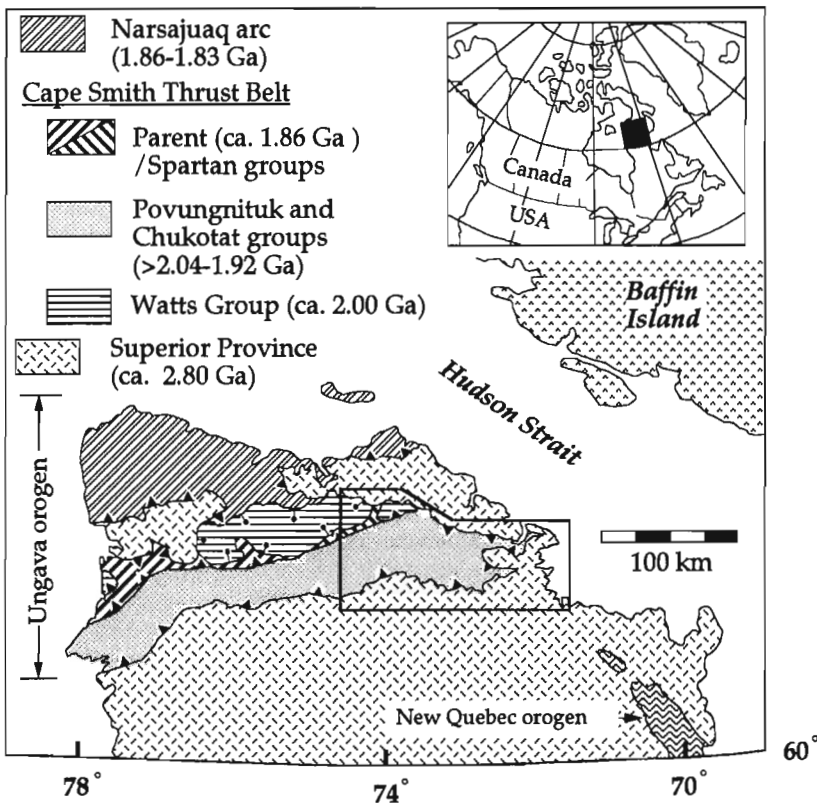


Figure 1. Map illustrating the tectonic elements of the Ungava Peninsula north of 60°N and highlighting the location of the eastern Cape Smith Belt map area. The location of the northern Ungava Peninsula is shown by the black box in the inset. U-Pb ages are from R. Parrish (1989, per. comm., 1991; see St-Onge et al., 1992) and Machado et al. (1991). Solid outline area corresponds to area of Figure 5.

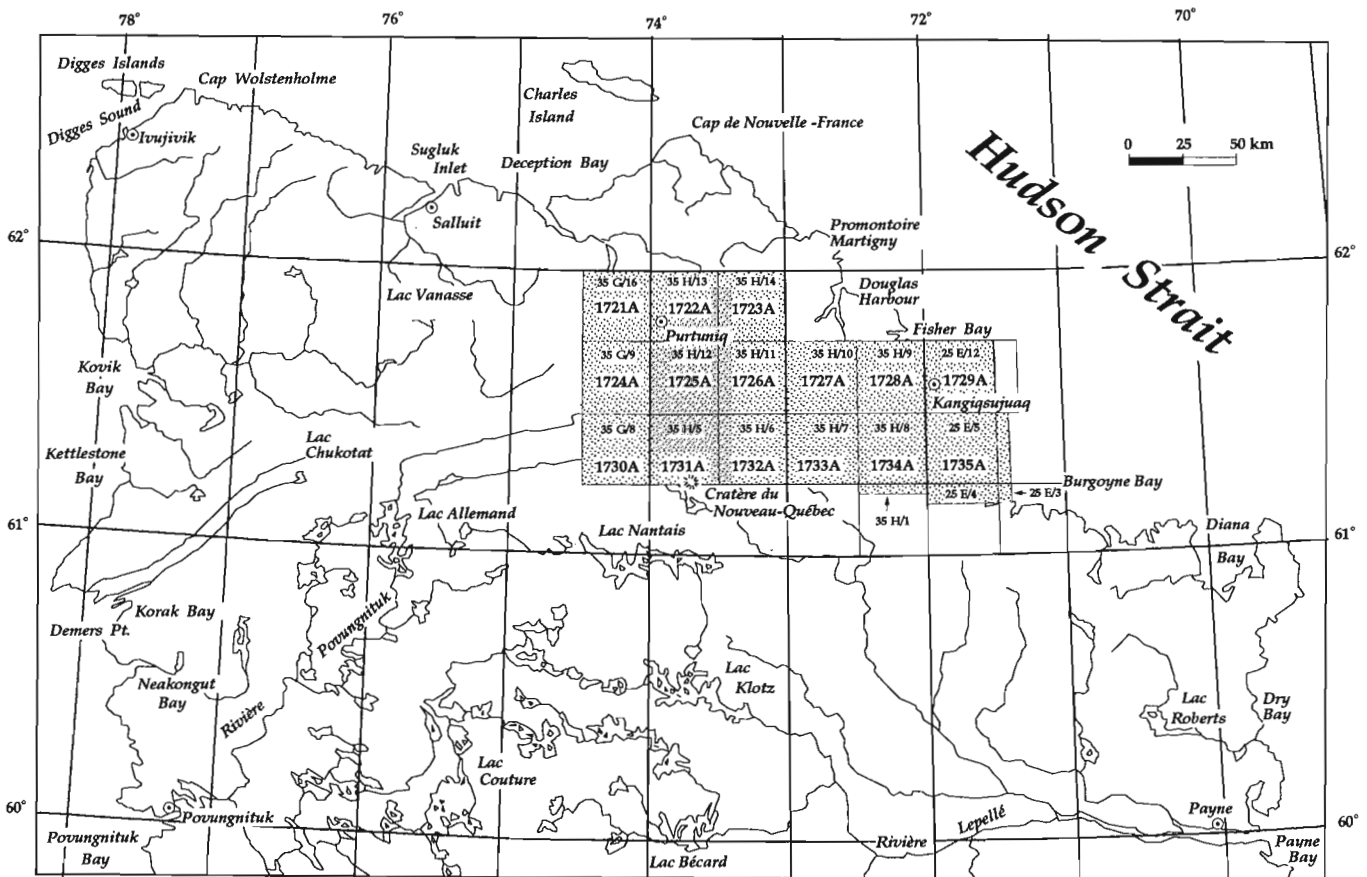


Figure 2. National topographic system reference and index to the fifteen published Geological Survey of Canada maps for the eastern Cape Smith Belt (St-Onge and Lucas, 1989a-c, 1990a-l).

Settlements

The Inuit village of Kangiqsujaq (population ca. 300) is located on the south shore of Wakeham Bay (1729A). Regular gas, diesel, and naphtha can be purchased from the Inuit Co-op store; groceries and smaller camping goods are available both from the Co-op and a Hudson Bay store. A post office, nursing station, and new airport (1989) provide necessary services. Pay telephones are found at the local transit house (run by the Inuit Co-op) or at the mayor's office. The only other habitation point in the map area is the Raglan mine site (1726A) where a fluctuating population of mine employees resides. The former Asbestos Hill mine site at Purtunig (1722A) is abandoned. Although in use more recently, the Kattiniq exploration site (1725A) was completely deserted during the years of field work for this project (1985-1987).

Climate and vegetation

The entire map area lies in the zone of discontinuous, but widespread permafrost (Brown, 1967), which at Purtunig (1722A) extends to a depth of more than 540 m. (Stewart, 1976). The mean annual air temperature isotherm of -7°C passes through Joy Bay (1729A) striking northeast.

Wakeham Bay (1729A) is free of ice from about the last week of June or the first week of July until mid-November when it completely freezes over (Drinnan and Prior, 1955). During the summers of 1985-1987, only low-lying areas (below 300 m) such as the western coast of Ungava Bay (1735A, 1729A) and the lac Watts (1721A) or rivièrè Wakeham (1728A) valleys were sufficiently free of snow for geological traverses in June. The highest ground (700 m) in the lac Cross (1724A), Kattiniq (1725A) and lac Vicenza (1733A) areas only became suitable for traversing in late July or early August. During the summers of 1985 and 1987, unusually warm weather cleared many outcrops not normally free of snow in the map area, whereas the higher elevation areas were covered with new snow starting August 9 in 1986.

The entire map area is in the barrens and only small alders and willows grow in sheltered spots at low elevation (e.g. lac Watts (1721A) and rivièrè Wakeham (1728A) valleys). Ground cover consists of grasses, mosses, and similar low-growing plants. Flowers such as *Dryas integrifolia* (mountain avens), *Epilobium latifolium* (broad-leaved willow-herb), *Papaver radicum* (arctic poppy), and *Pedicularis lanata* (woolly lousewort) add colour to the valleys from June to early August. Lichens partially cover most outcrops, unless the rocks lie under the more persistent snowbanks. Wildlife is generally scarce with caribou occupying the river valleys in the early part of the summer and higher elevations later in the season. Seals were noted along the coast of Ungava Bay (1735A, 1729A); snowy owls and geese were seen inland. No bears were observed during the course of the field work.

Physiography

The area covered by the mapping project includes three physiographic divisions; the Povungnituk Hills, the Sugluk Plateau, and the Larch Plateau (Bostock, 1970). The Povungnituk Hills transect the region in an east-west direction, in general consisting of a bedrock-controlled topography of elongate ridges and valleys in much of the map area south and southeast of lac Watts (1721A). In the Purtunig (1722A) and lac Watts area, the bedrock-controlled relief comprises hills that are larger and more rounded, whereas in the lac Rinfret (1726A), lac Wakeham (1727A), and lac Vicenza (1733A) areas, the extent of Quaternary cover yields a flat and bleak plateau. Hilltop elevations range between 300 and 610 m above mean sea level.

To the north of the Povungnituk Hills, the Sugluk Plateau is a flat, rocky surface that stands at ca. 610 m and is deeply dissected by a few north-flowing rivers. These rivers have cut steep-walled valleys that terminate along the coast as fiords such as Douglas Harbour (Fig. 2).

To the south, the Larch Plateau consists of a gently undulating surface with elevations between 300 and 520 m, which is deeply dissected by steep-walled valleys containing east-flowing rivers such as the rivièrè Laflau and the rivièrè Lataille (1734A). The generally flat southern skyline is broken only by the rim of the Cratère du Nouveau-Québec, which reaches an altitude of 660 m.

Previous and recent work

Some of the earliest geological observations of the Ungava Peninsula were made by Bell (1885) during a series of expeditions to Ungava Bay, Hudson Strait, and Hudson Bay in 1875, 1877, 1884 and 1885. Bell assembled a suite of samples from the Joy Bay area (Fig. 3) comprising 'gneiss, soapstone, quartz, feldspar, hornblende, mica-rock, epidote and iron pyrites' which he interpreted to be derived from 'ordinary Laurentian rocks'. To the west, Bell (1885) made a 'track-survey' of the western Digges Island (Fig. 3) which he concluded to be 'formed entirely of Laurentian gneiss'. An exploration of the coast south of Cape Wolstenholme (Fig. 3) led him to observe that the rocks consist of 'common forms of gneiss, with veins and patches of fine-grained red granite in some places'.

In 1897, Low explored the coastal regions of the Ungava Peninsula from Douglas Harbour (Fig. 3) on the south side of Hudson Strait to George River on the eastern side of Ungava Bay. In his report Low (1899) describes rusty masses of garnet amphibolite and hornblende schist among the biotite granitic gneiss of the Douglas Harbour area. To the south, between the two arms of Fisher Bay (Fig. 3) Low examined a section of interlayered garnetiferous mica-schist and hornblende schist cut by numerous quartz veins. Well banded, garnet-bearing rusty mica-schist, hornblende schist, and micaceous quartzite were observed by his party at the head of Wakeham Bay (1728A). In the Joy Bay and Whitley Bay area (1735A), Low (1899) described dark

amphibolite associated with grey siliceous mica-schist, dark-grey quartzite and rusty 'iron-bearing beds'. He distinguished the amphibolite from enclaves of foliated quartz diorite enclosed by pink granitic gneiss and not associated with 'iron ores'. Low (1899) also noted that where less 'disturbed', the schists appeared to rest upon domes of granitic gneiss. Finally, he concluded that beds of quartzite and associated shales or slates must have been locally 'shoved into ridges by over-thrust faults'. These descriptions comprise the first published observations on the metamorphosed and imbricated supracrustal rocks of the Cape Smith Belt.

In 1898 and 1899 Low explored the west coast of the Ungava Peninsula from Cape Wolstenholme (Fig. 3) to Cape Jones and then the eastern shores of James Bay south to the Rupert River. In the Cape Wolstenholme area, Low (1902) observed that dark, rusty gneisses and schists belonging to a 'more ancient bedded series' were 'altered' by the intrusion

of masses and sheets of granitic gneisses. From Kettlestone Bay (Fig. 3) to the south side of Korak Bay (Fig. 3) Low (1902) noted the predominance of 'trap' rock forming a range composed of several ridges of sharp hills which intersect the Hudson Bay coastline. There he observed that the 'trap' rock could have a diabase texture or be porphyritic. He noted that nearly everywhere the rock was 'fractured most often in irregular prisms' (i.e. pillows) and that the cracks were filled with quartz, calcite, epidote, prehnite and chlorite. Low (1902) also observed that 'various stages of schistosity are seen in the trap, varying from a slight elongation and rounding of the irregular prisms to an extreme phase where their shape and character are almost obliterated'. The deformed rocks are described as 'consisting of alternate dark and light-green bands of hornblendic and chloritic schists holding thin bands of calcite and quartz formed from the squeezing and lengthening of the masses of these minerals, which originally filled fissures between the trap prisms'. Low's (1902) report thus contains the first descriptions of the pillowed basalt

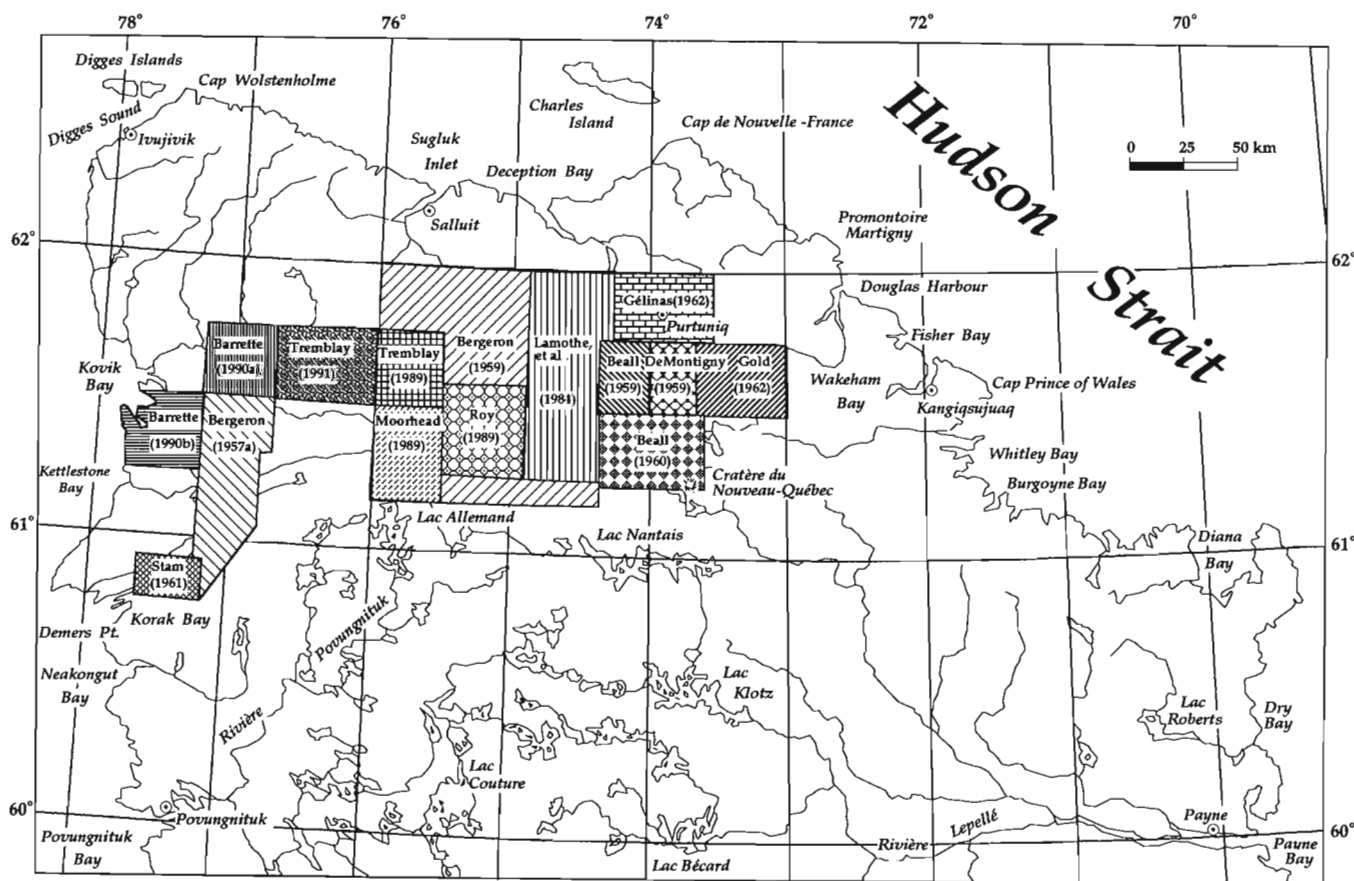


Figure 3. Previous and recent mapping in the Cape Smith Belt. Year in parentheses corresponds to year of map publication. In addition to the outlined maps, coastal maps for segments of Ungava Bay, Hudson Strait, and Hudson Bay were published by Bell (1885) and Low (1899, 1902) and the area around Korak Bay was mapped by Gunning (1934). Gunning (1934) also published M.E. Watts' outline for the western portion of the Cape Smith Belt. Kretz (1960) published a reconnaissance geological map of the entire Peninsula north of 60°N and Taylor (1982) published seven 1:250 000 scale geological maps north of 61°N. The area north and east of the map areas shown on Figures 2 and 3 was recently mapped at 1:100 000 scale by St-Onge and Lucas (1990n, 1992) and Lucas and St-Onge (1991). The nature and location of the more thematic studies completed in the Cape Smith Belt by a number of authors are given in the text.

flows of the Cape Smith Belt and their mineralogical and textural transition from low-grade basalts to amphibolite facies metabasites.

Based on Low's observations, the western portion of the Cape Smith Belt was prospected for base metals in 1931 and 1932 by Cyril Knight Prospecting Company Limited, Huronian Mining and Finance Company, Newmont Exploration Limited, and Quebec Prospectors Limited. The work was carried out by four men including M.E. Watts who produced a geological sketch map of their explorations on a scale of 1:506 880 and covering an area of over 12,800 km² (Gunning, 1934). Mineral showings in the western belt were found. In 1933, Gunning examined the sulphide deposits north of Korak Bay (Fig. 3) and made observations on the granites and supracrustal rocks exposed along the coast of Hudson Bay north to Kettlestone Bay (Fig. 3). In his report, Gunning (1934) describes the argillaceous to carbonaceous siliceous sediments and quartzites, the pillowed lava flows and the gabbro dykes and sills of the western Cape Smith Belt (Fig. 1). As well, the geological setting of the sulphide mineralization is outlined for a small area along the north shore of Korak Bay. There, the pillowed lava flows of the Cape Smith Belt are underlain by a band of folded sedimentary rocks into which are emplaced a series of gabbro sills. Sulphide mineralization (pyrrhotite, chalcopyrite, and pyrite) was reported by Gunning (1934) to be localized at the folded contacts between the gabbro bodies and the host sedimentary rocks.

With the discovery of nickel and other base metals in the Cape Smith Belt in 1955 - 1957, geologists from the Ministère de l'Énergie et des Ressources du Québec (formerly the Ministère des Mines du Québec and the Ministère des Richesses Naturelles du Québec) mapped several areas of the western and central belt (Fig. 3). Bergeron (1957a) published two maps with his early report on the Cape Smith Belt. One map, at a scale of 1:126 720 illustrates the geology of the belt along a north-south transect in the vicinity and south of lac Bilson (Fig. 3). A second map, at a scale of 1:1 013 760 shows the northern and southern boundaries of the Cape Smith Belt as well as a major thrust fault extending from Kettlestone Bay to southwest of Douglas Harbour (Fig. 3). In 1958, Bergeron covered 8282 km² southeast of lac Vanasse (Fig. 3) at 1:126 720 scale. In his report (Bergeron, 1959), two principal tectonostratigraphic groups are described north of the exposed Archean basement; an older Povungnituk Group comprising sedimentary and volcanic rocks and a younger Chukotat Group composed of dominantly pillowed basalts. Bergeron published the principal results of his field work in a number of short papers (Bergeron, 1957b, 1958). He also proposed regional correlations between the Cape Smith Belt and the Labrador Trough, the Mistassini and Otish basins, and the Belcher Islands (Bergeron et al., 1962).

In 1958, deMontigny mapped the area centered on the upper rivière Déception (1725A) at 1:63 360 scale (Fig. 3). Building on the work of Bergeron (1959), deMontigny (1959) distinguished two principal tectonostratigraphic groups and mapped a thrust fault placing Povungnituk Group conglomerates on Chukotat Group pillowed basalts. During

the same summer, Beall traversed in the area of lac Cross (1724A) and compiled a geological map at a scale of 1:63 360 (Fig. 3). Beall (1959) recognized three regionally extensive 'reverse faults' and a number of fold structures including the syncline at lac Cross. His senior mapping assistant subsequently completed a Ph.D. thesis on the geology and mineralogy of the lac Cross area (Shepard, 1960). In 1959, Beall (1960) worked at 1:63 360 scale (Fig. 3) in the lac Laflamme area (1730A, 1731A) where he documented the regional-scale northwest-trending cross-folds of sedimentary, volcanic, and intrusive units of the Povungnituk Group. He wrote a Ph.D. thesis on the petrology of layered gabbroic sills (Beall, 1962) and one of his senior mapping assistants completed an M.Sc. thesis on the metamorphism of iron-stones in the lac Laflamme area (Hashimoto, 1962). A final report on the lac Cross and lac Laflamme areas was published by Beall (1977).

Gold (1962) mapped the area of lac Rinfret (1726A) and lac Guindeau (1725A) in 1959 at 1:63 360 scale (Fig. 3) and interpreted the repetition of tectonostratigraphic units in this area as the result of displacements on major 'reverse' faults. As well, he concluded that the contact between units of the Cape Smith Belt and the exposed gneisses to the northeast was a fault. Following the discovery of an asbestos deposit at Purtuniqu (1722A) by M.E. Watts in 1957, Gélinas (1962) mapped the area between lac Watts (1721A) and the eastern rivière Déception (1722A) in 1960 at 1:63 360 scale (Fig. 3). He examined the quartzofeldspathic gneisses north of the Cape Smith Belt and concluded that these form the basement complex to the sedimentary and volcanic units of the belt. Gélinas documented a general increase in metamorphic grade in the supracrustal rocks, from greenschist facies in the south to amphibolite facies in proximity to the basement/cover contact. Finally, Gélinas (1962) mapped the major fault south of lac Watts which was first interpreted as a reverse fault by Bergeron (1957a).

In 1957, Stam mapped the southwestern corner of the Cape Smith Belt, northeast of Korak Bay (Fig. 3). In a very insightful paper, Stam (1961) presented the stratigraphic and structural evidence which led him to conclude that the Cape Smith Belt was predominantly a thrust belt. Contrary to the accepted view at the time, Stam also concluded that the southern contact of the belt was a thrust fault and not an unconformity as proposed by Bergeron (1957a) and his colleagues. In his paper, Stam provided the first structural cross-section of the western belt and in it showed three major thrust faults and seven minor reverse faults. As well, the Archean basement was clearly inferred to underlie the entire width of the supracrustal belt.

Following the detailed work in the central and western portions of the Cape Smith Belt in the late 1950s-early 1960s, several regional scale geological mapping projects and compilations were completed. As a member of a gravity survey team, Kretz (1960) made reconnaissance geological observations and published a map of the northern Ungava Peninsula at 1:506 880 scale. In 1973, Taylor (1974, 1982) mapped the peninsula north of 61°N at 1:250 000 scale. He outlined the dominant units and identified the major structures in the Cape Smith Belt and mapped the principal

contact between supracrustal and quartzofeldspathic units. In his set of seven 1:250 000 scale geological maps, Taylor (1982) provides the first subdivision of the gneisses and granites both south and north of the belt. Dugas (1971) published a list of mineral occurrences in the Cape Smith Belt and Avramtchev (1982) compiled a set of ten 1:250 000 scale maps showing the location, type, shape and size of mineral occurrences north of 60°N. Avramtchev (1982) used previously published geological information to construct the geological base used in his compilation.

A number of more thematic studies were undertaken in the Cape Smith Belt in the 1970s and early 1980s. Baragar (1974, 1983) studied the volcanic rocks and measured a number of stratigraphic sections in the western portion of the belt. Comparisons of units and volcanic structures preserved in the Cape Smith Belt with those found on the Ottawa and Sleeper islands in Hudson Bay were made by Baragar (1984), and Baragar and Piché (1982). The tectonic setting of sedimentation and volcanic activity in the Cape Smith Belt and regional correlations with other circum-Superior belts were topics addressed by several authors including Dimroth et al. (1970), Moore (1977) and Baragar and Scoates (1981). The geochemistry and petrogenesis of the volcanic suites in the central and western belt were presented by Schwarz and Fujiwara (1977), Francis and Hynes (1979) and Francis et al. (1981, 1983). The internal stratigraphy and petrogenesis of layered peridotite-gabbro sills in the medial portion of the belt were studied by Miller (1977), Francis and Hynes (1979) and Bédard et al. (1984).

The structural architecture of the central Cape Smith Belt from the southwestern corner of 1730A to the north end of lac Watts (1721A) was investigated by Hynes and Francis (1982). These authors viewed the belt as a composite of eight tectonostratigraphic blocks, each separated from the adjoining blocks by north-dipping, high-angle reverse faults. The petrology of metamorphosed siliceous ironstones in the lac Laflamme (1731A) and lac de la Grunérite (1734A) areas was documented by Hashimoto and Béland (1968). Variations of regional metamorphic grade in the Wakeham Bay (1729A) and lac Vicenza (1733A) areas were studied by Schimann (1978a, b), whereas Westra (1978) examined a suite of metamorphic samples from north of 61°N. Stewart (1976) published a summary of the mine geology at Purtuniqu (1722A) and Miller (1977) studied the petrology and geochemistry of a mineralized ultramafic sill in the Kattiniq area (1725A). Lastly, Hoffman (1985) reviewed available geological, gravity and magnetic data for the northern Ungava Peninsula and proposed a tectonic model for the Cape Smith Belt in which the thrust belt was considered to be a 20 000 km² klippe separated from a proposed root zone at Sugluk Inlet (Fig. 3) by a lower-plate antiform of Archean basement.

In 1983, the Ministère de l'Énergie et des Ressources du Québec initiated a seven year project to map the western portion of the Cape Smith Belt at 1:50 000 scale (Lamothe, 1986). Reports and maps stemming from this project are available for a number of areas (Fig. 3) including lac Beauparlant (Lamothe et al., 1984), lac Chukotat (Moorhead,

1986, 1989), lac Vanasse and Lessard (Tremblay, 1986, 1989, 1991), lac Bélanger (Roy, 1989), lac Bilson (Barrette, 1990a), and lac Bolduc (Barrette, 1990b). In addition, Hervet (1986) published a short paper on the area southeast of lac Vanasse (Fig. 3). Within the context of the mapping project, petrological and geochemical studies of volcanic rocks were completed by Picard (1986, 1989a, b) and Gaonac'h et al. (1989, 1992), detailed structural observations were made by Budkewitsh (1986), the petrology of layered sills was studied by Thibert et al. (1989) and the petrology of a late felsic pluton was examined by Feininger (1986). The magmatic evolution of the extrusive and intrusive units in the belt was considered in terms of a plate tectonic model by Picard et al. (1989, 1990). Studies on the occurrence and genesis of mineralization in the central and western portions of the belt are given in Giovenazzo (1986), Giovenazzo and Lefebvre (1986), Giovenazzo et al. (1989), Barnes and Giovenazzo (1990), and Barrette (1991).

In order to complement the work by the Ministère de l'Énergie et des Ressources du Québec in the western portion of the Cape Smith Belt, the Geological Survey of Canada initiated a three-year project in 1985 to map the eastern portion of the belt from Wakeham Bay (1729A) to Lac Watts (1721A; Fig. 2). It was agreed between the federal and provincial mapping agencies that the Geological Survey of Canada would focus its studies on (1) the tectonostratigraphy of the eastern part of the belt, (2) the structural and thermal evolution of the thrust belt, and (3) the tectonic evolution of the northern margin of the Superior Province. As well, the Ministère de l'Énergie et des Ressources du Québec would continue its long-term study of mineral deposits in the entire belt. In order to insure geological map coverage at a common scale from Ungava Bay to Hudson Bay, the eastern portion of the belt was mapped at 1:50 000 scale (Fig. 2).

Numerous interim and final papers on all aspects of the Geological Survey of Canada's work in the eastern portion of the Cape Smith Belt have been published by project participants. Preliminary field mapping results were presented in four Current Research reports (St-Onge et al., 1986, 1987, 1988b; Scott and Bickle, 1991), one Ministère de l'Énergie et des Ressources du Québec report (St-Onge and Lucas, 1986), and sixteen Open File maps (St-Onge et al., 1988a). Tectonostratigraphic units of the eastern belt were described by St-Onge et al. (1989), Scott et al. (1989, 1991, 1992) and St-Onge and Lucas (1990m). Geochronological constraints on the tectonic evolution of the Early Proterozoic belt were published by Parrish (1989). The structural evolution of the thrust belt and the interaction of structural and metamorphic processes were presented in Lucas (1989a, 1990), Lucas and St-Onge (1989a, b) and Lucas and Byrne (1992). Regional metamorphism, mineral reactions and geothermobarometric constraints were discussed by Bégin (1989a, 1992a,b) and St-Onge and Lucas (1989d, 1991). Isotopic constraints on the origin of tectonostratigraphic units in the eastern belt were published by Hegner and Bevier (1989, 1991). Finally three Ph.D. theses (Bégin, 1989b; Lucas, 1989b; Scott, 1990) and one B.Sc. thesis (Scott, 1986) form an integral and important part of the database for the eastern Cape Smith Belt project.

The information contained in this memoir is a compendium of the information presented in the publications listed above. The purpose of the memoir is to present the principal results of the eastern Cape Smith Belt mapping project in one venue in order to serve as a first order geological reference and complement the published Geological Survey of Canada maps (St-Onge and Lucas, 1989a-c, 1990a-l) for the eastern portion of the belt (Fig. 2).

In 1989, the Geological Survey of Canada initiated a second three-year geological mapping project in the Ungava Peninsula. The purpose of the project was to complement the work of the federal and provincial agencies in the Cape Smith Belt by mapping the area north of the belt at 1:100 000 scale. One aim of the new project was to further document the regional tectonic and structural context for the rocks of the thrust belt. Although the results of this second project will be the subject of a separate Geological Survey of Canada publication, the regional context provided by the later project will be used here in a review of the general geology of the Ungava Peninsula. Early results from recent field work north of the Cape Smith Belt have been published by Baragar et al. (1986), St-Onge and Lucas (1990n, 1992), Lucas and St-Onge (1991, 1992), Lucas et al. (1992), and St-Onge et al. (1992).

Radiometric age determinations on rocks of the Cape Smith Belt and adjacent gneisses have been made by a number of workers. Beall et al. (1963) compared K-Ar and whole-rock Rb-Sr dates from the eastern thrust belt and the northern portion of the Labrador Trough. A Rb-Sr study of an Archean granodiorite from north of Lac Nantais (Fig. 3) was published by Taylor and Loveridge (1981) and the results of a similar study of two plutons from the western portion of the belt were presented by Taylor and Loveridge (1985). Doig (1983, 1987) published Rb-Sr results for samples of Archean and Early Proterozoic gneisses in the Deception Bay and Sugluk Inlet areas (Fig. 3). Parrish (1989) derived U-Pb ages for critical intrusive and extrusive units within the central Cape Smith Belt and also for the Archean and Early Proterozoic gneisses to the north. More recent U-Pb age determinations by Parrish on units in and north of the belt are given in St-Onge et al. (1992). Machado et al. (1991) and N. Machado (pers. comm., 1992) produced a number of U-Pb dates for volcanic and plutonic units in the western Cape Smith Belt, thereby adding greatly to the geochronological data base of northern Ungava.

The Cratère du Nouveau-Québec (also known as Chubb Crater and Nunavik Crater) is a meteorite-impact structure formed in the gneisses south of the Cape Smith Belt in the lac Laflamme area (1731A). Lying along the southern boundary of the present project area (Fig. 3), the crater has been the focus of several field studies after the United States Air Force photographed it in 1943. Visits by Meen and Chubb (a prospector) in 1950 and Meen and Martin in 1951 led to several publications (Meen, 1950, 1951a, 1952, 1957). A profile study of the Cratère du Nouveau-Québec was published by Millman (1956). Currie and Dence (1963) measured sheeting in the crater rim whereas Currie (1965) described the geology of the crater area and Currie (1966) published a 1:6000 scale bedrock geological map. The

petrography of an impactite from the Cratère du Nouveau-Québec was summarized by Marvin et al. (1988). Whereas Meen considered the crater to be quite recent and post-last glaciation, a study by Harrison (1954) clearly shows that the Cratère du Nouveau-Québec has to be a preglacial structure. Subsequently, ^{40}Ar ^{39}Ar dating by Roddick (1990) yielded an age of $0.47 \pm 0.52 / -0.47$ Ma for a sample of impactite. Bouchard (1989) discussed the possible sedimentary record preserved at the bottom of the crater lake, and Bouchard and Péloquin (1989) provided a comprehensive review of the geology, geomorphology, Quaternary geology, flora, fauna, history of exploration, and archeology of the crater area.

A number of regional geophysical surveys have been completed over the Cape Smith Belt since the early 1960s. Gravity data and interpretations for northern Québec were published by Tanner and McConnell (1964) with subsequent interpretations by Innes et al. (1967, 1968) for the Hudson Bay area. A gravity map of Canada was published by Earth Physics Branch (1980) and a magnetic anomaly map for northern Quebec was published by the Geological Survey of Canada (1983). Using the results of the gravity surveys in conjunction with geological and geochronological arguments, Gibb and Walcott (1971), Thomas and Gibb (1977), Baer (1977), Gibb (1983), Gibb et al. (1983) and Feininger et al. (1985) have proposed and disputed a number of early tectonic models for the origin of the Cape Smith Belt (see review by Hoffman, 1985).

Until recently, the glacial and postglacial events in northern Ungava were studied only in the coastal areas of the peninsula. Matthews (1962, 1966, 1967a) published a series of papers on the glacial and postglacial geomorphology of the coast between Cape Wolstenholme and Sugluk Inlet (Fig. 3). In his publications, Matthews considered the question of postglacial land uplift in northern Ungava. Air photographs and available data on the Quaternary geology of northern Quebec were summarized by Prest (1970) and illustrated on a 1:5 000 000 scale map of Canada (Prest et al., 1968). St-Onge and Scott (1986) made notes on the geomorphology and Quaternary geology of the lac de la Grunérite area (1734A) and considered field evidence for the presence or absence of former proglacial lakes in the region. Bruneau and Gray (1991) published a 1:250 000 scale map of the Quaternary deposits and presented results of C^{14} dating for the area between Sugluk Inlet and the promontoire Martigny (Fig. 3). A short field study of possible rock pingos south of Purtuniqu (1722A) was presented by Seppälä (1988). In 1989, Daigneault (1990) initiated a three-year mapping project of the surficial deposits of the Ungava Peninsula north of 61°N . His field work and compilation of the unconsolidated sediments at 1:250 000 scale will fill a current void in the knowledge of the Quaternary geology of the northeastern Precambrian Shield.

Field methods and extent of mapping

Field work for the eastern Cape Smith Belt project was carried out during the summers of 1985-1987. The field party comprised five people during the first two years of field work; Marc St-Onge (Geological Survey of Canada),

Stephen Lucas (senior mapping assistant and graduate Ph.D. student at Brown University), Normand Bégin (senior mapping assistant and graduate Ph.D. student at Queen's University), David Scott (senior mapping assistant, undergraduate B.Sc. student at McMaster University and graduate Ph.D. student at Queen's University) and Janien Schwarz (camp cook and manager). In 1987, the crew of five was joined by William Marsh (June-July) and Jim Archibald (July-August), pilots of the Glanford Aviation helicopter used that summer.

Personnel, camp equipment, and fuel were brought to Wakeham Bay (1729A) (1985) and Purtuniqu (1722A) (1986) at the start of the field season with a chartered Air Inuit 748 from Kujjuaq. Every two weeks, provisions were purchased from Dorval Food Market in Dorval, Quebec and flown to Wakeham Bay or Purtuniqu with Air Inuit Twin Otter charters from Kujjuaq. Five camps were established in 1985, at the west end and south shore of Wakeham Bay, on the Wakeham River (1728A), at a mid-point between the rivière Wakeham and the rivière Laflau (1733A) and on lac de la Grunérite (1734A). In 1986 four camps were set-up, on the rivière Déception (1722A), the north end of lac Watts (1721A), at the south end of lac Cross (1724A), and at Purtuniqu (1722A). A sub-contracted helicopter from the Ministère de l'Énergie et des Ressources du Québec was used to transport personnel, material, and provisions to the new camp sites and to ferry rock samples and empty fuel drums to the Wakeham or Purtuniqu airstrips for shipment south.

In 1987, material was flown to Purtuniqu with a chartered Bradley Air 748 from Iqaluit (N.W.T.). Provisions were bought from Fraser's Meat Market in Almonte, Ontario and flown to Purtuniqu by chartered Bradley Air Twin Otter every two weeks. Two camps were established during the field season, one at lac Watts (1721A) and one on the river draining north into lac Tarraliaq (1723A). Local field transport was provided by a helicopter on contract to the Geological Survey of Canada field party.

Geological traverses were done exclusively on foot and an average distance of 15 to 20 km per day was mapped by individual geologists. Traverse spacing was 1 to 3 km depending on local geology. Transport to and from traverse was also generally by foot, although boats were used on Wakeham Bay and lac Watts (1985 and 1986) and in 1987 a helicopter stationed in camp provided the needed ferry service. Geological observations and measurements were recorded during traverse on 1:38 397 scale black-and-white airphotos. All the information was then compiled in camp on 1:50 000 topographic bases which were subsequently used to produce the fifteen colour maps published by St-Onge and Lucas (1989a-c, 1990a-l). Towards the end of systematic field work in 1987, spot checks were made in the map area where additional information was required to clarify data gathered during the systematic traversing.

Traversing started on June 22 in 1985, June 24 in 1986, and June 19 in 1987. Fieldwork was concluded on September 1 the first year, September 3 the second year, and August 26 the final year of the project. The weather was generally sunny and cool (but often windy) in 1985 and 1987 and therefore

good for traversing. However in 1986, after an unusually hot July, the summer weather ended August 9 and snowfalls began.

The aim of the mapping project was to examine the Early Proterozoic rocks of the eastern portion of the Cape Smith Belt at 1:50 000 scale. As such the surrounding Archean basement units were not mapped, although observations were made on the nature of the gneissic units immediately underlying the basal décollement of the thrust belt or those imbricated within the Early Proterozoic thrust stack.

Acknowledgments

The success of the eastern Cape Smith Belt project is in large part due to the enthusiasm and complete dedication of Normand Bégin (University of Calgary) and David Scott (GEOTOP). Their systematic independent mapping, hard work, and interest in geology during the three summers of field work were exemplary and made them superior senior field assistants. In camp, Janien Schwarz (University of Victoria) provided food, shelter, and warmth for the often wind-battered traversing parties. Her interests in the natural milieu greatly opened our eyes to the beauty of the barren lands we were living in. We are indebted to William Marsh and Jim Archibald of Glanford Aviation (Hamilton) for an impeccable and outstanding job with the helicopter during the summer of 1987. We are grateful to Daniel Lamothe (Ministère de l'Énergie et des Ressources du Québec) for the logistical co-operation and exchange of ideas during the course of the project. We thank Charlie Arngak, President of the northern Village of Kangiqsujuaq for his permission to map and camp on Category I land and for his help among the ice flows of Wakeham Bay. Our thanks to Peter Horsman of Trans-Québec Helicopters, Gaéthan Roby and Ken Stirmeay of Air Inuit, and Fred Alt of Bradley Air for co-operation with logistics. Falconbridge Limited and Delaware Resources Limited are gratefully acknowledged for subcontracting their Jet Ranger in 1986. We wish to acknowledge Asbestos Corporation and Falconbridge Limited for the use of their runways and installations during the course of the project.

We are grateful to Tim Byrne (Brown University), Dugald Carmichael (Queen's University), Herb Helmstaedt (Queen's University), Randy Parrish (GSC), John Scott (GSC), and Denis St-Onge (GSC), for their field visits to northern Quebec. Their mapping and sampling greatly contributed to our understanding of the bedrock and Quaternary geology of the project area. In particular we wish to acknowledge Herb Helmstaedt for his prediction of the existence and subsequent discovery of the sheeted dykes in the Watts Group. We thank Randy Parrish (GSC) for his careful and meticulous geochronological studies on samples brought back south.

Finally we are indebted to Ken Card (GSC) for his careful and timely critical review of a first version of this memoir. Denis St-Onge (GSC) and Dave Scott (GEOTOP) are also thanked for their reviews on the earlier manuscript. Michel Parent (CGQ) is acknowledged for critically reading the Quaternary section.

GENERAL GEOLOGY: TECTONIC DOMAINS OF THE UNGAVA OROGEN

The Cape Smith Belt is the foreland thrust belt of the Early Proterozoic Ungava orogen of northern Quebec (St-Onge and Lucas, 1990n; Fig. 1). The orogen is an arc-continent collisional belt (Lucas et al., 1992; St-Onge et al., 1992) which comprises tectonostratigraphic elements accumulated on or accreted to the northern margin of the Superior Province Archean craton during >0.2 Ga of divergent and convergent margin tectonic activity (Fig. 4). The tectonostratigraphic units of the eastern Ungava orogen can be grouped into three principal tectonic domains (Fig. 1, 5): (1) (par)-autochthonous plutonic and supracrustal rocks of the Superior Province (Lucas and St-Onge, 1991; St-Onge et al., 1992); (2) autochthonous and allochthonous sedimentary and volcanic units inferred to be associated with rifting of the Superior Province craton (Povungnituk and Chukotat groups; Hynes and Francis, 1982; Francis et al., 1983; Picard et al., 1990; St-Onge and Lucas, 1990m); and (3) allochthonous crustal components of assemblages interpreted as an ophiolite (Watts Group; St-Onge et al., 1988b; Scott et al., 1989; Scott and Bickle, 1991; Scott et al., 1991), and a

magmatic arc (Narsajuaq arc; St-Onge and Lucas, 1990n; Lucas and St-Onge, 1991). By definition (Bergeron, 1957a), the eastern Cape Smith Belt comprises the units of the orogen listed above minus the Archean basement of the Superior Province (domain 1) and the Early Proterozoic Narsajuaq arc of domain 3 (Fig. 1).

The rocks of domain 1 are Archean (ca. 2.93 - 2.57 Ga; Taylor and Loveridge, 1981; Doig, 1983, 1987; Parrish, 1989). They occur both as the stratigraphic or structural basement to the rocks of domain 2 and as the structural basement to the rocks of domain 3 (Fig. 4, 5). Domain 1 comprises older mafic-ultramafic units and sedimentary rocks intruded by voluminous tonalite and granite plutons.

Units in domain 2 are Early Proterozoic (ca. 2.04-1.92 Ga; Parrish, 1989; N. Machado, pers. comm., 1992) and outcrop as predominantly allochthonous cover in the southern portion of the Cape Smith Belt (Fig. 5). Two principal groups are recognized (Bergeron, 1959; Table 1); the older Povungnituk Group and the younger Chukotat Group. The Povungnituk Group contains a sedimentary and volcanic record of continental rifting. A lower sequence of clastic sedimentary rocks (conglomerate, quartzite, ironstone, semipelite, pelite)

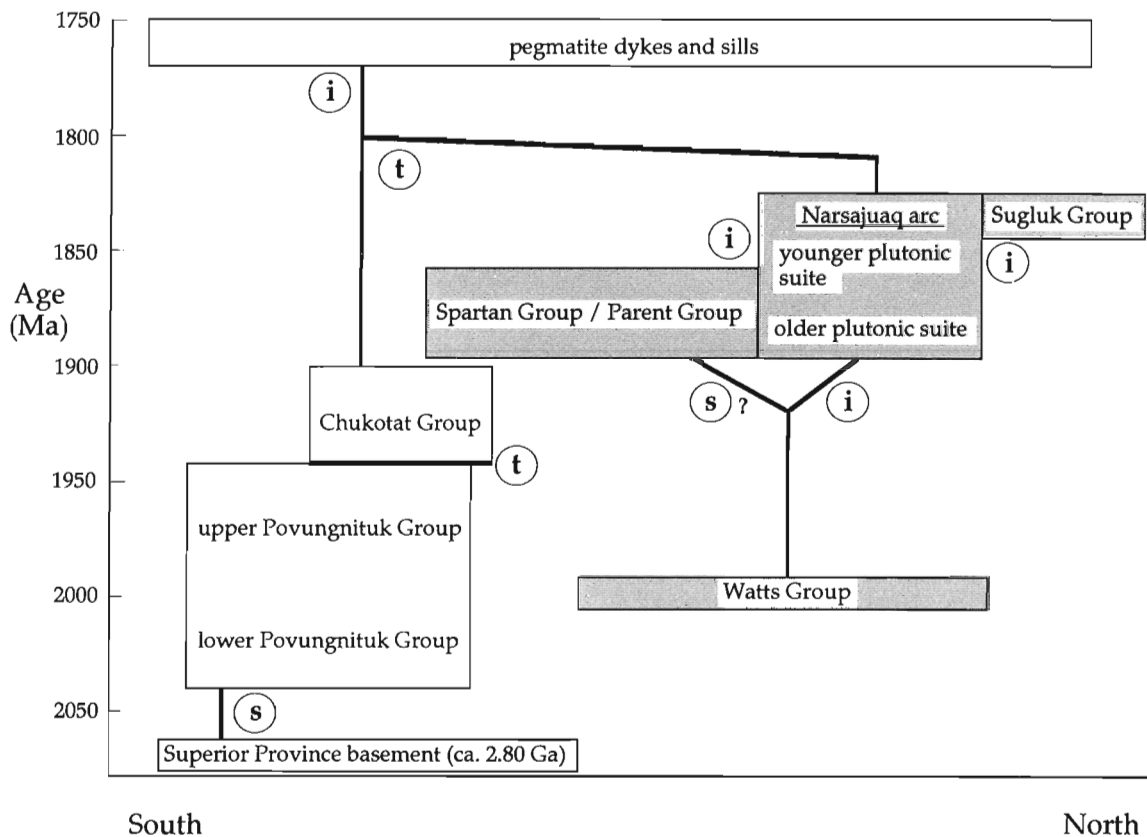


Figure 4. Space and time relationships for the tectonostratigraphic assemblages in the Ungava orogen. For reasons discussed in the text and in St-Onge et al. (1992), domain 3 units (shaded) are interpreted to be tectonostratigraphically 'suspect' with respect to the Superior Province continental-margin. The figure shows: (1) the accumulation interval represented by each assemblage; (2) interpreted (s, stratigraphic; t, tectonic; i, intrusive) and unknown (unspecified) spatial relationships between assemblages; and (3) the interpreted coalescence of domain 3 assemblages before accretion to the northern rifted margin of the Superior Province.

EARLY PROTEROZOIC

domain 3

tonalite

Spartan Group

graphitic pelite, semipelite, quartzite

Watts Group

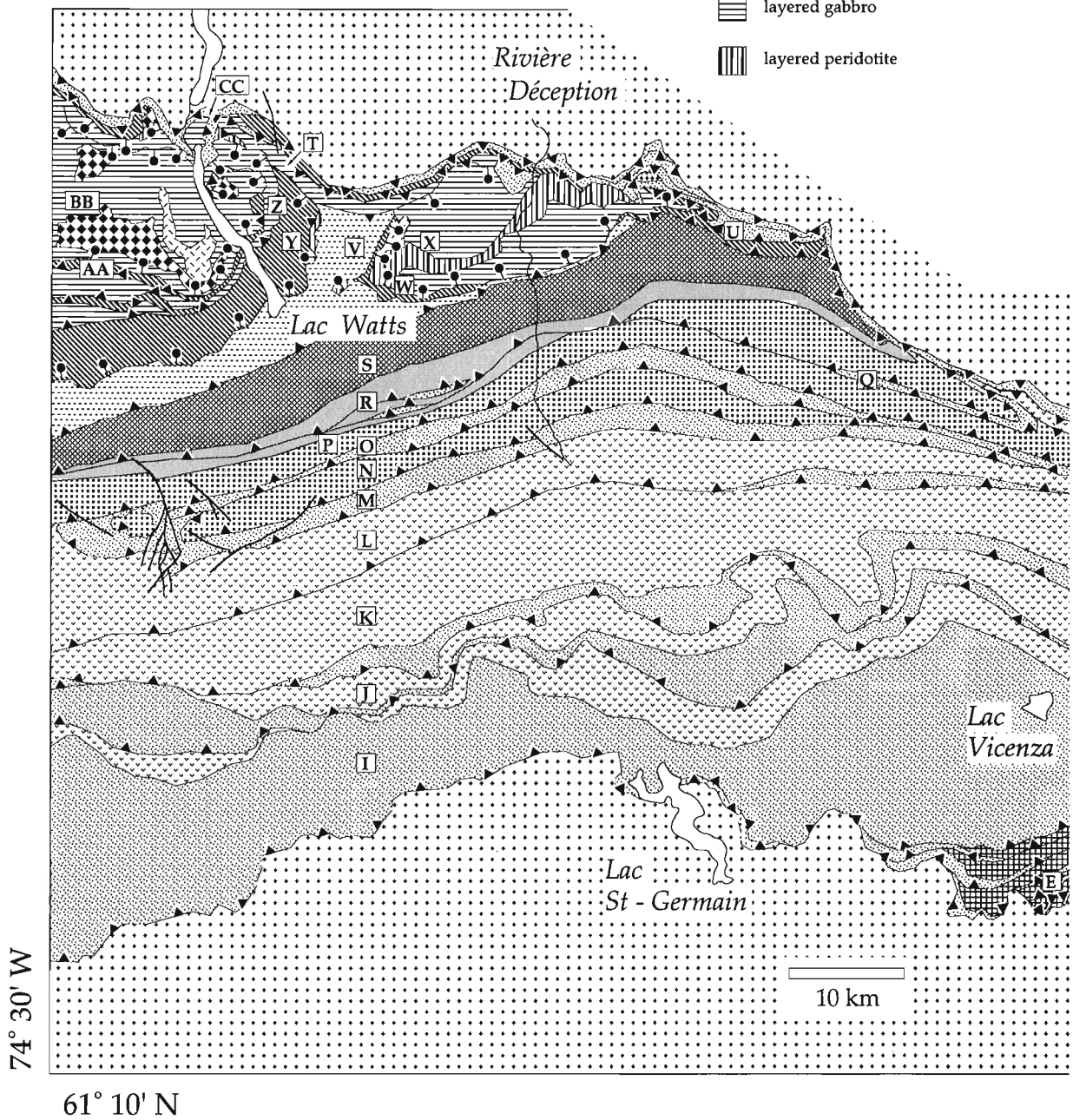
basalt, gabbro sills and sheeted dykes

pyroxenite

layered gabbro

layered peridotite

Figure 5. Geological compilation map for the eastern Cape Smith Belt. Boxed letters refer to thrust sheet labels which are used in the text. Area corresponds to that outlined in Figure 1.






ARCHEAN


domain 2

domain 1


Chukotat Group

Superior Province





-  dominantly plagioclase-phyric basalt, gabbro, peridotite
-  dominantly pyroxene-phyric basalt, gabbro, peridotite
-  dominantly olivine-phyric basalt, gabbro, peridotite






-  tonalite, granite, amphibolite

Upper Povungnituk Group

-  basalt, gabbro, peridotite

Lower Povungnituk Group

-  micaceous quartzite
-  semipelite, quartzite, ironstone, dolomite, conglomerate, basalt, volcanoclastic sedimentary rock, gabbro, peridotite
-  ironstone
-  arkosic quartzite, ironstone, conglomerate

-  oblique - slip fault
-  reverse fault
-  normal fault
-  thrust fault
-  geological boundary

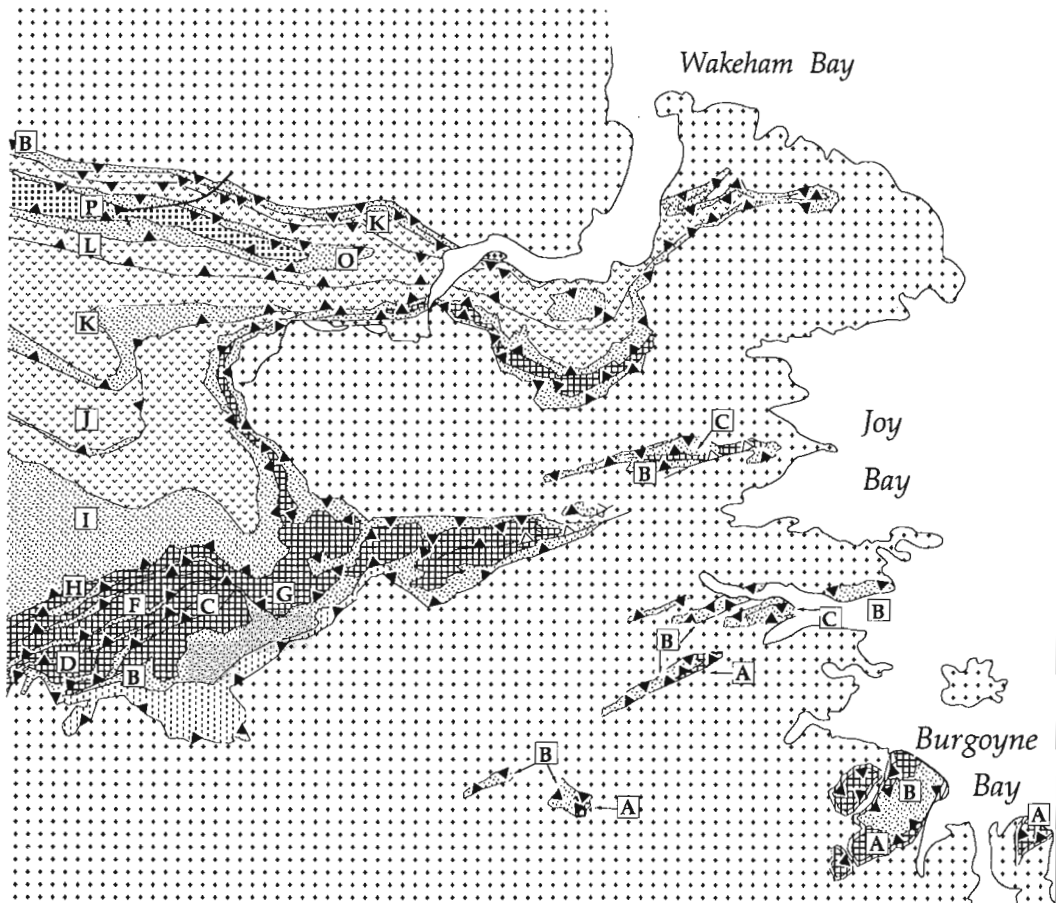


Table 1. Tectonostratigraphic table for the Wakeham Bay-lac Watts area

ERA	GROUP / SUITE	MAP SYMBOL	LITHOLOGY
LATE PROTEROZOIC		Pd	Diabase dykes
EARLY PROTEROZOIC	NARSAJUAQ	Pt	Tonalite
	SPARTAN	PSpe	Semipelite, pelite, quartzite, gabbro
	WATTS	PWb	Basalt, gabbro sills, sheeted gabbroic dykes
		PWpy	Pyroxenite
		PWg	Layered gabbro
		PWp	Layered peridotite
	CHUKOTAT	PCpl	Dominantly plagioclase phyrlic basalt, gabbro
		PCpy	Dominantly pyroxene phyrlic basalt, gabbro
		PCol	Dominantly olivine phyrlic basalt, gabbro, peridotite, layered gabbro-peridotite sills
EARLY PROTEROZOIC	UPPER POVUNGNITUK	PPb	Basalt, volcanoclastic sedimentary rock, rhyolite, minor semipelite and quartzite, gabbro, peridotite, layered gabbro-peridotite sills
		PPms	Micaceous quartzite
	LOWER POVUNGNITUK	PPv	Basalt, volcanoclastic sedimentary rock, rhyolite, minor quartzite, dolomite and calc-silicate, gabbro, peridotite, layered, peridotite-gabbro sills
		PPse	Semipelite, pelite, micaceous quartzite, quartzite, conglomerate, ironstone, dolomite, calc-silicate, minor basalt and volcanoclastic rocks, gabbro, peridotite, layered peridotite-gabbro sills
		PPi	Ironstone, minor quartzite and semipelite
		PPs	Quartzite, ironstone, conglomerate, semipelite
ARCHEAN		Agn	Tonalite, granite, amphibolite

and minor carbonate (dolomite) is overlain by a bimodal suite of basalt and rhyolite. Fault-scarp conglomerates and the distribution of tectonostratigraphic units indicate accumulation of the Povungnituk Group in a tectonically-active basin. The Chukotat Group includes pillowed and massive basalt flows and associated gabbro, peridotite and layered gabbro-peridotite sills. The dominantly igneous Chukotat Group seems to record the change from accumulation of continental rift-type volcanic rocks to the formation of transitional crust and possibly oceanic crust. Both the Povungnituk Group and the lower Chukotat Group contain numerous layered peridotite-gabbro sills. The chemistry of the sills suggests that these may represent a feeder system for the lower Chukotat Group flows (Bédard et al., 1984).

Rocks of domain 3 are also Early Proterozoic (ca. 2.00-1.80 Ga; R. Parrish, 1989, pers. comm., 1991) but they occur solely as allochthonous packages in the northern portion of the Ungava orogen (Fig. 1, 4). Two tectonostratigraphic groups are recognized in the eastern portion of the Cape Smith Belt (Fig. 5, Table 1). The Watts Group (Lamothe et al., 1984) comprises a distinctive assemblage of layered mafic and ultramafic rocks, massive and pillowed basalt flows, mafic sills and sheeted dykes, and plagiogranite intrusions. This group has been interpreted by St-Onge et al. (1988b) as a dismembered and metamorphosed ophiolite suite ('Purtuniqu ophiolite'). The Spartan Group (Lamothe et al., 1984) comprises mostly pelite interbedded with semipelite and fine-grained quartzite. St-Onge et al. (1992) have suggested that the Spartan Group might represent a clastic apron marginal to an island-arc complex. The Watts Group is intruded by a number of plutons of quartz diorite, tonalite, and monzogranite (Table 1). St-Onge et al. (1992) have proposed that the plutons may be associated with Early Proterozoic magmatism in the Narsajuaq arc which is preserved in crystalline thrust imbricates north of the Cape Smith Belt (Fig. 1).

Archean units in domain 1 are characterized by high-grade tectonic fabrics and mineral assemblages (Lucas and St-Onge, 1991) that predate the accumulation of the sedimentary and volcanic rocks of domain 2. The tectonostratigraphic units of domain 2 record the development of a foreland thrust belt characterized by south-verging faults ramping up from a basal décollement located at the Archean basement-Early Proterozoic cover contact (Fig. 5; Lucas, 1989a; St-Onge and Lucas, 1990m). The 'tectonically suspect' units of domain 3 were accreted to the thrust belt (Fig. 4) along south-verging faults which re-imbricated the foreland thrust belt, and which resulted in at least 100 km of displacement of domain 3 units with respect to the underlying autochthonous basement of domain 1 (Lucas, 1989a). Accretion of domain 3 units resulted in crustal thickening and consequent exhumation of high-pressure, greenschist- to amphibolite-facies metamorphic rocks in the Cape Smith Belt (Bégin, 1989a, 1992a,b; St-Onge and Lucas, 1991; Lucas and St-Onge, 1992).

Following the accretion of domain 3 units, both the allochthons and the autochthonous footwall basement of the Ungava orogen were deformed into regional-scale folds

during two post-thrusting folding episodes (east-trending and northwest-trending; St-Onge and Lucas, 1990m; Lucas and Byrne, 1992). As a result of the folding episodes, the eastern portion of the Cape Smith Belt is characterized by a large, west-plunging synform (Fig. 1) which exposes an oblique crustal cross-section allowing direct geological examination of more than 18 km of structural relief at the present erosion surface (Lucas, 1989a). In order to take full advantage of the oblique crustal-scale view preserved on the largely west-dipping cross-fold limbs, work by the Geological Survey of Canada between 1985 and 1987, focused on the eastern portion of the thrust belt (outlined area, Fig. 1).

All tectonostratigraphic units in the eastern Cape Smith Belt are deformed and metamorphosed. However, modifiers describing their deformation state (e.g., schist) or metamorphic character (e.g., meta-) are dropped for simplicity where appropriate in this memoir and on the fifteen companion maps (Fig. 2; St-Onge and Lucas, 1989a-e, 1990a-l). Unit designation letters utilized in the text correspond to those listed in the Tectonostratigraphic Table and to those shown on the fifteen companion geological maps (Fig. 2).

DOMAIN 1: PLUTONIC UNITS OF THE SUPERIOR PROVINCE

In the southeastern Ungava orogen (Fig. 5), the Archean Superior Province outcrops continuously from south of lac St-Germain (1731A), eastward to Wakeham Bay (1729A) and northward to the northern rivière Déception (1722A). South of Burgoyne Bay (1735A), the Archean units comprise the stratigraphic basement to unconformably overlying Early Proterozoic strata (Fig. 5; St-Onge and Lucas, 1990m). Elsewhere, the basement/cover contact is tectonic (Lucas, 1989a) and rocks of the Superior Province comprise the structural basement to the overlying Early Proterozoic thrust imbricates of the Cape Smith Belt (Lucas, 1989a; St-Onge and Lucas, 1990m). The Archean units are only very locally imbricated with Early Proterozoic strata, for example along

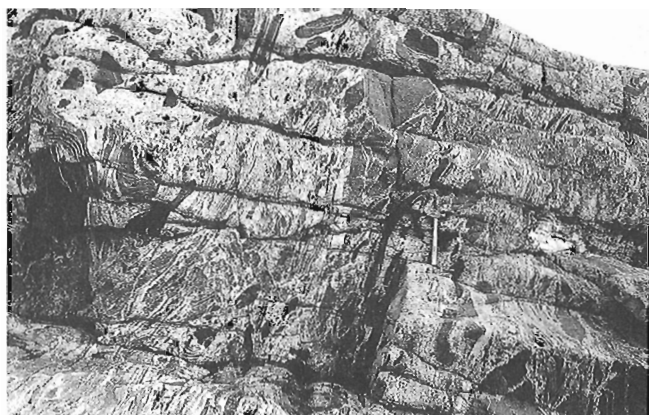


Figure 6. Foliated biotite-hornblende tonalite (light) with abundant mafic enclaves (dark) from the Superior Province on the north shore of Fisher Bay. (Fig. 3). Hammer is 39 cm long. (GSC 205313-N)

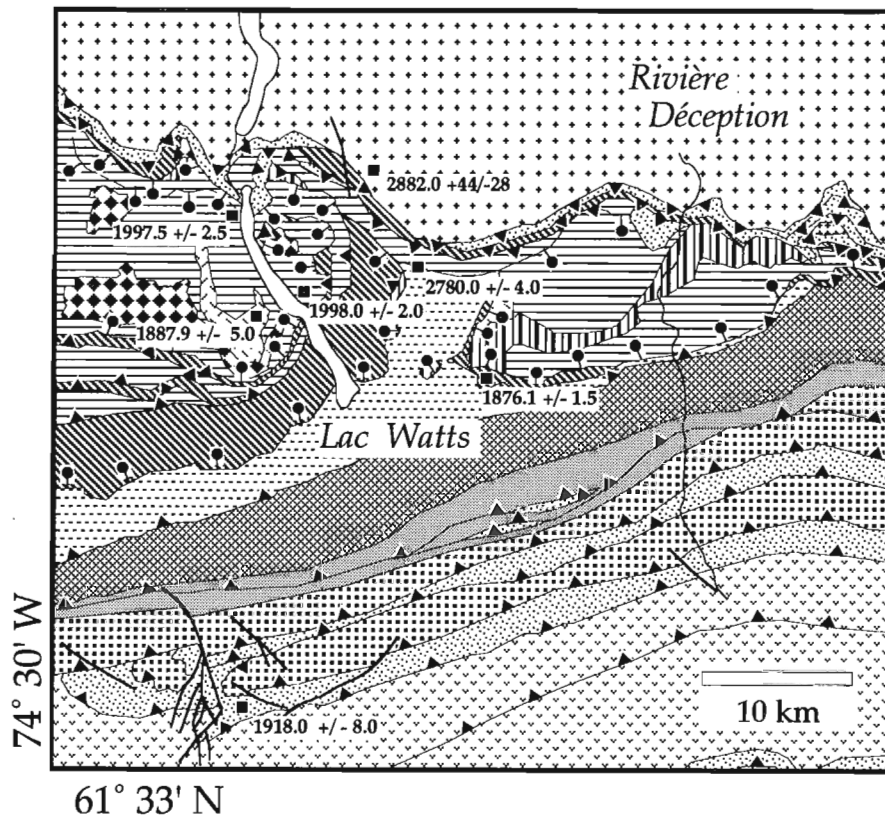
the northern basement/cover contact east of the rivière Déception (1722A). However, high-temperature mineral assemblages and fabrics (ranging from a weakly developed foliation to a mylonitic gneissosity) associated with Archean tectonism in the basement, were reworked on a regional scale during the Early Proterozoic (Lucas, 1989a; Lucas and St-Onge, 1991, 1992). At the scale of the orogen, the Superior Province units can be considered (par)-autochthonous with respect to the overlying thrust belt (Fig. 1).

Plutonic units (Agn)

In the northeastern Ungava Peninsula, the Superior Province is characterized by voluminous plutonic bodies which range in composition from hornblende ± biotite tonalite to biotite ± hornblende granite (Lucas and St-Onge, 1991). The plutonic bodies engulf early screens and rafts of peridotite, amphibolite (Fig. 6), quartz diorite, and rusty semipelite. Two samples of biotite ± hornblende tonalite (collected northeast of lac Watts, Fig. 7) have U-Pb (zircon) igneous crystallization ages of 2882 ± 44 – 28 Ma and 2780 ± 4 Ma (Fig. 8; Parrish, 1989). Since mapping of Archean basement units was beyond the scope of the eastern Cape Smith Belt project, the reader is referred to the results of the subsequent Geological Survey of Canada project in the northern Ungava Peninsula for a more complete description of these rocks (Lucas and St-Onge, 1991, 1992; St-Onge and Lucas, 1992).

DOMAIN 2: AUTOCHTHONOUS TO ALLOCHTHONOUS TECTONO-STRATIGRAPHIC UNITS OF THE CAPE SMITH BELT

The Early Proterozoic rocks of the eastern Cape Smith Belt have been divided into two tectonostratigraphic domains (2 and 3 from above) based on demonstrable stratigraphic or intrusive relationships (domain 2) or the lack of such relationships (domain 3) with the northern margin of the Superior Province (St-Onge and Lucas, 1992; see also Picard et al., 1990). Domain 2 comprises the Povungnituk and Chukotat groups, and occurs predominantly in the southern part of the belt (Fig. 5). Domain 3 includes the Spartan and Watts groups and it occurs in the northern part of the thrust belt. Within domain 2, three tectonostratigraphic subdivisions have been previously proposed (Fig. 4 and 5; reviewed in St-Onge and Lucas, 1990m): (1) autochthonous and allochthonous, dominantly sedimentary rocks of the lower Povungnituk Group; (2) allochthonous, dominantly volcanic rocks of the upper Povungnituk Group; and (3) allochthonous volcanic rocks of the Chukotat Group. Crosscutting field relationships and geochemical studies suggest that rocks of the Povungnituk and Chukotat groups were accumulated on or adjacent to the rifted Superior Province craton in the Early Proterozoic (Fig. 4; Hynes and Francis, 1982; Francis et al., 1983; Hegner and Bevier, 1989; Picard et al., 1990; St-Onge and Lucas, 1990m). In the following sections these Early Proterozoic units are described from south to north (Fig. 5), an order which reflects their



EARLY PROTEROZOIC

- domain 3
- tonalite
 - Spartan Group
 - graphitic pelite, semipelite, quartzite
 - Watts Group
 - basalt, gabbro sills and sheeted dykes
 - pyroxenite
 - layered gabbro
 - layered peridotite

- domain 2
- Chukotat Group
- dominantly plagioclase-phyric basalt, gabbro, peridotite
 - dominantly pyroxene-phyric basalt, gabbro, peridotite
 - dominantly olivine-phyric basalt, gabbro, peridotite
- Upper Povungnituk Group
- basalt, gabbro, peridotite
- Lower Povungnituk Group
- semipelite, quartzite, conglomerate, volcanoclastic sedimentary rock, gabbro, peridotite

ARCHEAN

- domain 1
- Superior Province
- tonalite, granite, amphibolite
- sample location
 - oblique - slip fault
 - normal fault
 - thrust fault
 - geological boundary

Figure 7. Location and U-Pb age determination for seven geochronology samples in the western portion of the map area (1721A-1726A). Ages are from Parrish (1989).

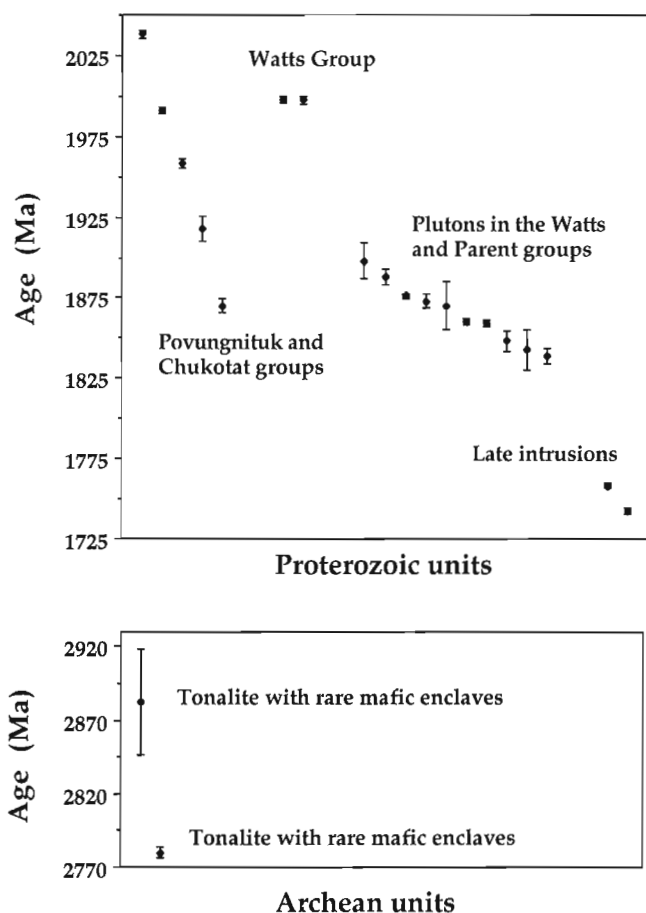


Figure 8. Summary of U/Pb (zircon and baddeleyite) data for the tectonostratigraphic units of the Cape Smith Belt and underlying Archean basement which are discussed in the text. Two sigma error bars are indicated. Data is from R. Parrish (1989, pers. comm., 1991), N. Machado et al. (1991) and Machado (pers. comm., 1992).

autochthonous to progressively more allochthonous nature with respect to the underlying Superior Province basement. The increasing allochthonous nature of the supracrustal units is a function of the age of emplacement, the displacement, and the stacking order of thrust sheets within the Cape Smith Thrust Belt (see Lucas, 1989a; St-Onge and Lucas, 1990m; Lucas and St-Onge, 1992).

Lower Povungnituk Group (PPs - PPms)

Autochthonous sedimentary rocks (PPs)

Autochthonous, clastic sedimentary rocks of the lower Povungnituk Group occur as areally-restricted, thin (less than 20 m thick) sequences along the southern margin of the main Cape Smith Belt (1732A, 1733A, 1734A) and in small erosional outliers south and west of Burgoyne Bay (1735A). Because of their size, only the autochthonous units in the Burgoyne Bay area are shown on Figure 5. In both the main belt and the outliers, the autochthonous sedimentary rocks rest unconformably on Archean tonalite or monzogranite (Fig. 9) which show no evidence of a penetrative Proterozoic fabric. The autochthonous units are capped by the high-strain basal décollement of the thrust belt (St-Onge et al., 1988b; Lucas, 1989a).

In the main belt, the autochthon comprises metre-scale lenses of either polymictic conglomerate (Fig. 10), quartz pebble-bearing arkosic grit (Fig. 11) and/or iron-rich quartzite. In the outliers of Burgoyne Bay (Fig. 9), the autochthon includes both carbonate- and quartz-rich ironstone beds (Fig. 12), well-laminated pelite and semipelite, and arkosic quartzite beds characterized by graded bedding and basal quartz pebble grits. The ironstone beds are 1-2 m thick, the arkosic quartzite beds 2-3 m thick, and the pelite and semipelite intervals 2-3 m thick. In the arkosic quartzite, rounded to subrounded feldspar and quartz

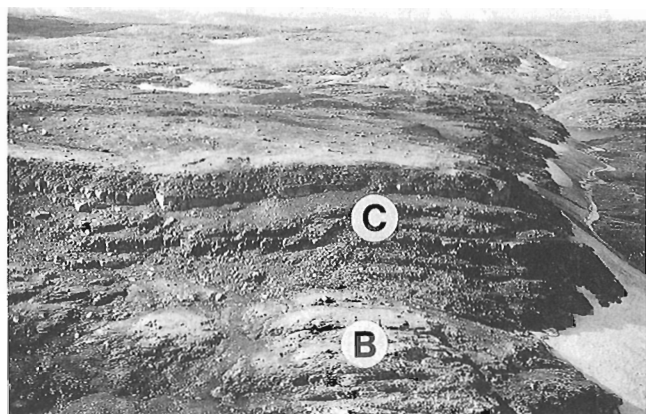


Figure 9. Aerial view of the autochthonous arkosic quartzites of the lower Povungnituk Group, 6km west of Burgoyne Bay (Fig. 5). Individual quartzite beds are 3 m thick. Letters identify the Early Proterozoic cover (C) and the Archean Superior Province basement (B). Thickness of cover section is 30 m. (GSC 204234-F)

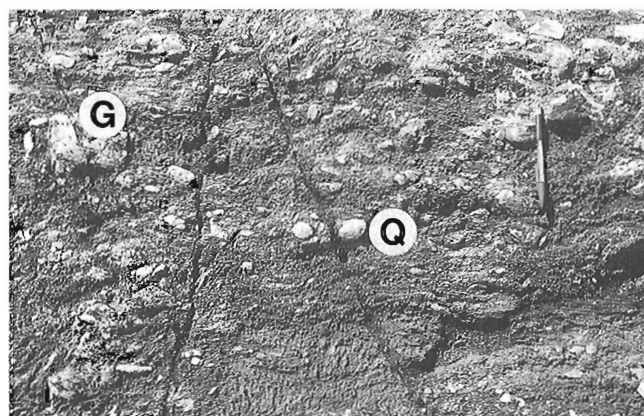


Figure 10. Basal, polymictic conglomerate of the lower Povungnituk Group, 29 km west of Joy Bay (Fig. 5). Granitoid (G) and quartz (Q) pebbles are present. Pen is 15 cm long. (GSC 1992-102P).

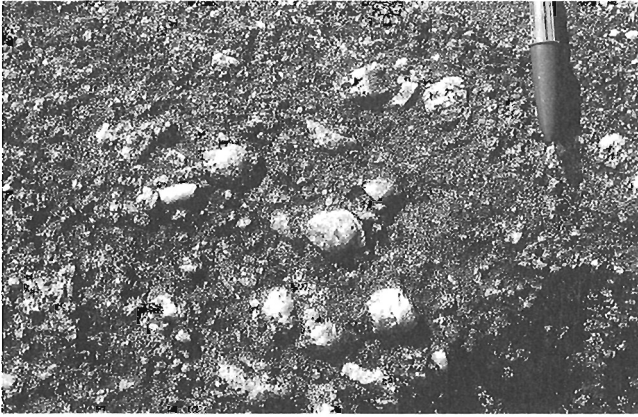


Figure 11. Quartz pebble-bearing arkosic grit of the lower Povungnituk Group, 3 km east of lac St-Germain (Fig. 5). Pen cap is 4.5 cm long. (GSC 1992-102AA)



Figure 13. Detail of arkosic quartzite bed showing trough crossbedding. Quartzite is of the lower Povungnituk Group 6 km west of Burgoyne Bay (Fig. 5). Pen is 15 cm long. (GSC 204234-G).

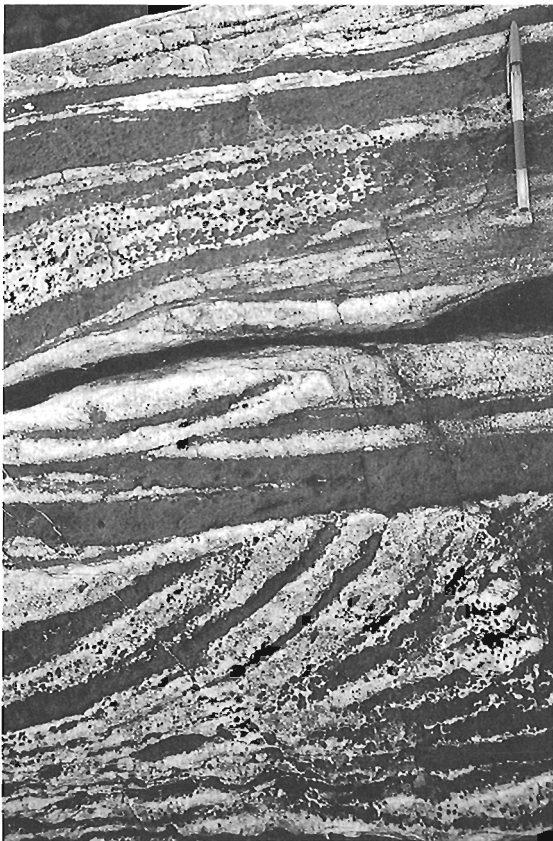


Figure 12. Crossbedded ironstone unit of the lower Povungnituk Group 5 km west of Burgoyne Bay (Fig. 5). Magnetite-rich beds (dark) alternate with quartz-rich beds (light). Pen is 15 cm long. (GSC 1992-102Z)

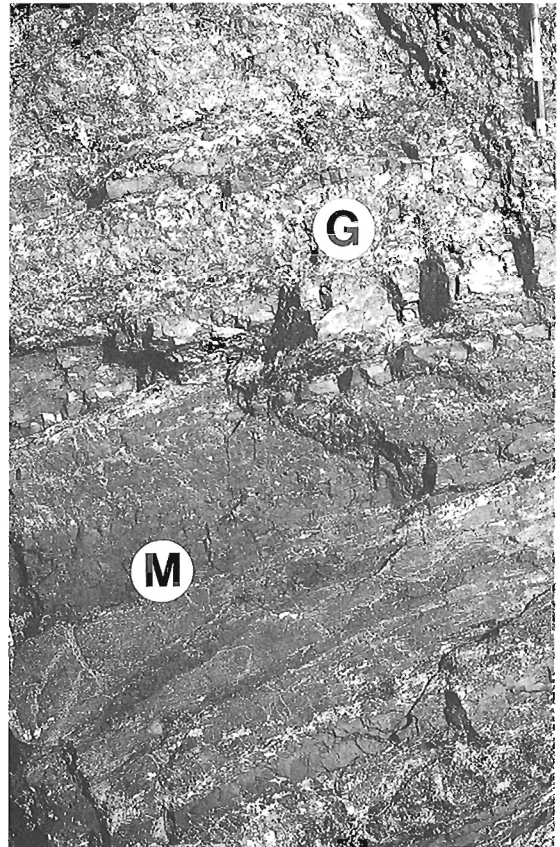


Figure 14. Interbedded magnetite (M) and grunerite (G) schist of the lower Povungnituk Group, 2 km north of lac de la Grunérite (1734A). Pen is 15 cm long. (GSC 204233-K)

grains vary from less than a millimetre to several millimetres in diameter. The matrix is silica-cemented. Some of the quartzite beds display well-developed trough crossbeds (Fig. 13), the orientation of which indicate south to north channelized flow. The autochthonous sequences of the lower Povungnituk Group have been interpreted by St-Onge et al. (1988b) and St-Onge and Lucas (1990m) as evidence of fluviodeltaic sedimentation. At the regional scale, the preserved autochthonous rocks provide a critical field relationship which links the lower Povungnituk Group units to the Superior Province basement in northern Quebec (Fig. 5).

Allochthonous sedimentary and volcanic rocks (PPI - PPms)

The bulk of the lower Povungnituk Group is allochthonous with respect to the underlying Archean basement (St-Onge et al., 1988b; Lucas, 1989a) and occurs in a series of thrust imbricates in the southern part of the thrust belt (Fig. 5). In the southernmost thrust sheets (thrust sheets A to D, Fig. 5), ironstone is overlain by semipelite interbedded with arkosic quartzite, minor ironstone, and dolomite. The semipelite is in turn overlain by a massive, homogeneous micaceous quartzite unit. Laterally and vertically, the ironstone and semipelite grade into mafic volcanoclastic rocks interlayered with basalt flows (1735A, 1730A, 1731A, 1733A, 1734A).

Ironstone (PPI)

The ironstone varies in thickness from 50 m to 650 m and includes (1) ferruginous quartzite, (2) interbedded, massive magnetite/grunerite schist (Fig. 14), (3) carbonate-rich grunerite schist and (4) garnet-biotite-hornblende-grunerite schist. These units are laterally discontinuous and therefore the ironstone is not subdivided in Figure 5, nor on the 1:50 000 scale geological maps for the eastern Cape Smith Belt (Fig. 2; St-Onge and Lucas, 1989a-c, 1990a-l). The greatest thickness of ironstone in the map area occurs west of lac de la Grunerite (1733A, 1734A) and east of lac St-Germain (1732A; Fig. 5).



Figure 15. Thinly bedded semipelite from the lower Povungnituk Group 5 km southeast of lac Vicenza (Fig. 5). Phyllosilicate rich intervals are more finely laminated than the more siliceous beds. Pen is 15 cm long. (GSC 1992-102A)

Semipelite, arkosic quartzite, dolomite (PPse)

Overlying the ironstone are 60 m to 960 m of interbedded semipelite, arkosic quartzite, and ironstone (Fig. 5). The semi-pelite is rusty, thinly bedded at the centimetre-scale (Fig. 15), locally graded, and characterized by parallel graphitic laminations at the top of beds. The arkosic quartzite is composed of subrounded to rounded, millimetre-scale, quartz and feldspar grains which are silica-cemented. Quartz constitutes 80% of the grains. Bed thicknesses range from 15 cm to over 2 m (Fig. 16). Some of the thicker beds contain quartz pebbles up to 2 cm in diameter in their basal zones. Graded bedding and channel structures (Fig. 17) are commonly preserved in the arkosic quartzite, which has been interpreted as a turbiditic deposit from a proximal fan environment (St-Onge and Lucas, 1990b). The ironstone is similar to that previously described and outcrops in discrete 1-2 m beds alternating with semipelite intervals tens of metres

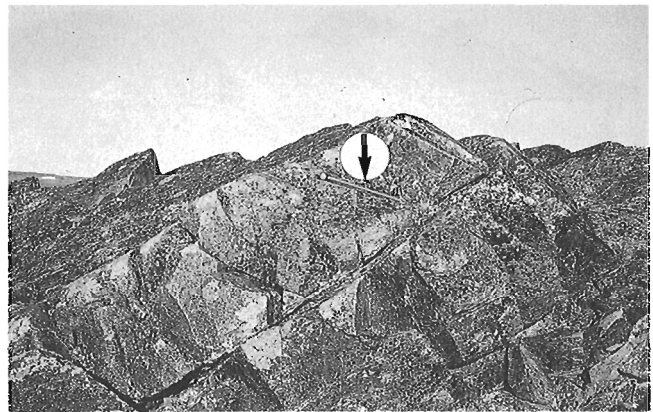


Figure 16. Arkosic quartzite beds of the lower Povungnituk Group from 2 km southeast of lac Vicenza (Fig. 5). The quartzite is interpreted as a turbiditic deposit from a proximal fan environment (see text). Arrow points to 80 cm long hammer. (GSC 204234-H)

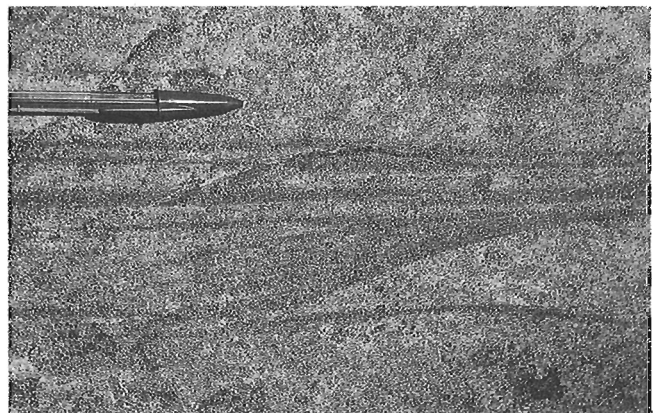


Figure 17. Channel structure in a proximal fan quartzite of the lower Povungnituk Group 2 km southeast of lac Vicenza (Fig. 5). Pen cap is 4.5 cm long. (GSC 1992-102BB)

in thickness. The base of the rusty semipelite and arkosic quartzite sequence is marked by a narrow, 2 m to 5 m thick, discontinuous interval of dolomite (Fig. 18) and associated calc-silicate rock.

Locally, polymictic conglomerate and arkosic quartzite beds occur within lower Povungnituk Group thrust sheets (1725A). The conglomerate is poorly sorted, with subangular to subrounded clasts of tonalite gneiss, basalt, gabbro, and argillite (Fig. 19). The centimetre- to metre-scale clasts form a framework filled with a matrix of quartz, feldspar, biotite, and chlorite. St-Onge and Lucas (1990b) have suggested that the conglomerate may be a fault scarp deposit related to normal faulting during accumulation of the Povungnituk Group, due to the unsorted nature of the clasts, the presence of both basalt and gabbro clasts, the lithological similarity of the granitoid boulders to the basement gneisses, and the laterally restricted occurrence of the unit.



Figure 18. Dolomite from the lower Povungnituk Group 10 km south of Wakeham Bay (Fig. 5). Other than compositional layering, no primary structures were noted in the domite. Back-pack is 1 m long. (GSC 204232-W)

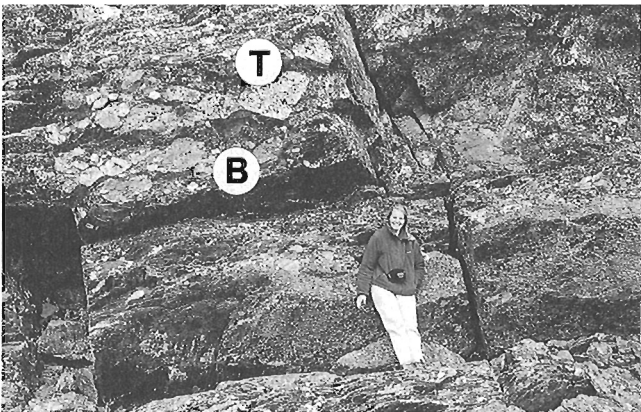


Figure 19. Polymictic conglomerate from the lower Povungnituk Group 9 km west of the upper rivière Déception (Fig. 5). Note the presence of large boulders of tonalite gneiss (T) and basalt (B). This unit is interpreted as a fault scarp deposit related to normal faulting (see text). Height of person is 1.8 m. (GSC 204767-A).

Basalt, volcaniclastic rock (PPv)

Thin pillowed or thicker tabular basalt flows and mafic volcaniclastic rocks are locally intercalated with the clastic sedimentary units of the lower Povungnituk Group. The volcanic and volcanic-derived units display a great degree of variability in tectonostratigraphic facies. Pillowed sequences grade laterally into mafic and felsic volcaniclastic units, dolomitic volcaniclastic rocks, calc-silicate bands, and semipelitic and quartzite beds. Thin (1 m) beds of dolomite are commonly associated with the lavas. The volcaniclastic rocks can contain felsic and mafic fragments up to 4 cm in diameter. The sequence also contains discontinuous layers of finegrained, aphyric to quartz-phyric rhyolite. Although very heterogeneous in the field, the common trait of this unit is the occurrence of interlayered mafic volcanic and clastic material at the outcrop scale, most notably in the area east of lac Forcier (1730A).

Micaceous quartzite (PPms)

The clastic and mafic units of the lower Povungnituk Group are overlain, by homogeneous micaceous quartzite (Fig. 20) in thrust sheets A to H (Fig. 5). The micaceous quartzite constitutes a distinct ridge-forming unit which varies in thickness from 70 m to 1700 m. This unit outcrops extensively in the area west of Joy Bay (1735A) north of lac de la Grunérite (1734A) and south of lac Vicenza (1733A; Fig. 5). The micaceous quartzite consists of quartz and up to 20% metamorphic biotite and muscovite. The quartzite is characterized by a uniform millimetre grain size and by abundant centimetre-scale quartz veins. It does not interfinger with volcanic rocks and it lacks any evidence of channelized flow. It is interpreted to mark the shallowing of a proximal basin, isolated from the main locus of crustal stretching and rift volcanism (upper Povungnituk Group; see below) by syndepositional normal faults (St-Onge and Lucas, 1990m).

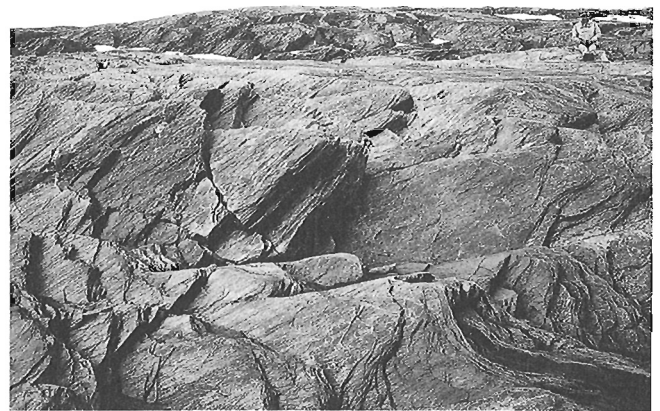


Figure 20. Micaceous quartzite unit of the lower Povungnituk Group, west end of Wakeham Bay (Fig. 5). Standing height of person sitting is 1.8 m. (GSC 204232-Z)

Northward change in tectonostratigraphic facies

The proportion of semipelite, ironstone, and quartzite within the lower Povungnituk Group changes systematically in each more internal (northerly) thrust sheet. Volumetrically less ironstone, proportionally more semipelite, and fewer quartzite beds (Fig. 21) characterize thrust sheets E to H (Fig. 5). This northerly increase in the semipelite to ironstone ratio, coupled with the transition to fewer and laterally more discontinuous quartzite beds, coincides in general with the decrease of dolomite beds, mafic volcanoclastic rocks, and basalt flows in the sequence.

Thrust imbricates I-M, O and Q (Fig. 5) are dominated by laminated semipelite interbedded with arkosic quartzites. The semipelite is thin-bedded (centimetre-scale) and commonly interfingers with beds of graphitic pelite (Fig. 22). The quartzite beds are tens of centimetres thick and are composed chiefly of rounded submillimetre quartz grains. In contrast to similar units in the southern thrust imbricates, the quartzite beds are laterally continuous and do not show evidence of channel structures or crossbedding (Fig. 23). St-Onge and Lucas (1990m) have suggested that they represent relatively distal turbidites. The finer grained, uniformly-bedded sedimentary rocks of these northern thrust sheets are thus interpreted as a more outboard, deeper-water facies of the lower Povungnituk Group. This interpretation is consistent with the fact that these thrust sheets occur more internally in the thrust belt, and thus that they are presumed to have travelled further southward than thrust sheets in their footwall (i.e. to the south) containing equivalent tectonostratigraphic units (Lucas, 1989a).

Gabbro sills (ga)

The apparent thickness of the sedimentary units in thrust sheets I, J, K, and L (Fig. 5) is greatly inflated by the emplacement of numerous gabbro sills. These are most



Figure 21. Interbedded semipelite (dark) and quartzite (white) beds of the lower Povungnituk Group 8 km east of lac Vicenza (Fig. 5). The sequence is interpreted as a distal fan deposit (see text). Outcrop is 15 m high. (GSC 204233-A)

numerous in the vicinity of lac Vicenza (1733A), east of lac St-Germain (1732A; Fig. 5) and north of the rivière Povungnituk (1730A). The mafic sills range from 10 m to 600 m thick and are essentially conformable with bedding defined by graphitic laminations in the clastic sedimentary rocks. The gabbro sills have narrow (less than 1 m) chilled margins and rarely show evidence of internal layering. The sills are interpreted to be part of the feeder system to the overlying volcanic rocks of the upper Povungnituk Group (see below).

Tectonostratigraphic interpretation and parentage of the lower Povungnituk Group

The tectonostratigraphic changes which characterize the allochthonous units of the lower Povungnituk Group are interpreted to reflect a progressive increase in water depth and the accumulation of units which represent more distal facies from south-to-north along a north-facing rift-margin (Baragar, 1974; St-Onge and Lucas, 1990m). These facies changes are consistent with a distal over proximal thrust stacking order and a north-to-south translation direction for thrust sheets in the southern part of the Cape Smith Belt (Lucas, 1989a).

The allochthonous clastic rocks of the lower Povungnituk Group (thrust sheets A-Q, Fig. 5) are interpreted to be correlative with the autochthonous strata in the Burgoyne Bay area (1735A) based on: (1) the presence of arkosic quartzites and ironstones in both the autochthon and allochthons; and (2) the regional, south-to-north, proximal-to-distal facies distribution in domain 2. This interpretation is consistent with U-Pb analyses of detrital zircons which show only Archean ages for the autochthonous and allochthonous quartzites of the Povungnituk Group (R. Parrish, pers. comm., 1991) in the map area. The correlation of the autochthonous and allochthonous strata along the southern margin of the thrust belt is critical in relating the bulk of the lower Povungnituk Group to the northern margin of the Superior Province.

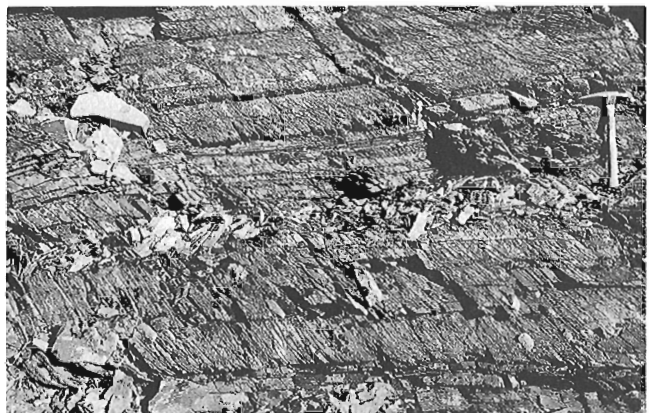


Figure 22. Interbedded semipelite and pelite from the lower Povungnituk Group within thrust sheet M (Fig. 5). The nearly horizontal bedding is outlined by dark graphite laminations at the top of individual 10-15 cm thick beds. The spaced slaty cleavage dipping to the bottom right of the photograph is related to a domain 2 D₂ fold structure discussed in the text. Hammer is 34 cm long. (GSC 1992-102HH)



Figure 23. Quartzite beds from the lower Povungnituk Group within thrust sheet M (Fig. 5). The laterally continuous, relatively thin quartzite beds are interpreted as distal turbidites (see text). Pen is 15 cm long. (GSC 1992-102D)



Figure 24. Pillowed basalt from the upper Povungnituk Group, 3 km west of Wakeham Bay (Fig. 5). Hammer is 34 cm long. (GSC 204232-L).

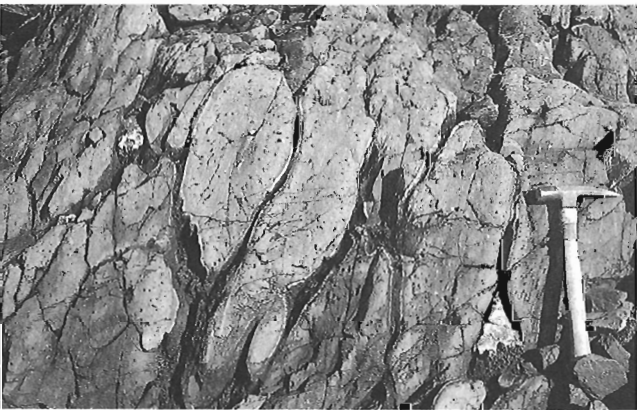


Figure 25. Irregular pillows in a tholeiitic basalt flow in the upper Povungnituk Group, 5 km south of the rivière Déception (Fig. 5). Hammer is 34 cm long. (GSC 1991-173A)

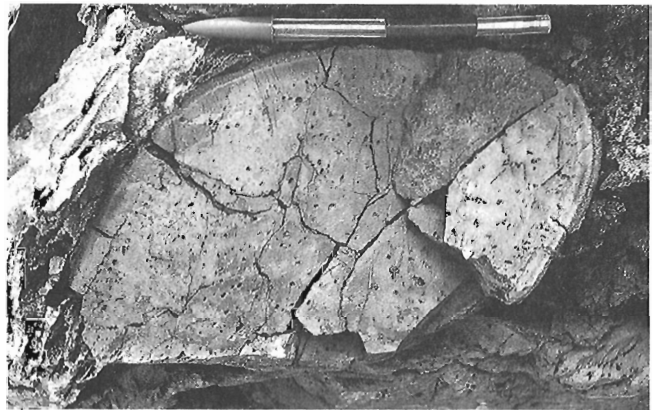


Figure 26. Vesicular basalt showing a well developed pillow structure and seldge rim. The vesicular basalt flow is from the upper Povungnituk Group 5 km south of the rivière Déception (Fig. 5). Pen is 15 cm long. (GSC 1992-102X)



Figure 27. Flow top breccia in a vesicular basalt sequence from the upper Povungnituk Group 5 km south of the rivière Déception (Fig. 5). Fragments of basalt are separated by a matrix of quartz and carbonate. Pen is 15 cm long. (GSC 1992-102 V).

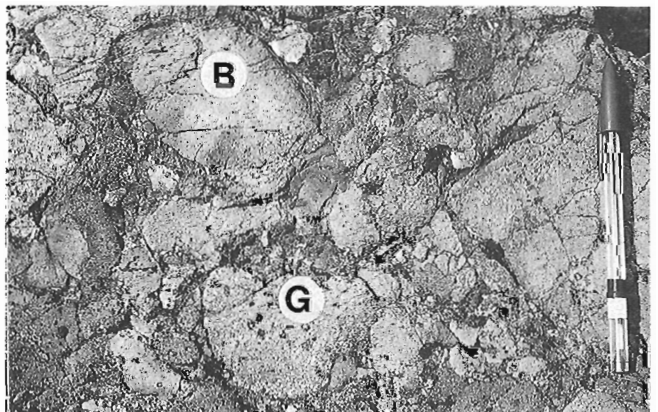


Figure 28. Mafic conglomerate from the upper Povungnituk Group 5 km south of the rivière Déception (Fig. 5). Note the angularity of the blocks and the presence of both gabbro (G) and basalt (B) clasts. The conglomerate is interpreted to be a fault-scarp deposit associated with synvolcanic faulting during accumulation of the upper Povungnituk Group (see text). Pen is 15 cm long. (GSC 204234-I).

The clastic sedimentary rocks of the Povungnituk Group are intruded by a small granodiorite body (Picard et al., 1990) southwest of lac Chukotat (Fig. 3). The intrusive body has been dated by U-Pb on zircon at 1991 ± 2 Ma (Fig. 8; Machado et al., 1991). More recently, a gabbroic sill emplaced in a sequence of rusty semipelite and quartzite (lower Povungnituk Group) northeast of Korak Bay (Fig. 3) has been dated at 2038 ± 2 Ma (Fig. 8; N. Machado, pers. comm., 1992). These ages provide minimum brackets for the onset of continental-margin subsidence and accumulation of sedimentary rocks along the northern margin of the Superior Province.

Upper Povungnituk Group (PPb)

Basalt flows of the upper Povungnituk Group conformably overlie or are interfingered with the upper clastic sedimentary rocks of the lower Povungnituk Group (Fig. 5). Both thin, pillowed mafic flows (Fig. 24, 25) and thicker, tabular flows are present. Vesicular flows (Fig. 26) and flow-top breccias (Fig. 27) are common. Dolomite and black semipelite occur between flows throughout the sequence, whereas mafic pyroclastic rocks are present in the lower part of the volcanic section. The base of the mafic pile is also characterized by isolated lenses of 5-10 m thick volcanogenic conglomerate, most notably northwest of lac St-Germain (1731A). The conglomerate is typically composed of subrounded to angular blocks of basalt and gabbro (Fig. 28) that range in diameter from a few centimetres to several metres. The blocks are clast-supported and the infilling matrix consists of millimetre-scale basalt rock fragments and carbonate. The presence of basalt and gabbro clasts and the limited lateral extent of the mafic conglomerate suggest that it may be related to synvolcanic, (normal?) faulting. Laterally discontinuous and thin (less than 50 m thick) rhyolite bodies within the mafic volcanic pile and a sequence of basanites/nephelinites and phonolites overlying the basalts (Gaonac'h et al., 1989, 1992) attest to the geochemical diversity of

Povungnituk Group volcanism. The volcanic and sedimentary rocks of the Povungnituk Group are intruded by massive gabbroic sills (Fig. 29), which are interpreted as part of a feeder system to the basalts of the upper Povungnituk Group.

The bulk of the mafic volcanic rocks have been described by previous workers (e.g. Hynes and Francis, 1982; Francis et al., 1983; and Picard et al., 1990) as Fe- and Ti-rich, LREE-enriched, continental tholeiites. The reader is referred to the above listed papers for a complete description of the geochemical characteristics of these lavas in the central portion of the Cape Smith Belt. A rhyolite sampled from near the top of the preserved volcanic sequence, east of lac Chukotat (Fig. 3) is dated (U/Pb on zircon) at $1959 +3.1/-2.7$ Ma (Fig. 8; Parrish, 1989).

The tectonostratigraphic evidence presented above and the regional distribution of the upper Povungnituk Group from Ungava Bay to Hudson Bay strongly suggest that this margin was a north-facing rift-margin of considerable lateral extent (at least 300 km; Fig. 1).

Tectonostratigraphic interpretation and parentage of the upper Povungnituk Group

The volcanic flows and volcanoclastic sedimentary units of the upper Povungnituk Group have been interpreted to be the result of voluminous magmatism associated with rifting of the Superior Province craton (Baragar, 1974; Hynes and Francis, 1982; Francis et al., 1983; Picard et al., 1990; St-Onge and Lucas, 1990m). Hot spot activity (e.g. White, 1987; White et al., 1987; McKenzie and Bickle, 1988; Richards et al., 1989; Behrendt et al., 1990) during the Early Proterozoic may explain the great thickness of the upper Povungnituk Group volcanic sequence (>5 km on Fig. 8 of Lucas, 1989a), the apparent lack of a continental-margin wedge of sedimentary rocks (Parrish, 1989), and the formation of the rift-margin itself.

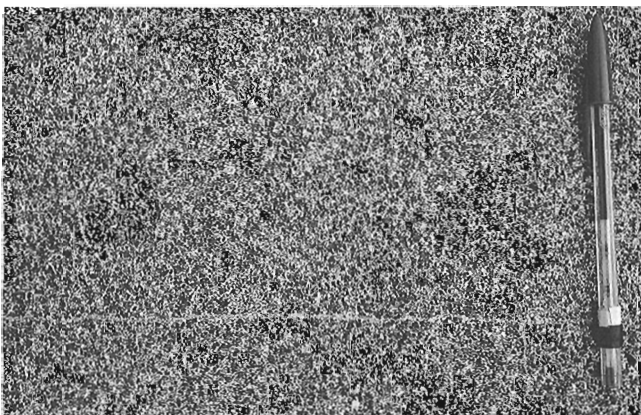


Figure 29. Massive gabbroic sill emplaced in the upper Povungnituk Group 12 km east of lac Vicenza (Fig. 5). The sills are interpreted to be part of a feeder system to the basalts of the upper Povungnituk Group (see text). Pen is 15 cm long. (GSC 1992-102EE)

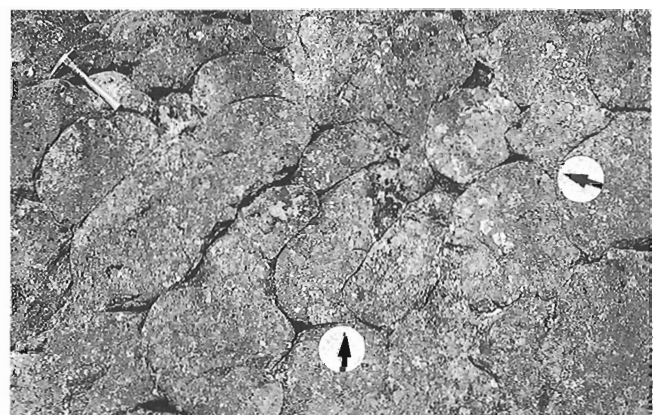


Figure 30. Pillow structures in an olivine-phyric basalt flow of the Chukotat Group (thrust sheet P 14 km south of lac Watts, Fig. 5). Arrows point to well developed pillow tails indicating stratigraphic tops to the upper left of photograph. Hammer is 34 cm long. (GSC 204233-X)

The gabbro sills emplaced into the rocks of the Povungnituk Group link the magmatism of the upper Povungnituk Group tholeiites to the underlying lower Povungnituk Group sedimentary sequence. The interpretation that the tholeiitic volcanic sequence is related to continental rifting is consistent with the hypothesis that accumulation of the lower Povungnituk Group occurred during progressive subsidence at a tectonically active continental-margin. As well, the rift setting is supported by the similarity of the basalts to modern, within-plate continental tholeiites, the occurrence of interbedded basalt and rhyolite flows, and the presence of alkaline basalts near the top of the volcanic sequence (Hynes and Francis, 1982; Francis et al., 1983; Gaonac'h et al., 1989, 1992; Picard et al., 1990; St-Onge and Lucas, 1990m).

Chukotat Group (PCol - PCpl)

Throughout the eastern portion of the Cape Smith Belt (Fig. 5), sedimentary and volcanic rocks of the Povungnituk Group are in thrust contact with the pillowed and massive basalt flows of the almost exclusively igneous Chukotat Group (St-Onge et al., 1987). In the Chukotat Group, lava flows range from 2 to 100 m in thickness. Volcanic structures, such as pillowed flows (Fig. 30), ropy lava (Fig. 31), lava withdrawal shelves (Fig. 32), pillow tubes (Fig. 33), and flow-top breccias are well preserved and indicate submarine accumulation (Francis and Hynes, 1979; Hynes and Francis, 1982; Francis et al., 1983). Fine examples of the primary textures and volcanic structures abound in the area east and north of lac Cross (1724A, 1725A). In thrust sheets N, P, R, and S (Fig. 5), three distinct basalt types (olivine-phyric,

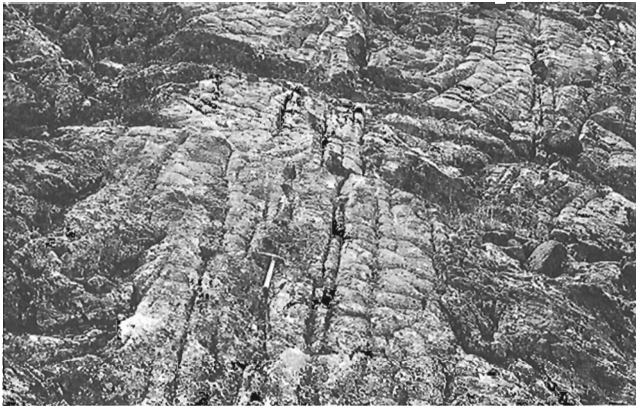


Figure 31. Ropy lava surface of an olivine-phyric basalt flow of the Chukotat Group (thrust sheet N, 18 km south of lac Watts, Fig. 5). Hammer is 34 cm long. (GSC 1992-102S)

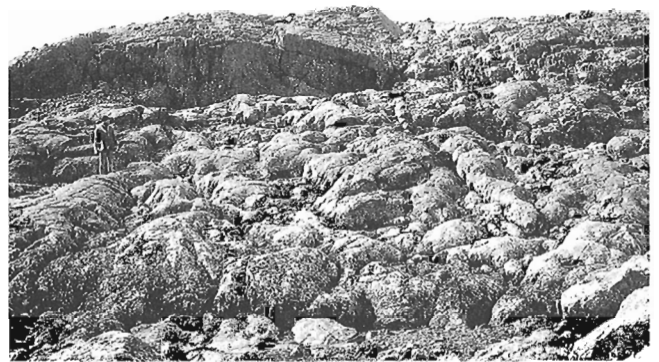


Figure 33. Pillow tubes in the olivine-phyric Chukotat Group from thrust sheet N, 18 km south of lac Watts (Fig. 5). Height of person is 1.8 m. (GSC 204234-J)

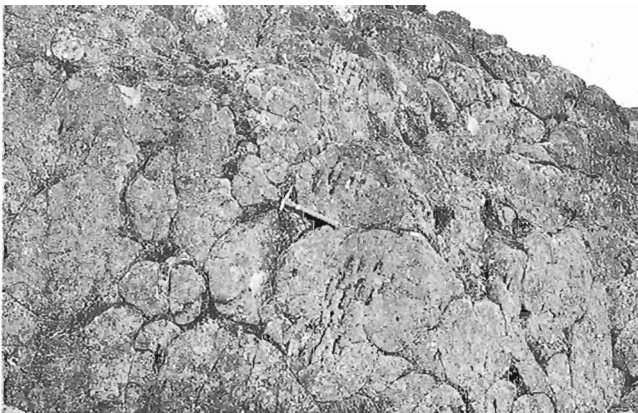


Figure 32. Pyroxene-phyric pillowed flows with lava withdrawal shelves (above and below hammer) from the Chukotat Group in thrust sheet P 14 km south of lac Watts. The pillow shelves allow a direct determination of the present attitude of the paleo-horizontal surface. Hammer is 34 cm long. (GSC 204234-C)

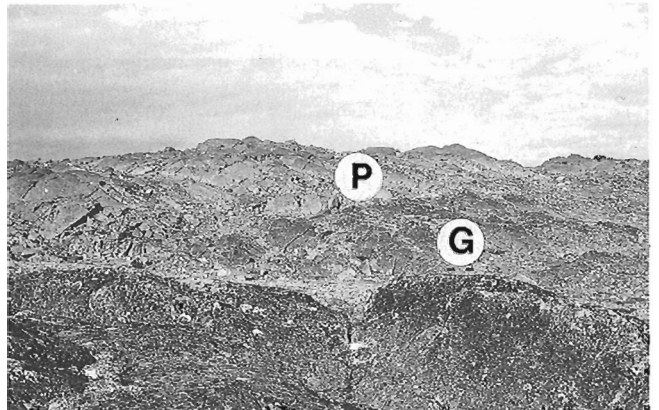


Figure 34. Layered peridotite (P) - gabbro (G) sill emplaced in the olivine-phyric Chukotat Group of thrust sheet P (27 km west of Wakeham Bay, Fig. 5). Thickness of peridotite shown is 20 m. (GSC 1992-102R)

pyroxene-phyric, and plagioclase-phyric) have been recognized based on the presence of the dominant pseudomorph phenocryst type (Francis and Hynes, 1979; Hynes and Francis, 1982; Francis et al., 1983; Picard et al., 1990).

The volcanic rocks of the Chukotat Group range in composition from Mg-rich komatiitic basalts (olivine-phyric basalt) to low-Ti, mafic lavas compositionally equivalent to modern n-MORBs (plagioclase-phyric basalt; Francis et al., 1981, 1983; Picard et al., 1990). A complete description of the geochemical characteristics of these lavas in the central portion of the Cape Smith Belt is given in Francis et al. (1981, 1983), Hynes and Francis (1982), and Picard et al. (1990).

Olivine-phyric basalt (PCol)

The olivine-phyric basalts have ropy to pillowed surfaces (Fig. 30, 31, 33) and are characterized by extensive polyhedral jointing. Red-weathering, well layered olivine-rich cumulate zones characterize the thicker flows. Quenched margins are pale green on fresh surfaces, and contain abundant light-green pseudomorphs after olivine phenocrysts. Microspinfex textures, characterized by randomly oriented platelets of olivine can be seen in the more magnesian flows and pillows (Hynes and Francis, 1982).

Pyroxene-phyric basalt (PCpy)

Pyroxene-phyric flows can be ropy or pillowed (Fig. 32) but often are characterized by hyaloclastite tops. They lack the polyhedral jointing of the olivine-phyric lavas. A diagnostic feature of the pyroxene-phyric basalts is the presence of a red-weathering selvage. As well, pillows in these flows tend to be more tabular in outline than those of the olivine-phyric basalt. Dark-green equant pseudomorphs after pyroxene phenocrysts are most notable near the pillow edges.

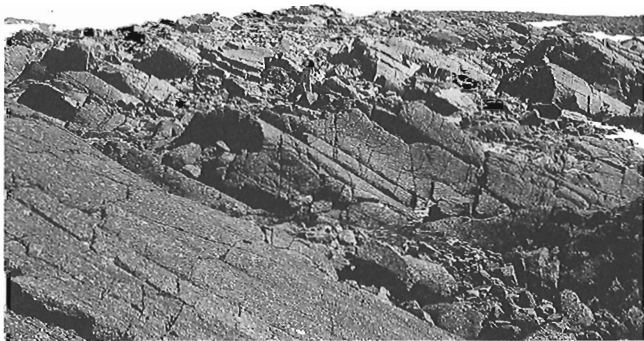


Figure 35. Peridotite at the base of a layered peridotite-gabbro sill which dips north (left). The sill is emplaced in the sedimentary rocks of the Povungnituk Group in thrust sheet M (19 km south of lac Watts, Fig. 5). The peridotite unit is 200 m thick and shows well developed columnar jointing. Height of person is 1.8 m. (GSC 1992-102Y)

Plagioclase-phyric basalt (PCpl)

Plagioclase-phyric lavas occur as thin pillowed or as thicker, tabular flows. Surfaces are undulatory, ropy, or locally brecciated (Hynes and Francis, 1982). Internal layering is not characteristic of even the thicker plagioclase-phyric units. Abundant white plagioclase phenocrysts characterize this basalt.

Layered mafic-ultramafic sills (pe, ga)

The lower Chukotat Group is host to numerous layered peridotite-gabbro sills (Fig. 34) which are tens to hundreds of metres thick (Bédard et al., 1984; St-Onge et al., 1987; Thibert et al., 1989). The sills are shown on the published 1:50 000 scale maps for the eastern Cape Smith Belt (Fig. 2; St-Onge and Lucas, 1989a-c, 1990a-l). The intrusive bodies are commonly characterized by a basal pyroxenite (chilled border phase) overlain by columnar-jointed peridotite (similar to Fig. 35) and capped by gabbro. Similar layered mafic-ultramafic sills up to several hundreds of metres thick and discordant dyke-sill complexes are found in thrust sheets I-M, O (Fig. 5) where they intrude the clastic sedimentary rocks and basalts of the Povungnituk Group. The intrusive bodies emplaced in the Povungnituk Group are most abundant in the lac Forcier - lac Vaillant area (1730A, 1731A) and in the lac Cross-Kattiniq-lac Félix zone (1724A, 1727A, 1726A, 1725A).

The gabbroic section in the thicker sills is marked by plagioclase cumulate layering (Fig. 36), ferrogabbro and quartz ferrogabbro (Fig. 37) zones, and in places is capped by a granophyric upper intrusive contact (Bédard et al., 1984; St-Onge et al., 1987; Thibert et al., 1989). When emplaced in sedimentary rocks, the upper zone of the layered bodies can be characterized by enclaves of quartzite or semipelite partially (Fig. 38) or completely (Fig. 39) detached from the host clastic unit. The sills and dykes intruding the lower

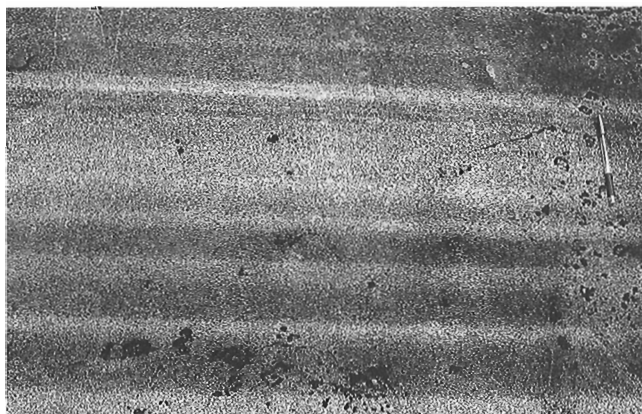


Figure 36. Plagioclase cumulate layering in the gabbroic portion above the peridotite base shown in Figure 35. The location of the sill is the same as for Figure 35. Pen is 15 cm long. (GSC 204234-B)

Povungnituk Group have been interpreted as being consanguineous with those found in the Chukotat Group (Bédard et al., 1984).

Major-element chemistry and abundance of lithophile elements in the sills suggests that they are comagmatic with the olivine-phyric basalts of the lower Chukotat Group and may represent their feeder system (Bédard et al., 1984; Thibert et al., 1989; Barnes and Giovenazzo, 1990). A sample of quartz ferrogabbro from a layered sill intruding the lower Povungnituk Group sedimentary rocks southeast of lac Cross (Fig. 7) has yielded a U/Pb age on baddeleyite of $1918 \pm 9/-7$ Ma (Fig. 8; Parrish, 1989).

Tectonostratigraphic interpretation and parentage of the Chukotat Group

Based on the chemistry of its basalt types, the Chukotat Group appears to record the change from accumulation of continental rift-type volcanic rocks to the formation of transitional crust, and finally the possible formation of LREE-depleted oceanic-type crust (Francis and Hynes, 1979; Francis et al., 1981, 1983; Hynes and Francis, 1982; Picard et al., 1990).

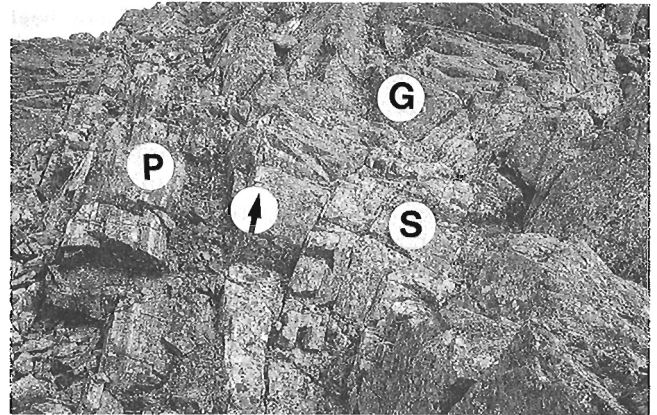


Figure 38. Upper contact of a layered peridotite-gabbro sill emplaced in the clastic sedimentary rocks of the lower Povungnituk Group (P). Note the sedimentary strata (S) partially detached from the wallrock by the granophyric portion (G) of the layered sill. The location of the sill is the same as for Figure 35. Arrow points at 15 cm long pen. (GSC 1992-102J)



Figure 37. Quartz ferrogabbro portion of the layered mafic-ultramafic sill shown in Figures 35 and 36. The location of the sill is the same as for Figure 35. Pen is 15 cm long. (GSC 1992-102II)

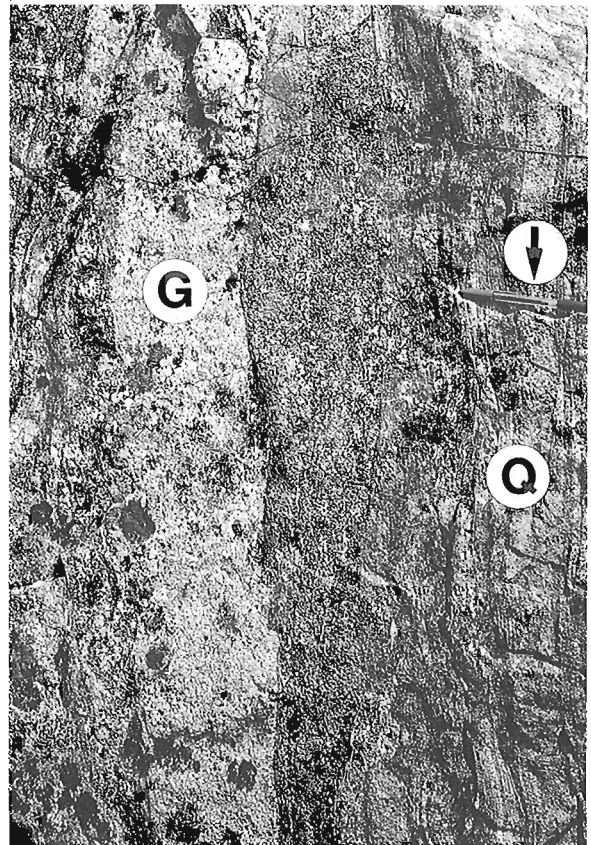


Figure 39. Enclave of quartzite (Q) engulfed in granophyre (G) near the upper intrusive contact of the layered mafic-ultramafic sill shown in Figures 35 to 38. The location of the sill is the same as for Figure 35. Arrow points at 15 cm long pen. (GSC 1992-102JJ)

Although the Chukotat Group is fault-bounded, the layered mafic-ultramafic sills appear to provide a magmatic link between the tectonostratigraphy of the Povungnituk and Chukotat groups suggesting that the latter is also related to the northern rifted margin of the Superior Province (Fig. 4). Based on the interpretation that the sills represent feeders to the Chukotat Group transitional-crust basalts, the existing U-Pb geochronology (summarized on Fig. 8) suggests that the rifting which was initiated by 2038 Ma, led to the accumulation of >5 km of continental tholeiitic basalts by 1959 Ma, and that it had evolved towards the formation of an oceanic basin by ca. 1918 Ma. The apparent hiatus in magmatism between 1959 Ma and 1918 Ma is not well understood. Alternative hypotheses for the Chukotat Group include derivation by back-arc spreading or magmatism in the foreland of the thrust belt (Parrish, 1989). However, the absence of arc rocks of ca. 1918 Ma age in the Ungava orogen argues against the first hypothesis, whereas the virtual absence of sedimentary rocks and the geochemical change within the Chukotat Group suggesting a continental rift to oceanic transition (Francis and Hynes, 1979; Francis et al., 1981, 1983; Hynes and Francis, 1982; Picard et al., 1990) do not support the second hypothesis.

DOMAIN 3: 'SUSPECT' TECTONO-STRATIGRAPHIC UNITS OF THE CAPE SMITH BELT

Domain 3 is an assemblage of distinct lithotectonic units which occurs in the northern portion of the Cape Smith Belt (Fig. 5). No tectonostratigraphic or magmatic link is known between domain 3 units and those of either domain 1 or 2, despite the fact that units of domains 1 and 2 are exposed well into the internal zone of the Ungava orogen (Fig. 1; Lucas and St-Onge, 1991). The units of domain 3 are therefore considered tectonically 'suspect' (in the sense of Coney et al., 1980) with respect to the Superior Province and the sedimentary and volcanic rocks of domain 2. Within domain 3, two principal fault-bounded assemblages have been recognized in the eastern Cape Smith Belt (Fig. 5): (1) ultramafic and mafic cumulates and mafic intrusive and extrusive units of the Watts Group, and (2) clastic sedimentary rocks of the Spartan Group.

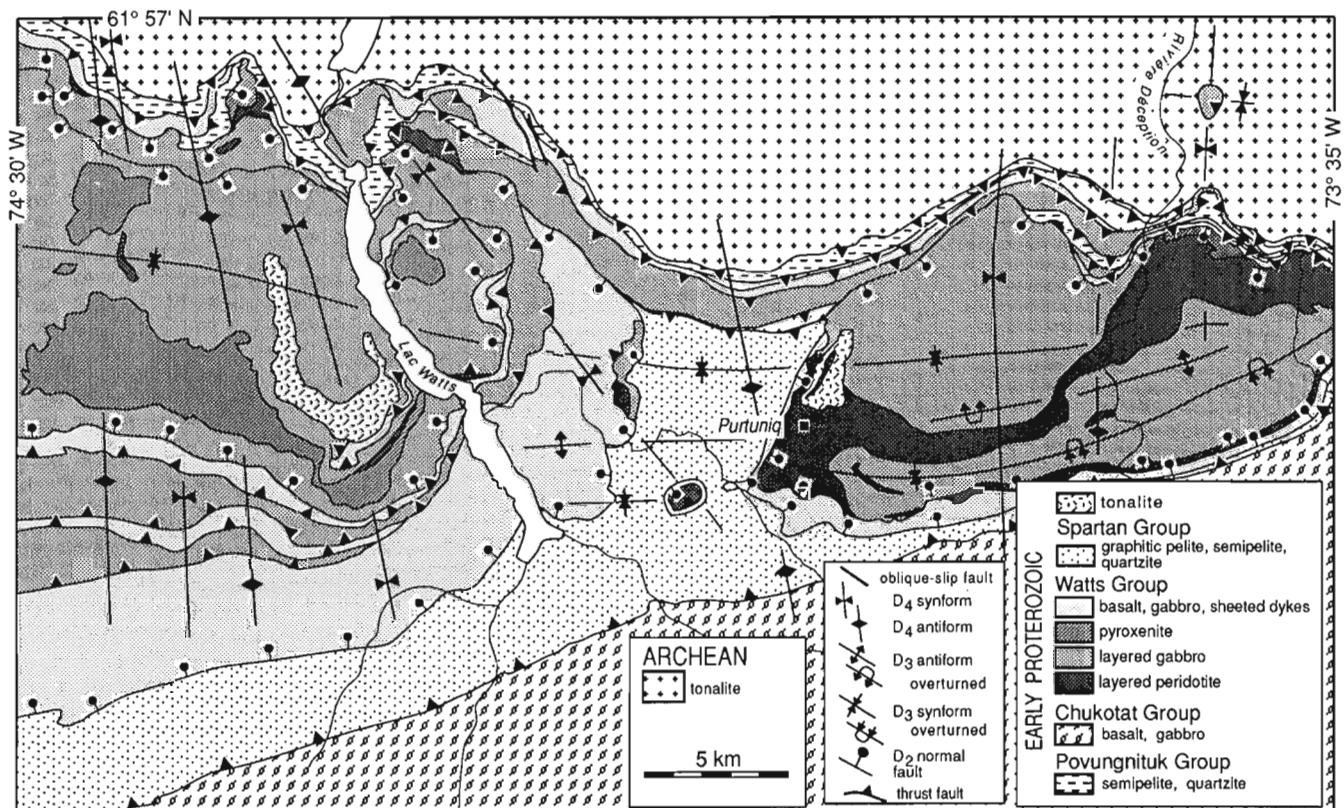


Figure 40. Simplified geological map for the eastern part of the Watts Group in the lac Watts (1721A) and Purtunig (1722A) area (modified from Scott et al., 1992).

Watts Group (PWp - PWb)

The Watts Group comprises a distinctive assemblage of layered mafic and ultramafic rocks, massive and pillowed basalt flows, mafic sills and sheeted dykes, and rare plagiogranite intrusions (St-Onge et al., 1988b; Scott et al., 1989, 1991; Scott, 1990; St-Onge and Lucas, 1990m). The Watts Group is fault-bounded and occurs within the structurally highest imbricates of the eastern Cape Smith Thrust Belt (Lucas, 1989a) in the vicinity of lac Watts (1721A) and Purtuniqu (1722A). The layered mafic and ultramafic rocks generally overlie strongly foliated extrusive and intrusive mafic rocks (St-Onge and Lucas, 1990m) such that the original stratigraphic sequence has been broadly tectonically inverted (Fig. 40, 41).

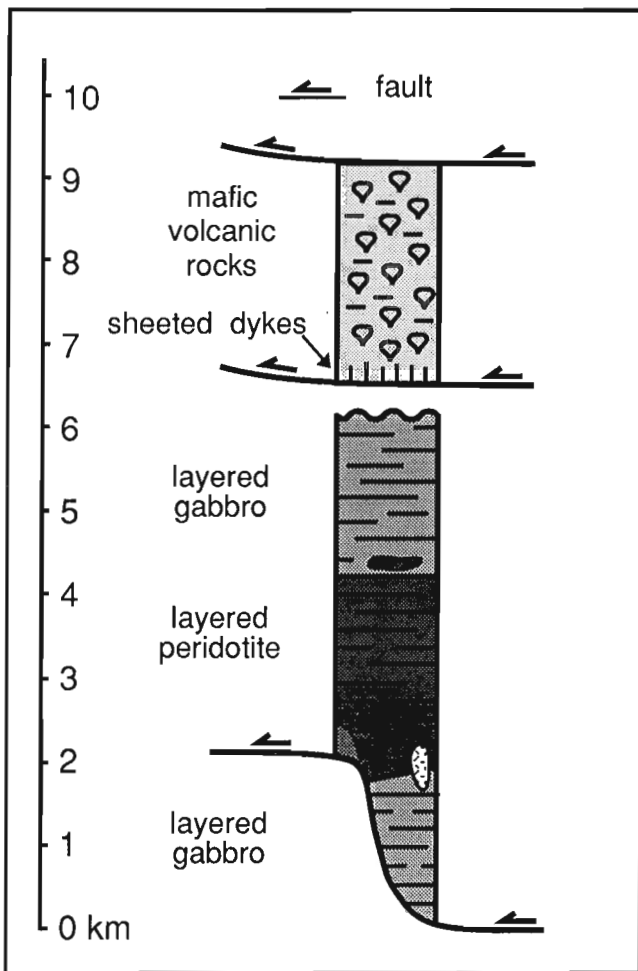


Figure 41. Reconstructed composite section through the rocks of the Watts Group in the lac Watts-Purtuniqu area (from Scott et al., 1992).

Layered peridotite (PWp)

Layered ultramafic rocks (dunite, wehrlite) of the Watts Group contain centimetre- to metre-scale compositional layers (Fig. 42) which correlate with modal variations in metamorphic mineral assemblages after olivine or pyroxene. The ultramafic plutonic rocks have been interpreted as principally cumulate in origin (Scott et al. 1989, 1991) based on well-developed adcumulate textures in thin-section and field observations of olivine-clinopyroxene modally-graded layers.

Two types of layered peridotite bodies are documented. Large bodies such as the one northeast of lac Watts (1721A; Fig. 40) are completely fault-bound and in tectonic contact with layered gabbroic units and clastic metasedimentary

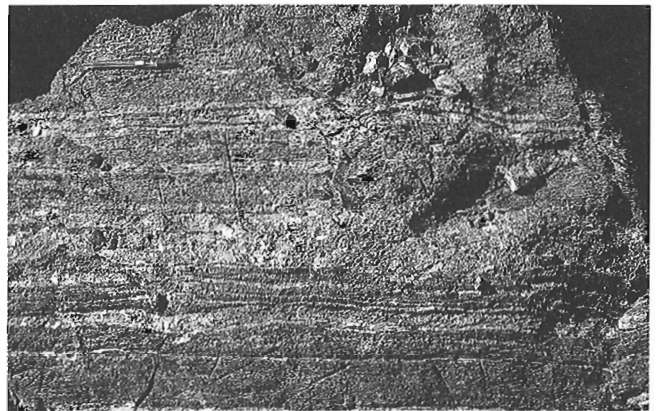


Figure 42. Layered peridotite from the Watts Group 3 km northeast of lac Watts (Fig. 5). Darker bands are clinopyroxene-rich and the lighter bands are dunitic. The layering in the ultramafic rock is interpreted as principally cumulate in origin (see text). Pen is 15 cm long. (GSC 1992-102T)

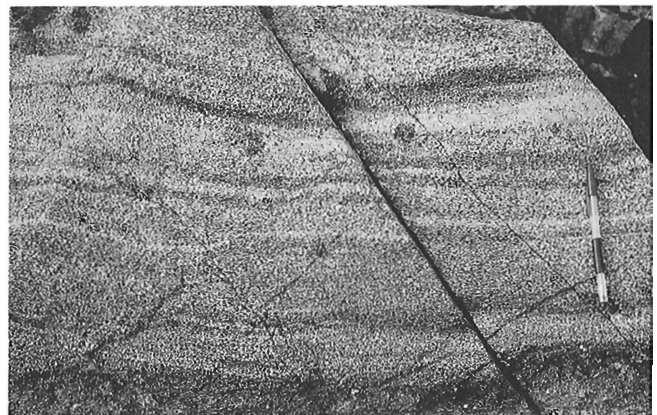


Figure 43. Medium grained layered gabbro from the Watts Group 11 km northeast of Purtuniqu (Fig. 40). Dark layers are metapyroxenitic in composition and light layers are anorthositic. The layering in the mafic rock is interpreted as principally cumulate in origin (see text). Pen is 15 cm long. (GSC 204234-Q)

rocks. In contrast, smaller layers and lenses of layered peridotite east of lac Watts and a large ultramafic body east of Purtuniqu (1722A; Fig. 40) apparently form an integral part of a continuous mafic/ultramafic sequence with layered gabbroic rocks. In the second type of ultramafic body, the contact between peridotite and gabbro is gradational and marked by an increasing proportion and thickness of plagioclase-bearing layers in the ultramafic rocks. The gradual contact is interpreted as a primary, igneous transition in a cumulate sequence (Scott et al., 1992).

Concordant layers of chromite are documented at several locations in the ultramafic rocks northeast of lac Watts and south of Purtuniqu, although these occurrences appear to be laterally discontinuous (Picard et al., 1990; Scott, 1990; Scott and Bickle, 1991).



Figure 44. Metre-scale layering in a gabbro of the Watts Group from the east shore of lac Watts (Fig. 40). The anorthositic layers (white) have a nonuniform appearance because of ductile deformation related to D₂ deformation. The hammer is 34 cm long. (GSC 204233-T)

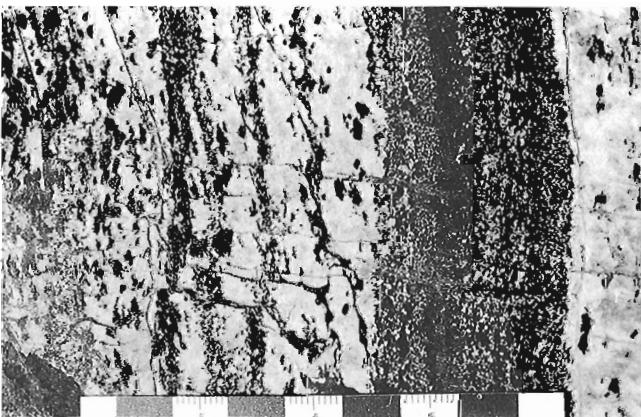


Figure 45. Centimetre-scale layering in a gabbro of the Watts Group northeast of Purtuniqu (Fig. 40). Dark layers are defined by grains of hornblende (after pyroxene) and light layers comprise plagioclase and zoisite (after primary plagioclase). Scale is in centimetres. (GSC 1992-102E)

Layered gabbro (PWg)

Coarse grained, compositionally layered gabbroic rocks form the volumetrically most important unit of the Watts Group (Fig. 40). The gabbro is characterized by centimetre- to metre-scale compositional layering (Fig. 43, 44) which is defined by the modal abundance of two end-member mineral assemblages: (1) hornblende (after primary pyroxene) which forms black metapyroxenite layers (Fig. 45); and (2) plagioclase-zoisite (after primary plagioclase) which forms white meta-anorthositic layers (Fig. 46). Petrographic study of the layered gabbroic rocks indicate a cumulate origin (Scott, 1990). Their geochemical composition is tholeiitic, suggesting that this unit represents mafic cumulates of oceanic layer 3 (Scott, 1990). U-Pb analyses of zircons from two layers of gabbroic composition in the mafic cumulates (on the east side and at the north end of lac Watts; Fig. 7) have yielded ages of 1998 ± 2 Ma and 1997.5 ± 2.5 Ma respectively (Fig. 8; Parrish, 1989).



Figure 46. Deformed anorthositic layer in a gabbro of the Watts Group 1 km east of lac Watts. Such layers are principally composed of zoisite and plagioclase derived from a more calcic primary plagioclase. Pen cap is 4.5 cm long. (GSC 1992-102L)

Pyroxenite (PWpy)

Large, kilometre-scale pyroxenite bodies occur on the west side of lac Watts (1721A). The pyroxenite is massive, shows no internal layering, and is essentially composed of coarse (millimetre to centimetre-size) primary clinopyroxene. Hornblende after primary clinopyroxene is observed in the smaller bodies along the northern margin of the belt. Field crosscutting relationships and the regional map pattern (Fig. 5) suggest that the pyroxenite is intrusive into the surrounding layered gabbroic unit. Locally near their margins, the pyroxenite bodies contain xenoliths of layered gabbro which is similar to the regional mafic cumulate unit (Fig. 47; St-Onge et al., 1988b; Scott, 1990).

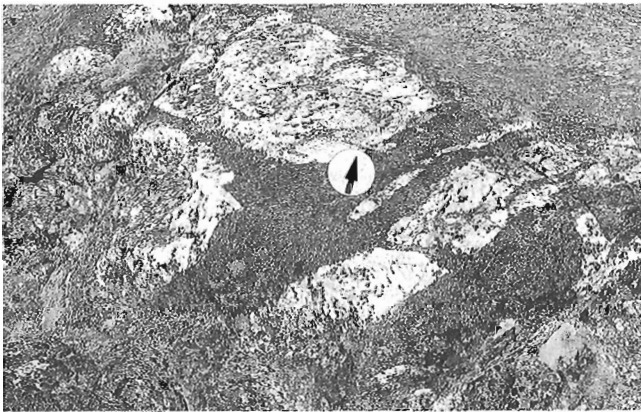


Figure 47. Large xenoliths of layered anorthositic gabbro (white) in pyroxenite (dark). The pyroxenite is part of the large intrusive body on the west side of lac Watts (Fig. 40). Arrow points at a 15 cm long pen. (GSC 1992-102DD)

Basalt, gabbro sills, sheeted dykes, and plagiogranite (PWb)

A complex of sheeted dykes with screens of fine- and coarser-grained amphibolite (St-Onge et al., 1988b) is preserved within the Watts Group, 5 km east of lac Watts (1721A) and 6.5 km west of Purtuniqu (1722A; Fig. 40). The dyke complex, which outcrops on a prominent hill (245 m high), is exposed over an area approximately 400 m wide and 700 m long. Within the complex, individual north-northeast striking dykes are 20-60 cm wide (Fig. 48) and dip steeply toward the east-southeast, roughly perpendicular to the orientation of the overlying flows (Scott et al., 1992). Most dykes have 2-3 mm wide chilled margins on one side. Adjacent dykes are distinguished petrographically by grain-size variations and the presence or absence of coarser amphibole or plagioclase crystals, presumably pseudomorphs after primary phenocrysts (Scott and Bickle, 1991).

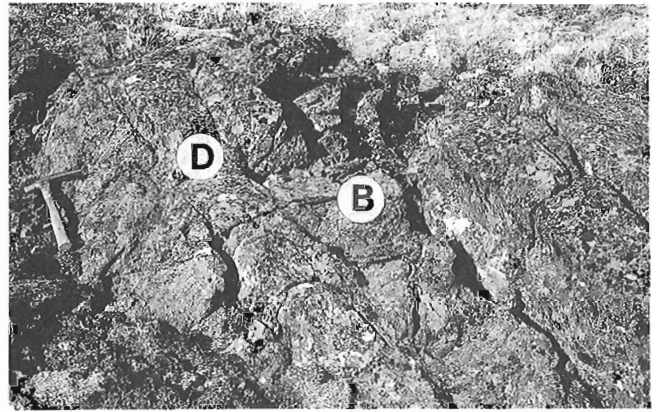


Figure 49. Zone of basalt (B) intruded by discrete gabbroic dykes (D), 3 km east of lac Watts (Fig. 40). This zone is transitional between areas of 100 % sheeted dykes (Fig. 48) and an extensive unit of deformed pillowed basalts (see Fig. 50) in the Watts Group. Outside the field of view, the basalt (B) is pillowed. Hammer is 34 cm long. (GSC 204234-N)



Figure 48. Sheeted dykes from the Watts Group 5 km east of lac Watts (Fig. 40). The outcrop is 100% half-dykes which dip steeply to the east (right-hand side of photograph). The hammer is 34 cm long. (GSC 204234-O)



Figure 50. Pillowed basalt of the Watts Group from the east side of lac Watts (Fig. 40). Pillow selvages are outlined by epidote. Pen is 15 cm long. (GSC 1992-102U)

Geochemical and isotopic analyses show that two compositionally distinct populations of dykes are present in the sheeted dyke complex. The older population is tholeiitic (n-MORB) in composition, with $E_{Nd}(2.0 \text{ Ga})$ values which range from +4.0 to +4.7 (Hegner and Bevier, 1991; Scott, 1990; Scott and Hegner, 1990). These dykes, which comprise the bulk of the sheeted dyke complex, are petrographically, compositionally and isotopically similar to rocks formed at modern oceanic spreading ridges (Scott et al., 1991). The second population of dykes, which crosscut the n-MORB dykes (Scott et al., 1989; Scott, 1990; Scott and Hegner, 1990), are tholeiite to basaltic komatiite in composition and have trace element patterns (REE, Zr, Ti, Nb) similar to tholeiitic rocks from hot-spot related oceanic islands such as Hawaii (Scott, 1990). The $E_{Nd}(2.0 \text{ Ga})$

values of +3.0 to +3.4 indicate that these rocks had a mantle source which was isotopically distinct from the older population of n-MORB dykes. Both populations of dykes are crosscut by narrow, chlorite-rich dykes at intervals of several metres (Scott and Bickle, 1991).

A partly tectonized, upward stratigraphic transition from sheeted dykes to an extensive unit of deformed pillowed basalts, inferred to be essentially primary in origin, has been documented in the Watts Group, east of lac Watts (1721A; Fig. 40). The transition (Fig. 49) comprises a zone of alternating dykes, massive fine- to coarse-grained amphibolites, and pillowed basalt passing upward into a more-continuous outcrop of deformed pillowed basalts, over an across-strike distance of approximately 300 m (Scott and Bickle, 1991; Scott et al., 1992). The deformed pillows are outlined by ~5 cm thick epidote-rich selvages. The pillows are up to 1-2 m long and variably elongate in the principal foliation plane (Fig. 50). The basalt flows are tholeiitic with n-MORB-like major and trace element compositions (Scott et al., 1989, 1991). Neodymium isotopic compositions range from +3.3 to +3.9. Rare lava withdrawal shelves and locally well-preserved pillow shapes allow the orientation and facing direction of the sequence to be determined as northwestward. The minimum stratigraphic thickness of the sequence has been determined by down-plunge cross-section reconstruction to be 2.5 km (Fig. 41; Lucas, 1989a; Scott, 1990; Scott et al., 1992).

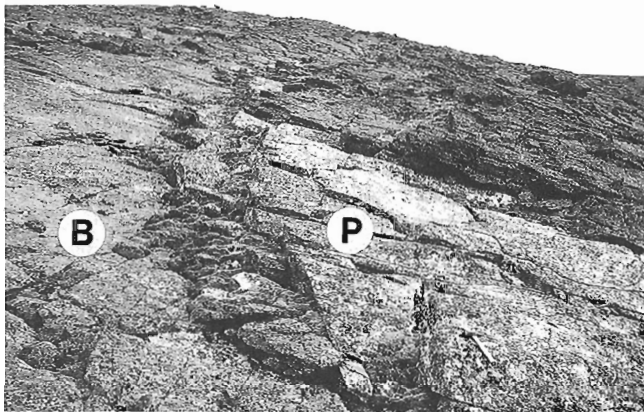


Figure 51. Plagiogranite sill (P) intruding the pillowed basalts (B) of the Watts Group 2 km east of lac Watts (Fig. 40). Hammer is 34 cm long. (GSC 1992-102Q)

The pillowed basalt and layered gabbro of the Watts Group are intruded in several localities east and west of lac Watts (1721A) by small plagiogranite bodies. The plagiogranites are typically 1-5 m thick sills (Fig. 51), 50-100 m long, fed by felsic dykes which cut part of the

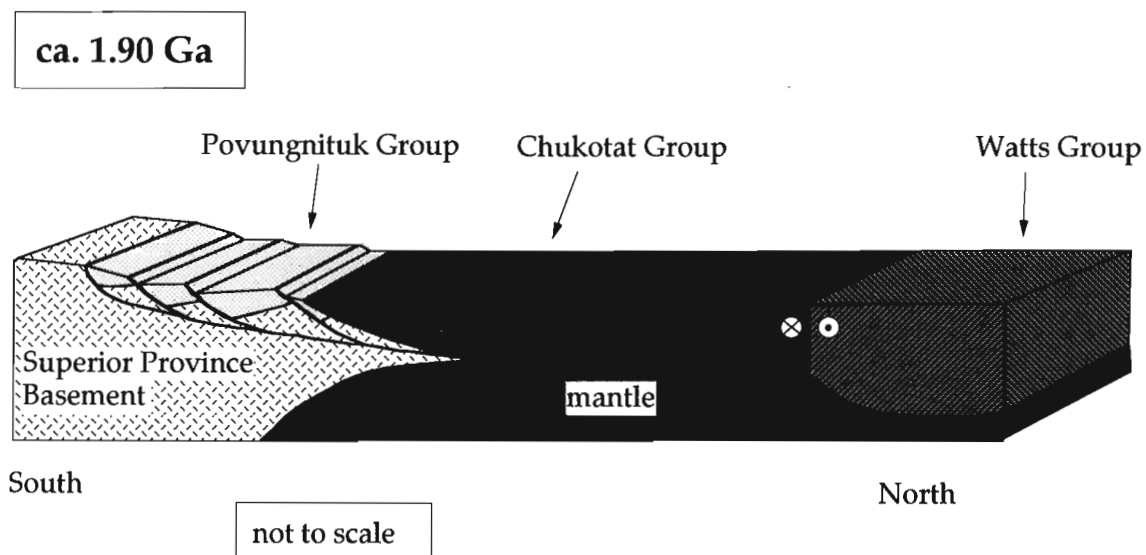


Figure 52. Schematic block diagram illustrating the proposed plate tectonic setting for the tectonostratigraphic units of the Cape Smith Belt at 1.9 Ga. Constraints for the model are given in the text. The boundary between the Chukotat and Watts groups at this stage is inferred to be a dextral transform plate boundary. Circled dot indicates movement to the east; circled 'X' indicates movement to the west.

pillowed basalts. In turn, the plagiogranites are cut by the narrow, late chlorite-rich dykes also found in the sheeted-dyke complex (Scott and Bickle, 1991).

Tectonostratigraphic interpretation and parentage of the Watts Group

The occurrence of sheeted dykes and pillowed basalts in stratigraphic sequence and their association with layered mafic and ultramafic rocks and rare plagiogranite intrusions led St-Onge et al. (1988b) to suggest that the rocks of the Watts Group may represent the crustal remnants of a tectonically dismembered ophiolite suite (e.g. Moores, 1982). The ophiolite appears to comprise rocks which formed at an oceanic spreading ridge (MORB-suite) and were subsequently intruded by rocks of the ocean island-like suite (Scott, 1990; Scott et al., 1992). Subsequent petrographic, chemical, and isotopic analyses of these rocks support this interpretation (Hegner and Bevier, 1989; Scott, 1990; Scott et al., 1991).

Based on the 1998 Ma age obtained for the MORB-like rocks of the ophiolite and the 1918 Ma age for the transitional oceanic domain of domain 2, two principal tectonic models (St-Onge et al., 1989) have been proposed for the Watts

Group. In a ‘two-basin’ model, the Watts Group is presumed to have formed in an older northern basin which would have predated the opening of a separate southern basin into which accumulated the bulk of the Povungnituk and Chukotat groups (Picard et al., 1989, 1990). Alternatively, in a ‘one-basin’ model, continental rifting (leading to mid-ocean ridge spreading) would have propagated over an along-strike distance consistent with the geochronological diachroneity (Hegner and Bevier, 1989; Scott et al., 1989, 1991). In the latter model, eventual juxtaposition of older oceanic and younger transitional oceanic crust is presumed to have occurred along a transform plate boundary (Fig. 52; St-Onge et al., 1992).

Both models are consistent with the available geochronological constraints. One difficulty with the ‘two-basin’ model is that no evidence has been found of the crust that would have separated the older oceanic basin (Watts Group) from the younger basin (Povungnituk and Chukotat groups; St-Onge et al., 1989; Picard et al., 1990). A difficulty with the ‘one-basin’ model is the apparent absence of structural evidence for lateral translation of the older ophiolitic units (Watts Group) relative to the younger Superior Province margin units (Picard et al., 1990). However, in either tectonic scenario, the Watts Group appears to be geochronologically and tectonostratigraphically distinct with respect to units in domain 2 (Fig. 4). Thus the Watts Group is considered ‘suspect’ with respect to the northern rifted margin of the Superior Province and the units of domain 2 (St-Onge et al., 1992).

Spartan Group (PSpe)

Sandwiched between the mafic and ultramafic units of the Watts Group and the pillowed basalts of the Chukotat Group are the fault-bounded sedimentary rocks of the Spartan Group (Fig. 5; Lamothe et al., 1984). The Spartan Group clastic sedimentary sequence comprises mostly laminated dark pelites and semipelite (Fig. 53). Fine grained quartzites (Fig. 54) occur towards the structural top of the Spartan

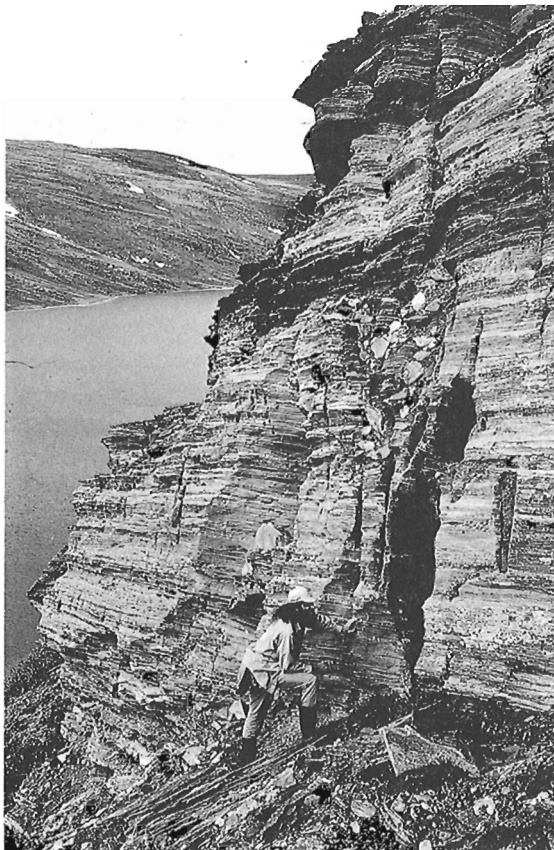


Figure 53. Interbedded graphitic pelite and semipelite of the Spartan Group at the south end of lac Watts (Fig. 5). The sequence is interpreted as a relatively deep water deposit (see text). Height of person is 2.0 m. (GSC 204234-S)



Figure 54. Fine grained quartzite from the Spartan Group west of lac Watts (Fig. 5). The quartzite is interpreted as a distal fan turbidite deposit (see text). Arrow points to hammer which is 34 cm long. (GSC 1992-102GG)

Group thrust sheet at the south end of lac Watts (1721A; Fig. 5). Graded bedding is preserved in some of the quartzite beds but in general, the strong bedding-parallel schistosity obscures primary features. South of lac Watts, the clastic rocks of the Spartan Group are intruded by a set of finegrained mafic sills of undetermined age.

Tectonostratigraphic interpretation and parentage of the Spartan Group

The sedimentary rocks of the Spartan Group are interpreted as having been deposited in a relatively deep water (pelagic?) environment, with the monotony of the sequence interrupted near the top by distal fan turbidite beds (St-Onge et al., 1988b). In the eastern Cape Smith Belt, the Spartan Group is in fault contact with both the underlying Chukotat Group and the overlying Watts Group (Fig. 5). This structural position is analogous to that of the dominantly volcanic Parent Group (Picard et al., 1990) in the western portion of the belt (Fig. 1). The lithological and geochemical characteristics of the Parent Group have led Picard et al. (1990) to suggest that it comprises units accumulated in a subduction-related, calc-alkaline magmatic arc. To date, no direct or indirect tectonostratigraphic links have been established between the Spartan and Parent groups. However, if the two groups are lateral equivalents as suggested by St-Onge et al. (1992), then the Spartan Group may represent a clastic apron marginal to the Parent Group magmatic arc (fore-arc basin deposits; Fig. 55). Alternatively, the Spartan Group may represent distal deposits associated with the northern rift-margin of the Superior Province. In either case, the apparent absence of direct tectonostratigraphic links between the Spartan Group

in the north and the Chukotat-Povungnituk groups to the south makes the former tectonostratigraphically 'suspect' with respect to the rifted northern margin of the Superior Province (Fig. 4 and 55; St-Onge et al., 1992).

Tonalite intrusions (Pt)

In the eastern Cape Smith Belt, rocks of the Watts Group are intruded by fourteen kilometre-scale plutons of biotite ± hornblende tonalite (Fig. 56). The plutons, occur in the lac Watts (1721A) and Purtuniqu (1722A) area and only the two larger bodies are shown on the compilation map of Figure 5. The plutons are part of a suite that is emplaced in the Watts and Parent groups and which varies in composition from hornblende-biotite quartz diorite, biotite ± hornblende tonalite to biotite monzogranite (Taylor, 1982; Feininger, 1986; Lamothe, 1986; Picard et al., 1990; St-Onge and Lucas, 1990m). Locally, the plutons are muscovite ± garnet bearing (St-Onge et al., 1987) when emplaced in clastic sedimentary rocks. U-Pb (zircon) dating of several of the intrusive bodies (Parrish, 1989; Machado et al., 1991; N. Machado, pers. comm., 1992) has documented two distinct geochronological suites (Fig. 8): (1) an older suite of foliated plutons ranging in age from 1898 Ma to 1860 Ma; and (2) a younger suite of weakly foliated to massive plutons ranging in age from 1848 Ma to 1839 Ma (St-Onge et al., 1992). In the map area, one tonalite west of lac Watts, was dated (U-Pb on zircon) at 1888±5 Ma and another tonalite north of Purtuniqu at 1876±1.5 Ma (Fig. 7; Parrish, 1989).

Lucas et al. (1992) and St-Onge et al. (1992) have suggested that the quartz diorite to granite plutons emplaced in the Watts and Parent groups are correlative with the plutonic rocks of the Early Proterozoic Narsajuaq arc which

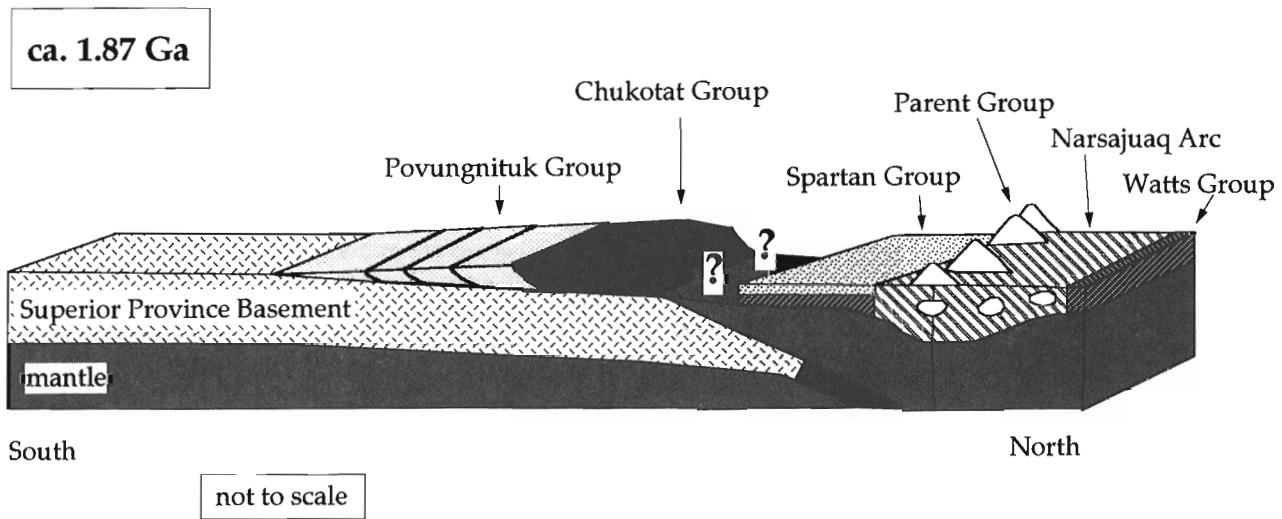


Figure 55. Schematic block diagram illustrating the proposed plate tectonic setting for the tectonostratigraphic units of the Ungava orogen at 1.87 Ga. Constraints for the plate tectonic model are given in the text and in St-Onge et al. (1992). The imbricated Povungnituk and Chukotat groups represent the early stage of formation of the Cape Smith Thrust Belt. The question marks refer to the unknown relationship between the units of domain 3 and the continental-margin thrust belt at 1.87 Ga.

are preserved in a series of crystalline thrust imbricates north of the Cape Smith Belt (Fig. 1). A description of the Narsajuaq arc is beyond the scope of this report and the interested reader is referred to Lucas et al. (1992) and St-Onge et al. (1992) for more information.

LATE DIABASE DYKES

Two late Proterozoic diabase dykes were mapped south of lac Vicenza (1733A; Fig. 5) and south of the rivière Povungnituk (1730A). The dykes trend west-northwest and are vertical. One is 1 km, the other is 5 km in length and both are on average 50 m thick. The dykes which crosscut both the Archean units of the Superior Province and the allochthons of the Cape Smith Belt are interpreted to be part of the Franklin diabase swarm of Fabrig et al. (1971).

STRUCTURAL HISTORY OF THE CAPE SMITH BELT: OVERVIEW

From a structural perspective, the Cape Smith Belt is best described as an Early Proterozoic thrust belt which is preserved in a doubly-plunging synclinorium (Hoffman, 1985; Lucas, 1989a; St-Onge and Lucas, 1990m) that extends



Figure 56. Medium grained biotite tonalite from the west side of lac Watts (Fig. 5). (GSC 1992-102FF)

across the entire Ungava Peninsula (Taylor, 1982). The deformation history of the rocks in the map area has been subdivided into distinct structural-metamorphic episodes for each of the three principal tectonostratigraphic domains defined above: ((1) Archean basement, (2) Povungnituk and Chukotat groups, and (3) Watts and Spartan groups (St-Onge et al., 1986; Lucas, 1989a; Lucas and St-Onge, 1992). The structural and metamorphic histories for each domain are correlated in both a relative and absolute time framework in Table 2 (modified from Lucas and St-Onge, 1992). The principal correlation tool is the relationship between deformation and metamorphism, as observed at map- to thin section-scale and especially the relationship between deformation and the thermal peak of metamorphism (Lucas, 1989a, 1990; St-Onge and Lucas, 1990m; see 'Metamorphic History of the Cape Smith Belt'). The use of the metamorphic thermal peak as a relative chronometer for deformation in the thrust belt is based on the assumption that thermal peak conditions were reached coevally at comparable structural levels throughout the thrust belt (Lucas, 1989a; St-Onge and Lucas, 1991).

The deformation leading up to and including the collision between the Superior Province continental margin and the Narsajuaq arc of domain 3 (St-Onge et al., 1992; Lucas and St-Onge, 1992) is characterized by a complex interplay between thrusting, penetrative bulk shear, and metamorphism (Table 2; Lucas 1989a, 1990; St-Onge and Lucas 1990m). These "thin-skinned" deformation episodes were succeeded by regional-scale folding of the Cape Smith Belt, the Narsajuaq arc, and the underlying Superior Province basement about east-trending axes (Table 2). The east-west folds are coaxial with the thrust belt structures and generally have a south-verging asymmetry. These observations, coupled with metamorphic data (see below), have led to the suggestion that the "thick-skinned" folding represents the terminal stage of collisional deformation (Lucas and St-Onge, 1989a; St-Onge and Lucas, 1990m), possibly related to continent-continent collision between the Superior and Rae cratons (Hoffman, 1988).

The final deformation episode was responsible for cross-folding of the thrust belt and its footwall basement about north- to northwest-trending axes. All of the Early Proterozoic deformation episodes (Table 2) resulted in crustal shortening and are probably related in a general sense to the continent-scale Trans-Hudson orogen (Lewry and Stauffer, 1990). As a consequence of exhumation following the cross-folding of the belt, the eastern portion of the Cape Smith Belt exposes over 18 km of structural relief and provides a natural depth section of the thrust belt and its footwall (Lucas, 1989a). Structural sections of the belt have been constructed using the structural relief and rendering the natural depth section into a true section of the thrust belt. The assumptions and methodology associated with construction of the structure sections are outlined in the following section, setting the stage for the subsequent descriptions of the history of thin-skinned deformation in each tectonostratigraphic domain.

A consistent terminology for faults and shear zones is used in describing the structural history of the Cape Smith Belt. Fault refers to the discrete surface marking the boundary between hangingwall and footwall, while shear zone refers to the zone of penetrative non-coaxial deformation extending above and below the fault. As an example, the basal décollement for the Cape Smith Belt is consistently recognized as a major lithological contact separating Early Proterozoic hanging wall rocks from an Archean footwall and can be viewed conceptually as a fault (Lucas, 1989a). However, both hanging wall and footwall rocks adjacent to the basal décollement contain penetrative

ductile deformation fabrics which have collectively been described as relating to a basal shear zone (Lucas, 1989a, 1990).

STRUCTURAL SECTIONS OF THE CAPE SMITH BELT

Structural sections of the Cape Smith Belt have been constructed using the axial or "down-plunge" projection technique (e.g., Argand, 1911; Mackin, 1950; Stockwell, 1950; King, 1986), utilizing geological information obtained over the range of exposed depth levels (Lucas, 1989a). The

Table 2. Correlation of structural-metamorphic histories between principal tectonostratigraphic domains

Age (Ga)	Superior Province (domain 1)	Cape Smith Belt	
		Povungnituk and Chukotat groups (domain 2)	Watts and Spartan groups (domain 3)
ca. 2.7-2.8	D1 Truncurrent (?) deformation, granulite-facies metamorphism and plutonism		
<2.00, >1.88			D1 Faulting, foliation development
<1.92 (<1.87?)	D2 Penetrative shear adjacent to basal décollement, retrograde metamorphism	D1 Piggyback-sequence thrusting, folding, foliation development, pre-thermal peak metamorphism	
1.83 - 1.80 (Arc - continent collision)	D3 Basement imbrication, penetrative shear, retrograde metamorphism	D2 Out-of-sequence thrusting, thermal peak metamorphism (syn-D2 in HW, static in FW)	D2 Accretion (obduction), out-of-sequence thrusting during thermal peak metamorphism, normal (?) faulting during retrograde metamorphism
ca. 1.76 (?)	D4 Folding about E-W axes	D3 Folding about E-W axes	D3 Folding about E-W axes
<1.76, >1.74 (?)	D5 Folding about N-S axes	D4 Folding about N-S axes	D4 Folding about N-S axes

basic assumption inherent in the construction these sections is that any geological structure being projected has a predictable ("cylindrical") geometry at the scale of the projection area (here termed "regional-scale"). In other words, all structural plunge must be explained by one or more regionally significant and predictable models which cumulatively account for the plunge. There are two principal models for the origin of the undulating east-west plunge in the Cape Smith Belt: (1) original variations in the amplitude of D₃ folds, and consequently, D₄ folds (Table 2); and (2) D₄ cross-folding about axes oriented approximately perpendicular to the thrust belt and D₃ structures. The plunge models do not include lateral thrust ramps and related folds because these structures do not have significance at the regional scale. As such, any east-west plunge introduced by these lateral structures cannot be used in constructing axial projection-based sections. Conversely, any plunge due to

non-predictable (non-cylindrical) geometries that is not removed prior to projection will generate an error in the sectional representation of the projected structure.

Strike-parallel sections (approximately east-west) were constructed (Lucas, 1989a) to establish the variation in structural level exposed along the strike length of the belt (Fig. 57). In order to prepare the strike-parallel sections, the exact geometry of the plunging pre-D₄ belt was established. Thrust-related and D₃ fold axes provide the best monitor of east-west structural plunge because these axes originated with an east trend and an assumed subhorizontal plunge. St-Onge et al. (1986) demonstrated that D₃ outcrop- to map-scale folds were statistically coaxial with east-trending thrust-related map-scale folds. As a result, both thrust-related and D₃ outcrop- to map-scale fold axes were utilized to outline domains of approximately constant plunge across the map area (Fig. 57). Statistically large populations (25-100 measurements) were employed in calculating the

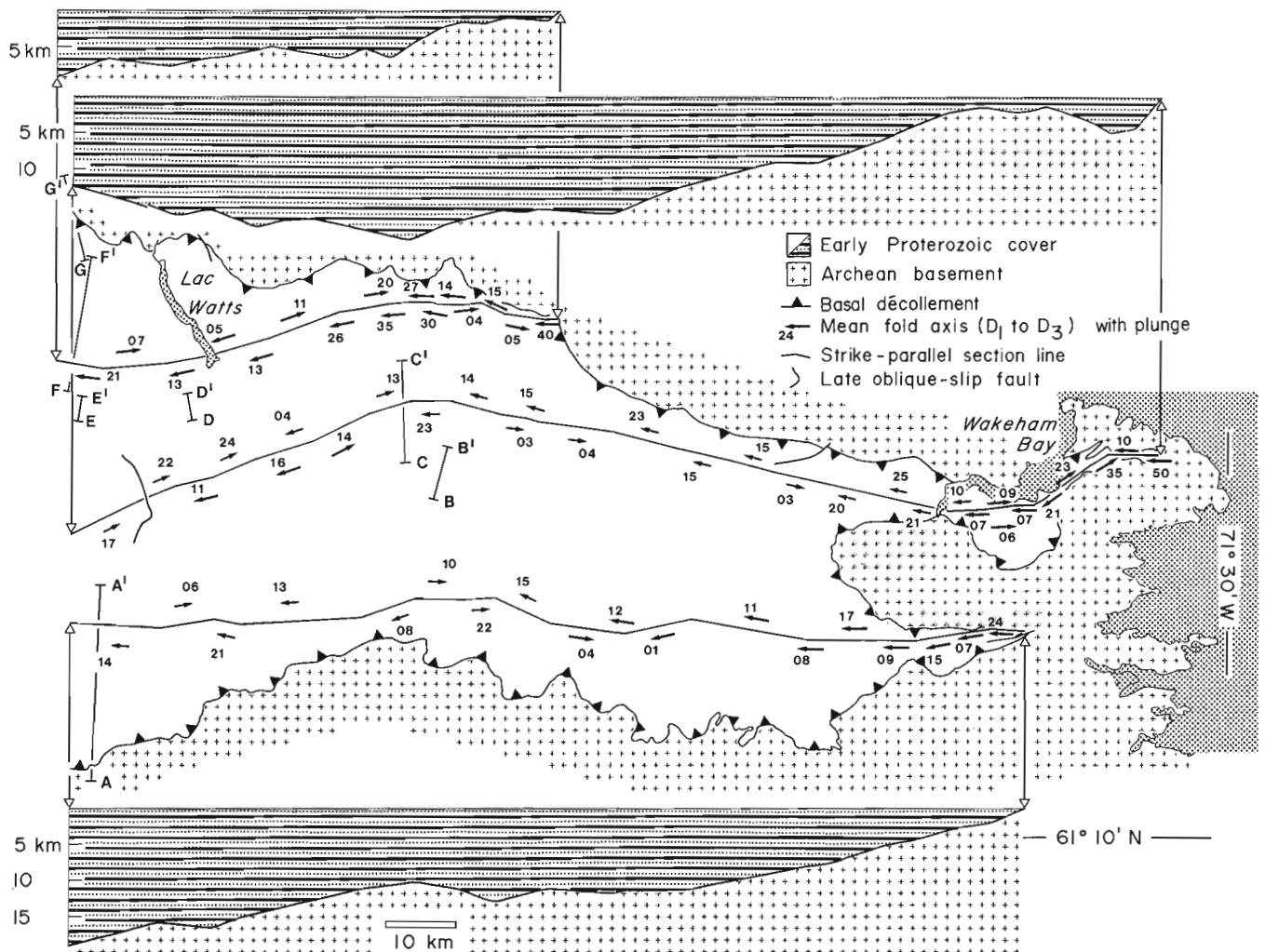


Figure 57. Strike-parallel sections of the eastern portion of the Cape Smith Belt. The mean D₁ to D₃ fold axis plunges used to construct the sections are shown. Section lines A-A' to G-G' represent the lines along which the downplunge constrained strike perpendicular cross-section (Fig. 58) is hung (see text for a discussion of the construction techniques).

mean axes to eliminate any "noise" in the outcrop-scale D₃ fold axis data due to local non-cylindrical effects. The strike-parallel sections were constructed by projecting the position of the exposed basement-cover contact onto vertical planes using the mean fold axes for the plunge domains encountered along the section lines (Fig. 57). The strike of each domainal segment of the section plane ("section line" in map view) is parallel to the trend of the mean fold axis for that domain. The mean fold axes, section lines, and the strike-parallel sections are all illustrated in Figure 57.

The validity of the strike-parallel sections in terms of adequately representing the geometry of the basement-cover contact at depth can be demonstrated at the scale of the map area (Fig. 5). Two principal observations attest to the legitimacy of these sections (Lucas, 1989a): (1) the close correlation between structural level predicted by the strike-parallel sections and the geology of the erosion surface; and (2) the relatively close agreement between present-day crustal thicknesses estimated from the sections and those determined from crustal models based on detailed gravity profiles (Feininger et al., 1985). The regional-scale predictability of the thrust faults is qualitatively suggested by their extensive along-strike continuity (e.g., thrusts I, K, L, M, O, and V, Fig. 5). The continuity shows that the faults do not have laterally unpredictable geometries such as: (1) significant changes in slip magnitude, or (2) major lateral ramps, transferring displacement to another horizon or fault system.

The strike-perpendicular cross-section (Fig. 58) was built from over 50 independently established down-plunge projections prepared in domains of statistically constant east or west plunge. Individual down-plunge projections were constructed by projecting the erosion surface geology onto the profile plane corresponding to the mean fold axis for that domain. The actual assembly of the composite down-plunge section (Fig. 58) involves stacking the individual projections up from the basement-cover contact in accordance with their relative structural level as predicted by the strike-parallel sections (Fig. 57). This ensures that the amount of structural relief employed in building the final composite section corresponds to that determined by the strike-parallel sections using the mean fold axis data. The individual projections are stacked up from the basement-cover contact because it is the only iso-structural relief datum in the study area.

The distortional effects of stacking non-coplanar projections (derived from nonparallel plunge axes) were eliminated by proportionally adjusting adjacent projections on the basis of the relative obliquity of their axes from the average plunge axis orientation. This specifically avoids gaps or overlaps which are created when non-coplanar projections are assembled. As a result, the section is termed "down-plunge constrained" because it was not built solely from unmodified projections. Cross-section lines representing the structurally highest projections used are shown in map view (Fig. 57). These lines give an erosion

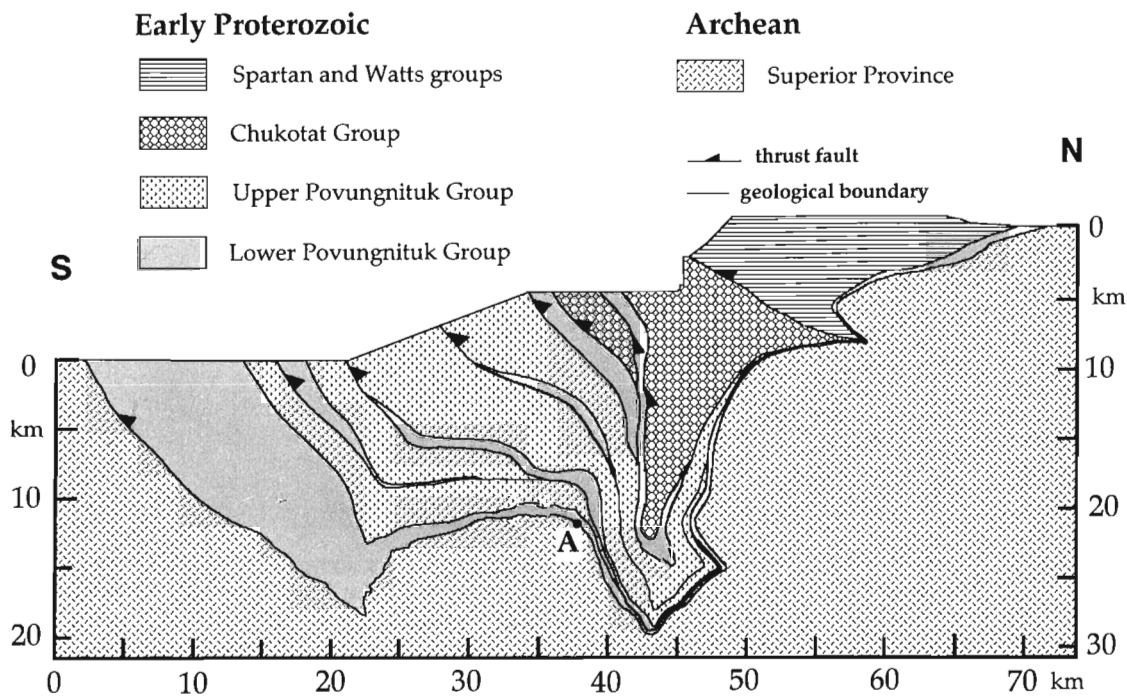


Figure 58. Downplunge constrained strike-perpendicular cross-section of the eastern portion of the Cape Smith Belt. The cross-section is of the thrust belt following D₃ folding but prior to D₄ folding. The segmented nature of the top of the cross-section is an artifact of the construction method used (see text for a discussion of the construction techniques). Point "A" refers to the site of D₃ pressure determinations described in the text.

surface trace from which to "hang" the cross-section. For reasons of clarity the remainder of the section lines for the individual projections are not illustrated in Figure 57.

The resulting down-plunge constrained cross-section (Fig. 58) reveals a striking south-to-north increase in the amount of structural relief (from 18 to 30 km). The structural relief gradient is illustrated at the top of the cross-section because the individual projections are stacked up from the

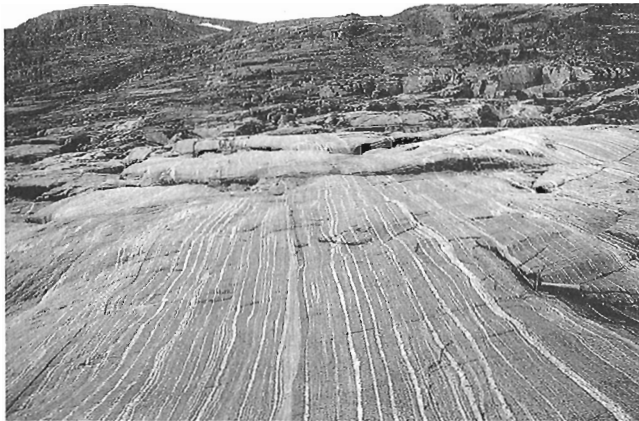


Figure 59. Archean tonalite gneiss on the east shore of Wakeham Bay (Fig. 5). Steeply-dipping tonalite bands (dark) are interlayered with monzogranite veins (light). Hammer is 34 cm long. (GSC 204233-H)

basement-cover contact, the only iso-structural relief datum in the study area. The south-to-north structural relief gradient is attributed to an increase in the amplitude of the D₃ and D₄ regional-scale folds towards the north. Initially, the D₃ regional-scale folds appear to have developed with a progressive south-to-north increase in amplitude. Subsequent D₄ cross-folding of this heterogeneous D₃ geometry consequently resulted in higher amplitude D₄ structures towards the north. The overall effect of the D₃-D₄

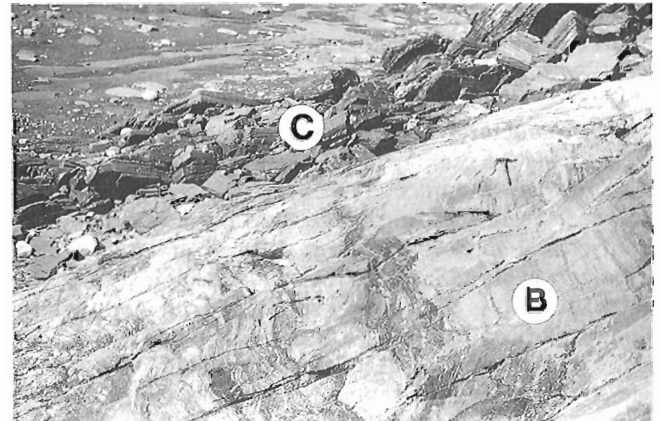


Figure 61. Detail of the basement/cover contact in the area shown on Figure 60. The gneissosity in the Archean basement (B) away from the basement/cover contact is parallel to the hammer and clearly at a high angle to the tectonic fabric in the overlying cover units (C). Hammer is 34 cm long. (GSC 204636-Y)

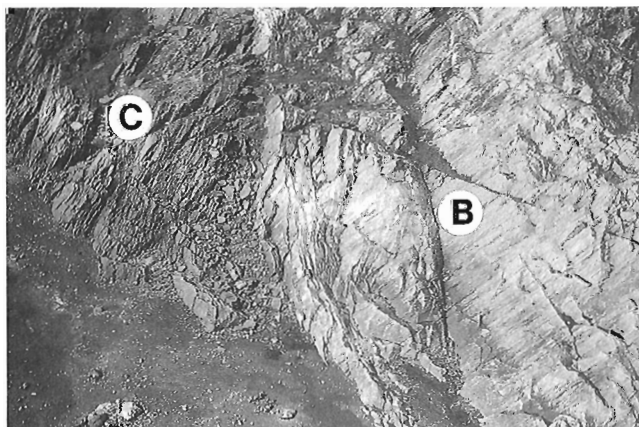


Figure 60. Tectonic contact between the Archean basement (B) and the Early Proterozoic cover (C) on the northwest shore of Wakeham Bay (Fig. 5). The basement in this locality is a biotite hornblende tonalite with mafic enclaves. It is characterized by a vertical gneissosity except in the immediate (3 m) area of the basement/cover contact (see text and Fig. 62 and 63). The cover comprises semipelite and quartzite from the lower Povungnituk Group. A strong schistosity is developed in the cover units parallel to the basement/cover contact (dipping moderately (45°) to the southwest (left-hand side of photograph)). Length of exposed shoreline is 300 m. (GSC 204636-O)

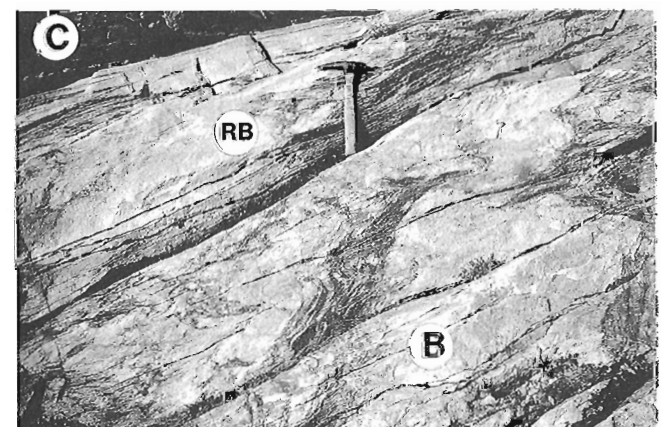


Figure 62. Reworked Archean basement (RB) in the shear zone beneath the basement/cover contact from the locality documented in Figures 60 and 61. The entire thickness of the transposition zone (RB) is shown in this photo, from the vertical Archean gneissosity in the lower right corner (B) to the moderately dipping contact with the cover units (C) in the top left corner. Hammer is 34 cm long. (GSC 204235-J)

amplitude gradient is a continuous south-to-north increase in east or west structural plunge. In summary, the total east-west plunge can be factored into two components: (1) plunge generated by the D₃-D₄ south-to-north amplitude gradient (model 1), and (2) plunge generated by D₄ cross-folding (model 2). However, there is no basis for systematically-distinguishing structural plunge derived from either model. Given that D₃-D₄ amplitude gradients are most likely non-cylindrical effects, any plunge generated as a result of these gradients will lead to the propagation of errors into the sections, necessarily reducing their validity.

It is important to recognize that essentially all of the information on the strike-perpendicular section (Fig. 58) is contained on the geological map of the Cape Smith Belt (Fig. 5). The section is generalized to the extent that structures that are not regionally predictable are not included. The section was not built on a vertical plane, but instead on the locally established profile planes of the map-scale D₃ folds. Consequently, it represents a pre-D₄ view of the thrust belt, its autochthonous basement, and the D₃ map-scale folds which deform them. Finally, an independent test of the crustal thicknesses portrayed in the cross-section is provided by pressure-temperature (P-T) determinations for D₃ assemblages. The D₃ pressure determinations for point "A" on Figure 58 cluster at 5 kbar (St-Onge and Lucas, 1990m), matching well the 16 km (~5 kbar) of D₃ structural section determined to be above point "A" based on the cross-section.

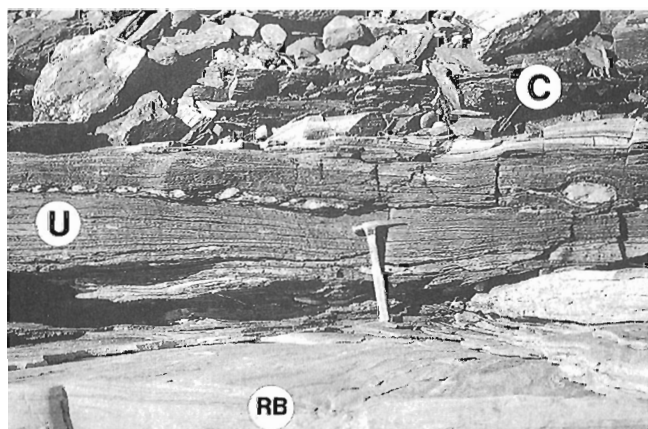


Figure 63. Detail of the ultramylonite zone derived from the Archean basement gneiss during D₂ shear zone deformation in the locality shown in Figures 60 to 62. View is orthogonal to the transport direction. Boudinaged quartz veins in the ultramylonite document that fluids were introduced into the footwall and that the quartz-feldspar-mica ultramylonite was apparently weaker than the veins (see text). Hammer is 34 cm. Abbreviations; (C) cover, (RB) reworked basement, (U) ultramylonite zone. (GSC 204636-A)

ARCHEAN BASEMENT (DOMAIN 1) DEFORMATION HISTORY

D₁ structures

All units within the Superior Province basement (Fig. 5), except undeformed gabbro dykes of presumed Early Proterozoic age (St-Onge et al., 1992), are characterized by a variably developed foliation (Fig. 6; Table 2). The foliation within individual lithological units is generally defined by a shape fabric of deformed quartz and feldspar, the alignment of xenolithic material and/or aligned crystals of metamorphic minerals (e.g., biotite, hornblende, clinopyroxene). Where high-grade assemblages are preserved, orthopyroxene crystals aligned in the foliation indicate that the planar fabric developed at granulite-facies conditions (Lucas and St-Onge, 1992). A gneissosity is produced in some units by the interlayering of tonalite±diorite with monzogranite veins (Fig. 59). The steeply-dipping foliation/gneissosity generally trends east and locally contains a subhorizontal stretching lineation. The lineation is defined principally by quartz-feldspar rodding, and less commonly by hornblende, clinopyroxene, or orthopyroxene crystals.

The regional distribution of strain is highly variable, although older plutonic units (e.g., tonalites) and their enclaves appear to record a generally higher bulk strain than younger units (e.g., granites; Lucas and St-Onge, 1992). However, even within the tonalites, enclaves with pre-existing foliations rarely show evidence of significant re-orientation or shape change during tonalite deformation. Local high-strain zones (metre- to kilometre-scale) occur in the tonalites,

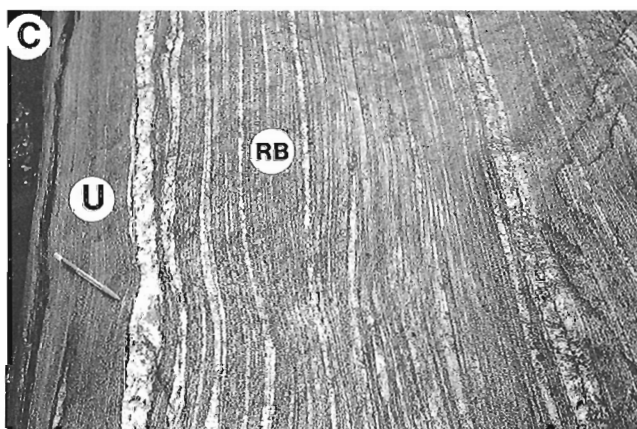


Figure 64. Reworked Archean basement gneiss (RB) and ultramylonite zone (U) immediately beneath the contact with the cover units (C) on the east shore of Wakeham Bay (Fig. 5). The ultramylonite zone (U) shows a marked grain-size reduction of the reworked tonalite/monzogranite gneiss in this locality. Pen is 15 cm long. (GSC 204233-F)

characterized by a well developed, often flaggy, foliation and a stretching lineation (Lucas and St-Onge, 1992). While evidence for bulk shear deformation exists along these zones, their regional significance and kinematics are as yet unresolved. The variably deformed state of the plutonic bodies coupled with the presence of abundant syntectonic granite veins suggest that the D₁ event in the Archean basement (Table 2) was coeval with magmatism (2.7-2.9 Ga; Parrish, 1989) as well as granulite-facies metamorphism (Lucas and St-Onge, 1992). Lucas and St-Onge (1991) have proposed that this Archean event (D₁) occurred in response to transpression of an active magmatic arc.

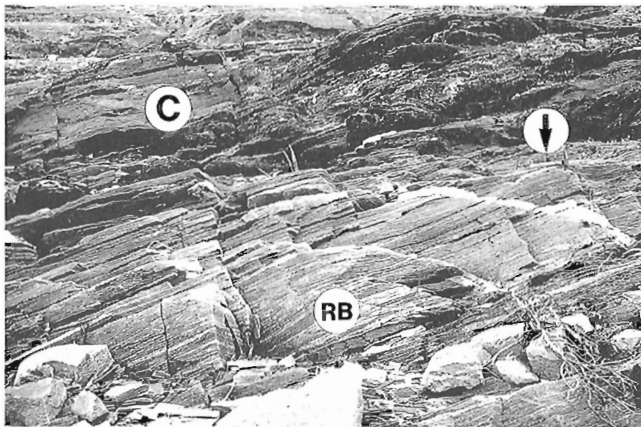


Figure 65. Reworked mylonitic basement (RB) and overlying sheared cover units (C) from the basement/cover contact on the south side of Wakeham Bay (Fig. 5). Arrow points to 34 cm long hammer. (GSC 204233-G)



Figure 67. Transverse stretching/mineral lineation defined by rodding of recrystallized quartz and feldspar and growth of garnet. Lineation is developed in the ultramylonite derived from the Archean basement gneisses in proximity to the basement/cover contact on the north shore of Wakeham Bay (Fig. 5). The plane containing the lineation is within a few centimetres of the basement/cover contact in this locality. Pen is 15 cm long. (GSC 204637)

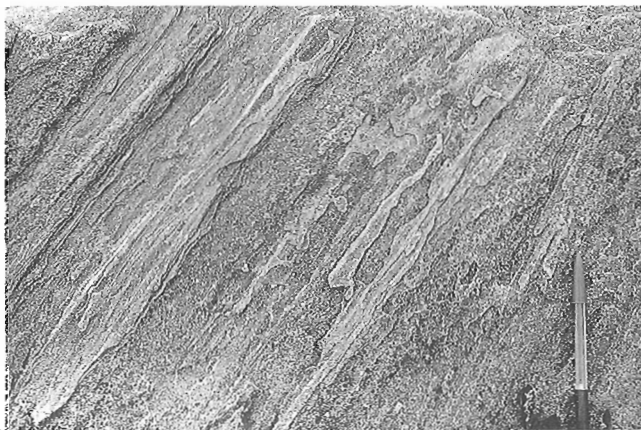


Figure 66. Transverse stretching lineation defined by rodding of recrystallized quartz and feldspar in the reworked Archean basement gneiss underlying the basement/cover contact. Location is the same as for Figure 65. Note pen for scale. (GSC 204233-J)



Figure 68. Asymmetric fold of reworked basement consistent with southward top-side-over (left-side-of-photo-down) displacement. Location is the same as for Figure 67. Pen is 15 cm. (GSC 204233-E)

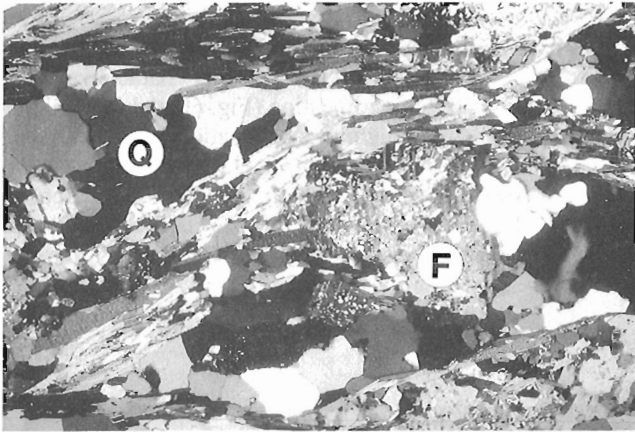


Figure 69. Photomicrograph of a shear zone in reworked Archean tonalite near the basement/cover contact on the north shore of Wakeham Bay (Fig. 5). A spaced mica foliation anastomoses around quartz (Q) and feldspar (F) grains and defines a C/S fabric which indicates a top-to-the-south (top-side-to-the-left) displacement. Horizontal field of view is 6 mm. (GSC 204636-Z)

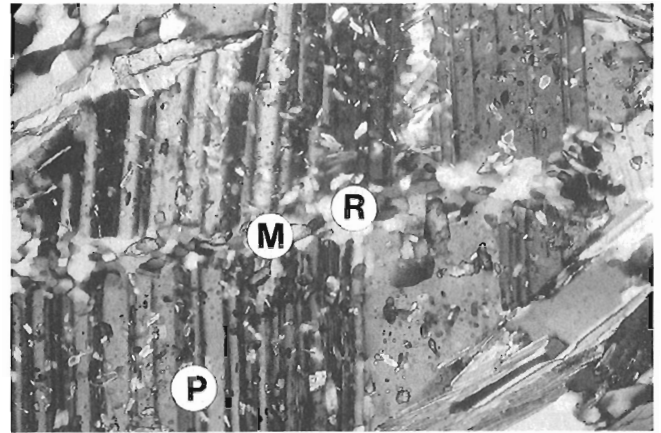


Figure 71. Photomicrograph showing a portion of a plagioclase porphyroblast (P) in a protomylonite derived from an Archean tonalite gneiss near the basement/cover contact 1 km east of the rivière Déception (Fig. 5). The porphyroblast is internally altered to white mica (M) and recrystallization (R) occurred along the microcrack. Horizontal view is 1 mm. (GSC 205208-D)

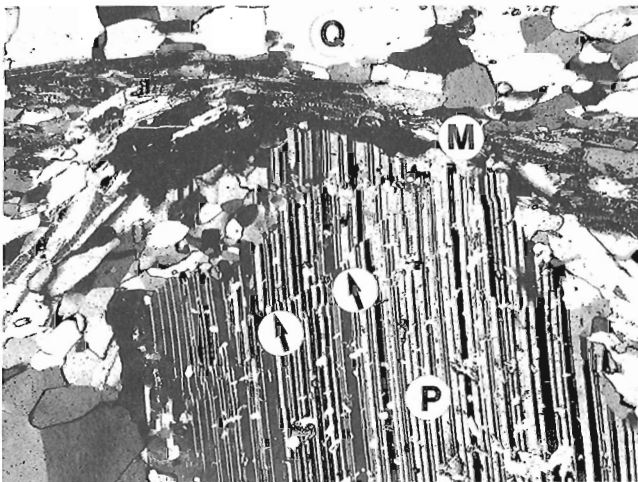


Figure 70. Photomicrograph of a plagioclase porphyroblast (P) in a protomylonite derived from an Archean tonalite gneiss near the basement/cover contact 1 km east of the rivière Déception (Fig. 5). The microstructure is typical of the basement involved in shear zones associated with thrust belt deformation in the Cape Smith Belt. A C-plane seam of muscovite and biotite (M) separates a quartz band (Q) from the feldspar. The plagioclase grain contains microcracks (arrows) and is partly altered internally to white mica. In addition, partial recrystallization has occurred at the upper left grain margin and along the microcracks (see Fig. 71). Horizontal field of view is 6 mm. (GSC 204664-D)

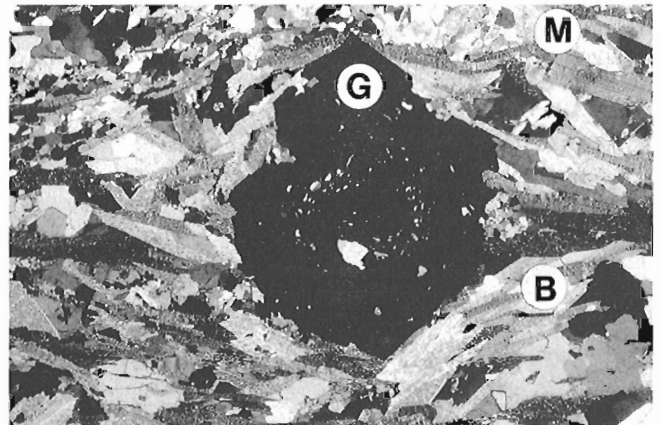


Figure 72. Photomicrograph of garnet (G), biotite (B), and muscovite (M) in a reworked Archean tonalite gneiss near the basement/cover contact 1 km east of the rivière Déception (Fig. 5). The lower amphibolite facies assemblage is the result of retrogression of the Archean granulite-facies assemblage during D₂ deformation of the basement (see text). Horizontal field of view is 4 mm. (GSC 1992-106I)

D₂ structures

The Superior Province basement contains a relatively narrow zone of penetrative strain adjacent to the contact with the Early Proterozoic rocks of the Cape Smith Belt (Lucas, 1989a; Fig. 5, 60 to 63). The zone is characterized by a foliation in which the Archean D₁ gneissosity is transposed into parallelism with the foliation in the overlying Early Proterozoic rocks (Fig. 60 to 63), and varies in width from approximately 0.5 m (lac St-Germain area (1732A); Fig. 5) to 3 m (Wakeham Bay area (1728A); Fig. 5). The basement

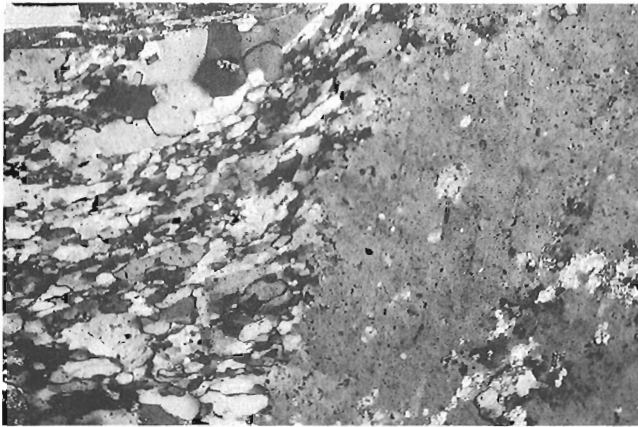


Figure 73. Photomicrograph of reworked Archean basement tonalite north of the basement-cover contact, 1 km east of the rivière Déception (Fig. 5). Feldspar porphyroclast is recrystallizing along its margins to smaller, oriented grains of feldspar defining the Proterozoic fabric in the basement rock. Horizontal field of view is 5 mm. (GSC 204636-I)

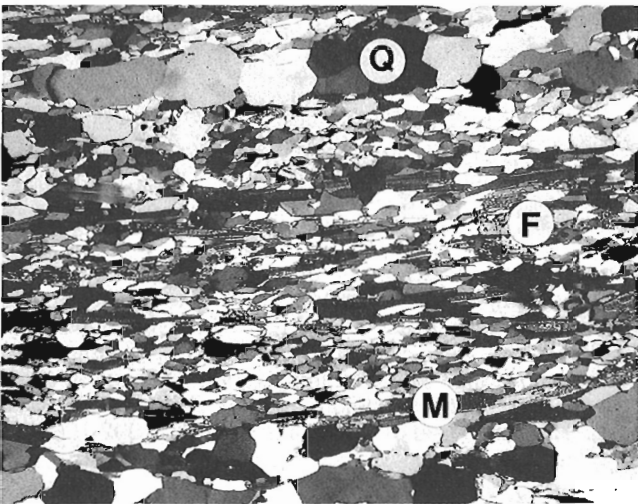


Figure 74. Photomicrograph of a reworked Archean tonalite adjacent to the basement-cover contact 1 km east of the rivière Déception (Fig. 5). Feldspar porphyroclasts have completely recrystallized and formed 'new' grains (F) in feldspar rich layers. The reworked compositionally defined foliation has quartz (Q), feldspar (F), and muscovite-biotite (M) layers. Horizontal field of view is 22 mm. (GSC 204664-I)

rocks are transformed into mylonites immediately adjacent to the basement/cover contact (Fig. 63 to 65). The narrow zone of penetrative deformation is further characterized by a north-trending stretching lineation (Fig. 66 and 67) which is parallel to the stretching/mineral lineation in the overlying Early Proterozoic rocks (St-Onge et al., 1986; Lucas, 1989a). The parallelism of the planar and linear structures immediately above and below the basement-cover contact suggests that the basement structures are of Early Proterozoic

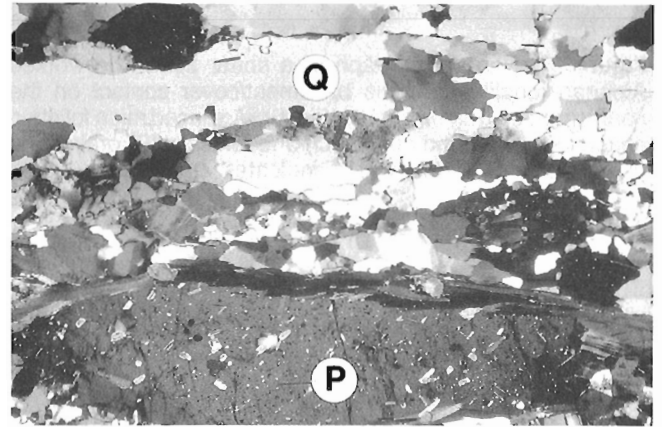


Figure 75. Photomicrograph of a reworked Archean basement tonalite 100 m north of the basement-cover contact, 1 km east of the rivière Déception (Fig. 5). Quartz ribbons (Q) in the reworked tonalite are polycrystalline and oriented parallel to a deformed plagioclase porphyroclast (P). Horizontal field of view is 6 mm. (GSC 1992-106M)

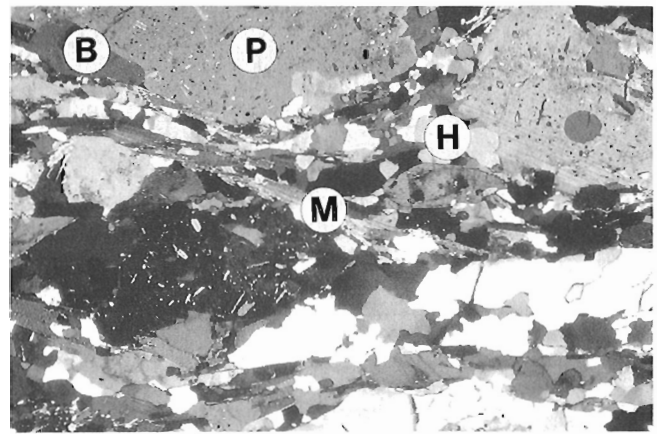


Figure 76. Photomicrograph of reworked Archean tonalite north of the basement-cover contact, 1 km east of the rivière Déception (Fig. 5). Retrograde muscovite (M), biotite (B), and chlorite (not shown) are derived at the expense of plagioclase (P) and hornblende (H). Horizontal field of view is 6 mm. (GSC 1992-106N)

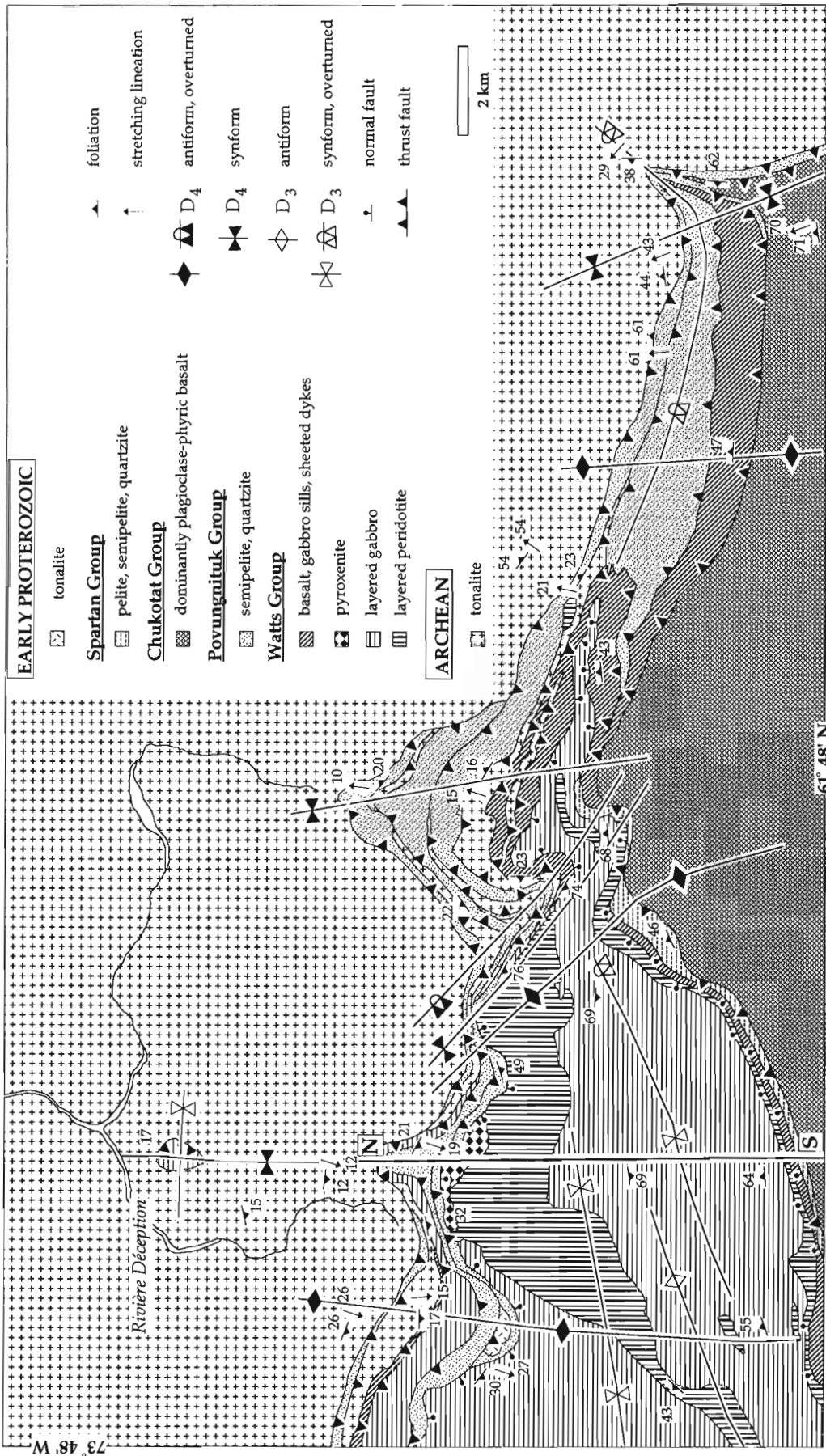


Figure 77. Simplified geological map of the northern margin of the Cape Smith Belt in the rivière Déception area (1722A, 1723A). This area is characterized by D₃ imbricates of Archean basement which vary in width from several metres to several hundred metres. Section line N-S represents the line along which the downplunge constrained strike-perpendicular cross-section shown on Figure 80 is hung.

age, and are here termed D₂ structures with respect to the basement deformation history (Table 2; Lucas and St-Onge, 1992).

The narrow zone of progressive ductile transposition of the Archean D₁ gneissosity is characterized by folds of the gneissic layering (Fig. 68) that are cut by small-scale, décollement-parallel shears (Fig. 62). In the reworked basement these shear zones are characterized by a spaced mica foliation anastomosing around quartz and feldspar grains. The foliation occasionally defines a C/S fabric (Berthé et al., 1979) which indicates a top-to-the-south displacement (Fig. 69), consistent with kinematic indicators in the thrust belt. The shear foliation throughout most of the transposition zone is defined by mica and by elongate polycrystalline aggregates of quartz and feldspar. The small-scale shears increase in density across the transposition zone until they form a penetrative, mylonitic to ultramylonitic foliation about 1 m below the décollement (Fig. 62 and 63).

Development of the mylonitic foliation in footwall Archean gneisses appears to result from fluid influx, retrograde, mica-producing reactions, and ductile deformation of quartz and feldspar (Lucas, 1990). The presence of deformed quartz veins (Fig. 63) indicates that fluids were able to penetrate into the basement from the dehydrating sedimentary rocks above the décollement. Two possible mechanisms may explain the fluid flow down into the basement (Lucas, 1990): (1) flow along a chemical potential gradient from the dehydrating sedimentary rocks into the "dry" basement gneisses; and (2) local fluid influx along fractures generated as a result of high fluid pressures along the décollement. Metamorphism of the basement gneisses during D₂ deformation is characterized by retrogression of the Archean granulite-facies assemblage to the ambient Proterozoic greenschist to lower amphibolite facies conditions. This was accomplished by the hydration of feldspars and hornblende, and the growth of retrograde white mica, biotite, and chlorite

(Fig. 70 and 71) and, rarely, garnet (Fig. 72). Feldspar grain size reduction in the transposition zone occurred by grain-scale faulting and rotation of fragments during early D₂ deformation, and later (most importantly) by dislocation creep with recrystallization localized at grain margins (Fig. 73) and along microcracks (Fig. 70 and 71).

The ultramylonite zone directly below the the basement/cover contact contains compositional layering in which quartz ribbons are interlayered with completely recrystallized feldspar bands and narrow mica seams (Fig. 74). The ribbons are polycrystalline quartz aggregates with a weak crystallographic preferred orientation (judged by the gypsum plate effect), and with individual grain boundaries at high angles to the length of the ribbons (Fig. 75). The quartz microstructure probably results from some combination of (1) recovery and recrystallization during deformation; and (2) annealing and grain growth following deformation. In contrast to the coarser grained quartz aggregates, the feldspar bands contain 50 to 100 μm grains displaying both a shape and an apparent crystallographic preferred orientation.

Basement deformation during D₂ in the map area is probably limited by the depth of penetration of the hydration-retrogression front (Lucas, 1989a). A similar mechanism was proposed by Bartley (1982) to explain limited involvement of underthrust Baltic Shield basement in the Caledonian orogeny. The zone of retrograde mica-production extends beyond the transposition zone into the basement below the basement/cover contact. This spatial evidence suggests that the hydration-retrogression front temporally preceded the deformation front's progress structurally downwards into the basement during D₂ (Lucas, 1989a, 1990). The most important consequence of the retrogression was probably the production of micas, a less competent mineral which lowered the yield stress for the gneisses (cf. Tullis and Mardon, 1984; Jordan, 1987).

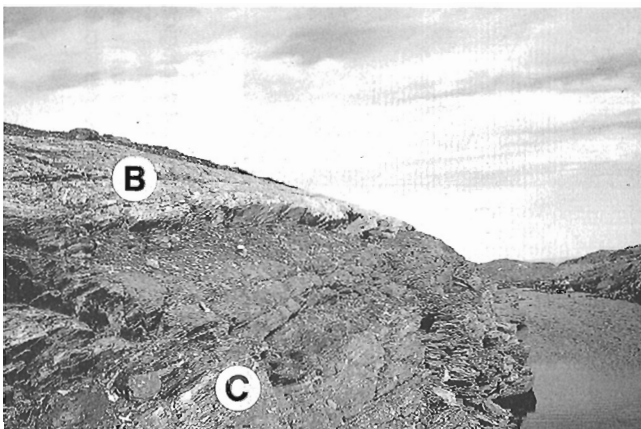


Figure 78. Imbricate of Archean tonalite gneiss (B) in thrust contact with clastic sedimentary rocks of the lower Povungnituk Group (C), 6 km east of the rivière Déception (Fig. 77). Height of section is 15 m. (GSC 204232-M)

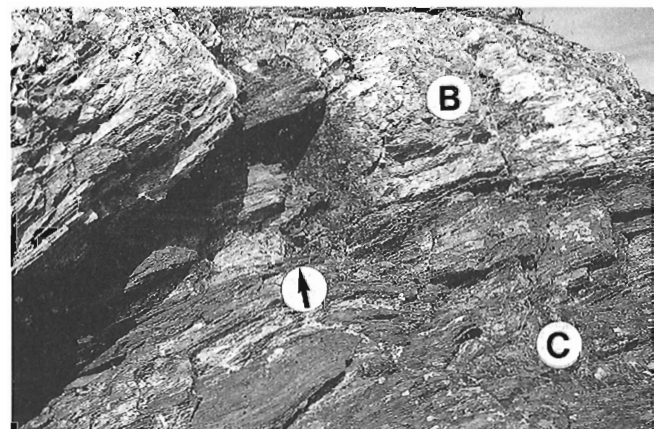


Figure 79. Detail of the contact between the basement imbricate (B) and the cover units (C) at the locality of Figure 78. The mylonitic foliation observed at the bottom of the basement slice is interpreted to have been generated during emplacement into the thrust belt (see text). Arrow points to 15 cm long pen. (GSC 1992-106V)

D₃ structures

The D₃ deformation event in the Archean basement is characterized by both ductile shear of the gneisses below the basement/cover contact and by thrust imbrication of basement slices with cover rocks of the Cape Smith Belt (Table 2; Lucas, 1989a, 1990; St-Onge and Lucas, 1990m; Lucas and St-Onge, 1992). Structures related to D₃ are localized along the northern margin of the Cape Smith Belt (lac Watts (1721A)-rivière Déception (1722A) area; Fig. 5). The basement shear zone is marked by up to 200 m of well foliated and lineated protomylonites below the basement/cover contact. This contrasts with the previously described, relatively narrow D₂ shear zones (0.5 to 3 m) preserved along the eastern and southern margins of the Cape Smith Belt. Metamorphic assemblages in the reworked gneisses are characterized by retrograde muscovite, biotite, and chlorite derived at the expense of feldspar and hornblende (e.g. Fig. 76). The broader basement shear zone probably reflects a longer deformation history (D₂ + D₃) during which bulk weakening by hydration and phyllosilicate growth occurred.

The zone of most pervasive shear in the basement coincides with the area of basement imbrication (rivière Déception (1722A)-lac Lecorré (1723A) area; Fig. 77). The basement thrust slices vary in width from several metres to several hundred metres (Fig. 78) and are discontinuous along strike, with strike lengths ranging from only several tens of metres to over ten kilometres (Fig. 77). These observations indicate that the basement slices in the Cape Smith Belt are not equivalent to the major basement slabs which characterize of the internal parts of some collisional belts (e.g., Mattauer, 1986; Dewey et al., 1989). Five basement imbricates are present in this fault system, and are individually interleaved

with thrust sheets of Povungnituk Group sedimentary rocks (Fig. 77). Mapping of the Superior Province basement for many kilometres structurally below the basal décollement has also demonstrated that major detachments do not occur within the exposed structural levels (Fig. 5; Lucas and St-Onge, 1991, 1992).

The basement slices are characterized by a protomylonitic foliation in their interior grading into an ultramylonitic foliation adjacent to their top and bottom contacts (Fig. 79). No Archean gneissic fabrics are preserved in the slices. The high strain zone at the top of the slices probably represents a localized ductile shear zone that developed during movement on the (now abandoned) D₂ décollement. This suggests that the basement slices experienced significant ductile deformation below the basement/cover contact prior to thrust imbrication. The ultramylonite zone observed at the bottom of the basement slices (Fig. 79) was most likely generated during their emplacement into the thrust belt. The older (D₂) basement/cover fault (or décollement) is interpreted to have been truncated and abandoned during D₃ emplacement of the basement slices (Fig. 80). It has been suggested (Byrne and Lucas, 1988; Lucas and Byrne, 1992) that basement thrusting may not have occurred until the rheological contrast between the thrust belt and the relatively stronger footwall was reduced by weakening of the footwall basement through retrogression and development of a mylonitic foliation. In total, the nature of Superior Province basement involvement in Early Proterozoic deformation appears to evolve from passive underthrusting during D₂ to more pervasive shear deformation and limited imbrication during D₃ (Table 2; Lucas 1989a; Lucas and Byrne, 1992; Lucas and St-Onge, 1992).

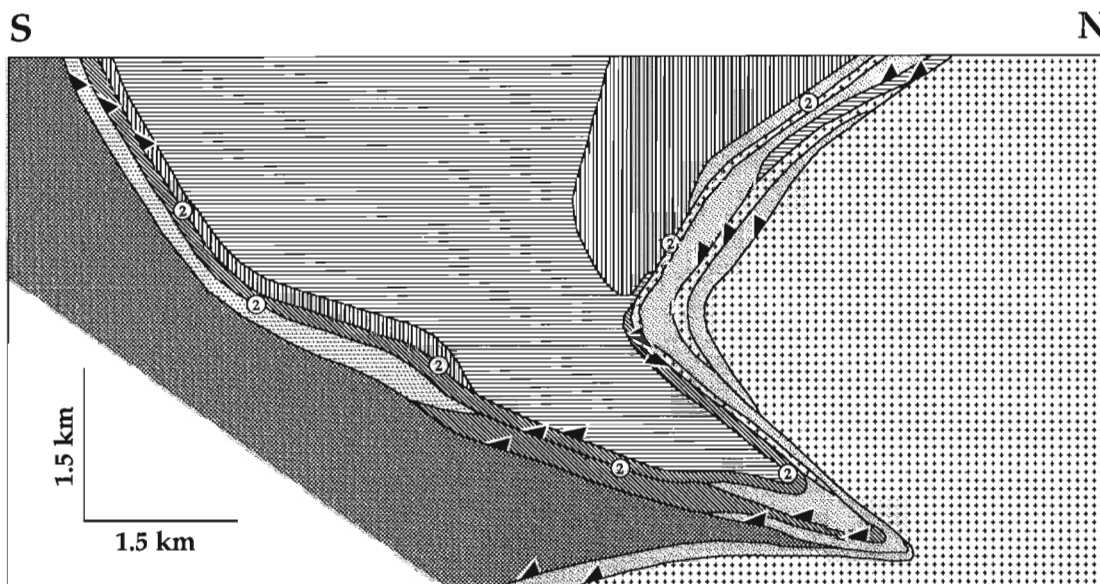


Figure 80. Detailed downplunge constrained cross-section of the area illustrated in Figure 77. Lithological legend is given in Figure 77. All faults are identified with triangular arrows; circled twos refer to normal faults.

POVUNGNITUK AND CHUKOTAT GROUPS (DOMAIN 2) DEFORMATION HISTORY

D₁ structures

The oldest tectonic structures observed in the Early Proterozoic Povungnituk and Chukotat groups are found at relatively high structural levels in the most external part of

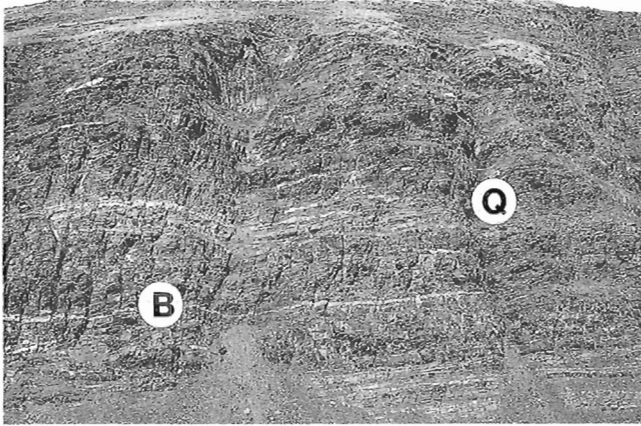


Figure 81. Early *D₁* thrust fault placing quartzites (Q) of the lower Povungnituk Group in hanging wall on basalt (B) of the upper Povungnituk Group in footwall. The cliff section is 150 m high and the fault juxtaposes thrust sheets I and K, 3 km southwest of Wakeham Bay (Fig. 5). (GSC 204232-V)

the orogen, and are interpreted to have formed during a thrusting episode (*D₁*) which accomplished north-south shortening and vertical thickening (Lucas, 1989a; St-Onge and Lucas, 1991). The structures are preserved because they escaped subsequent penetrative ductile strain during prograde metamorphism, which overprints older structures at deeper levels within the external part of the belt (e.g., adjacent to the basement-cover contact, Fig. 5 and 58). The preserved early structures include a sequence of low angle faults which repeat stratigraphic units (Fig. 81), minor folds of bedding, and a cleavage spatially associated with the faults and folds. The fault separating the Archean basement from the Early Proterozoic rocks, hereafter referred to as the basal décollement (Lucas, 1989a), is inferred to have had an important early movement history.

Basal décollement

A regional basal décollement separates the Early Proterozoic rocks of the Povungnituk and Chukotat groups from Archean basement in the map area. The basal décollement is localized at the basement/cover contact within the main Cape Smith Belt (Fig. 82). The basal décollement not only marks a major boundary between tectonostratigraphic domains 1 and 2, but it also separates highly deformed rocks in the hanging wall from footwall gneisses with <3 m of penetrative Proterozoic foliation immediately below the contact. In a series of outliers in the Burgoyne Bay area (1735A; Fig. 83), approximately 30 m of autochthonous lower Povungnituk Group sedimentary rocks separate highly deformed Proterozoic rocks from the underlying Archean basement

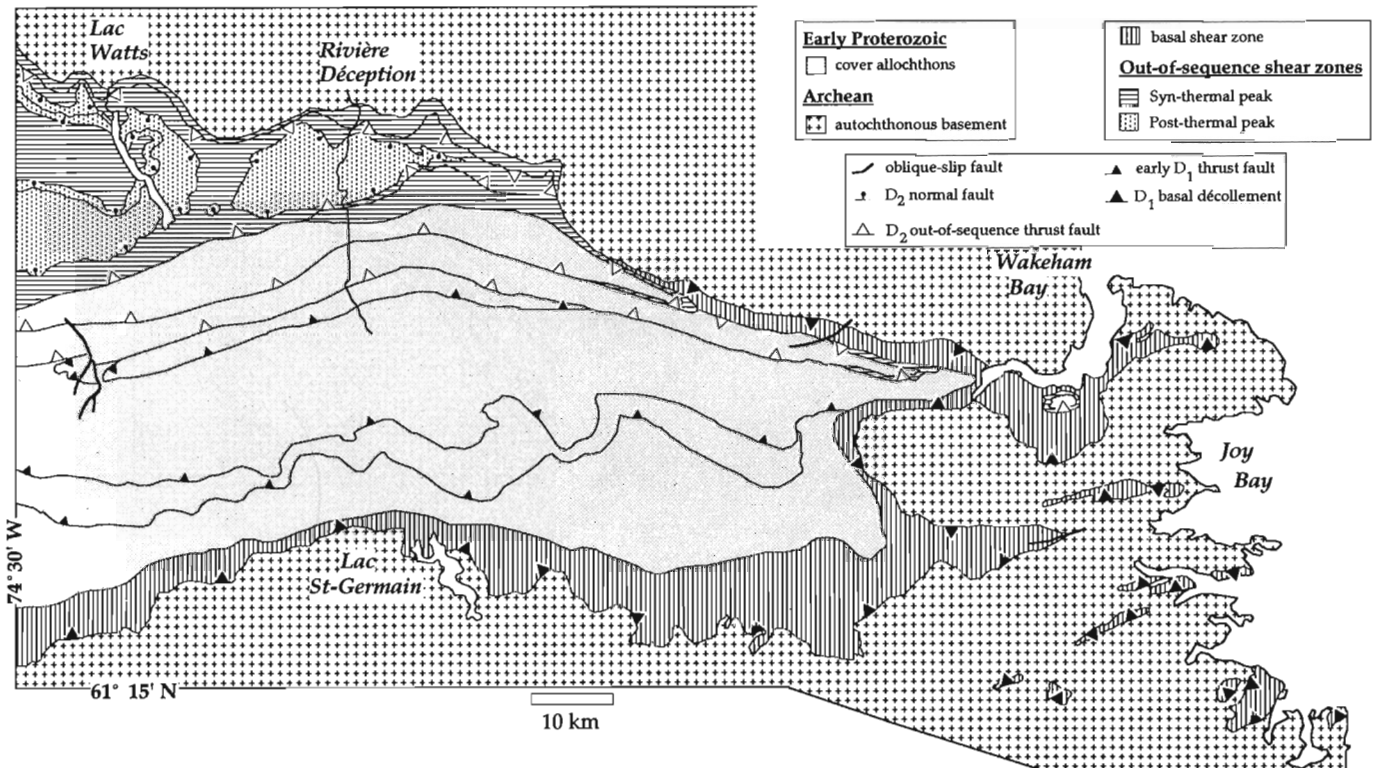


Figure 82. Regional extent of ductile shear zones in the eastern portion of the Cape Smith Belt (see text).

gneisses (Fig. 9). The contact between highly deformed and undeformed rocks of the Povungnituk Group is interpreted to be the same basal décollement that separates Archean and Proterozoic rocks to the north. This north-to-south change in the footwall stratigraphic level of the décollement must then mark the position of a major ramp in the décollement's trajectory. The tectonic significance of the basal décollement is that it separates *allochthonous* Early Proterozoic rocks of the Povungnituk Group and Chukotat groups from *autochthonous* Povungnituk Group and Archean rocks (St-Onge et al., 1986; Lucas, 1989a).

Lucas (1989a) has suggested that the trajectory of the décollement was influenced by the structure of the underthrust continental rift margin. A ramp in the décollement climbs through hanging wall tectonostratigraphy (thrust sheets C to H, south of lac Vicenza, Fig. 5) to a structurally higher glide horizon of pelite and semipelite (PPse; 1733A) to the west (thrust sheet I, Fig. 5). This ramp may have developed at the south margin of the rift basin containing the micaceous quartzite unit (PPms; 1733A), re-utilizing a presumed north-dipping normal fault. Evidence for this normal fault is indicated by the abrupt truncation of the southern margin rift-sediment duplexes against the basal décollement (Fig. 5).

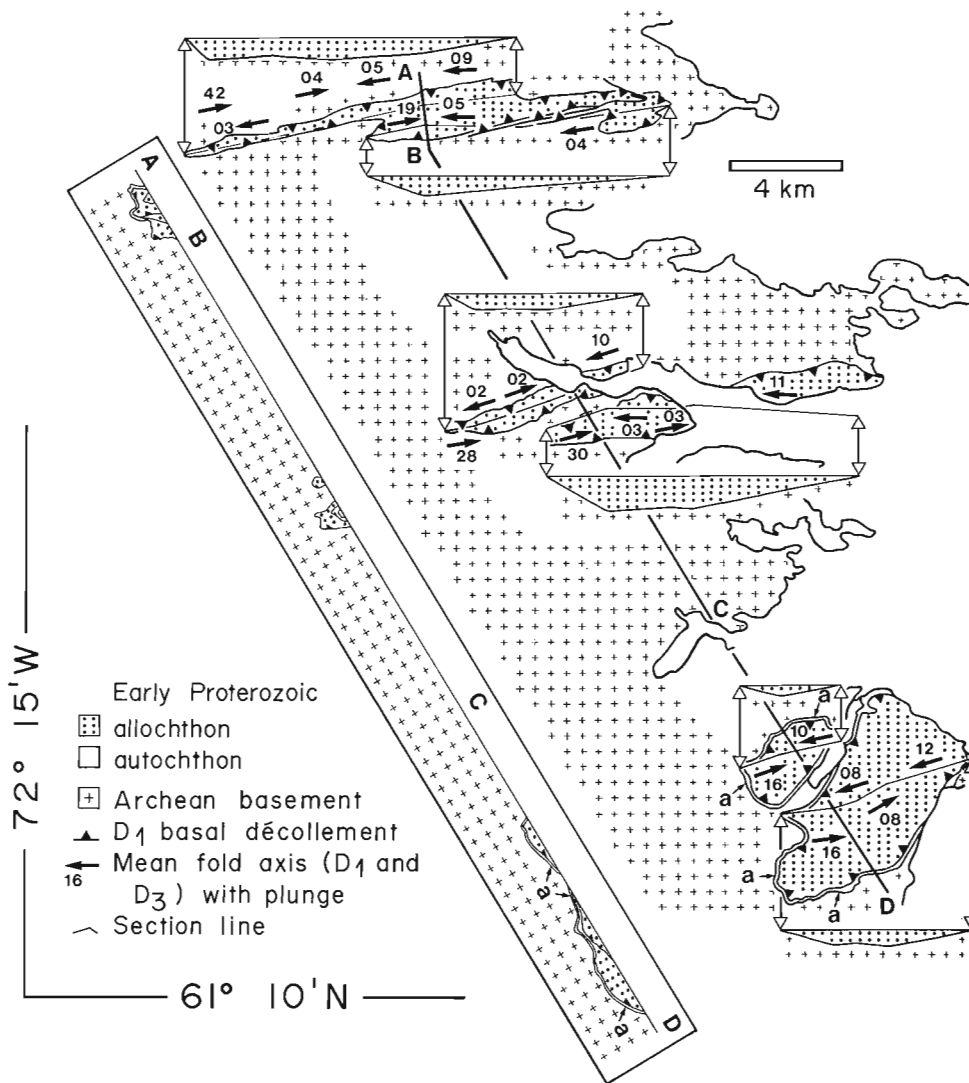


Figure 83. Strike-parallel and strike-perpendicular cross-sections of outliers of Early Proterozoic rock found southeast of the Cape Smith Belt in the Burgoyne Bay area (1734A, 1735A). The strike-perpendicular cross-section (ABCD in box) and the strike-parallel sections have no vertical exaggeration, and are at the same scale as shown in map view. Heavy line A-B-C-D represents the line of section for the strike-perpendicular cross-section in box. Letters 'a' refer to autochthonous strata depicted on the map and cross-section.

Piggyback-sequence thrust system

Map-scale structures

A thrust system linked to the basal décollement outcrops in the southern and eastern portions of the Cape Smith Belt (Fig. 5). Thrust faults bound packages of Povungnituk Group sedimentary and volcanic rocks (thrust sheets A to L, Fig. 5). The thrusts are responsible for thickening the Povungnituk Group rift sequence from at least 7 km (maximum stratigraphic thickness of Povungnituk Group; thrust sheet K, Fig. 5) to a minimum of 20 km (Fig. 58). Thickening was accomplished through progressive translation of more distal units (e.g., thrust sheet I, Fig. 5) onto more proximal units (e.g., thrust sheet G, Fig. 5). Thrust faults B to J (Wakeham Bay-lac Vicenza area, Fig. 5) appear to have developed in the footwall of thrust K in a foreland-propagating fashion. A lateral ramp connects thrust fault K to the basal décollement south of Wakeham Bay (Fig. 5), indicating that the basal décollement is part of the D1 thrust system. However, this thrust ramp is not included in the cross-section (Fig. 58) because lateral structures cannot be projected onto strike-perpendicular sections (Lucas, 1989a).

D1 thrust faults are characterized by a north-to-south movement direction and minimum displacements of up to 10 km. The north-to-south transport direction is documented by (1) the generally east-trending and north-dipping attitude of thrust ramps (Fig. 5, 58), and (2) the consistent juxtaposition of more distal sedimentary and/or volcanic facies onto more proximal facies. Matching hanging wall cut-offs with the corresponding footwall truncations for several of the major faults in this system (e.g. thrust faults J and K, Fig. 5) indicates that minimum displacements for individual faults are on the order of 10 km. Given these minimum displacements for individual faults and the fact that the thrust faults progressively climb up from the décollement from north to south (Fig. 58), the minimum displacement on the décollement at the northern margin is estimated to be on the order of 100 km. This is consistent with the observation that the Archean basement in the mapped area (Fig. 5) shows no evidence for crustal stretching (Hoffman, 1985; St-Onge et al., 1986). The décollement in the Wakeham Bay-Burgoyne Bay area (1735A, 1729A; Fig. 5) is characterized by carrying the same tectonostratigraphic unit in the hanging wall for approximately 70 km parallel to the north-south transport direction (thrust sheet B, Fig. 5). The hanging wall glide

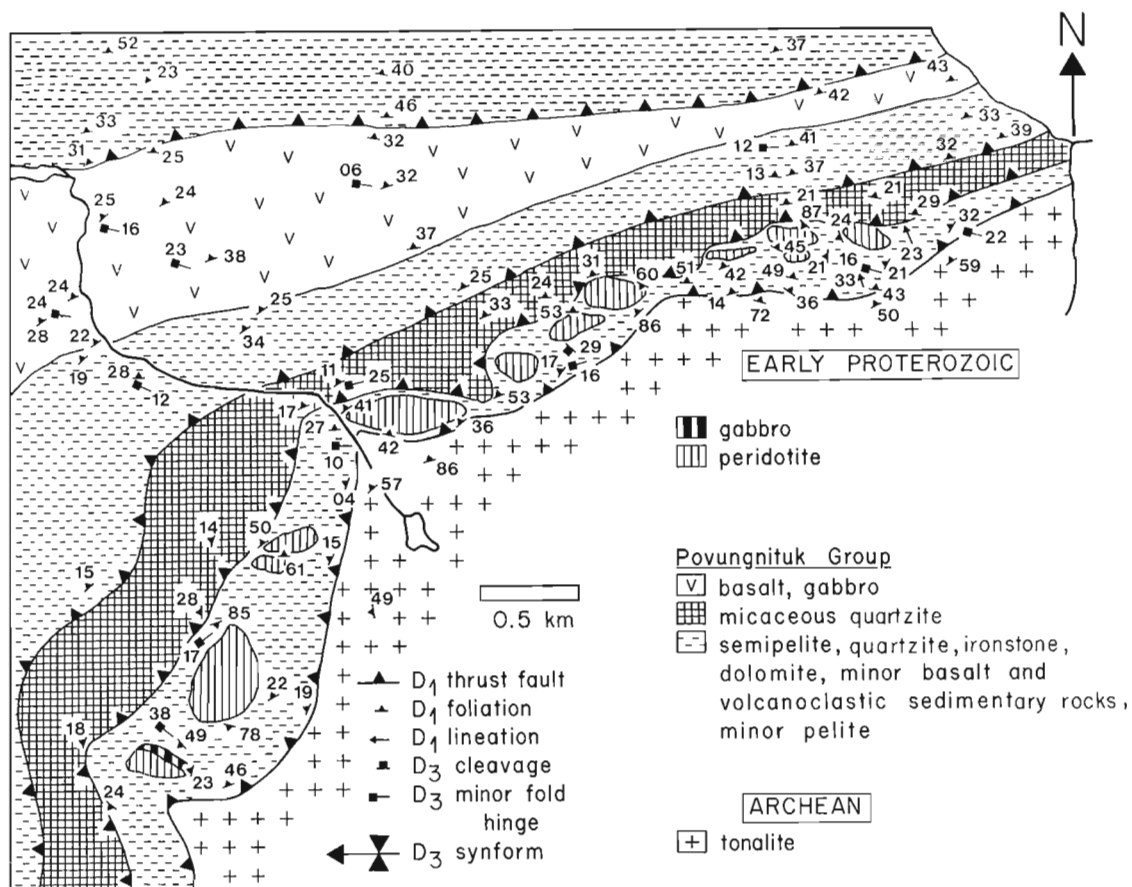


Figure 84. Geological map of a boudined mafic-ultramafic sill southwest of Wakeham Bay (1727A, 1728A). Flow of the overlying thrust sheet (carrying micaceous quartzite) into the interboudin gaps indicates that this ductile deformation (resulting from synmetamorphic movement along the basal décollement) must have occurred after emplacement of the thrust sheet. Location of the map is indicated in Figure 85 with "b".

horizon for this area is generally in semipelite (PPse) of the lower Povungnituk Group. The isostratigraphic hanging wall position of the basal décollement is also consistent with a large décollement displacement (>70 km).

Several lines of evidence suggest that the system of D₁ thrust faults accreted in a piggyback-stacking (i.e., foreland-propagating) sequence (Elliott and Johnson, 1980; Boyer and Elliott, 1982). First, fault-bend folds (Suppe, 1983) associated with ramps in structurally lower thrust faults deform older hanging wall thrust faults. As an example, thrust I was folded during translation of the hanging wall thrust stack through a footwall ramp of thrust G, located at the eastern edge of the southern margin duplexes (southeast of lac Vicenza, 1733A; Fig. 5). Second, overlying thrusts were deformed during synmetamorphic movement along the underlying basal décollement (which produced the basal shear zone; see below). As illustrated in Figure 84, ductile deformation in the basal shear zone resulted in boudinage of a layered mafic-ultramafic sill and consequent ductile flow of the overlying material, including the inactive thrust G (placing micaceous quartzite on semipelite and boudinaged sill, Fig. 84), into the interboudin gaps. These two examples suggest that the overall age progression for D₁ accretion of thrust sheets was from north to south.

Two distinct styles of imbrication are indicated by the geometry of the thrust sheets and faults in the southern portion of the map area (faults A to L, Fig. 5). Thrust sheets characterized by sedimentary rock overlain by basalt are typically 3-7 km thick and laterally extensive (e.g. thrust sheets I to L, Fig. 5). The rift basalts generally account for over 75% of the thrust sheet volume. In contrast, the imbricates that developed solely in the sedimentary rocks of the belt's southeastern corner are much thinner (0.4-2.5 km) and are relatively restricted in areal extent by thrust ramps (e.g. thrust sheets C to H, Fig. 5). The two imbrication styles are consistent with a model in which the number and spacing of thrust faults is a function of the strength of the component lithologies and the thickness of rheologically-competent units, such as basalt (Johnson, 1980). Development of the two imbricate styles clearly indicates that the rift margin stratigraphy and structure (described above) played an influential role in determining thrust geometry and the location of ramps.

The contrasting styles of imbrication are further indicated by different footwall ramp geometries. The footwall geometry of the thrust sheets dominated by basalt is characterized by (1) an initial flat segment in sedimentary rock, followed by (2) a ramp through several kilometres of rift basalt, and finally by (3) a long flat or gently ramping

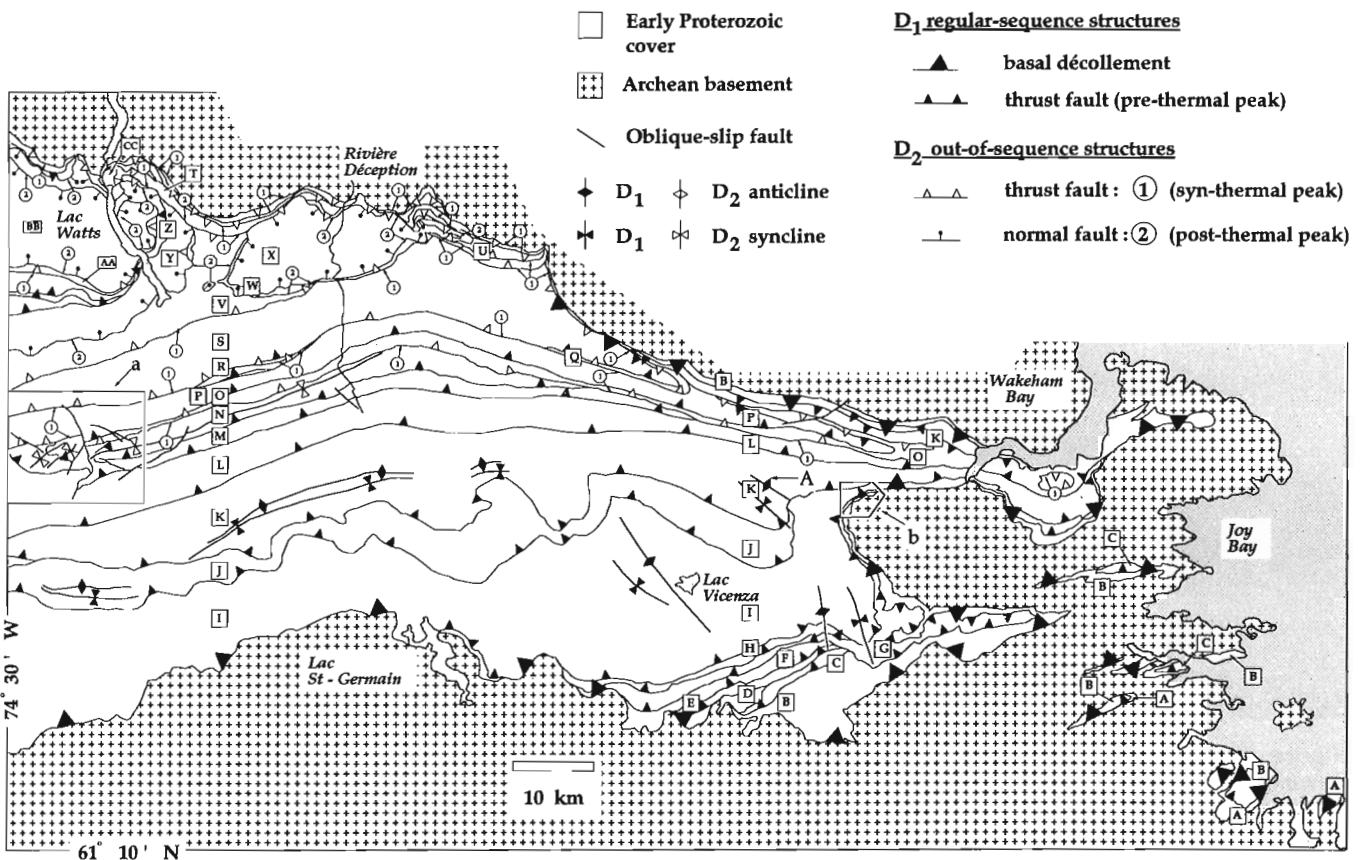


Figure 85. Compilation of D₁ and D₂ thrust faults and associated folds for the eastern portion of the Cape Smith Belt. Regular-sequence and out-of-sequence thrust faults are distinguished on this map by closed and open thrust fault teeth, respectively. Boxed letters label thrust sheets referred to in the text. Areas "a" and "b" refer to areas shown by Figures 109 below and 84, respectively.

(<5°) segment in basalt (Fig. 58). The basalt-dominated thrust sheets have only one or two major ramp segments (Fig. 58), with step-up angles averaging 20°. In contrast, the sedimentary-dominated imbricates along the southern margin form two duplex structures with hinterland-dipping horses (thrust sheets C-D-E-F, and thrust sheet H, Fig. 5; Boyer and Elliott, 1982).

The relative absence of D₁ fault-propagation folds (Suppe, 1983) provides another example of how the geometrical evolution of the thrust belt was influenced by the stratigraphy of the underthrust continental margin. Map-scale folds appear to be restricted to several hanging wall fault-bend fold pairs (Fig. 85) developed at the top of footwall ramps through the rift basalt succession. An example is the anticline-syncline pair developed in thrust sheet K (marked with "A" in Fig. 85). The lack of folds in comparison to fold-and-thrust belts involving sedimentary rock-dominated passive margin sequences (e.g., Helvetic Nappes, Ramsay et al., 1983) probably reflects (1) the absence of a repeated stair-step trajectory of the thrust faults through the rift basalts; and (2) the difficulty in forming fault-propagation folds in a relatively strong basalt sequence without significant rheological layering.

The absolute timing of D₁ deformation is poorly constrained. Lucas and St-Onge (1992; see also St-Onge et al., 1992) have suggested that it began between 1918 Ma and 1870 Ma (Table 2). The minimum age bracket refers to a U/Pb age (R. Parrish, pers. comm., 1991) for a gabbroic sill intruding Chukotat Group basalt (PCpl) west of the map area (east of Kettlestone Bay, Fig. 2). The basalt is interpreted as being equivalent to modern n-MORBs (Francis et al., 1983; Picard et al., 1990). The sill is inferred to postdate overthrusting of the basalt onto Superior Province crust

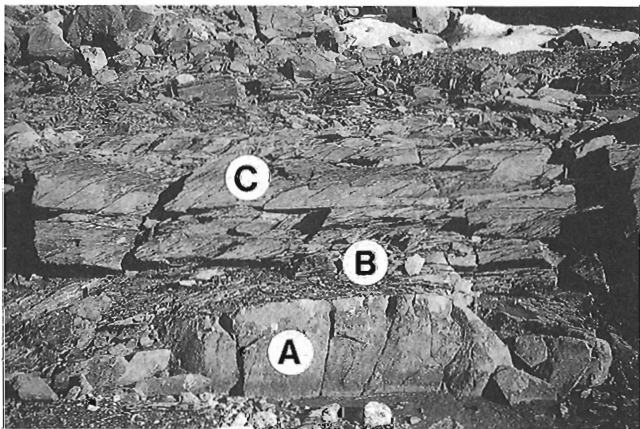


Figure 86. Siliciclastic sedimentary rocks of the lower Povungnituk Group with early D₁ cleavages from 8 km east of lac Vicenza (Fig. 5). The cleavages developed during movement on an underlying thrust fault (approximately 10 m below the bottom of the photo). A cleavage is absent from bed A (arkosic quartzite), subparallel to bedding in bed B (semipelite), and oblique to bedding in bed C (quartzite with a bimodal grain distribution), reflecting variations in grain size and quartz/mica ratio. Thickness of bed A is approximately 0.5 m. (GSC 204636-F)

because the sill contains Archean-aged zircon xenocrysts, apparently inconsistent with the oceanic nature of the basalt (Lucas and St-Onge, 1992; St-Onge et al., 1992). The question of why the continental thrust belt initiated prior to the principal collision (<1825 Ma; St-Onge et al., 1992; Lucas and St-Onge, 1992) between the Superior Province continental margin (domains 1 and 2) and the oceanic and magmatic arc units (domain 3) preserved in the orogen is difficult to resolve with the present data. Impingement of an upper plate oceanic, accretionary prism, or island arc terrane against the underthrust Superior Province continental margin could have generated the continent-verging thrust belt (Lucas and St-Onge, 1992) in a manner analogous to the ongoing collision in Taiwan. However, existing geochronology precludes collision of any units prior to 1839 Ma except the undated Spartan Group (Parrish, 1989; St-Onge et al., 1992). This question may in part be resolved if the collision was oblique, and the early colliding upper plate units were translated laterally out of the exposed part of the orogen on the Ungava Peninsula.

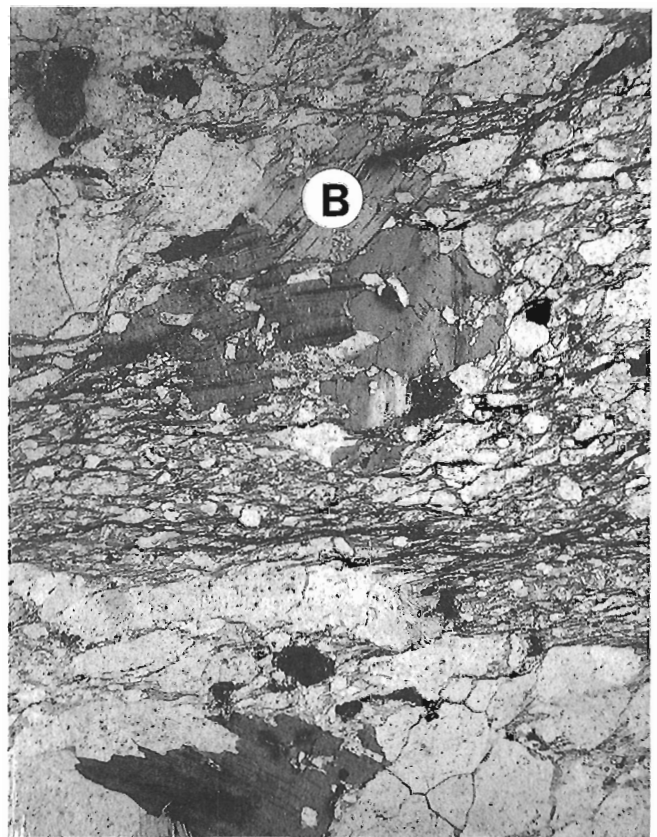


Figure 87. Photomicrograph of pressure solution cleavage (subhorizontal) in a quartzite of the lower Povungnituk Group with a bimodal grain size distribution (similar to bed C in Fig. 86). The quartzite is from an early D₁ fault zone, within 5 m of a thrust fault 8 km east of lac Vicenza (Fig. 5). The biotite porphyroblasts (B) postdate the development of the cleavage. The horizontal field of view is 12 mm. (GSC 204664-A)

Grain-scale structures

Field and thin section observations indicate that the fault zones preserved at high structural levels in Povungnituk Group sedimentary rocks are D₁ in age and predate the thermal peak of metamorphism. The fault zones studied are generally associated with the relatively large displacement thrusts (~10 km; see Lucas, 1989a) carrying sedimentary and mafic volcanic rocks (thrusts J to N, Fig. 5). Penetrative deformation in the hanging wall fault zones is restricted to relatively narrow widths, varying from 1 m in basalt to approximately 10 m in sedimentary rock. A typical sequence of deformed sedimentary rocks located approximately 10 m above a fault is illustrated in Figure 86. The pre-thermal peak, D₁ age of fault zone fabrics is indicated by two observations. First, unoriented biotite (thermal peak) porphyroblasts overgrow fault zone cleavages in quartzites (Fig. 87). Second, a D₁ thrust fault is folded in the footwall of a younger (D₂) thrust fault (west end of thrust fault N, Fig. 85). D₁ fault-related microstructures are preserved in the

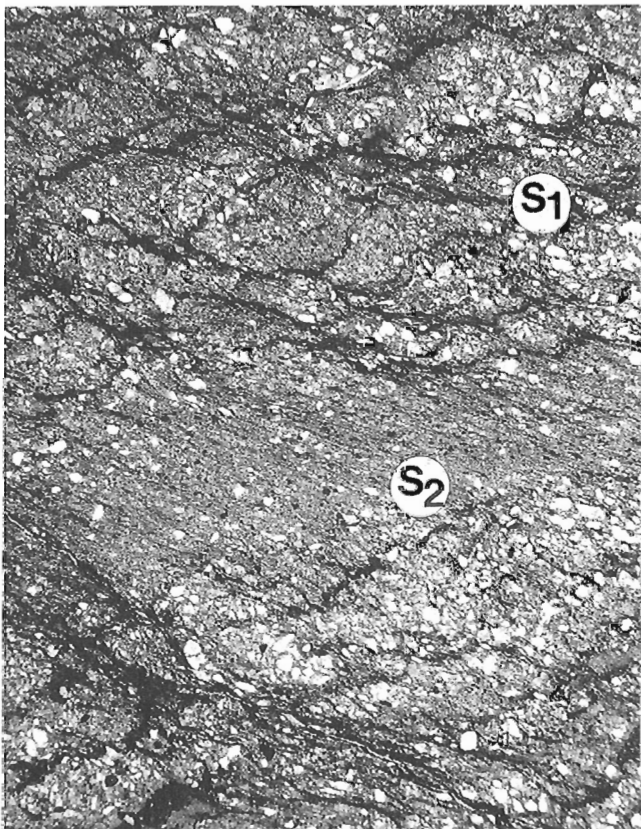


Figure 88. Photomicrograph of a semipelitic of the lower Povungnituk Group from the footwall fault zone of a folded early D₁ thrust fault at relatively high structural levels (area "a" on Figure 85). Early D₁ bedding-parallel pressure solution cleavage (S₁) is overprinted by a transecting pressure solution cleavage (S₂). The first cleavage developed during movement on the overlying early D₁ fault (thrust N, Fig. 5), located 10-15 m above the sample. The overprinting cleavage formed as the rocks were folded in the footwall of a D₂ out-of-sequence thrust fault (thrust O, Fig. 5). The horizontal field of view is 15 mm. (GSC 204664)

footwall syncline, although they are overprinted by a transecting D₂ cleavage related to flattening of the syncline during movement on the younger fault (Fig. 88; see 'D₂' section below).

Fine grained pelitic and semipelitic sedimentary rocks in the fault zones are characterized by a penetrative slaty cleavage. The cleavage is parallel to layering (transposed bedding) immediately adjacent to the faults, and generally oblique to bedding (Fig. 89) or axial planar to minor folds of bedding (Fig. 90) beyond about 5 to 10 m from the faults. The slaty cleavage microstructure is marked by (1) fine grained, aligned muscovite and chlorite, (2) lozenge-shaped quartz grains with apparently no crystallographic preferred orientation, and (3) dark seams of opaque minerals which anastomose around quartz grains (Fig. 88). These observations are consistent with the dominant deformation mechanism in quartz being pressure solution and with the growth of chlorite and muscovite resulting from metamorphic reactions (e.g., Beach, 1979; Robin, 1979).

Arkosic quartzite beds in pre-thermal peak D₁ fault zones record heterogeneous bulk deformation and cleavage development during fault movement. The development of cleavages in quartzite beds is primarily a function of (1) proximity to the fault, (2) clast size and distribution, and (3) the proportion of pelitic matrix. Coarser grained (0.2 to 1 mm) arkosic quartzite with a relatively uniform grain size distribution appear macroscopically undeformed beyond 2 to 3 m from faults (e.g., bed A, Fig. 86). However, thin section study reveals embayed quartz-quartz grain contacts, fractured feldspars and growth of white mica along grain boundaries and adjacent to feldspars (Fig. 91). In contrast, quartzites with a bimodal grain size distribution (coarse quartz and

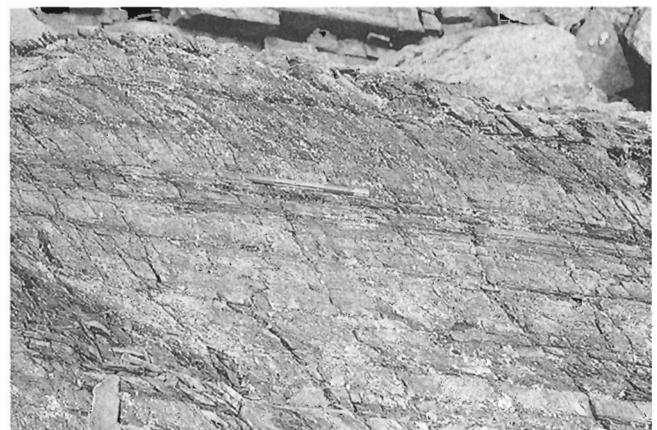


Figure 89. Slaty cleavage developed in a semipelitic from the lower Povungnituk Group 20 km southwest of lac Watts (thrust sheet M, Fig. 5). The cleavage is oblique to bedding (dipping to the right) which is marked by variations in the silica/mica/graphite ratio of the rock. Pen is 15 cm long. (GSC 1992-106W)

feldspar grains in a finer grained quartz-feldspar-mica matrix) have a macroscopically visible spaced cleavage (e.g., bed C, Fig. 86). The cleavage develops in the finer grained domains and is defined in thin section by seams of opaque minerals and aligned new grains of muscovite and chlorite (Fig. 87). Cleavage intensity increases substantially within about 2 to 3 m of faults, culminating in a penetrative layer-parallel cleavage in quartzite beds adjacent to faults.

Thin section observations on fault zone quartzites suggest that quartz deformation was accomplished by both pressure solution and dislocation creep while feldspar deformation was accomplished by cataclasis accompanied by the breakdown of feldspar to micas. Quartz microstructures include embayed grain contacts (Fig. 92), undulose extinction, optical subgrains, and some very fine grained mantles of quartz around detrital grains. Both plagioclase and K-feldspar deformed primarily by intragranular faulting along cleavages, and appear to have undergone breakdown reactions to white mica at the strain shadow ends and along the faults (Fig. 91). The occasional presence of very fine grained feldspar next to larger detrital clasts with serrated edges suggests that the clasts locally underwent

strain-induced grain boundary migration recrystallization (e.g., Tullis and Yund, 1985). These observations are consistent with early D₁ faulting occurring at relatively low temperatures. Early D₁ temperatures for these structural levels are bracketed between approximately 300°C (quartz brittle-ductile transition; Tullis and Yund, 1980) and 400°C (lower limit of biotite stability, given post-deformation growth of biotite porphyroblasts; Fig. 87).

The deformation of basalt in early D₁ fault zones included extensional and shear fracturing coupled with development of narrow, fault-parallel shear zones. Transgranular, dilatant fractures (Fig. 93) characterize deformation at the edge of the fault zones, generally 1 to 3 m away from the actual fault. Both extensional and shear fractures contain curved actinolite and chlorite fibres, suggesting a bulk shear

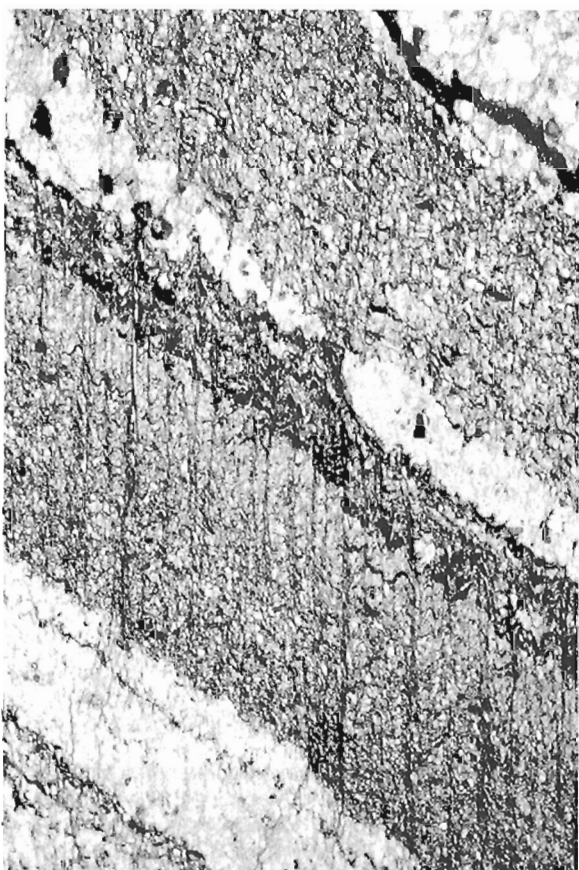


Figure 90. Photomicrograph of slaty cleavage in a semipelite of the lower Povungnituk Group, 8 km east of lac Vicenza (Fig. 5). The cleavage is axial planar to minor folds of bedding which are outlined by laminae of quartz and graphite. (GSC 1992-106D)

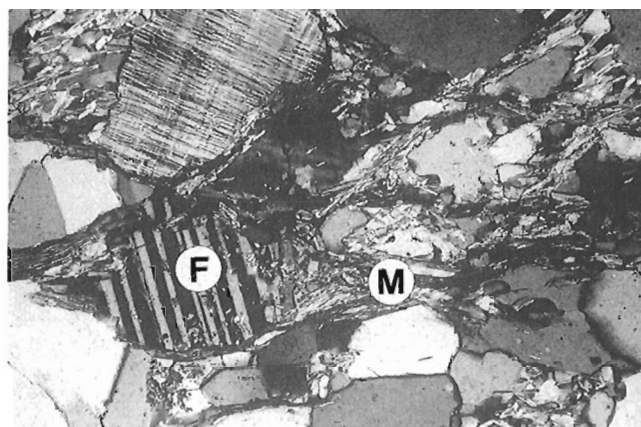


Figure 91. Photomicrograph of an arkosic quartzite from the lower Povungnituk Group, 8 km east of lac Vicenza (Fig. 5). Note the growth of white mica (M) along and adjacent to the feldspar grains (F). Horizontal field of view is 4 mm. (GSC 205208-E)

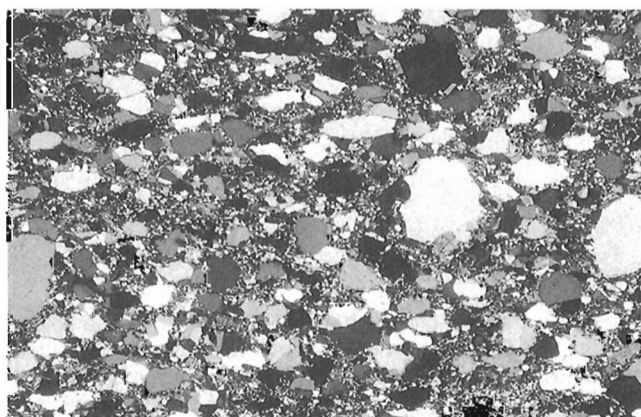


Figure 92. Photomicrograph of a quartzite from the lower Povungnituk Group 8 km east of lac Vicenza (Fig. 5). Where in mutual contact the larger quartz grains display embayed grain edges. The finer matrix comprises quartz, feldspar, biotite, and muscovite. Horizontal field of view is 10 mm. (GSC 1992-1020)

deformation. Intragranular fracturing occurs in actinolite grains (pseudomorphs of primary pyroxenes) adjacent to larger transgranular fractures, with actinolite fibres filling the dilatant fractures. Narrow (50 to 100 μm), fault-parallel shear zones increase in frequency towards the fault, but appear to form a penetrative foliation only within about 0.5 m of the fault. Shear zone foliations are characterized by actinolite and chlorite fibres growing on actinolite grain fragments produced by cataclasis, and by areas of extensive chlorite growth. The chlorite-rich areas may represent primary finer grained zones (e.g., chilled pillow or flow margins), suggesting that these may have played a role in determining where the shear zones initiated.



Figure 93. Photomicrograph of dilatant fractures filled with carbonate (C) in a metamorphosed basalt of the Povungnituk Group from thrust sheet L at the western margin of the map area (Fig. 5). Horizontal field of view is 8 mm. (GSC 1992-106S)

Most of the strain accumulated during early D_1 thrusting appears to have been partitioned into narrow zones immediately adjacent to the faults, and into finergrained sedimentary rocks away from the faults. Initial brittle deformation of pyroxene, amphibole, and plagioclase appears to have facilitated hydration reactions, resulting in growth of finer grained white mica, chlorite, and/or actinolite and the development of fault-parallel foliations (e.g., O'Hara, 1988). Fluid was most likely supplied by dehydration reactions in the sedimentary rocks and channelled along the thrust faults. Independent evidence for fluid movement along fault zones is given by the prevalence of quartz and quartz-carbonate veins within fault zones as compared to less-deformed rocks away from the fault zones.

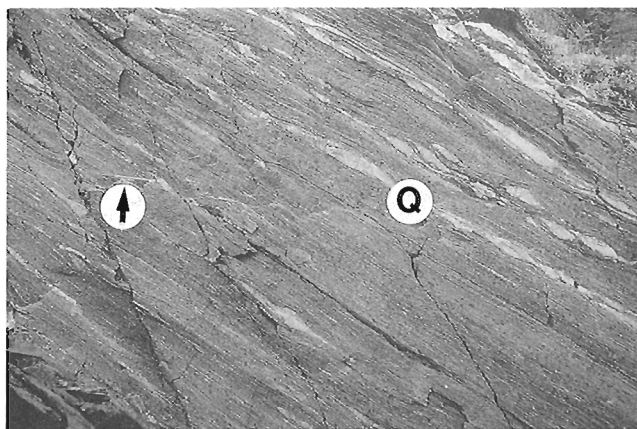


Figure 95. Micaceous quartzite (lower Povungnituk Group) with deformed quartz veins (Q) showing a well developed penetrative foliation dipping to the right-hand side of the photograph. The quartzite is in the basal shear zone on the west shore of Wakeham Bay (Fig. 82). All planar features (bedding, foliation, and quartz veins) are parallel. Arrow points to 15 cm pen. (GSC 204636-T)

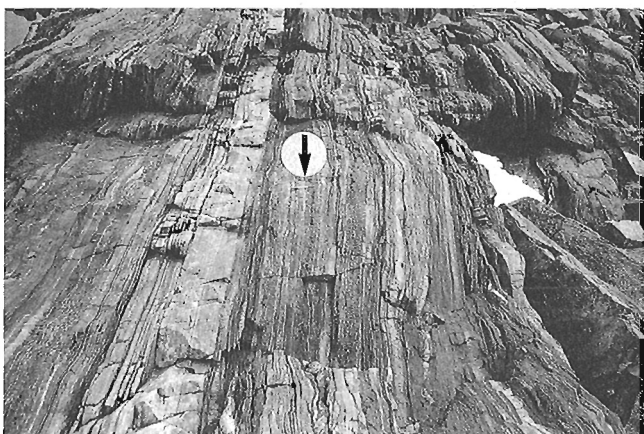


Figure 94. The D_1 basal shear zone (see text) on the east shore of Wakeham Bay (Fig. 82). The highly strained clastic sedimentary rocks and basites are part of the lower Povungnituk Group. The arrow points to a 15 cm long pen. (GSC 1992-106Y)

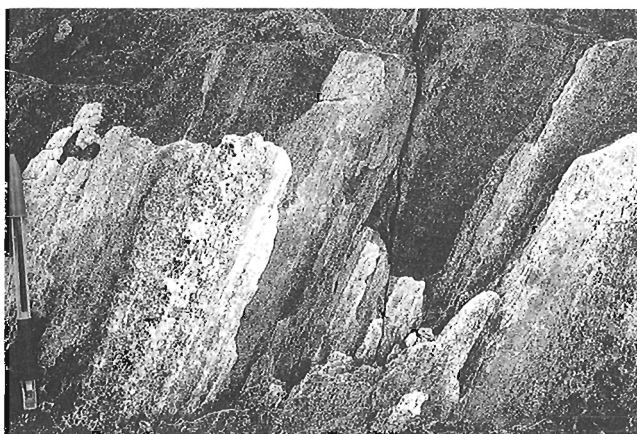


Figure 96. Quartz-plagioclase "smears" defining a transverse stretching lineation in the basal shear zone on the west shore of Wakeham Bay (Fig. 82). The lineation is developed in a mafic sedimentary rock of the lower Povungnituk Group. Pen is 15 cm long. (GSC 204233-C)

Basal shear zone

A ductile shear zone is present immediately adjacent to the basal décollement in the southern and eastern parts of the Cape Smith Belt (Fig. 82), and has been termed the basal shear zone (St-Onge et al., 1986; Lucas, 1989a, 1990). The shear zone crosscuts or deforms thrust faults of the early D₁ system (Fig. 82), and therefore must postdate the development of this thrust system. This interpretation is supported by observations of prethermal peak minerals overgrowing early D₁ foliations above the basal shear zone but growing and deforming within the shear zone itself. These relationships also suggest that during basal shear zone deformation the overlying early D₁ thrust sheets did not accumulate significant penetrative strain.



Figure 97. Deformed plagioclase phenocrysts defining a transverse stretching lineation in a deformed porphyritic basalt of the upper Povungnituk Group. Rock is from the basal shear zone on the west shore of Wakeham Bay (Fig. 82). Pen is 15 cm long. (GSC 204232-N)

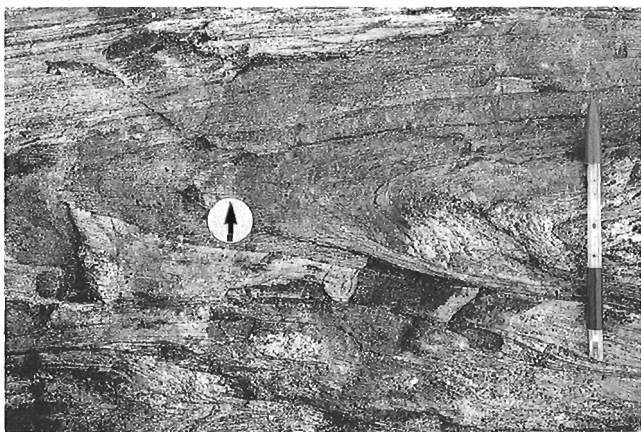


Figure 98. Tight fold of micaceous quartzite (lower Povungnituk Group) in the basal shear zone 30 km east of lac St-Germain (Fig. 82). The penetrative foliation which characterizes the basal shear zone is axial planar to the fold (arrow) and is defined by aligned biotite porphyroblasts. Pen is 15 cm long. (GSC 204232-R)

Map- and outcrop-scale structures

The basal shear zone is recognized at outcrop scale by a penetrative foliation (Fig. 94 and 95) and, in general, a stretching lineation (Fig. 96 and 97). Bedding and primary magmatic layering are transposed into the shear zone foliation (Fig. 98 and 99), which parallels the basement-cover contact (Fig. 82). These fabrics are developed in all Cape Smith Belt rocks within the shear zone except the interiors of the most competent ultramafic sills. Deformation of the sills in the shear zone occurred in at least one case by boudinage (Fig. 84; Lucas, 1989a). The separation of the boudins shown in Figure 84 represents an extension of approximately 100%, attesting to the severity of basal shear zone deformation.

The extent of the synmetamorphic basal shear zone (Fig. 82) was outlined using several field- and thin section-scale criteria (St-Onge et al., 1986; Lucas, 1989a, 1990). These criteria include: (1) presence of a well developed tectonic foliation and/or stretching lineation (Fig. 94 to 97); (2) parallelism of all planar features (e.g., bedding, foliation, quartz-veins; Fig. 95); (3) demonstrable or inferred strain-induced grain size reduction; (4) presence of non-coaxial flow indicators; (5) boudinage of competent bodies (e.g., the boudined mafic-ultramafic sill illustrated in Fig. 84); and (6) rotation of fold axes towards the transport direction (sheath fold development, Cobbold and Quinquis, 1980). Applying these criteria, the basal shear zone includes up to 5 km of clastic sedimentary rock and basalt directly above the basement/cover contact, and the uppermost 0.5 to 3 m of the gneisses below the basement/cover contact (described in the D₂ event for the Archean basement; Lucas, 1989a).

The basal shear zone contains a suite of kinematic indicators which document a top-to-the-south sense of movement (St-Onge et al., 1986; Lucas, 1989a; St-Onge and Lucas, 1990m). These asymmetric structures are found in both the thrust belt and basement rocks involved in the basal



Figure 99. Deformed pillowed basalt of the upper Povungnituk Group within the basal shear zone on the south shore of Wakeham Bay (Fig. 82). Pillow elongation is parallel to the penetrative foliation which characterizes the basal shear zone. Hammer is 34 cm long. (GSC 205208-L)

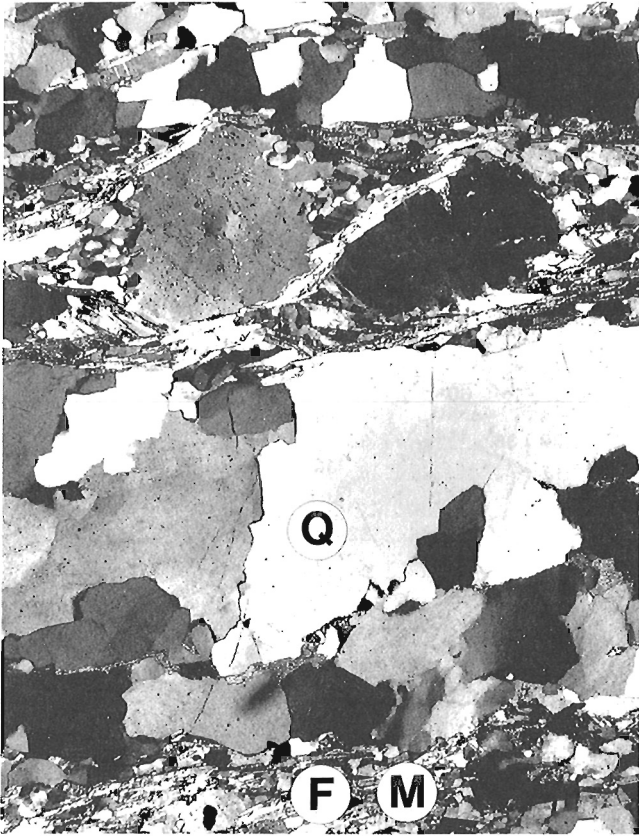


Figure 100. Photomicrograph of an arkosic quartzite of the lower Povungnituk Group deformed in the basal shear zone 10 km southwest of Wakeham Bay (Fig. 82). Compositional layering is defined by quartz (Q) and feldspar-mica (F, M) layers. Alignment of micas obliquely to the compositional layering defines "C/S" fabrics suggesting top-side-to-the-right displacement. Recrystallization at the margins of the feldspar porphyroclasts suggests that they deformed by dislocation creep (see text). Horizontal field of view is 15 mm. (GSC 204664-F)

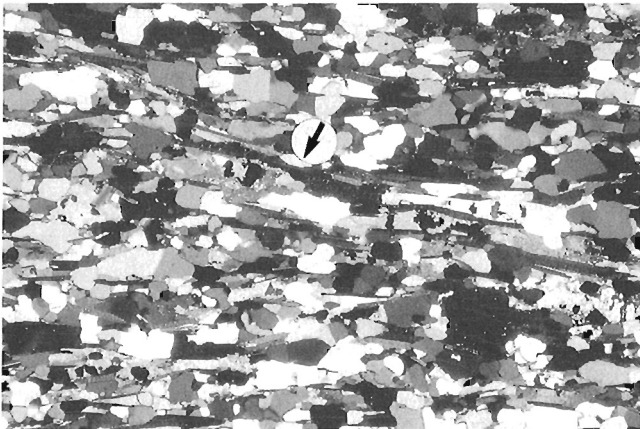


Figure 101. Photomicrograph of a shear band in micaceous quartzite of the lower Povungnituk Group. The shear band is defined by aligned muscovite (arrow). The quartzite is from the basal shear zone 10 km west of Joy Bay (Fig. 82). Horizontal field of view is 5 mm. (GSC 1992-106F)

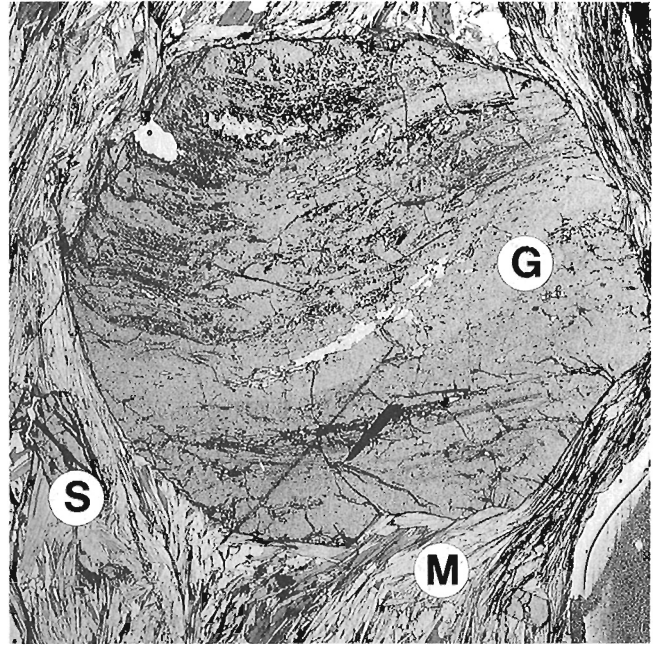


Figure 102. Photomicrograph of a garnet porphyroblast (G) in a muscovite (M) - staurolite (S) pelitic schist from the lower Povungnituk Group, 2 km west of Wakeham Bay (Fig. 5). The curved inclusion trails within the garnet record a significant amount of syn-growth rotation during deformation in the basal shear zone (see text). Horizontal field of view is 10 mm. (GSC 204234-D)

shear zone. The kinematic indicators that were used include (1) C/S fabrics (Fig. 100); Berthé et al., 1979); (2) shear band foliations (Fig. 101); White et al., 1980; Platt and Vissers, 1980); (3) porphyroblasts recording syn-growth rotation in the inclusion trails (Fig. 102); and (4) asymmetric folds of the shear zone fabric showing various stages of fold axis rotation into the shear direction. It should be noted that for any portion of the shear zone, a suite of kinematic indicators was employed to avoid potentially ambiguous individual observations (e.g., shear bands; Harris and Cobbold, 1985). However, all observations consistently gave the same, south-directed sense of shear.

Stretching lineations are well developed in the basal shear zone (Fig. 96 and 97) and record an approximately north-to-south shear flow direction (Fig. 103; Lucas, 1989a). The consistent presence and asymmetry of kinematic indicators in the XZ plane of shear zone finite strain ellipsoids demonstrates that the flow direction is parallel to the stretching (i.e., finite extension) direction. The mean north-northwest stretching lineation trend, unaffected by subsequent deformation, is best observed along the southern margin and the western boundary of the map area (Fig. 103). The parallelism of the early D₁ thrust transport direction (approximately north to south, as documented above) and the subsequent shear flow direction (south-southeastward) suggest that the tectonic transport direction did not vary significantly throughout the D₁ event.

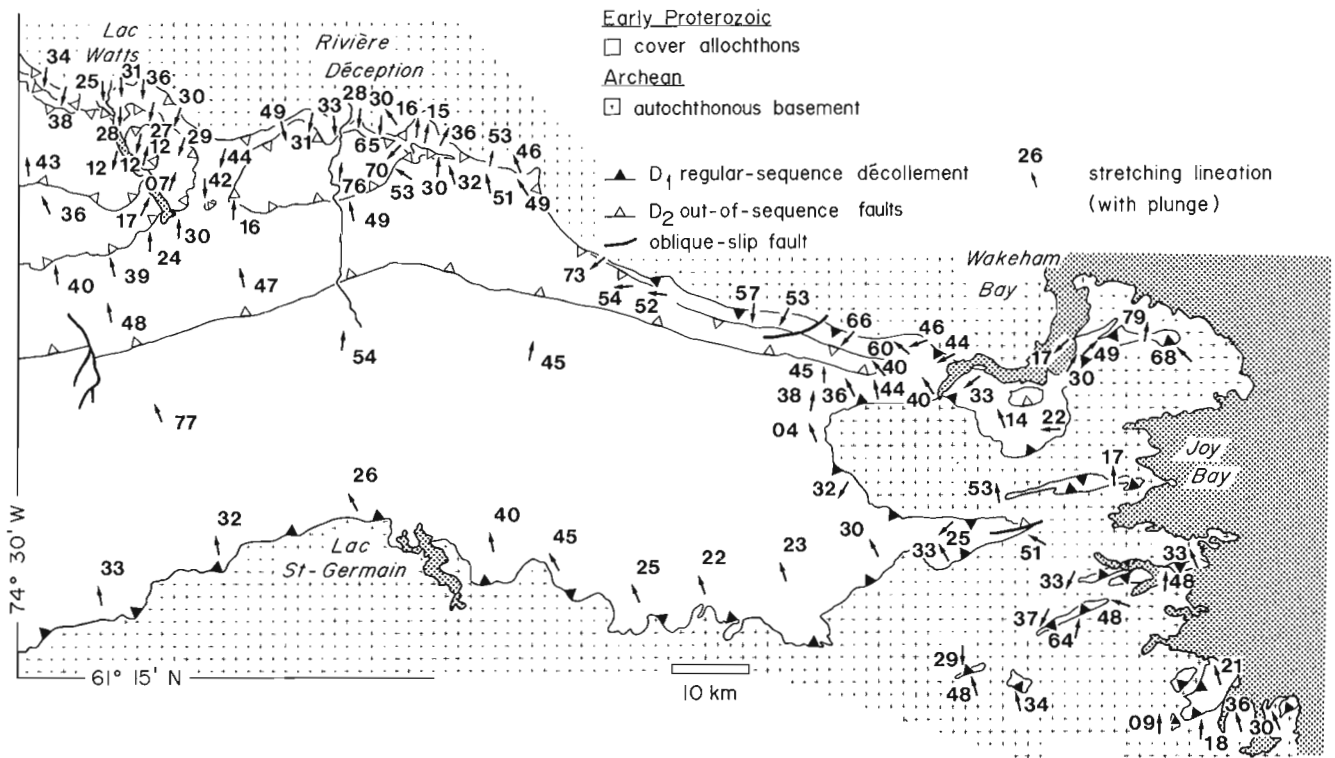


Figure 103. Compilation of the mean orientations of stretching lineations in the map area. Each arrow represents the Fisher vector mean of stretching lineation orientations in a domain (Lucas, 1989a,b). Arrows are plotted in the centre of the domains.

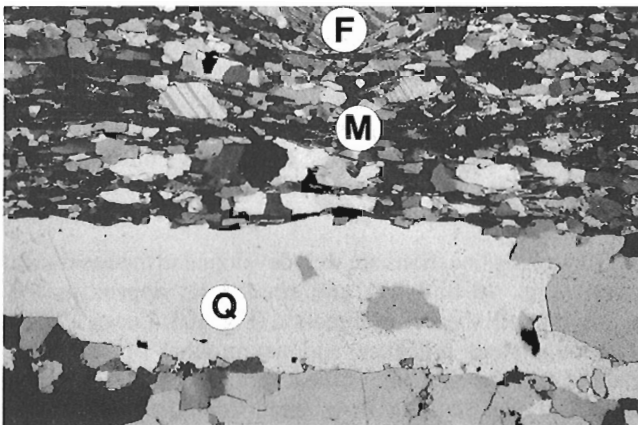


Figure 104. Photomicrograph of an arkosic quartzite of the lower Povungnituk Group in the basal shear zone 3 km west of Wakeham Bay (Fig. 82). Compositional layering is defined by alternating bands of recrystallized quartz (Q) and feldspar (F)/mica (M). Horizontal field of view is 3 mm. (GSC 1992-106J)

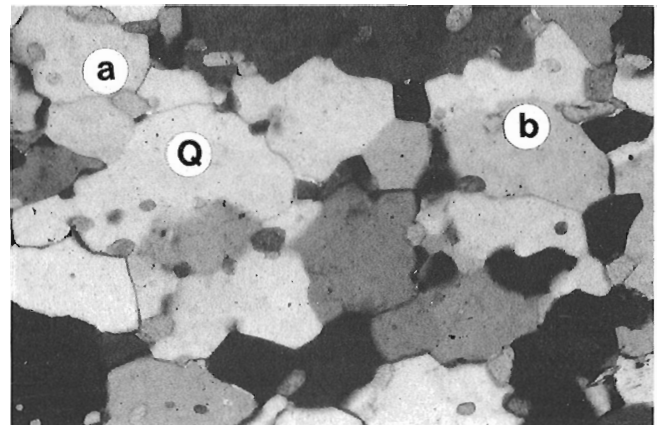


Figure 105. Photomicrograph of a quartzite from the lower Povungnituk Group, 3 km west of Wakeham Bay (thrust sheet B, Fig. 5). Locally the original carbonate cement is preserved at the junctions of several quartz grains (Q) such as in "a"; elsewhere the quartz grains have overgrown and entrapped the carbonate material such as in "b". The entrapped carbonate "blebs" are an indication that the quartzite underwent posttectonic annealing and grain growth (see text). Horizontal field of view is 4 mm. (GSC 1992-106E)

The trends of stretching lineations in the basal shear zone locally show a significant dispersion from the mean north-northwest/south-southeast trend (Fig. 103). The variable distribution can be attributed to deformation during the two post-D₁ events (Lucas, 1989a): (1) folding of the shear zone fabrics during the D₃ and D₄ episodes (discussed below) without any significant penetrative strain; and (2) passive rotation and transposition of D₁ fabrics into the axial plane of tight D₃ folds in zones of high D₃ penetrative strain. A good example of the fold limb dispersion effect (factor 1) is found in the lac Watts area (1721A; Fig. 103), where the D₃-D₄ dome-and-basin fold interference pattern is well developed near the basement/cover contact. The penetrative D₃ deformation effect (factor 2) is well illustrated along the tight northern keel from Wakeham Bay (1729A, 1728A) to the west (Fig. 104; see also Fig. 58 for the D₂ fold geometry).

The evolution from basal décollement to basal shear zone has been interpreted to represent a transition from discontinuous strain along a narrow fault zone to continuous ductile strain in a broad shear zone (Lucas, 1989a, 1990). Basal shear zone ductile deformation initiated at the basal décollement. Widening of the shear zone into the hanging wall and footwall of the décollement's is thought to result from strain- and metamorphism-induced softening at the base of the thrust belt (Lucas, 1989a, 1990). The growth of the basal shear zone was probably limited at the scale of the thrust belt by two lithological factors: (1) thick basalt sequences overlying the basal Povungnituk Group thrust sheets containing sedimentary rocks, and (2) "dry" Archean gneisses in the footwall basement. Povungnituk Group basalts appear to delimit the upward extent of the shear zone (compare Fig. 5 and 82). Lucas (1990) suggested that the contrast in yield strength between the sedimentary rocks and the overlying basalt was sufficient to partition most of the deformation into the sedimentary rocks of the lower Povungnituk Group.

Grain-scale structures

Povungnituk Group sedimentary rocks in the basal shear zone underwent a combination of grain size reduction and textural reconstitution due to both metamorphic reactions and deformation (Lucas, 1990). The outcrop appearance and microstructure of sedimentary rocks deformed in the shear zone can be compared directly with those in early D₁ fault zones because similar stratigraphic units can be traced from high structural levels down into the basal shear zone (Fig. 5 and 82). As an example, the well foliated quartzite-semipelite sequence in Figure 94 is stratigraphically equivalent to the variably cleaved sequence shown in Figure 86. The difference in deformation mechanisms and conditions is further emphasized when optical photomicrographs are compared for quartzite from an early D₁ fault zone (Fig. 87) and from the basal shear zone (Fig. 100).

The development of a thin section-scale compositional layering in arkosic quartzite deformed in the shear zone (e.g., Fig. 100 and 104) appears to result from dislocation creep deformation of both quartz and feldspar combined with the

growth of micas (Lucas, 1990). Climb-accommodated dislocation creep (Tullis and Yund, 1985) is interpreted to be the dominant deformation mechanism in quartz because it forms polycrystalline aggregates (Fig. 100 and 104) which appear to retain moderate crystallographic preferred orientations (as judged by a gypsum plate effect). The quartz grains within these aggregates are relatively coarse (1 to 5 mm), often with grain boundaries at high angles to the aggregates. This microstructure may result from syntectonic recrystallization at amphibolite grade conditions and/or from posttectonic annealing and grain growth (e.g., Fig. 105). In contrast, detrital plagioclase grains are preserved and are mantled by relatively small (100 to 250 μm) new grains at their strain shadow margins (Fig. 100). The morphology of the new grains coupled with their apparent crystallographic preferred orientation (strong gypsum plate effect) led Lucas (1990) to suggest that they were produced during recrystallization-accommodated dislocation creep (Tullis and Yund, 1985) of plagioclase. Growth of white mica and biotite is localized in the feldspar-rich layers of the shear zone quartzites (Fig. 100). The white mica probably results from the hydration and breakdown of feldspar, while biotite is most likely derived from reactions involving pelitic material in the sandstones. The presence of the micas may have restricted posttectonic growth of quartz and feldspar by "pinning" grain boundaries (Fig. 104 and 106; Lucas, 1990).

Complete reconstitution of primary igneous textures in basalt to penetrative foliations with plagioclase stretching lineations is attributed to both deformation and metamorphic processes (Lucas, 1990). Mafic rocks in the basal shear zone are virtually free of amphibole porphyroclasts. The syntectonic amphibole microstructure is dominated by oriented, elongate, fine grained crystals (Fig. 107). This suggests that the grain size reduction processes operative in

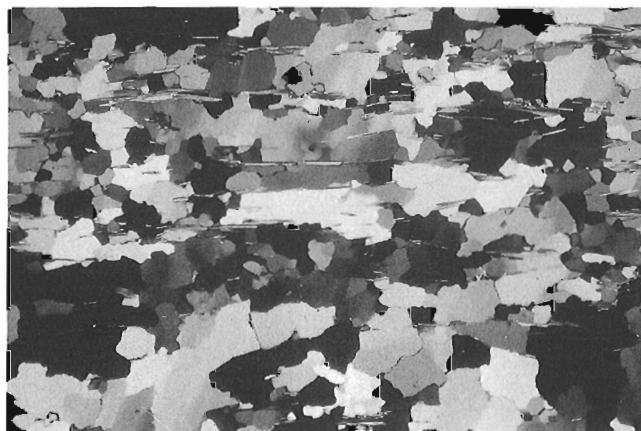


Figure 106. Photomicrograph of a quartzite from the lower Povungnituk Group 20 km east of the rivière Déception, a few metres south of the basement/cover contact (Fig. 5). The preservation of numerous small quartz grains defining the basal shear zone fabric is thought to be due to the presence of micas which may have restricted any posttectonic growth of quartz (i.e. Fig 104 and 105) by "pinning" the grain boundaries. Horizontal field of view is 10 mm. (GSC 204636-X)

the amphiboles (cataclasis, mineral reactions, and possibly intracrystalline plasticity) were able to completely destroy primary textures. Posttectonic mimetic growth of coarser actinolite and/or hornblende (0.5 to 1 mm) generally masks the older microstructure. The last growth increments are generally manifest as random crystals overgrowing the foliation (Fig. 108). The presence of fine grained (50 to 100 μm) aggregates of plagioclase grains in the basalt with an apparent crystallographic preferred orientation (strong gypsum plate effect) suggests that the feldspars probably deformed by recrystallization-accommodated dislocation creep.

Thermally-activated plastic deformation mechanisms appear to have replaced cataclastic ones in feldspar and (?) amphiboles as a result of continued D_1 deformation during prograde metamorphism. Feldspar in arkosic quartzite and basalt of the Povungnituk Group and in Archean basement gneisses exhibits optical microstructures consistent with early intragranular faulting (Fig. 70) being succeeded by recrystallization-accommodated dislocation creep (Fig. 70, 74, 100) during basal shear zone deformation (Lucas, 1990). The occurrence of pervasively foliated basalt from the Wakeham Bay area towards the northwest (Fig. 82) may reflect a transition from microcracking to intracrystalline plasticity as the most important deformation mechanism in hornblende (Lucas, 1990). Limited experimental and field evidence suggests that this transition should occur at about 600°C (see review by Brodie and Rutter, 1985), which corresponds to the peak temperatures for the Wakeham Bay area (Bégin, 1989a, 1992a; St-Onge and Lucas, 1990m; see below).



Figure 107. Photomicrograph of the basal shear zone fabric in a mafic volcanoclastic unit of the upper Povungnituk Group, 3 km west of Wakeham Bay (thrust sheet K, Fig. 5). The shear zone fabric is defined by the alignment of hornblende (H), epidote, chlorite, calcite, quartz and ilmenite. Horizontal field of view is 3.5 mm. (GSC 205165-A)

D₂ structures

Map- and outcrop-scale structures

Distinctive fault and fold structures that clearly postdate the development of the D_1 thrust faults have been mapped within the Povungnituk and Chukotat groups (St-Onge et al., 1987; Lucas, 1989a), and are here termed D_2 structures (Fig. 85). These structures can be linked to faults bounding units of the Watts and Spartan groups in the lac Watts (1721A) - rivière Déception (1722A) area of the Cape Smith Belt (Fig. 85). The D_2 faults have been described as out-of-sequence thrust faults (after Searle, 1985) based on their crosscutting relationships with the older, D_1 piggyback-sequence faults (Lucas, 1989a; St-Onge and Lucas, 1990m). Out-of-sequence faults in the eastern Cape Smith Belt were identified using several independent criteria (Lucas, 1989a). These include: (1) thrusts cutting down section in the transport direction, resulting in elimination of stratigraphic section in the footwall; (2) truncation of previously developed thrust structures in the footwall; and (3) truncation of metamorphic isograds. D_1 thrust faults may have been re-used during out-of-sequence (D_2) faulting but ductile (re)deformation of hanging wall and footwall rocks during D_2 faulting makes this difficult to prove.

Ductile deformation of rocks of the Povungnituk and Chukotat groups occurred adjacent to the out-of-sequence thrust faults (Lucas, 1990). In contrast to D_1 ductile shearing of these units, D_2 deformation occurred at thermal-peak conditions. It is difficult to determine when D_2 faulting began because of the synthermal peak nature of the

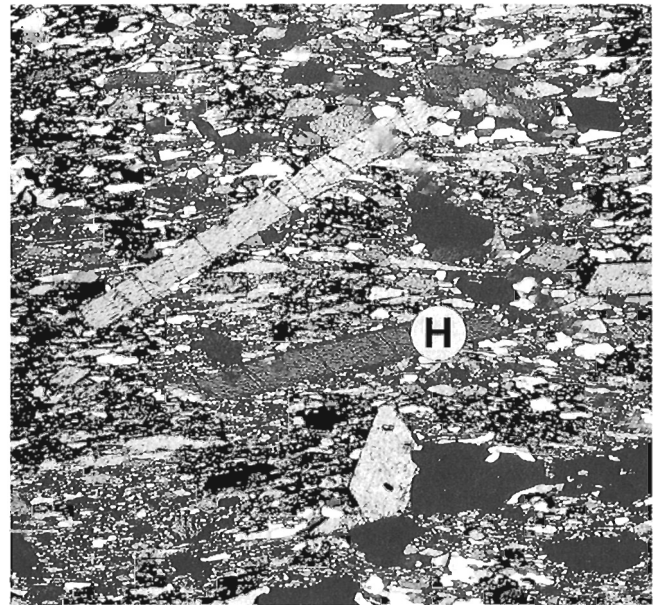
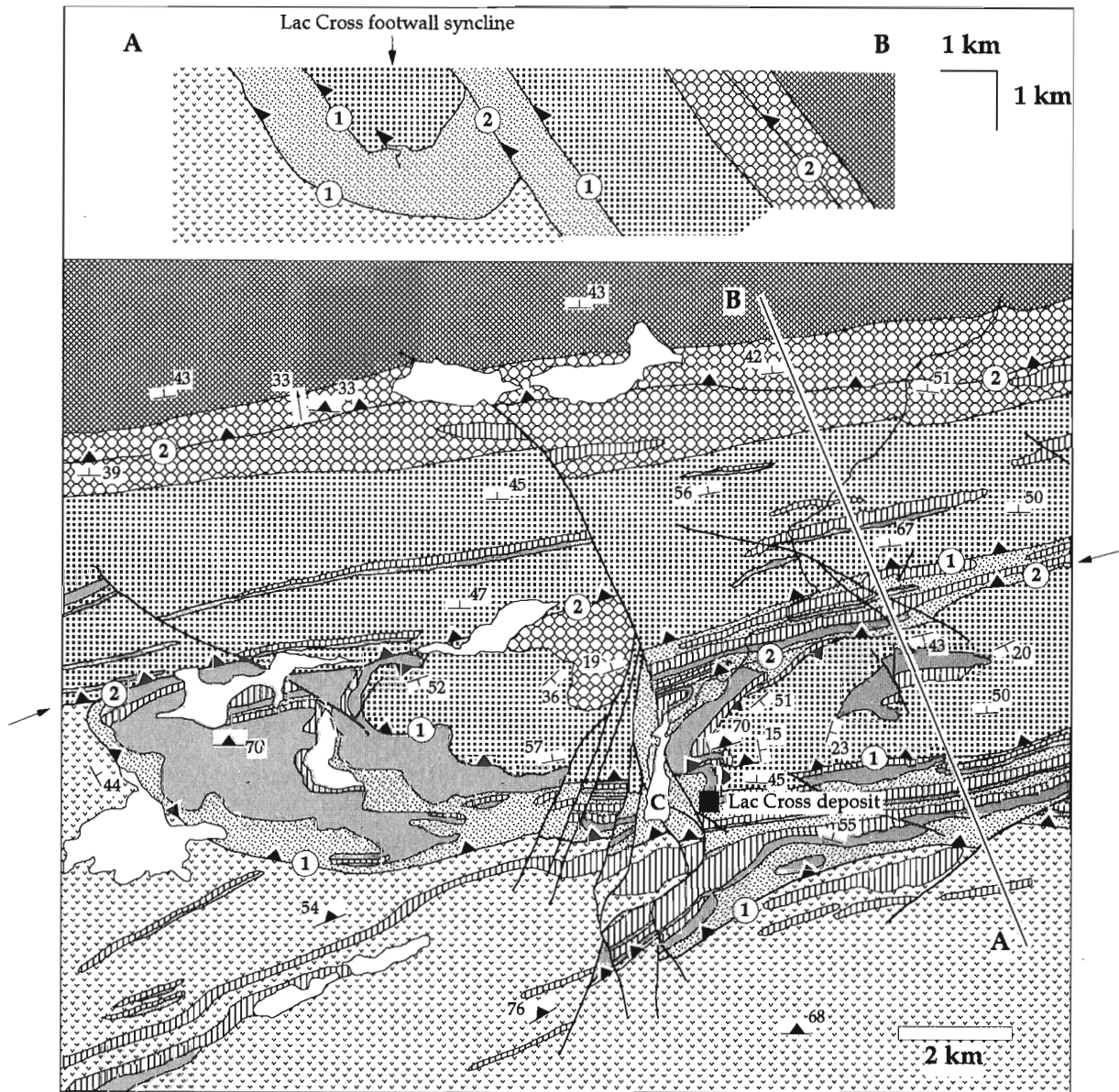







Figure 108. Photomicrograph of the basal shear zone fabric in a metabasalt from the upper Povungnituk Group 4 km west of Wakeham Bay (thrust sheet K, Fig. 5). The larger crystals of hornblende (H) randomly overgrow the shear zone fabric defined by the alignment of finer grains of hornblende, plagioclase, and epidote. Horizontal field of view is 2.5 mm. (GSC 204637-C)




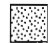
EARLY PROTEROZOIC





-  gabbro
-  peridotite


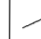

Chukotat Group

-  dominantly plagioclase-phyric basalt
-  dominantly pyroxene-phyric basalt
-  dominantly olivine-phyric basalt

Povungnituk Group

-  basalt, gabbro
-  semipelite, quartzite

-  oblique-slip fault
-  D₂ thrust fault
-  D₁ thrust fault
-  geological boundary

-  D₁ foliation
-  D₁ lineation
-  bedding

C lac Cross

Figure 109. Simplified geological map and downplunge constrained cross-section of the lac Cross area (1724A). Note the truncation of the early D₁ thrusts by the north-dipping, D₂ (out-of-sequence) thrust fault (arrows). The location of the map in the eastern Cape Smith Belt is indicated on Figure 85 by "a". Section line A-B represents the line along which the downplunge constrained strike perpendicular cross-section is hung.

deformation, but it is plausible that it was initiated during basal shear zone (D_1) deformation (Lucas, 1989a). Ductile shear zones developed both above and below the D_2 faults, affecting entire thrust sheets at the deepest structural levels (Povungnituk Group along the north margin of the Cape Smith Belt; Chukotat Group in footwall of thrust V east of rivière Déception; Fig. 5) but only narrow zones (<5 m) at higher structural levels (adjacent to thrust O, Fig. 5). The D_2 faults record a southward sense of displacement, based on an analysis of stretching lineation orientations coupled with outcrop and thin section observations of shear sense indicators (see the discussion of D_2 structures in the 'Watts and Spartan groups (domain 3) deformation history' below), parallel to that of the D_1 thrusts.

Deformation related to out-of-sequence thrusting at relatively high structural levels (lac Cross area, Fig. 85) is responsible for folding, faulting, and internally deforming D_1 thrust sheets. The structural evolution of the lac Cross area is documented in Figure 109 with a map and down plunge-constrained cross-section. A fault-propagation fold (Suppe, 1983) developed in front of the D_2 out-of-sequence fault and, as a result, folded the D_1 thrust faults. The out-of-sequence thrust then sliced the fault-propagation fold and stranded a footwall syncline at lac Cross (see cross-section, Fig. 109). Finally, tightening of the footwall syncline during deformation related to further displacement along the out-of-sequence fault resulted in development of (1) a north-dipping cleavage overprinting the fold, and (2) a south-verging out-of-syncline thrust in the core of the fold (Fig. 109). Footwall deformation at the relatively high

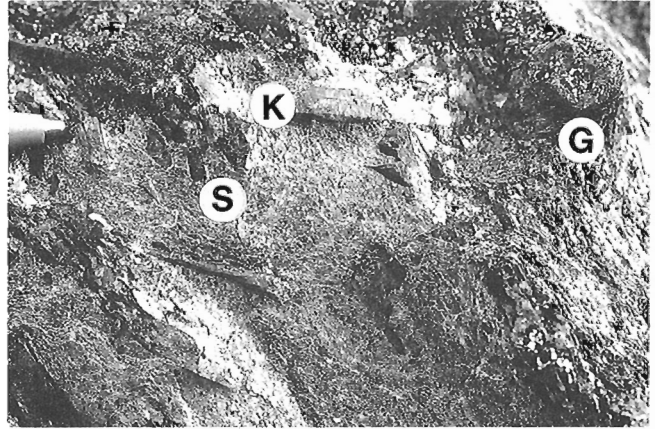


Figure 111. Posttectonic kyanite (K), garnet (G), and staurolite (S) in a muscovite-biotite pelitic schist from the lower Povungnituk Group 6 km west of Wakeham Bay (Fig. 5). Note that the higher temperature porphyroblasts (kyanite, garnet, and staurolite) overprint the lower temperature basal shear zone fabric defined by the alignment of biotite and muscovite. Tip of pen is 2 mm wide. (GSC 204232-Y)

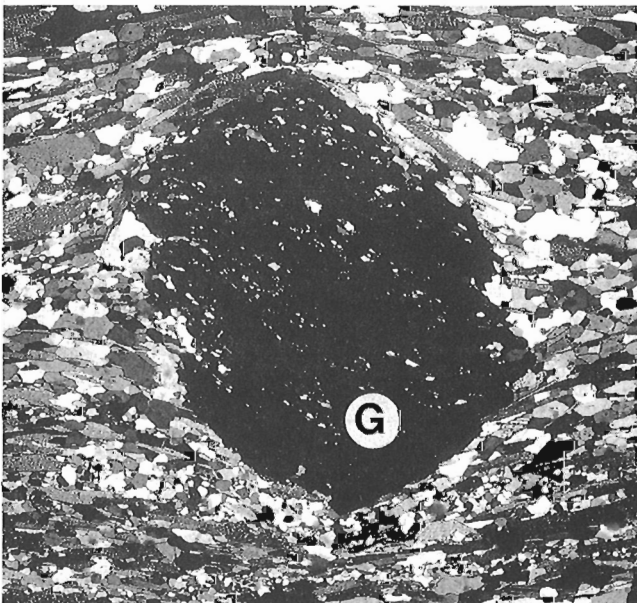


Figure 110. Photomicrograph of a syntectonic garnet (G) in a prograde D_2 shear zone 5 km northeast of lac Watts (Fig. 82). The shear zone fabric in the semipelite from the lower Povungnituk Group is defined by the alignment of biotite, plagioclase, and quartz. Note that inclusion trails within the garnet are continuous with the matrix foliation. Horizontal field of view is 7 mm. (GSC 205165-C)

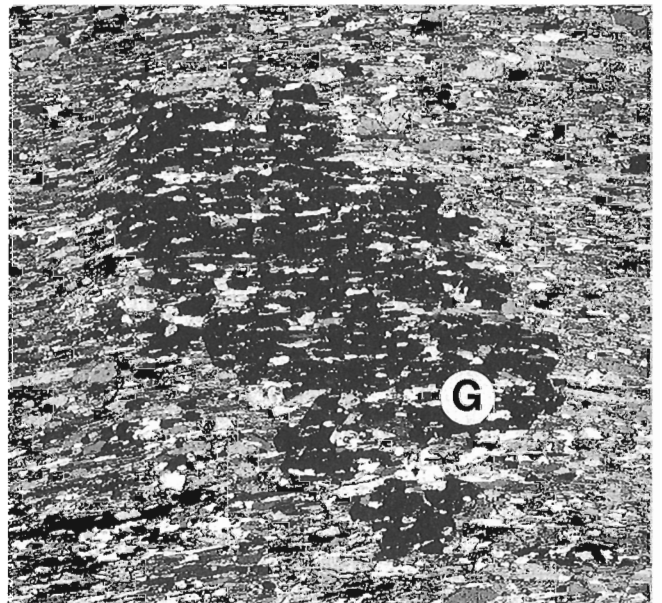


Figure 112. Photomicrograph of a thermal peak garnet (G) statically overgrowing the basal shear zone fabric in a metabasalt of the upper Povungnituk Group. Sample is from the basal shear zone on the south shore of Wakeham Bay (Fig. 82). The shear zone fabric is defined by the alignment of hornblende, plagioclase, and ilmenite. Horizontal field of view is 15 mm. (GSC 205165-B)

structural level of lac Cross is thus primarily limited to the rocks involved in the fault-propagation syncline. At least 7.5 km of hanging wall uplift (relative to footwall rocks) must have occurred during movement on this D₂ fault as a result of ramping through rocks of both the Povungnituk and Chukotat groups (Fig. 58; Lucas, 1989a).

Footwall cut-off angles for D₂ faults measured on the composite down-plunge cross-section (Fig. 58) average 25° in Chukotat Group basalt, 20° in Povungnituk Group sedimentary rocks, and 10° in Povungnituk Group basalt.

Grain-scale structures

Microstructural studies of sedimentary and mafic rocks in D₂ shear zones clearly show that the thermal peak minerals are both deformed and growing in the foliation (Fig. 110). In contrast, Povungnituk and Chukotat group units unaffected by D₂ penetrative deformation (e.g., Wakeham Bay area, Fig. 82) are marked by the static growth of thermal-peak porphyroblasts over the D₁ foliation (Fig. 111 and 112). Greenschist grade shear zones developed adjacent to the most external (southern) portions of the out-of-sequence thrust faults (O and R, south of Lac Watts, Fig. 85). The shear zones are relatively narrow (1 to 5 m wide), and are characterized by the development of a penetrative fault-parallel foliation destroying primary volcanic or sedimentary structures (compare Fig. 32 and 113).

The transition between relatively undeformed pillow basalt (Fig. 32) and a shear zone marked by mafic schist (Fig. 113) has been studied along thrust S (Fig. 85; Lucas, 1990). For each fault, the mafic schist is characterized by millimetre-scale compositional banding, defined by alternating layers of actinolite-chlorite, plagioclase, and calcite (Fig. 114). Microstructural changes with increasing strain (i.e., towards the fault) in the basalt include (1) rotation and oriented growth of actinolite and chlorite; (2) development

of actinolite-chlorite and plagioclase layers (Fig. 114); (3) transposition of calcite±quartz±plagioclase veins (Fig. 114); and (4) an overall decrease in the thickness and increase in the regularity of the compositional layers. Processes contributing to the development of the compositional layering in metabasalt may include metamorphic reactions aided by stress-induced diffusion transfer (e.g., Robin, 1979), and ductile deformation of plagioclase, quartz, and calcite (Lucas, 1990). Penetrative deformation of Chukotat Group basalt in the footwall of thrust V south of lac Watts (Fig. 85) is limited to within 3 m of the fault, and records a similar microstructural evolution to thrust S involving calcite veining, vein transposition and oriented chlorite growth (Fig. 115; Lucas, 1990).

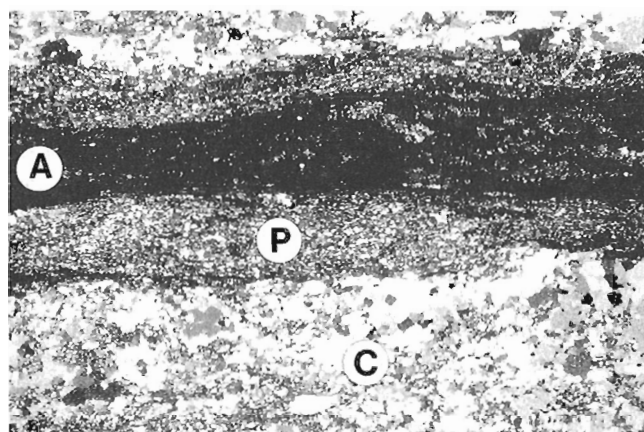


Figure 114. Photomicrograph of the mafic schist along thrust fault S 12 km south of lac Watts (Fig. 85). The schist is characterized by millimetre-scale compositional banding defined by layers of actinolite-chlorite (A), plagioclase (P) and calcite±quartz±plagioclase (C). Horizontal field of view is 12 mm. (GSC 204832-B)

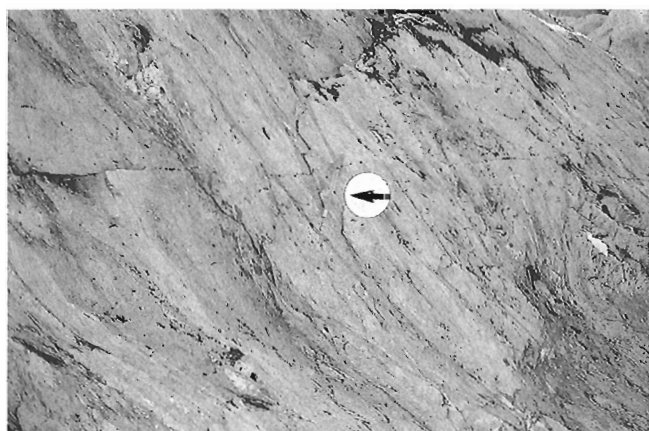


Figure 113. Deformed pyroxene-phryic pillowed basalt of the Chukotat Group. Deformation zone is in the footwall of the D₂ out-of-sequence fault S, 12 km south of lac Watts (Fig. 85). Arrow points to 15 cm long pen. (GSC 204233-Y)

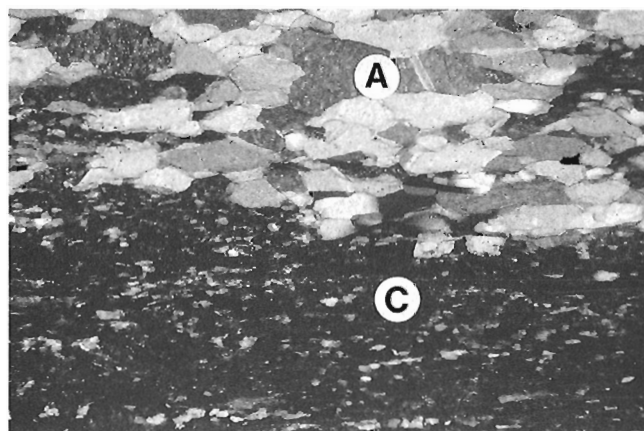


Figure 115. Photomicrograph of deformed Chukotat Group basalt in the footwall of thrust V, 3 km south of lac Watts (Fig. 85). Layering is defined by actinolite-chlorite-plagioclase (C) bands and transposed calcite veins (A). Horizontal field of view is 3 mm. (GSC 1992-106P)

WATTS AND SPARTAN GROUPS (DOMAIN 3) DEFORMATION HISTORY

D₁ structures

The oldest structures mapped in the the Watts and Spartan groups are faults which are cut by an 1888 Ma tonalite pluton (west side of lac Watts, Fig. 40; Parrish, 1989; St-Onge and Lucas, 1990m; St-Onge et al., 1992). The faults juxtapose layered gabbro and peridotite of the Watts Group (hanging wall) against basalt and sedimentary rocks of the Spartan and Watts groups (footwall), suggesting that they may be thrusts (St-Onge et al., 1988b; Lucas and St-Onge, 1992). A foliation which predates the thermal peak of metamorphism is developed adjacent to the faults.

The nature of the proposed pre-1888 Ma (*D₁*) deformation in the Watts and Spartan groups is not well understood. Except for the faults described above, fabrics or other structures potentially related to *D₁* deformation are not recognized in the two tectonostratigraphic groups. It is plausible that the accreted portions of the two groups may have largely escaped the intense syn-plutonic deformation and granulite-grade metamorphism documented to the north in the Narsajuaq arc (Fig. 1; Lucas and St-Onge, 1992). Such an explanation can be considered if the Watts and Spartan groups represent relatively outboard fragments of the arc complex (Lucas et al., 1992; St-Onge et al., 1992). The pre-1888 Ma structures may thus be the products of deformation external or possibly even unrelated to the principal Narsajuaq arc deformation zone (e.g., accretionary prism deformation; Lucas and St-Onge, 1992).

D₂ structures

Two distinct systems of *D₂* faults have been mapped in the Watts and Spartan groups: (1) pre- to syn-thermal peak (abbreviated to thermal peak), and (2) post-thermal peak (Fig. 85). The relative ages of these two systems were established on the basis of the metamorphic grade of fault zone mineral assemblages, and the truncation relationships between intersecting faults. Both systems of *D₂* faults are responsible for reformation of pre-existing structures in the northern (internal) part of the Cape Smith Belt. The internal part of the Cape Smith Belt is considered to be all units in the hanging wall of the most southerly out-of-sequence fault (fault O, Fig. 5). The structural position of the two fault systems appears to vary with age: the youngest (post-thermal peak) faults are the structurally highest and the most internal (northern) (Fig. 85).

Thermal peak fault system

Map- and outcrop-scale structures

Detailed mapping of the thermal peak out-of-sequence faults in the Cape Smith Belt documents their role as basal thrusts for the Watts and Spartan groups (Lucas 1989a; St-Onge and Lucas 1990m; Lucas and St-Onge, 1992). These *D₂* faults in general emplace units of the Watts and Spartan groups on either Povungnituk Group sedimentary and mafic rocks

(northern margin of the Cape Smith Belt, Fig. 5) or Chukotat Group basalt (along the orogen-scale fault V; Fig. 1 and 5). The *D₂* faults along the northern margin of the Cape Smith Belt can be traced southward as out-of-sequence thrust faults (described above) which re-imbricate Povungnituk and Chukotat Group units (see above; Fig. 5, 85, and 109). Structurally higher *D₂* thermal peak faults in the lac Watts (1721A) - rivière Déception (1722A) area are truncated off by an overlying post-thermal peak *D₂* fault (Fig. 82 and 85).

Detailed mapping has also shown that the faults carrying thrust slices of Archean basement into the Cape Smith Belt along its northern margin (see above) are contiguous with or cut by thermal peak *D₂* faults bounding imbricates of the Watts and Povungnituk groups (Fig. 77 and 80). The zone of interleaving of basement, Povungnituk Group, and Watts Group rocks appears to have an overall duplex geometry (east of rivière Déception (1722A, 1723A), Fig. 77; Lucas, 1989a). The Watts Group ophiolitic rocks locally lie directly on basement, indicating that their basal fault can at least locally displace the pre-existing Povungnituk and Chukotat groups thrust stack preserved in the southern portion of the Cape Smith Belt (Lucas, 1989a). Along the northern margin of the belt, both the hanging wall and footwall of the *D₂* faults are characterized by highly deformed, mylonitic rocks (Fig. 116 and 117; Lucas, 1990) consistent with the relatively deep structural levels exposed (ca. 1 GPa peak pressures; St-Onge and Lucas, 1991).

The thermal peak *D₂* faults record a southward sense of displacement, based on an analysis of stretching lineation orientations (Fig. 103 and 118) coupled with outcrop and thin section observations of shear sense indicators (Lucas, 1989a). A south-directed displacement sense is recorded by a suite of kinematic indicators in the ductile shear zones adjacent to the faults (Lucas, 1989a). The principal kinematic indicators preserved in the thermal peak shear zones are (1) C/S fabrics (Berthé et al., 1979), (2) shear bands (Fig. 119; White, et al., 1980; Platt and Vissers, 1980) and

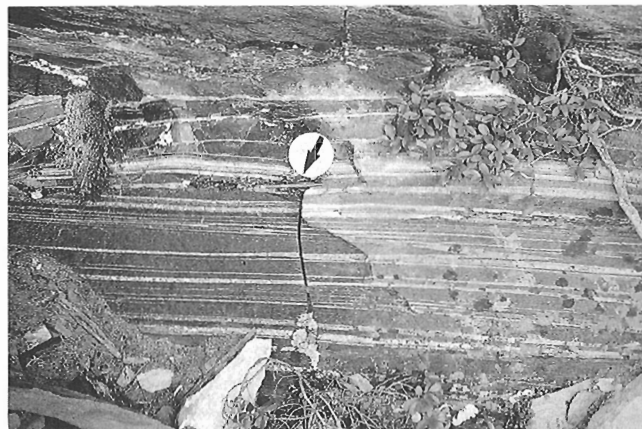


Figure 116. Straight gneiss derived from a Watts Group layered gabbro. The ductile high-strain zone is found in the hanging wall of a *D₂* thermal peak fault, on the west shore of lac Watts (Fig. 85). Arrow points to 15 cm long pen. (GSC 204233-U)

(3) rotated syn-deformation porphyroblasts (Fig. 120). The southward sense of displacement for the D₂ thrusts is parallel to that documented for the D₁ and D₂ thrusts in the Povungnituk and Chukotat groups.

The kinematics and regional geometry of the D₂ thermal peak faults involving the Watts and Spartan groups are consistent with their interpretation as thrust faults (St-Onge et al., 1988b; Lucas, 1989a; St-Onge and Lucas, 1990m; Lucas and St-Onge, 1992). Furthermore, stretching lineations in the ductile shear zones associated with these D₂ thrusts are parallel to the north-northwest-trending lineations that characterize the older basal shear zone to the southeast (Fig. 103). This suggests that a relatively constant tectonic transport direction was maintained during the D₁-D₂ (Povungnituk and Chukotat groups) and D₂ (Watts and Spartan groups) deformation episodes (see Table 2; Lucas,



Figure 117. Sheath fold of Povungnituk Group quartzite, 20 km east of rivière Déception (thrust sheet U, Fig. 5). The sheath fold structures are in the hanging wall of a thermal peak D₂ thrust fault. Arrow points to 15 cm pen. (GSC 204234-M)



Figure 118. D₂ stretching lineation in a quartzite of the lower Povungnituk Group from the northern margin of the Cape Smith Belt west of rivière Déception (Fig. 5). The stretching lineation is defined by the rodding of quartz and feldspar in the principal shear zone foliation plane. Pen is 15 cm long. (GSC 204233-P)

1989a; Lucas and St-Onge, 1992). A minimum displacement estimate of 50-100 km for the thermal peak (D₂) thrust system indicates that it was responsible for significant translation of Watts and Spartan groups rocks in the internal part of the Cape Smith Belt (Lucas, 1989a). In the absence of corresponding hanging wall and footwall cut-offs, this estimate is based on measurements of fault length parallel to the movement direction (i.e., in the cross-section, Fig. 58). The displacement estimate is of the same order of magnitude as that inferred for the D₁ basal décollement (Povungnituk and Chukotat groups) described above.

Grain-scale structures

All units of the Watts and Spartan groups between the northern margin of the belt and thrust fault V (Fig. 5) are ductily-deformed in shear zones associated with the thermal peak D₂ thrusts. Both the thermal peak faults and shear zones are truncated and/or reworked against the post-thermal peak D₂ faults (Fig. 82 and 85). Microstructural studies of Spartan Group sedimentary units and Watts Group basalt and mafic/ultramafic plutonic rocks in these shear zones clearly show that the thermal peak minerals are both deformed and growing in the foliation (e.g. Fig. 119 and 120; Lucas, 1990).

Thrust fault V, a D₂ thermal peak thrust (Fig. 85) exposed at intermediate structural levels of the thrust system (Fig. 58) is characterized by a penetratively deformed hanging wall and an essentially undeformed footwall. Spartan Group sedimentary rocks (hanging wall) have a fault-parallel foliation which results from bulk shear deformation during fault movement at upper greenschist grade (Lucas, 1990).

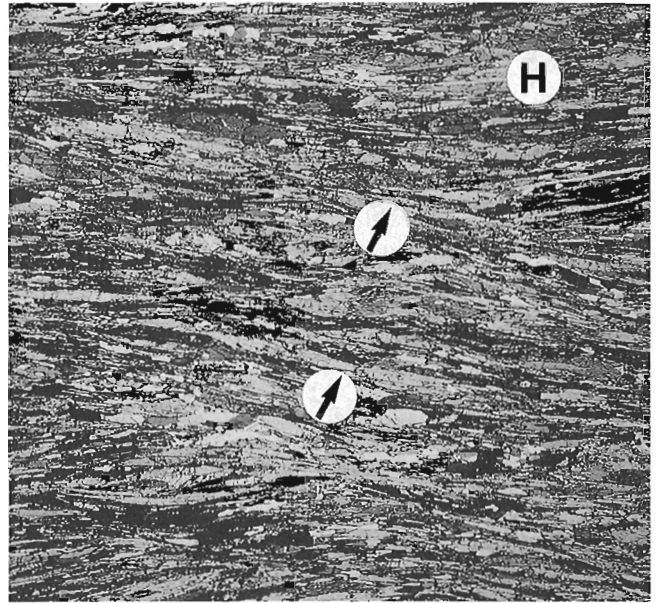


Figure 119. Photomicrograph of a shear band fabric in a deformed gabbro of the Watts Group 4 km west of lac Watts (Fig. 5). The D₂ thermal peak foliation is defined by the alignment of hornblende (H) crystals and the shear bands (arrows) indicate a top-side-to-the-right (south) translation. Horizontal field of view is 11 mm. (GSC 204637-D)

Foliation development was accomplished by dislocation creep of quartz in Spartan Group quartzites. In semipelites and pelites, it was accomplished by a combination of growth and rotation of micas, and pressure solution and dislocation creep of quartz. Hanging wall pelites immediately adjacent to the fault (within 3 m) are characterized by an intense foliation (slaty cleavage) and lineation, and by abundant deformed quartz veins (Fig. 121).

The northern part of the D₂ thermal peak thrust system (north of thrust sheet V, Fig. 85) is marked by a broad region of penetratively deformed, well lineated metamorphic rocks derived from Watts Group (ophiolitic) units (Fig. 5). Relict thermal peak assemblages in the overlying post-thermal peak shear zones (Fig. 82) suggest that the thermal peak tectonites were probably much more extensively developed than is preserved in the Cape Smith Belt (Lucas, 1989a). The bulk shear deformation was accomplished by cataclasis

(plagioclase and hornblende), dynamic recrystallization (plagioclase and possibly hornblende; Fig. 122) and climb-accommodated dislocation creep (quartz) (Lucas, 1990). Amphibole-, clinozoisite- and phyllosilicate-producing reactions contributed to foliation development through the growth and subsequent rotation of elongate, oriented crystals (e.g., hornblende and clinozoisite, Fig. 120 and 123). The presence of rotated minerals (e.g. garnet, Fig. 120) and oblique fabrics (e.g. C/S) with consistent asymmetries suggest that the shear zones record a component of non-coaxial deformation (discussed above).

The thermal peak shear zones appear relatively homogeneous at map-scale (Fig. 82) but are in fact heterogeneous at smaller scales as a result of deformation partitioning in the compositionally layered rocks (Lucas, 1990). Deformation partitioning results from ductility contrasts between materials, and can occur at scales varying

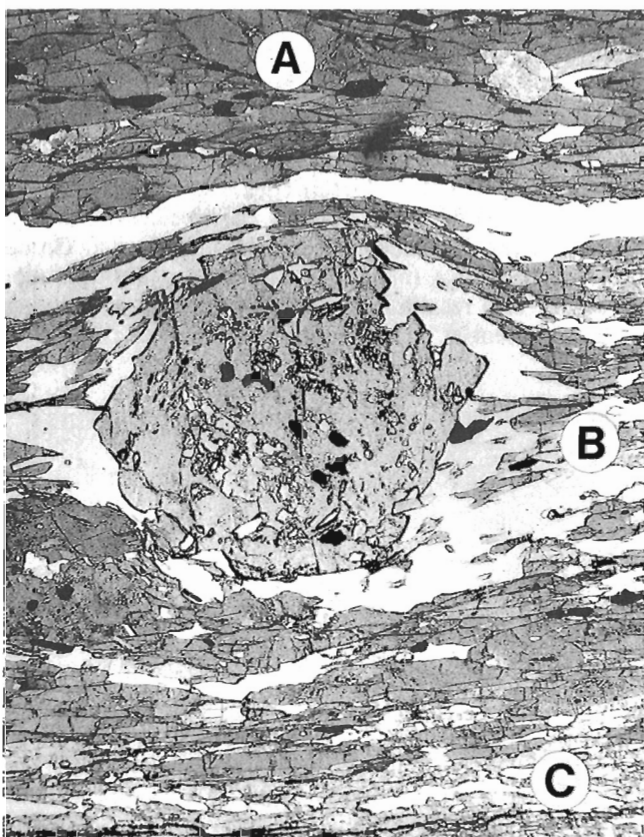


Figure 120. Photomicrograph of a metamorphosed layered gabbro from the Watts Group 2 km west of rivière Déception and three kilometres south of the basement/cover contact (Fig. 5). The syntectonic garnet indicates a top-to-the-left (south) sense of shear, consistent with the south-directed shear sense reported from other kinematic indicators in the D₂ out-of-sequence shear zones. Three compositional layers are present: (A) hornblende layer, (B) hornblende-plagioclase-quartz-garnet layer; and (C) clinozoisite-plagioclase-chlorite layer. The syntectonic nature of all metamorphic phases indicates that deformation occurred at thermal peak conditions. Horizontal field of view is 18 mm. (GSC 204664-B)

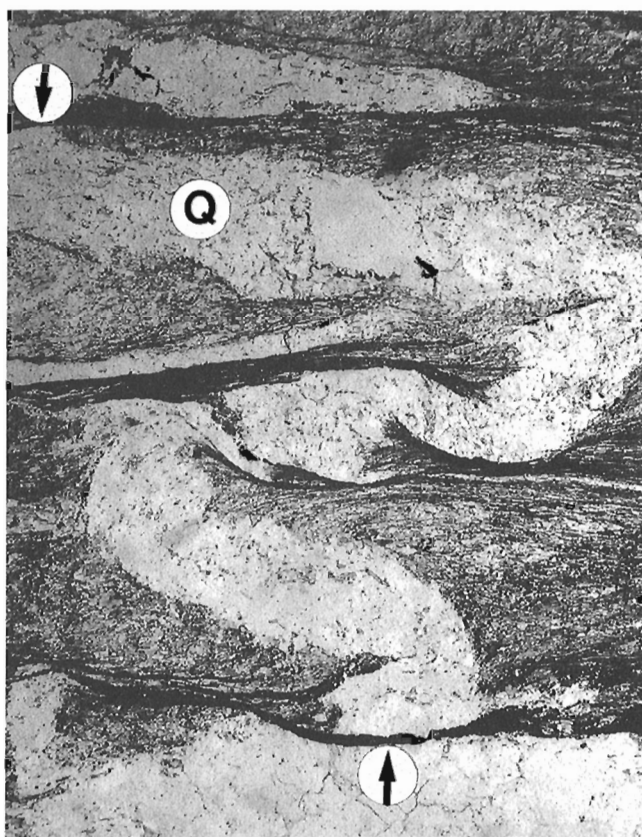


Figure 121. Photomicrograph of a deformed quartz vein (Q) in a pelite of the Spartan Group. The sample is from the hanging wall of out-of-sequence thrust V south of lac Watts (Fig. 5 and 85). Synthrusting quartz veins are folded and possibly faulted, although the apparent offsets (see arrows) may simply reflect volume loss during pressure solution-accommodated deformation of the veins. The pelite itself has an intense pressure solution cleavage defined in part by oriented muscovite crystallites. Horizontal field of view is 14 mm. (GSC 204664-H)

from individual grains to crustal layers (Bell, 1981, 1985). Compositional layering in the Watts Group ophiolitic rocks was either generated (e.g., in basalt) or enhanced (e.g., in layered gabbro, Fig. 124) during the bulk shear deformation. Processes which may have generated layering or enhanced pre-existing layering include (Lucas, 1990): (1) metamorphic reactions which may change the grain size and/or strengths of products relative to reactants; (2) metamorphic segregation or stress-induced diffusion transfer between phases of differing strength and solubility (Robin, 1979; Sawyer and Robin, 1986); and (3) mechanical differentiation of phases with differing strengths in which a weak phase can effectively isolate grains of the stronger phase (Sclar, 1965; Shelley, 1974; Dell'Angelo and Tullis, 1982). An example of the inter-relationship between compositional layering and deformation partitioning is shown in Figure 122: mechanical differentiation leads to the development of hornblende and plagioclase-zoisite layers, with the result that deformation is accommodated largely by the plagioclase-zoisite layers (Lucas, 1990).



Figure 122. Heterogeneous deformation of a layered gabbro from the Watts Group at the north end of lac Watts (Fig. 5). Hornblende tails (black) are developed adjacent to coarse hornblende porphyroclasts. White bands are zoisite-plagioclase. Ductile shear deformation is associated with movement on an underlying D₂ out-of-sequence fault at amphibolite grade (thermal peak) conditions. Length of pencil is 3.5 cm. (GSC 204636-K)

Post-thermal peak fault system

Map- and outcrop-scale structures

Two major post-thermal peak faults (Fig. 125) are present in the lac Watts (1721A)-rivière Déception (1722A) area (Fig. 85; Lucas, 1989a; St-Onge and Lucas, 1990m). These faults are responsible for the final southward displacement of the ophiolitic rocks relative to footwall units of the Spartan and Povungnituk groups. The faults bound "klippen" of Watts Group basalt, sheeted dykes and mafic and ultramafic cumulates (Fig. 5) which sit on top of D₂ thrust sheets. These faults invert the stratigraphic order of the Watts Group

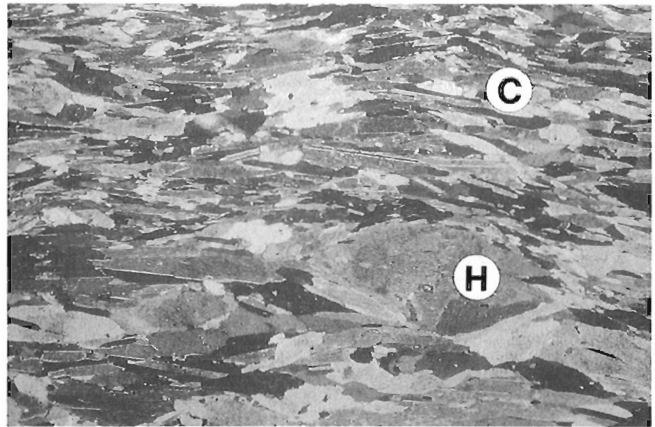


Figure 123. Photomicrograph of the D₂ shear zone foliation in a gabbro of the Watts Group, east shore of lac Watts (Fig. 5). The foliation which developed at thermal peak conditions is defined by the alignment of hornblende (H) and clinozoisite (C) crystals. Horizontal field of view is 3 mm. (GSC 204637-A)

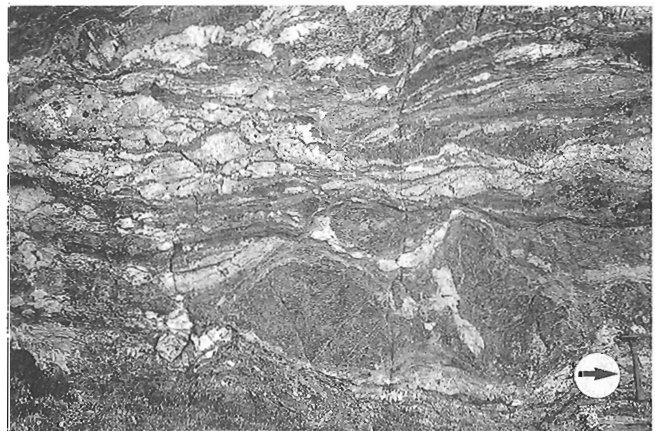


Figure 124. Sheared and boudined layered gabbro from the Watts Group, east shore of lac Watts (Fig. 5). Disaggregated white layers are plagioclase-clinozoisite-rich; dark layers contain hornblende-actinolite-plagioclase. The two large boudins in the lower centre-right of the photograph are metapyroxenite. The arrow points to a 34 cm long hammer. (GSC 204233-S)

ophiolite, placing layered gabbro (sheet BB, Fig. 5) on top of pillowed basalt and sheeted dykes (sheet Y; Fig. 5; Lucas, 1989a). The relative ages of the two principal post-thermal peak faults could not be determined because they do not intersect or interact within the Cape Smith Belt (Fig. 5 and 85).

The post-thermal peak faults are characterized by their (1) truncation of footwall thermal peak (D_2) thrusts, and (2) syn-movement growth of post-thermal peak mineral assemblages in the ductile shear zones that developed adjacent to the faults. Shear zones associated with the post-thermal peak faults appear to record a top-to-the-south

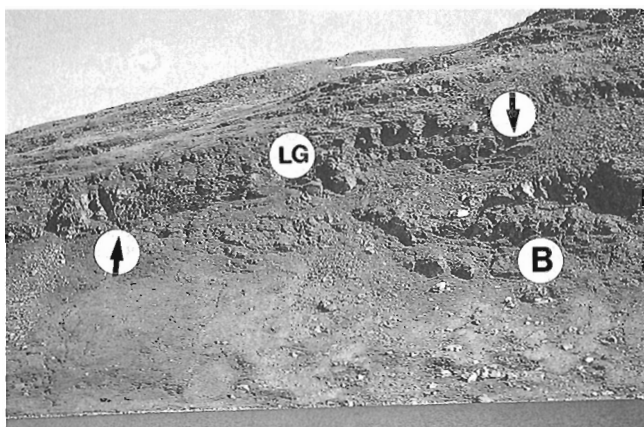


Figure 125. Post-thermal peak fault BB on the east shore of lac Watts (Fig. 5). The fault juxtaposes layered gabbro (LG) of the Watts Group in its hanging wall on basalt and gabbro (B) of the Watts Group in its footwall. The trace of the fault is indicated by the two arrows. Height of hill on right-hand side of photograph is 330 m. (GSC 1992-106BB)

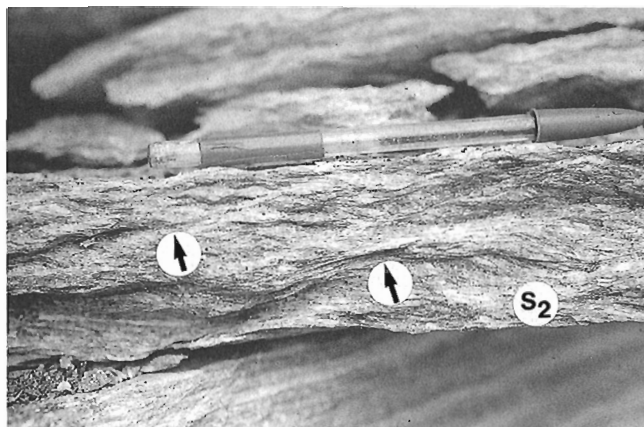


Figure 126. Shear bands (arrows) deforming thermal peak foliation (S_2) in a deformed gabbro from the Watts Group on the east shore of lac Watts (Fig. 5). The retrograde assemblage along the shear bands indicate that they are post-thermal peak in age. The predominance of the south (left) -dipping set of shear bands is consistent with a top-to-the-south sense of movement. Length of pen is 15 cm. (GSC 204233-V)

sense of movement. Kinematic indicators include: (1) shear bands (Fig. 126 and 127; Platt and Vissers, 1980; White et al., 1980), (2) C/S fabrics (Berthé et al., 1979), (3) back-rotated boudins (Hanmer, 1986), and (4) rotated syn-deformation porphyroblasts (Fig. 128). The post-thermal peak fault system records at least 50 km of movement, as constrained by measurements of fault length parallel to movement direction (Fig. 5; Lucas, 1989a).

In contrast to the kilometre-scale shear zones associated with the thermal peak D_2 thrusts, relatively narrow shear zones (1 to 10 m) occur adjacent to the post-thermal peak faults (Lucas, 1989a; St-Onge and Lucas, 1990m). The shear zones immediately above the post-thermal peak faults are characterized by greenschist-grade "mylonites" (Fig. 129) derived from amphibolite-grade D_2 tectonites (e.g., layered gabbro in sheet BB or gabbro sills within sheet Y, Fig. 5; Fig. 130 and 131). Rotated, internally foliated boudins of anorthosite and pyroxenite in the mafic mylonites (Fig. 132 to 134) are interpreted to result from disaggregation of relatively competent layers during ductile flow in the enveloping gabbroic layers (St-Onge et al., 1987; Lucas, 1989a, 1990). Complete isolation of individual boudins within the surrounding mafic mylonites (Fig. 132 to 134) qualitatively attests to the large strains accumulated along the shear zones during post-thermal peak D_2 deformation.

The thermal peak foliation in the hanging walls of the late peak faults was reworked along a network of small-scale shear zones (Lucas, 1989a, 1990). Similar to the mylonitic fault zones, the small-scale shear zones are characterized by partial replacement of amphibolite-grade assemblages by greenschist-grade minerals (Bégin, 1989b). The geometry of the hanging wall shear zones (Fig. 126) suggests that they

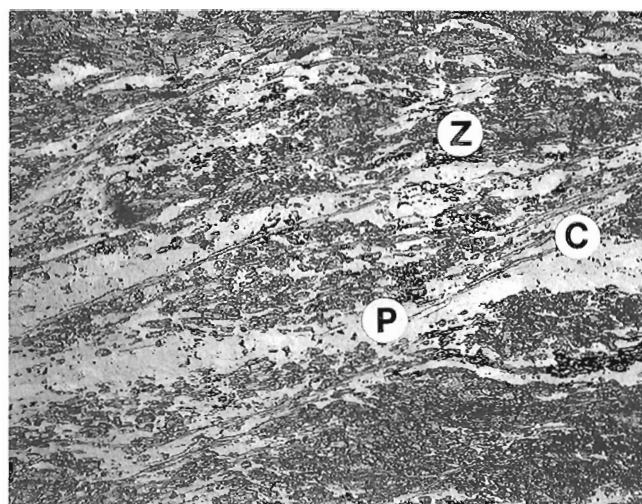


Figure 127. Photomicrograph of late D_2 shear bands in an anorthositic layer of a layered gabbro in the Watts Group, east shore of lac Watts (Fig. 5). The shear bands are defined by chlorite blades (C) and plagioclase (P). Plagioclase and chlorite are the products of retrograde reactions consuming the thermal peak assemblage zoisite (Z)-plagioclase-hornblende. The thermal peak foliation (horizontal) is preserved between the shear bands. Horizontal field of view is 20 mm. (GSC 204664-J)

represent conjugate shear bands or extensional crenulation cleavages (Platt and Vissers, 1980). They are oriented subparallel to the syn-thermal peak foliation and dip 20° to 40° shallower or steeper (Fig. 126). The shear zones vary in width from micron- to metre-scale and are heterogeneously distributed throughout the thrust sheets, in contrast to the pervasively-developed thermal peak foliation. Their specific distribution reflects local compositional, and hence rheological, variations (Lucas, 1990). Outcrop and thin section observations indicate that several generations of the shear bands often developed, each successive one deforming and rotating older sets. All sets of these relatively discrete

shears generally contain a stretching lineation subparallel to the thermal peak lineation (Fig. 103; Lucas, 1989a). The predominance of the south-dipping conjugate set of shear bands (Fig. 126) suggests that the rocks experienced a non-coaxial deformation with a hanging wall-to-the-south sense of displacement.

Lucas and St-Onge (1992) have interpreted the post-thermal peak D₂ faults as normal faults along which the hanging walls were translated southward relative to the footwalls. The basis for this interpretation is derived in part

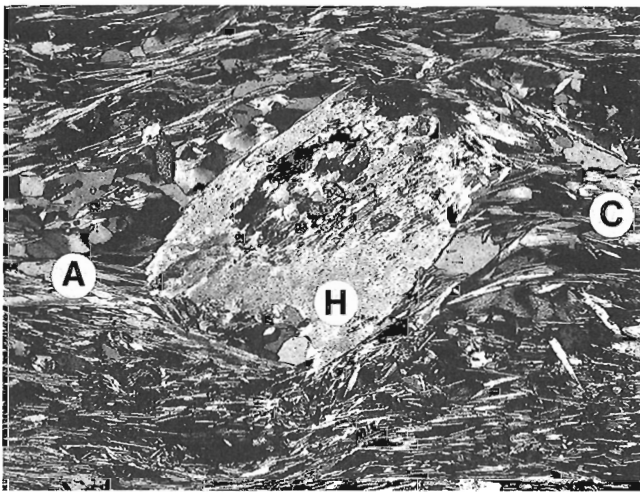


Figure 128. Photomicrograph of the late D₂ ultramylonite shown in Figure 132 (below). Hornblende porphyroblast (H) is reacting to actinolite (A) and chlorite (C). Strain shadows contain quartz, plagioclase, and chlorite. Location is the same as for Figure 132 (below). Horizontal field of view is 10.5 mm. (GSC 204664-C)

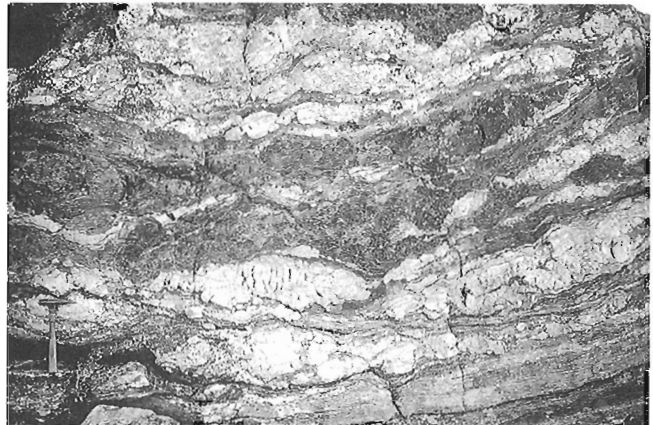


Figure 130. Sheared and boudined layered gabbro from the Watts Group, east shore of lac Watts (Fig. 5). Disaggregated white layers are plagioclase-clinozoisite-rich; dark layers contain hornblende-actinolite-plagioclase. A shear zone associated with an underlying (<10 m below photograph) D₂ post-thermal peak fault occurs in the lower right-hand corner of the photograph. There the rock records the change from a heterogeneously deformed layered gabbro (upper portion of outcrop) into a more homogeneous chlorite-actinolite-plagioclase schist. Hammer is 34 cm long. (GSC 204636-J)

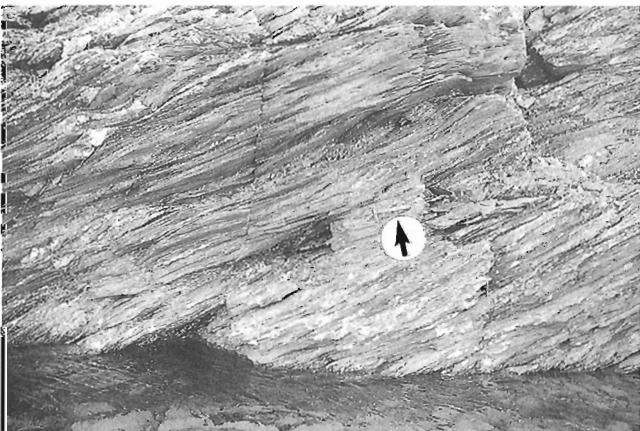


Figure 129. Greenschist grade mylonite derived from layered gabbro of the Watts Group on the east shore of lac Watts (Fig. 5). The mylonite is a chlorite-actinolite-plagioclase schist which contains preserved porphyroclasts of hornblende (e.g. Fig. 128). Arrow points to 34 cm long hammer. (GSC 204636-U)

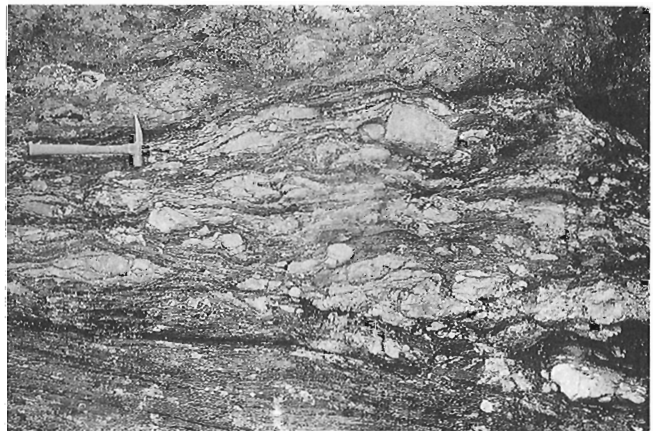


Figure 131. Detail of the zone of transition from the heterogeneously deformed layered gabbro of Figure 130 to the chlorite-actinolite-plagioclase schist (ultramylonite) of Figure 132 (below). Location is to the bottom left of the outcrop shown in Figure 130. Note the disaggregating layer of anorthosite. Hammer is 34 cm long. (GSC 204636-J)

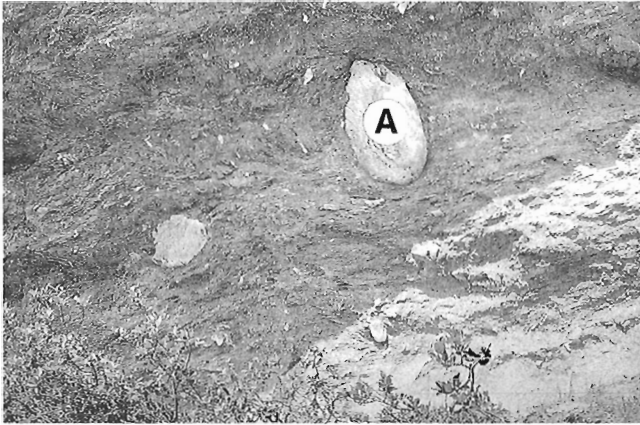


Figure 132. Ultramylonite derived principally from a layered gabbro of the Watts Group, east shore of lac Watts (Fig. 5). The ultramylonite is related to movement on an underlying post-thermal peak fault (<3 m below photo). Boudins are derived from anorthositic (A) layers. Chaotic appearance of the mafic schist is due to intense microfolding of the retrograde chlorite-actinolite-plagioclase schistosity during a post-D₂ folding event. Long dimension of the larger anorthositic boudin is 75 cm. (GSC 204233-W)

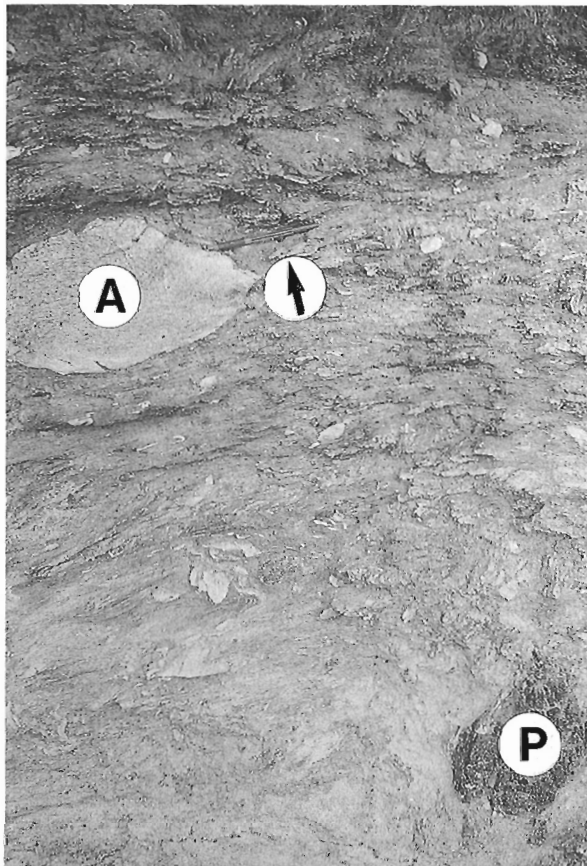


Figure 133. Boudins of anorthosite (A) and pyroxenite (P) in the ultramylonite shown in Figure 132. Location is the same as for Figure 132. Arrow points to 15 cm long pen. (GSC 204636-C)

from mapping to the north and west of the Cape Smith Belt map area (St-Onge and Lucas, 1990c; Lucas and St-Onge, 1991). The structurally-higher of the two faults (fault BB; Fig. 5) carries Watts Group mafic and ultramafic cumulate rocks and can be traced to the northwest where it forms the "roof" fault to the Narsajuaq arc (Fig. 1; Lucas and St-Onge, 1992).

Lucas and St-Onge (1992) present several independent lines of evidence to support the interpretation of the "roof" fault to Narsajuaq arc as a normal fault. First, it is characterized by syntectonic retrograde metamorphic assemblages in its hanging wall (Watts Group; Bégin 1989a) and syntectonic thermal peak assemblages in its footwall (Watts and Povungnituk groups; Bégin 1989a, 1992a). Second, studies on growth-zoned garnets from pelitic schists in the footwall of the fault indicate near-isothermal decompression trajectories consistent with arrested heating due to burial and relatively rapid, tectonically-driven exhumation (St-Onge and Lucas, 1991). These paths contrast with those recorded in rocks buried to similar depths at more external locations in the thrust belt (see 'Analytically-derived P-T paths in pelites' section below). Third, the 1888 Ma arc pluton intruding the Watts and Spartan groups west of lac Watts (1721A; Fig. 7) contains muscovite at its margins (in contact with sedimentary rocks) which yields a K-Ar age of 1824 ± 17 Ma (Hunt and Roddick, 1991). This low-temperature cooling age is broadly consistent with the estimated age of the collision between the Narsajuaq arc and the lower-plate (i.e., between 1826 Ma and 1758 Ma; St-Onge et al., 1992).

The fault geometry, kinematics, and the three lines of evidence summarized above from Lucas and St-Onge (1992) are consistent with the interpretation that post-thermal peak fault BB (Fig. 85) is a normal fault. The structurally lower post-thermal peak fault Y (Fig. 85 and 135) is also interpreted as a hanging wall-down-to-the-south normal fault, given its macro- to micro-scale similarities to the "roof" fault of the Narsajuaq arc.



Figure 134. Detail of the anorthositic boudin of Figure 133, showing preservation of the foliation that developed during thermal peak D₂ deformation. Location is the same as for Figure 132. Pen is 15 cm long. (GSC 204636-B)

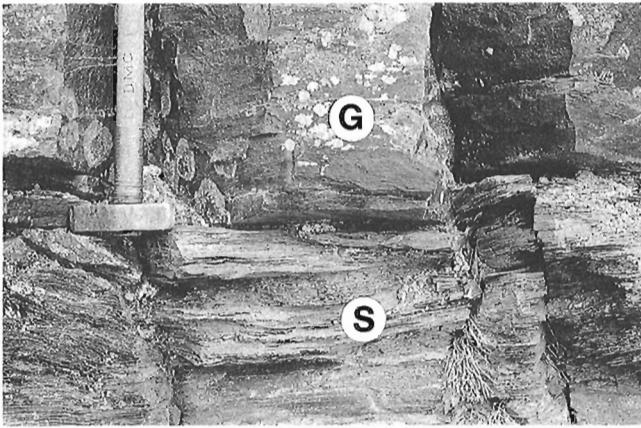


Figure 135. Hangingwall (within <5 m) of fault Y on the east side of lac Watts (Fig. 5). The fault places the mafic intrusive and extrusive units of the Watts Group on the clastic sedimentary rocks of the Spartan Group. Note the development of a retrograde mafic schist (S) from the overlying gabbroic rocks (G) which is similar to features described for post-thermal peak fault BB (see text). (GSC 1992-106X) Note hammer for scale.

The extensional faulting apparently recorded in the northern portion of the Cape Smith Belt may have been triggered by the wedging of the kilometre-scale Narsajuaq arc (e.g., Price, 1986; Dorsey, 1992) into the base of the thrust belt during an inferred ca. 1.8 Ga arc-continent collision (Fig. 1; St-Onge and Lucas, 1991; Lucas and St-Onge, 1992). A similar scenario has been proposed for the Tauern Window extensional faulting in the eastern Alps, where extension appears to follow emplacement of the Zentralgneiss crystalline thrust sheets at deeper structural levels (Selverstone, 1988; Ratsbacher et al., 1989). In the Cape Smith Belt, the extensional deformation can be viewed as gravitationally-driven backsliding along the roof fault to the Narsajuaq arc (assumed to be south-dipping; Lucas and St-Onge, 1992).

Grain-scale deformation

Penetrative fault-parallel shear zones are restricted to narrow bands adjacent to the post-thermal peak D₂ faults (faults Y and BB, Fig. 85; Lucas, 1989a). The shear zones are typically around 10 m wide and are characterized by a foliation defined by retrograde chlorite and actinolite (after hornblende; Bégin, 1989b) in both Watts Group basalt and layered gabbro. Strain is not homogeneously distributed through these zones, but appears to be localized in a 2 to 3 m wide band of penetratively foliated and largely retrograded schist containing boudined fragments of relatively competent anorthositic and pyroxenitic layers directly above the faults (Fig. 129, 132 and 133).

Several processes contributed to the development of the "melange-like" schist (Fig. 132 and 133) from layered gabbro (Lucas, 1990). The thermal peak foliation in gabbro layers was reworked into a finer grained, more homogeneous schistosity (compare Fig. 120 with Fig. 128) as the result of

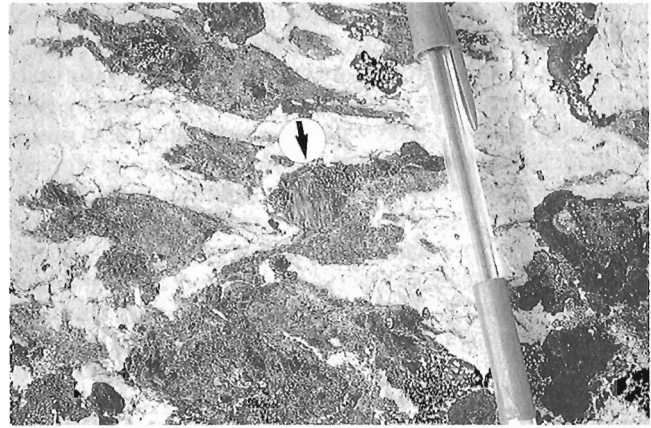


Figure 136. Hornblende porphyroclasts (arrow) reacting to actinolite tails in a layered gabbro of the Watts Group at the northwest end of lac Watts (Fig. 5). Note pen for scale. (GSC 204233-R)

dynamic recrystallization of plagioclase combined with complete breakdown of thermal peak mafic phases (e.g., hornblende to actinolite and chlorite, Fig. 128 and 136). Development of this retrograde fabric appears to have weakened the gabbro layers (see below) relative to the anorthosite and pyroxenite layers. Boudinage of the anorthosite and pyroxenite layers (Fig. 132 to 134) occurred by both ductile necking and the development of extensional shear zones (Lucas, 1990).

Anorthositic layers in Watts Group gabbro within 10 m of a post-thermal peak fault contain the retrograde metamorphic assemblage zoisite-plagioclase-chlorite± muscovite along shear bands (Fig. 126 and 127) and at boudin necks (Lucas, 1990). In contrast, the thermal peak zoisite-plagioclase±hornblende assemblage defines the older penetrative foliation in lozenges that are rotated by the shear bands (Fig. 127). The proportion of plagioclase relative to zoisite is significantly higher in the late D₂ structures (>10:1) as compared to the thermal peak foliation (<1:5; see Fig. 127). Microprobe analyses of anorthosite samples (approximately 5 m above fault BB along the east shore of lac Watts, Fig. 85) indicate that plagioclase, zoisite, and chlorite record the same mineral chemistries in both the retrograde and thermal peak assemblages (Lucas, 1990). Plagioclases are uniformly albitic (An₀₋₁), while zoisite records 2.8 mole percent pistacite compositions (mole percent pistacite=Fe³⁺/(Fe³⁺+Al)). These results suggest that although retrograde reactions changing the relative amounts of minerals are spatially restricted to late D₂ structures, compositions throughout the anorthositic layers have been homogenized. This apparent microchemical homogeneity (equilibrium?) may be explained by a flux of fluid into the anorthositic layers during or after retrograde metamorphism. An influx of fluid is further suggested by: (1) the absence of phases which gained Ca²⁺ during retrograde metamorphism, indicating that it was apparently lost from the layers (see below); and (2) the presence of muscovite along shear bands, which appears to require the addition of K⁺ to the layers (Lucas, 1990).

Plagioclase derived from retrograde reactions along shear bands in anorthositic layers appears to record dislocation creep deformation (Lucas, 1990). Plagioclase microstructures in the shear zones are characterized by fine (50 to 300 μm long) recrystallized grains with aspect ratios up to 3:1 and an apparent crystallographic preferred orientation (suggested by a strong gypsum plate effect; Lucas, 1990). The processes directly responsible for the plagioclase microstructure are difficult to constrain without detailed TEM studies. One possibility is that plagioclase deformed primarily by climb-accommodated dislocation creep resulting in plastic grain strain (as in quartz; Tullis and Yund, 1985). However, experimental and field studies have shown that climb in plagioclase may not be important at temperatures below about 600°C (Tullis, 1983; White and Mawer, 1986). Alternatively, plagioclase may have deformed by recrystallization-accommodated dislocation creep (e.g., Tullis and Yund, 1985) but developed the elongate grains as the result of some subsequent (syn and/or post-deformation) process(es). Potential processes include stress-induced diffusion transfer and oriented grain growth (Lucas, 1990).

In general, the post-thermal peak shear zones appear to have experienced an influx of fluids which promoted retrogression of thermal peak assemblages, supplying H_2O and CO_2 for reactions and providing a transport medium for both reactants and products (Lucas, 1990). The source of the fluids is unknown at present, but may be meteoric water channelled down along the normal faults from higher crustal levels. As a consequence of the fluid influx, the retrograde metamorphism occurred in an open chemical system at the scale of the shear zones (Lucas, 1990). Water supplied during deformation permitted hydration and equilibration of thermal peak assemblages to the post-thermal peak conditions (e.g., hornblende+ H_2O to actinolite+chlorite). In addition, the fluid acted as a transport medium for the diffusion of alkalis between mafic cumulate layers and across the faults. Retrograded meta-anorthositic layers appear to have gained K^+ and lost Ca^{2+} , while more mafic rocks both above and below the thrusts gained Ca^{2+} , as indicated by the growth of calcite porphyroblasts. The growth of calcite porphyroblasts also suggests that the fluids that were channelled along the fault zones were CO_2 -bearing (i.e. $X_{\text{H}_2\text{O}} < 1$).

In hanging wall rocks structurally above the penetrative post-thermal peak shear zones, retrograde metamorphic assemblages are largely restricted to shear bands (Fig. 126 and 127). Retrograde (shear band) assemblages in Watts Group gabbroic rocks include actinolite-chlorite-plagioclase ($< \text{An}_3$) \pm quartz \pm calcite. In contrast, the prograde assemblages defining the penetrative thermal peak foliation in gabbroic layers include relatively coarse grained (1 to 4 mm) hornblende-plagioclase ($> \text{An}_{20}$) \pm clinozoisite \pm actinolite (Fig. 120). Where coarser grained hornblende porphyroblasts are preserved in shear bands, they have composite retrograde tails of actinolite followed by chlorite (Fig. 136; Bégin, 1992a).

CORRELATION OF DEFORMATION HISTORIES BETWEEN TECTONOSTRATIGRAPHIC DOMAINS

Distinct structural-metamorphic histories have been documented for the (1) Archean Superior Province basement, (2) Povungnituk and Chukotat groups, and (3) Watts and Spartan groups. The structural-metamorphic histories presented above have been correlated between the three tectonostratigraphic domains by recognizing common, interdomainal structures and metamorphic assemblages. Geochronological data on the orogen (discussed above; see also St-Onge et al., 1992) have been utilized to constrain the ages of both independent and common tectonic events. Table 2 presents the structural-metamorphic episodes by domain, their correlations, and the available absolute age constraints.

Synmagmatic, granulite-grade deformation in the Superior Province basement (D_1 , Table 2) is constrained to be Archean based on (1) U-Pb ages for major plutonic units (2.7-2.9 Ga, Parrish, 1989) and (2) the angular unconformity locally observed at the base of the Povungnituk Group. The D_2 - D_3 foliations and associated lineations in the basement are parallel to the D_1 - D_2 foliations in the Povungnituk and Chukotat groups and are defined by similar amphibolite-grade mineral assemblages. Furthermore, kinematic indicators associated with D_2 - D_3 foliations in the basement give the same sense of shear as do those associated with D_1 - D_2 foliations in the Early Proterozoic rocks. These observations indicate that D_2 and D_3 deformation in the basement correlate with D_1 and D_2 in domain 2, respectively (Table 2).

The tectonostratigraphic record indicates that the 'tectonically suspect' Watts Group was obducted onto the Superior Province continental margin following intrusion of the youngest arc-related pluton (1839 Ma) in the Watts Group (see above; St-Onge et al., 1992). As illustrated in Table 2, D_2 out-of-sequence faults in the Povungnituk and Chukotat groups can be linked to D_2 thrust faults bounding the Watts and Spartan Group units and to the D_3 faults responsible for interleaving basement and cover rocks along the northern margin of the belt (St-Onge and Lucas, 1990m; Lucas and St-Onge, 1992). Simply put, accretion of Watts and Spartan Group units (D_2) correlates with out-of-sequence faulting (D_2) in the Povungnituk and Chukotat groups, and Archean basement thrusting (D_3). Furthermore, this regional thrusting event is interpreted to be coeval with accretion of the Narsajuaq arc to the continental margin thrust belt (Lucas and St-Onge, 1992). Collision between the Narsajuaq arc and the Superior Province continental margin is constrained to have occurred between 1826 Ma (youngest plutonic units of the Narsajuaq arc; see above) and 1758 Ma the age of syenogranite dykes which stitch together all elements of the orogen (Parrish, 1989; St-Onge et al., 1992).

Accretion of domain 3 units (Watts and Spartan groups, Narsajuaq arc) to the Superior Province continental margin occurred along the regional-scale out-of-sequence fault system that represents the fundamental "suture" in the Ungava orogen (Fig. 85; Lucas and St-Onge, 1992). In the map area, the "suturing" thrust system carries (1) Spartan Group in its most external position on thrust fault V (Fig. 5); and (2) Watts Group ophiolitic rocks along the northern margin of the Cape Smith Belt on faults X to BB (Fig. 5). Northwest of the map area, Narsajuaq arc units structurally overlies rocks of the Watts and Povungnituk groups (St-Onge and Lucas, 1990m) and its sole thrust can be traced along strike as the "suturing" D₂ thrust system (Lucas and St-Onge, 1992). Displacement estimates can be made for domain 3 units based on their structural overlap on the autochthonous Superior Province basement (Fig. 1). Based on measurements parallel to the accretion-related stretching lineation (Fig. 103 and 118), minimum displacements for the Narsajuaq arc and the Watts Group are estimated to be 65 km and 100 km, respectively (Lucas and St-Onge, 1992).

POST-THRUSTING, THICK-SKINNED DEFORMATION EPISODES

Map-scale folds deform the thrust belt, its footwall basement and the thermal peak mineral isograds (Fig. 5, 58, and 137; see 'Metamorphic mineral zones in mafic rocks of the Povungnituk, Chukotat and Watts groups' section below; St-Onge et al., 1986; Lucas, 1989a; St-Onge and Lucas,

1990m; Lucas and Byrne, 1992). The large-scale folds are west-trending and are approximately coaxial with commonly observed outcrop-scale minor folds (Fig. 138 to 140). These structures overprint the thin-skinned compressional structures in all three tectonostratigraphic domains and fold the proposed normal faults (post-thermal peak D₂ faults) involving units of the Watts and Spartan groups. Consequently, the west-trending folding event is termed D₃ for the Cape Smith Belt and D₄ for the Archean basement (Table 2). The west-trending structures are refolded by northwest-trending cross-folds which also involve both thrust belt rocks and the footwall basement (Fig. 137). This final regional deformation event is termed D₄ for the Cape Smith Belt and D₅ for the Superior Province Archean basement (Table 2). The involvement of Archean basement in the folding events has led to the deformation being describe as thick-skinned, in contrast to the thin-skinned thrust deformation which occurred above a mid-crustal, basement-cover décollement (see also King, 1986; Hoffman et al., 1988; Lucas and Byrne, 1992).

The principal consequences of the two post-thrusting deformation episodes are: (1) development of the west-trending, orogen-scale synclinorium in which the Cape Smith Belt is preserved and the anticlinorium to the north in which the autochthonous Superior Province basement is exposed (Fig. 1); and (2) creation of the northwest-trending, orogen-scale synclinal saddle into which the synclinorium-anticlinorium pair plunge, generating >20 km of structural relief on the saddle's flanks (Fig. 1 and 58; Lucas, 1989a). It is the structural relief generated by the

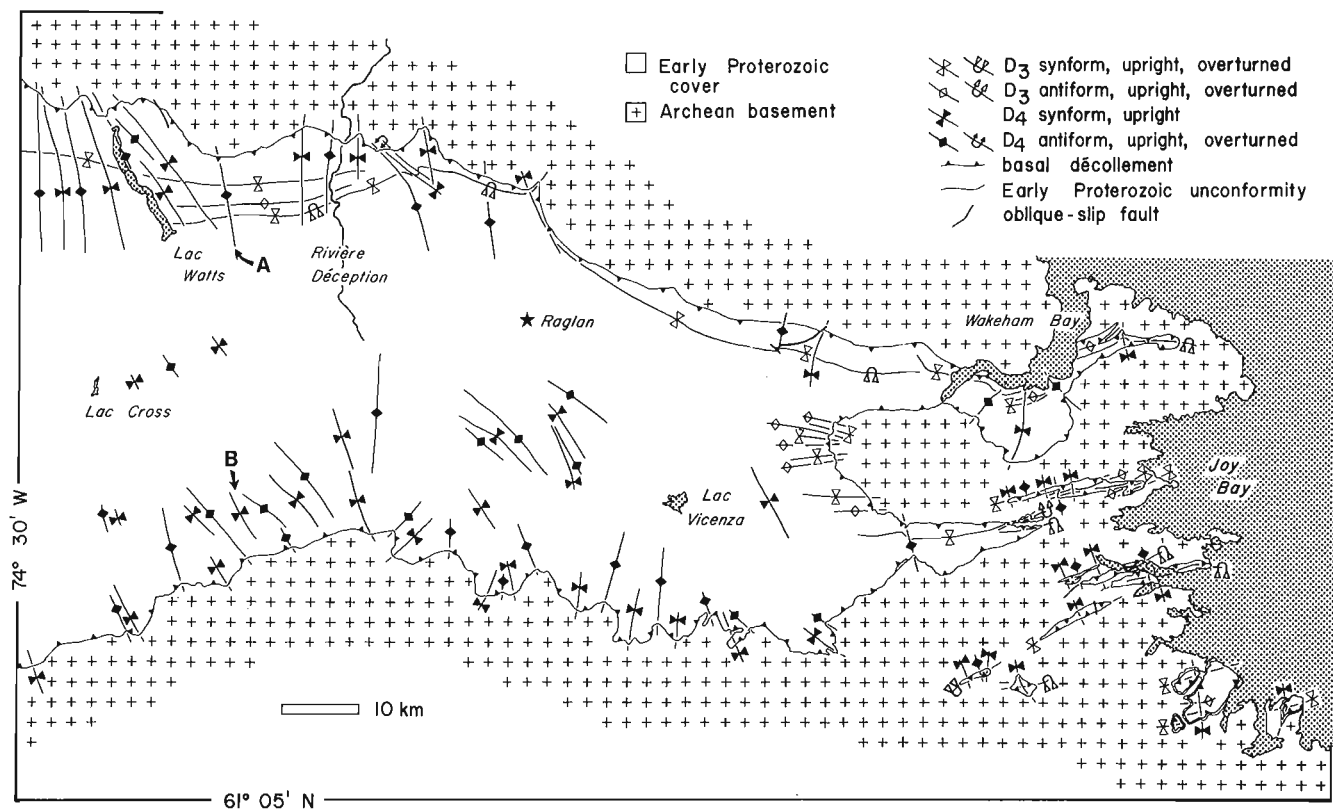


Figure 137. Compilation of axial traces for D₃ and D₄ macroscopic folds in the eastern Cape Smith Belt map area.

cross-folding event that has resulted in the post-peneplanation exposure of oblique cross-sections of the orogen and which has been utilized to construct structure sections of the eastern portion of the Cape Smith Belt (Fig. 58; Lucas, 1989a).

The map-scale folds appear to be localized in two principal settings: (1) at major viscosity interfaces, such as the basement/cover contact (i.e., basal décollement) (Fig. 137); or (2) where strong mechanical layering is present, such as mafic-ultramafic sills in sedimentary rocks (Fig. 141). The map- to outcrop-scale nature of the thick-skinned fold structures and associated cleavages are described in the following two sections, while the mechanics of the folding deformation is described in a third section.

West-trending folds

The geometry of west-trending folds has been studied in three areas within the Cape Smith Belt: (1) the Joy Bay-Burgoyne Bay area (eastern outliers; 1734A, 1735A; Fig. 83), (2) the Wakeham Bay - lac de la Grunérite area (eastern end of the belt; 1727A, 1728A, 1729A, 1733A, 1734A; Fig. 138), and (3) the lac Watts-rivière Déception area (northern margin; 1721A, 1722A; Fig. 137). The well exposed outliers provide a good opportunity to study map-scale fold styles and folding

mechanisms, and are discussed first in this section. A significant contrast in the regional-scale fold structure between the Wakeham Bay area and the northern margin (Fig. 58 and 137) suggests that there may be lateral and vertical variations in fold geometry within the Cape Smith Belt. The map-scale folds of the eastern end and northern margin areas are described after those of the outliers. Finally, the question of how the shortening strain indicated by the map-scale folds (e.g., basement-cover contact, Fig. 141) is accommodated at mesoscopic and microscopic scales is discussed.

Eastern outliers

Outliers of Early Proterozoic rocks southeast of the Cape Smith Belt are preserved in a dome-and-basin fold interference pattern (Fig. 83) (St-Onge and Lucas, 1990m; Lucas and Byrne, 1992). At the outcrop scale, west-trending minor folds and associated fabrics are systematically re-oriented along north-trending outcrop- to map-scale fold trains, indicating that the north-trending folds were superposed on the west-trending structures. The west-trending map-scale folds have a 0.5 to 2.0 km wavelength, and are highlighted because each outlier is preserved in one or more doubly-plunging synforms (Fig. 83). The west-trending structures in the southern outliers are broad, open

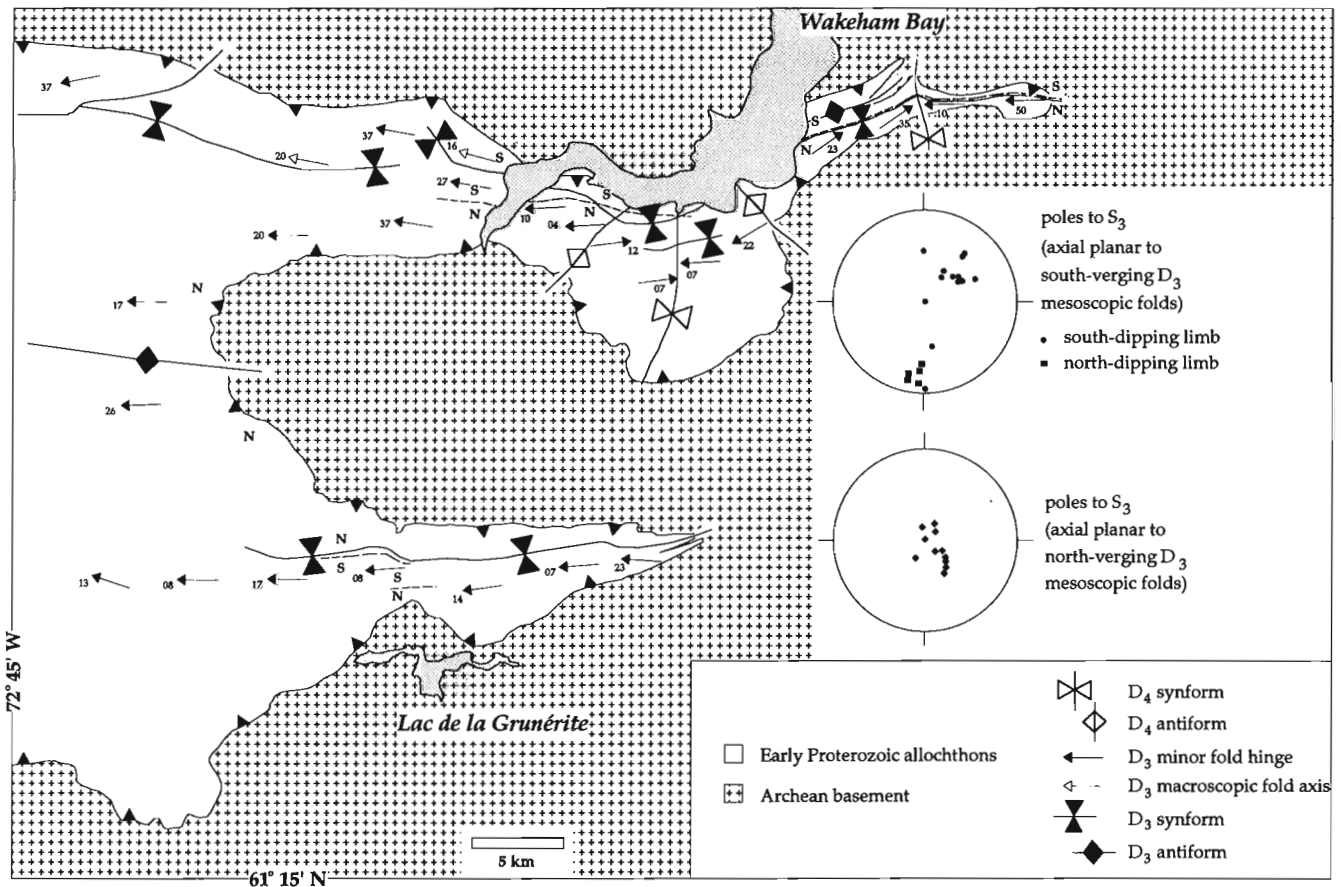


Figure 138. Compilation of mesoscopic and macroscopic D₃ fold axial traces in the Wakeham Bay area (1727A, 1728A, 1729A, 1733A, 1734A). Hinges are grouped into north (N) or south (S) verging domains based on fold asymmetries.

folds with limb dips not exceeding 30° (Fig. 9 and 83). In contrast, the northern outliers are characterized by asymmetric, south-verging structures with Povungnituk Group units preserved in the pinched (cusped) keels (Fig. 83). The chevron-style synforms have steep to overturned northern limbs and moderately north-dipping southern limbs (Fig. 83). Lucas and Byrne (1992) have suggested that the geometries of the west-trending outlier folds are consistent with an origin related to buckling during layer-parallel shortening (e.g., Fletcher 1974).

Cross-sections of the outliers (Fig. 83) indicate that the north-to-south change in west-trending fold geometry coincides approximately with the edge of a southward-thickening sequence of autochthonous quartzites (Fig. 5 and 9). Although the change in fold geometry could reflect an increase in folding strain towards the north, it seems fortuitous that it occurs at the location of a major change in the lithological composition of the footwall to the thrust belt. The transition in outlier fold geometry may thus correspond to a change in the rheological structure of the Povungnituk Group with the appearance of the massive, thick (~3 m) quartzite beds in the autochthonous footwall (Lucas, 1989b; St-Onge and Lucas, 1990m). In the northern outliers, the penetrative foliation in the Povungnituk Group thrust sheets and the upper few metres of footwall basement probably contributed to the development of more cusped, chevron-style fold profiles during folding. The massive quartzite beds lying unconformably on basement in the southern outliers do not provide a similar fine-scale rheological layering or mechanical anisotropy for chevron-style buckling, and thus may have resulted in relatively low amplitude/wavelength fold profiles (Lucas, 1989b).

Eastern end of the belt

The geometry of the west-trending folds in the Wakeham Bay-lac de la Grunérite area (1727A, 1728A, 1729A, 1733A, 1734A; Fig. 138) is best illustrated in the down-plunge

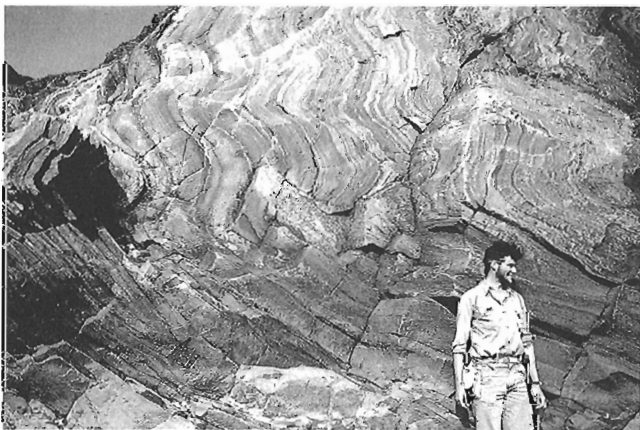


Figure 139. Mesoscopic D₃ folds of quartzite from the lower Povungnituk Group west of Wakeham Bay (Fig. 5). Note person for scale. (GSC 204233-D)

cross-section (Fig. 58). At the level of the basal décollement (basement/ cover contact), the regional-scale folds have a striking "W-shaped" geometry (Fig. 58). These folds have a relatively high amplitude to wavelength ratio (20 km/30 km), and a profile characterized by two cusped synclinal keels separated by a lobate medial antiform (Fig. 58 and 138; St-Onge and Lucas, 1990m; Lucas and Byrne, 1992). A minimum strike length of 150 km for the "W-shaped" D₃ profile is suggested by gravity data from a detailed survey conducted 10 km west of the map area (Feininger et al., 1985). The cusped-lobate geometry is commonly observed in the deeply eroded cores of other folded orogenic belts (e.g. Helvetic Nappes of the Swiss Alps, Ramsay et al., 1983; Wopmay Orogen, King, 1986; Needle Mountains, Colorado, Harris et al., 1987). It has been modeled as a buckling instability between two non-Newtonian materials with different viscosities (Smith, 1975).

Northern margin

The D₃ map-scale geometry at the structural levels exposed in the western and northern parts of the map area (Fig. 80 and 137) departs significantly from the "W-shaped" profile that underlies the belt. At the relatively high structural levels exposed in the southwestern part of the map area (Fig. 57), units of the Povungnituk and Chukotat groups occur in a north-dipping monocline (Fig. 58). The monocline was presumably steepened from its thrust belt attitude during west-trending folding. The Wakeham Bay synform (1729A, 1728A; Fig. 5) can be traced westward from Wakeham Bay as a upright to overturned, tight to isoclinal fold (Fig. 58) whose axial trace is adjacent and approximately parallel to the basement/cover contact (Fig. 137). Fold geometries near the basement/cover contact north of Raglan (Fig. 137) are complex. The Wakeham Bay synform steps to the northwest in an en echelon fashion to become the lac Watts-rivière Déception (1721A, 1722A) west-trending synform (Fig. 137). However, a younger, northwest-trending synform



Figure 140. Mesoscopic D₃ folds of well-foliated upper Povungnituk Group basalt at the southwest end of Wakeham Bay (Fig. 5). The spaced crenulation cleavage parallel to the hammer is associated with the D₃ folding. The hammer is 34 cm long. (GSC 204232-U)

appears to parallel and overprint the Wakeham Bay synform north of Raglan, thus making its geometry near the en echelon step difficult to resolve in detail (Fig. 137).

East of rivière Déception (1722A, 1723A; Fig. 137), the northern synform is overturned with an axial surface dipping 30° to the north (Fig. 80). The overturned segment of this synform is laterally discontinuous, and like the Wakeham Bay synform (Fig. 5 and 58), may reflect local oversteepening

of the basement/cover contact along the northern synformal limb. To the west, the lac Watts-rivière Déception synform progressively becomes a more open structure with an upright axial surface (Fig. 137). The variable dip of the northern synformal limb may result from lateral inhomogeneities in the growth rate of the basement-cored antiform to the north, possibly due to local gravitational enhancement during buckling (Lucas and Byrne, 1992).

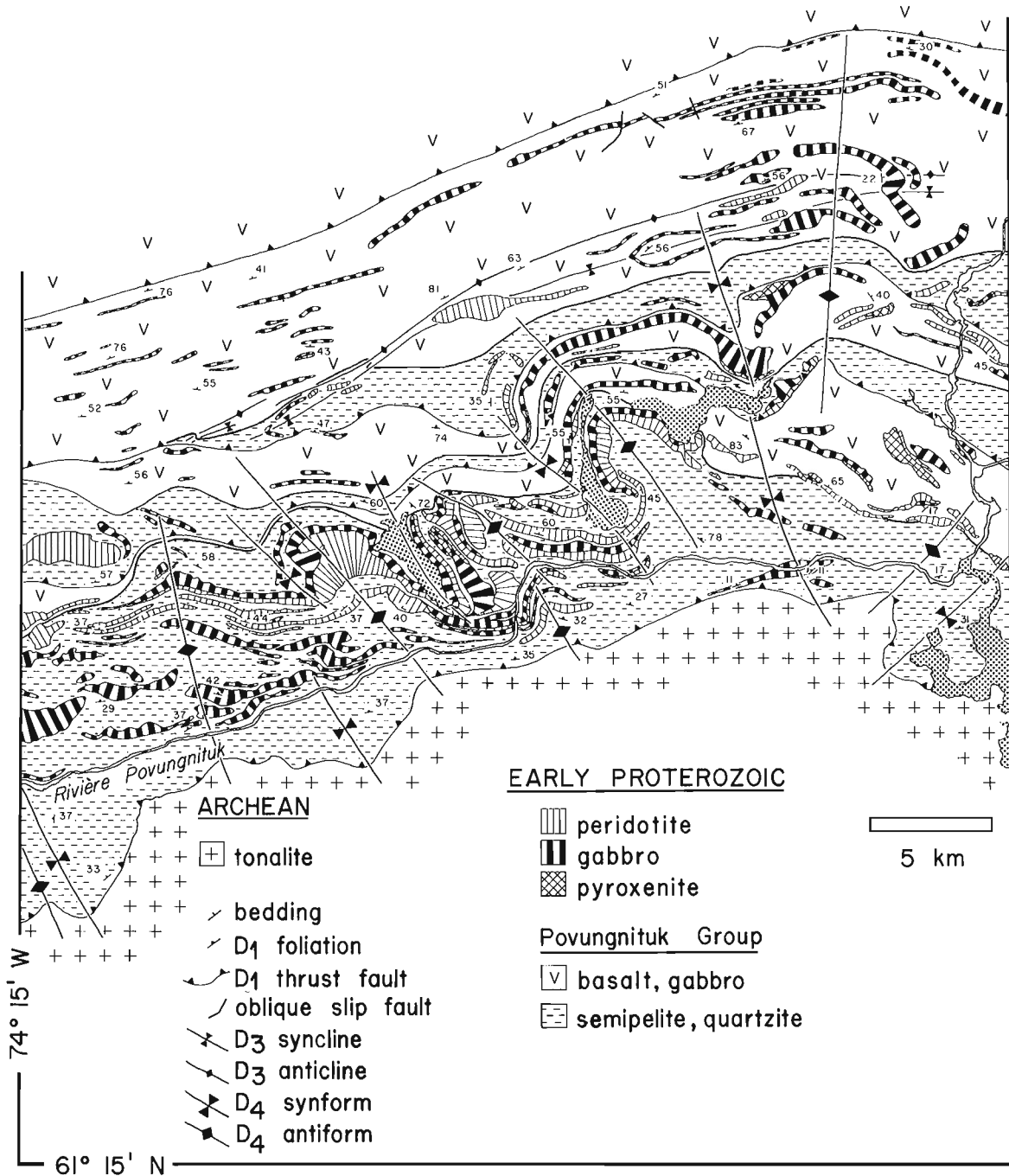


Figure 141. Simplified geological map for the area northwest of lac St-Germain (1731A). The D4 map-scale folds are localized at the basement/cover contact and in areas where mafic-ultramafic sills are emplaced in the sedimentary rocks of the lower Povungnituk Group. Lake in southeast corner is lac St-Germain.

Outcrop- and grain-scale folding

Map-scale folding of the Cape Smith Belt and its Archean footwall basement was accommodated at the grain- and outcrop-scales by several mechanisms (Lucas, 1989b; St-Onge and Lucas, 1990m). Folding strain (>50% shortening at the level of the basement/cover contact; Fig. 58) appears to have been accommodated by either (1) the development of minor folds with associated cleavages, or (2) a more distributed deformation without the development of folds or cleavages. In areas with a strong pre-folding anisotropy (e.g., shear zones; see Lucas, 1989a), the principal outcrop- to grain-scale deformation structures are minor folds at wavelengths ranging from metres for folded layers (Fig. 142) to sub- millimetre for individual grains (Fig. 143). Crenulation cleavages are associated with many of the minor fold hinges (Fig. 140), and are often marked by the growth of new phyllosilicates (Fig. 144) or amphiboles and/or evidence of pressure solution strain.

Minor folds are relatively rare structurally away from the pre-folding shear zones. This mechanical behaviour in unfoliated rocks may result from a lack of rheological layering with an appropriate layer thickness or competency contrast to form buckle folds at the centimetre- to metre-scale (Johnson, 1980). The basement gneisses probably did not develop minor, west-trending folds because the Archean gneissosity was in an unsuitable orientation for buckling. In both the basement and unfoliated Proterozoic rocks, shortening may have been accommodated by some combination of distributed grain-scale deformation and/or heterogeneous deformation involving the development of an array of shears (e.g., Jacob et al., 1983; Lucas and St-Onge, 1991). The occurrence of D₃ cleavages in basement lithologies was studied in the hinge zones of the D₃ synforms in the outliers west of Burgoyne Bay (1734A, 1735A; Fig. 5; Lucas, 1989b). In the tight synformal hinges of the northern outliers (Fig. 83), a spaced D₃ cleavage persists for at least 10 m below the basement/cover contact (St-Onge and Lucas, 1990m). In contrast, D₃ fabrics are not observed in the



Figure 142. Asymmetric, south facing D₃ folds of Archean basement tonalite along the north margin of the Cape Smith Belt, west of Wakeham Bay (Fig. 5). The tonalite displays a strong pre-folding anisotropy due to reworking by the D₁ basal shear zone of the thrust belt. Length of pen is 15 cm. (GSC 204901)

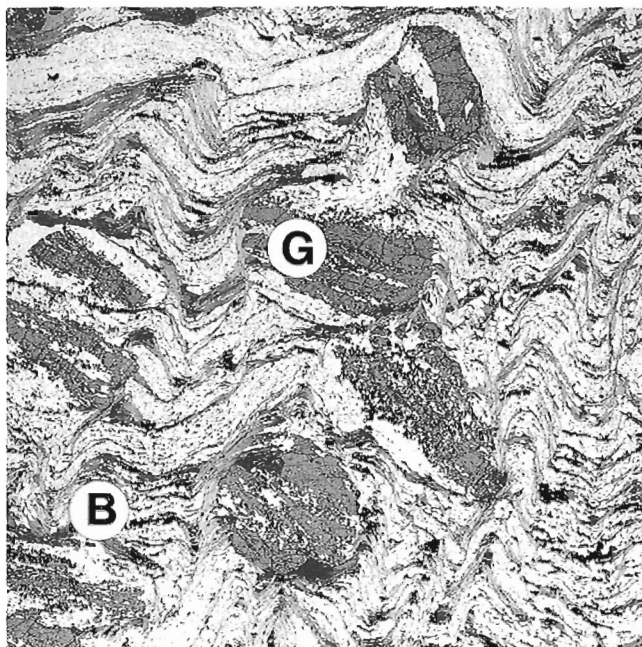


Figure 143. Photomicrograph of crenulated garnet (G) - biotite (B) semipelite from the lower Povungnituk Group, 13 km southwest of Wakeham Bay (Fig. 5). The D₃ crenulations deform the D₁ basal shear zone fabric defined by the alignment of biotite and compositional layering in the semipelite. The garnet overgrows the D₁ fabric and is in turn enveloped by the D₃ crenulation fabric. Horizontal field of view is 15 mm. (GSC 1992-106B)

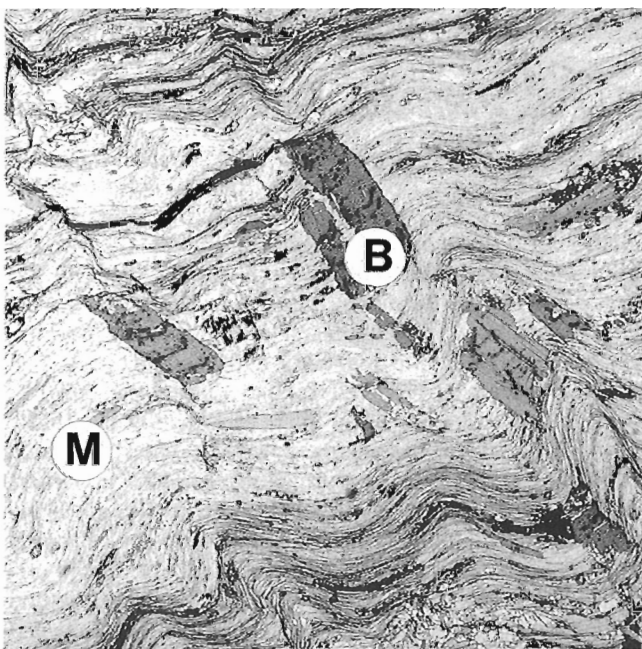


Figure 144. Photomicrograph of crenulated muscovite (M) pelite from the lower Povungnituk Group, 10 km southwest of Wakeham Bay (Fig. 5). Late biotite porphyroblasts (B) are axial planar to the D₃ microfolds of the D₁ basal shear zone foliation. Horizontal field of view is 7 mm. (GSC 1992-106A)

basement underlying the southern outliers, which are characterized by open D₃ map-scale folds (Fig. 9 and 83). This suggests that a minimum amount of D₃ shortening may be required to produce penetrative deformation in more competent units, and that below this amount fold-accommodation strain is accomplished very inhomogeneously (Lucas, 1989b).

Cross-folds

West-trending folding was succeeded by a deformation episode which produced a suite of north- to northwest-trending folds (cross-folds; Lucas, 1989b; St-Onge and Lucas, 1990m). As with the west-trending folds, the cross-folds involve both basement and cover at wavelengths ranging from millimetre scale to more than 100 kilometres (Fig. 137). The regional cross-fold saddle which transects the center of the Ungava orogen (Fig. 1; St-Onge and Lucas, 1992) appears to have a wavelength of at least 300 km. However, two cross-fold wavelengths dominate at map scale: (1) a 50 km wavelength, with the folds deforming the entire Proterozoic tectonostratigraphy and the basement (e.g., A, Fig. 137); and (2) 5 to 10 km wavelengths, which are restricted to the area of the basement/cover contact (e.g., south of lac Vicenza, Fig. 137) or to thrust sheets with mafic or ultramafic sills intruding sediments (e.g., B, Fig. 137; Fig. 141). A possible explanation for the limited occurrence of the smaller wavelength folds is that they are restricted to zones in the thrust belt tectonostratigraphy which have rheological layering appropriate to buckle (Lucas, 1989b; St-Onge and Lucas, 1990m). Cross-folding strain at structural levels which do not display outcrop- or map-scale folds must have shortened by either grain-scale deformation or small-scale faulting, as suggested above for the west-trending folding event.

Mechanics of thick-skinned folding

Lucas and Byrne (1992; see also St-Onge and Lucas, 1990m; Lucas and St-Onge, 1992) proposed that the west-trending folds resulted from horizontal compression during north-south intracontinental shortening of the orogen following arc-continent collision. A similar scenario has been proposed for the Early Proterozoic Wopmay orogen, where deformation progressed from synmetamorphic basement-involved thrusting (King, 1986; St-Onge and King, 1987) to basement-involved folding during the terminal stages of the collision (King, 1986; Hoffman et al., 1988). Similar, late stage, basement-cored folds have also been recognized in the New Quebec (Hoffman, 1988), Damara (Jacob et al., 1983), and Appalachian (Van Staal et al., 1990) orogens. In fact, many of these orogenic belts are relatively well preserved because they occur as keels or synclinoria within the folded footwall basement. Detailed structural studies in the Norwegian Caledonides by Steltenpohl and Bartley (1988) have shown that the regional pattern of structural culminations and synformal basins transverse to the orogen is the result of post-thrusting cross-folding. Furthermore, they have re-interpreted the classic gneiss domes (Ramberg, 1966; and references therein) as the result of dome-and-basin fold interference patterns generated by two

episodes of post-collisional (post-metamorphic), basement-involved folding. Low amplitude arches in the northwestern Gulf of Mexico basin have been interpreted as folds (300 km wavelength) generated by horizontal compression related to late Cretaceous to early Tertiary deformation in the Mexican fold and thrust belt (Laubach and Jackson, 1990). Stephenson et al. (1990) have described lithosphere-scale folds in the Tertiary Eureka orogen of Arctic Canada with wavelengths of 200 km and they have attributed their development to shortening of a lithosphere with a weak lower crust and a relatively strong upper mantle. Long-wavelength fold structures have been documented in the Indian Ocean lithosphere, and explained by large-scale buckling of viscosity interfaces in response to horizontal compression related to India-Asia convergence (McAdoo and Sandwell, 1985; Zuber, 1987).

However, two other major hypotheses exist to explain the origin of the regional-scale, west-trending fold structures (Lucas and Byrne, 1992): (1) gravitational collapse of density inversions established during thrusting (i.e., diapirism; Ramberg, 1966); and (2) hanging wall antiforms above ramps in major crustal detachments (e.g., Ando et al., 1984). The second hypothesis can be eliminated for two reasons: (1) no thrust faults are observed in association with any of the folds in the thrust belt or footwall basement (St-Onge and Lucas, 1990m; Lucas and St-Onge, 1991); and (2) west-trending structures are continuous over several wavelengths at all scales.

Geological tests for a gravitational collapse hypothesis are largely provided by theoretical (e.g., Fletcher, 1972) and experimental (Ramberg, 1966) studies. The results of one such study involving centrifuge modelling of the growth of gravitational instabilities in a greenstone belt (Dixon and Summers, 1983) predict: (1) varying subsidence, and hence domes and basins, along strike; and (2) extensional structures across the crests of the antiforms. The "W-shaped" profile at the basal décollement (Fig. 58) appears to have a minimum strike length of 150 km (T. Feininger pers. comm., 1985) with no evidence of syn-folding subsidence along strike (Lucas, 1989a). Detailed examination of outcrop-scale, west-trending folds and associated fabrics across the regional-scale antiform at the east end of the belt (south west of Wakeham Bay; 1734A, 1728A; Fig. 5) indicate that the crest of the antiform did not experience syn-D₂ extensional strain (St-Onge et al., 1986; Lucas, 1989b; St-Onge and Lucas, 1990m).

The conspicuous limb asymmetry of the west-trending outcrop-scale folds (e.g. Fig. 142) bears no direct relation to the map-scale fold geometry, even though the asymmetry maps out into distinct domains (Fig. 138). A possible explanation for the asymmetry changes on the limbs of map-scale folds (Fig. 138) is that the minor folds developed prior to final tightening of the map-scale folds, and were rotated through their hinges (Lucas, 1989b; St-Onge and Lucas, 1990m). The fold hinge migration explanation is best illustrated in the Wakeham Bay area (1728A), where south-verging minor folds occur on both the north and the south limbs of the synform and the change in asymmetry to north-verging occurs on the south limb (Fig. 138). The hinge migration hypothesis is further supported by a clockwise

rotation of initially coplanar cleavage (axial planar to south-verging folds) from the north to the south limb of the Wakeham Bay syncline (top stereonet, Fig. 138). Hinge migration of this scale through a synclinal keel is inconsistent with the kinematic patterns predicted by the Dixon and Summers (1983) diapir models.

The fact that the west-trending fold geometries do not pass the principal tests of either the diapiric or ramp antiform hypotheses suggests, but does not prove, a horizontal compression origin for the structures (Lucas and Byrne, 1992). Similarly, the chevron to rounded fold styles observed at outcrop (e.g., Fig. 139, 140, and 142) and map scales (e.g., Fig. 138) suggest that the folds developed in response to layer parallel shortening but this does not prove the horizontal compression hypothesis. Although the origin of the northwest-trending structures has not been discussed, their similarity at all scales to the older west-trending structures suggests that they may have also been generated by horizontal compressional deformation (Lucas, 1989b). Lucas and St-Onge (1989a) proposed that the northwest-trending structures in the Cape Smith Belt developed during late-stage shortening in the New Quebec orogen (see also Hoffman, 1988).

The west-trending folds with an approximately 30 km wavelength (Fig. 58 and 138) may have resulted from amplification of buckling instabilities arising at the basal décollement, which was buried at about 15-20 km at the time of folding (St-Onge and Lucas, 1990m). The strain indicated by these map-scale folds is substantial (at least 50% shortening), although the high fold amplitude and locally significant vertical stretching along the northern margin of the Cape Smith Belt (Lucas, 1989a) makes it difficult to accurately constrain the shortening by folding. The density inversion established during thrusting (mafic-dominated allochthons overlying felsic basement) may have enhanced the amplitude growth rate of buckling instabilities initiated at the basement/cover contact (e.g., Neurath and Smith, 1982). The wavelength of the Cape Smith Belt synclinorium is estimated to be about 150 km (Fig. 1), the same order of magnitude as the wavelength of the orogen-scale, northwest-trending synform (approximately 300 km). These structures may represent the finite products of amplification of buckling instabilities arising at deep interfaces such as the Moho (Lucas and Byrne, 1992).

METAMORPHIC HISTORY OF THE CAPE SMITH BELT: OVERVIEW

Recent studies (e.g., Jamieson and Beaumont, 1988) have shown that the thermal history of a material point in a thrust belt is strongly influenced by the point's uplift mechanism, uplift rate, and its structural position in the thrust belt. Regional metamorphism has been studied in the eastern portion of the Cape Smith Belt using a multidisciplinary approach which considers these factors in addition to the classic qualitative and quantitative descriptions of preserved metamorphic history (St-Onge and Lucas, 1989d, 1990bm 1991). These studies have shown that the tectonothermal evolution of the Cape Smith Belt is characterized by an interaction between (1) deformation, (2) uplift and erosion,

and (3) thermal equilibration of thickened crust. In addition, this approach has led to the quantitative derivation of P-T (pressure-temperature) paths and qualitative P-T-t-d (pressure-temperature-time-deformation) paths for pelitic rocks in the Cape Smith Belt (St-Onge and Lucas, 1991). The P-T paths have provided important constraints for investigations of the thrust belt's structural history and associated deformation processes (Lucas, 1989a, b, 1990; Lucas and St-Onge, 1992).

Four principal methods have been used to study the metamorphic and tectonothermal history of the Cape Smith Belt: (1) field and petrological identification of metamorphic mineral zones in mafic units of the thrust belt (Fig. 145 and 146; St-Onge et al., 1986; Bégin, 1989a, b, 1992a); (2) qualitative evaluation of mineral growth and deformation relationships (Lucas, 1989a, 1990; St-Onge and Lucas, 1990m, 1991); (3) quantitative (analytical) derivation of P-T paths with growth-zoned garnets in pelitic units (St-Onge and Lucas, 1990m, 1991); and (4) finite difference modelling of vertical heat conduction and numerical derivation of theoretical P-T paths (Lucas, 1989b; St-Onge and Lucas, 1991). The results from the first three methods will be presented (in the same order) in the following sections. As was outlined in the 'Structural History' section, the Cape Smith Belt has been divided into two distinct tectonic domains or parts. The internal part of the Cape Smith Belt is considered to be all units in the hanging wall of the most southerly out-of-sequence fault (fault O, Fig. 5), while the external part is considered to be all units in the footwall of this fault.

EARLY D₁ THERMAL CONDITIONS IN THE POVUNGNITUK AND CHUKOTAT GROUPS






The oldest preserved metamorphic assemblages in the Cape Smith Belt are found in the Povungnituk and Chukotat groups and appear to be associated with early D₁ piggyback-sequence thrusting (Table 2; Lucas, 1989b, 1990; St-Onge and Lucas, 1991). Metamorphic conditions during early D₁ crustal thickening cannot be established at the base of the thrust belt because of overprinting during synmetamorphic basal shear zone deformation. However, at structural levels above the basal shear zone (Fig. 82), the high strain zones associated with individual early D₁ thrust faults are preserved. The mineral assemblages and microstructures found in the early D₁ fault zones (Fig. 87) north of lac Vicenza (1733A; Fig. 5) suggest that deformation occurred over the range of physical conditions bracketed by the quartz brittle-ductile transition (approximately 300°C and the biotite stability field (approximately 400°C; discussed above in 'Structural History of the Cape Smith Belt'; Lucas, 1989b). Given the 5 km average thickness for thrust sheets in this area (Fig. 5 and 58), early D₁ pressure estimates for the base of the thrust belt may have been in the range of 3-5 kbar. These constraints on the early D₁ P-T conditions suggest that at the onset of D₁ thrusting in the Cape Smith Belt, there was no significant residual heat from lithospheric thinning and/or rift margin magmatism associated with formation of the north-facing rift margin (i.e. accumulation of the Povungnituk and Chukotat groups; St-Onge and Lucas, 1991).

METAMORPHIC MINERAL ZONES IN MAFIC ROCKS OF THE POVUNGNITUK, CHUKOTAT, AND WATTS GROUPS



The geometry of the thermal peak metamorphic culmination was established at the regional scale by systematic mapping of metamorphic mineral assemblages in mafic extrusive and intrusive rocks (Fig. 145 and 146; Bégin, 1989a, b, 1992a). Field work (St-Onge et al., 1986, 1987, 1988b) constrained the locations of three mineral isograds: hornblende-in, actinolite-out, and garnet- or clinopyroxene-in. This was

followed by a detailed petrological study of the metamorphic mineral assemblages in the mafic units by Bégin (1989b, 1992a). Bégin's (1989b, 1992a) petrological study refined the position of the mapped mineral isograds and defined the position of an oligoclase-in isograd with petrographic and microprobe work. The mineral isograds in the external part of the belt are shown on Figure 145 and those in the lac Watts (1721A) area of the internal domain are detailed on Figure 147. The underlying Superior Province basement lacks sufficient mafic rocks to constrain the mineral isograds with the same precision as in the thrust belt. However, recent

Povungnituk Group

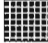
-  actinolite - albite zone
-  hornblende - actinolite - albite zone
-  hornblende - actinolite - oligoclase zone
-  hornblende - oligoclase zone
-  hornblende - oligoclase - garnet/clinopyroxene zone

Chukotat Group


-  actinolite - albite zone
-  actinolite - oligoclase ± hornblende zone

Watts Group

thermal peak mineral zones

-  hornblende - actinolite - albite to hornblende - oligoclase - garnet/clinopyroxene

post - thermal peak mineral zones

-  actinolite - chlorite - albite overprint on greenschist to amphibolite grade assemblages

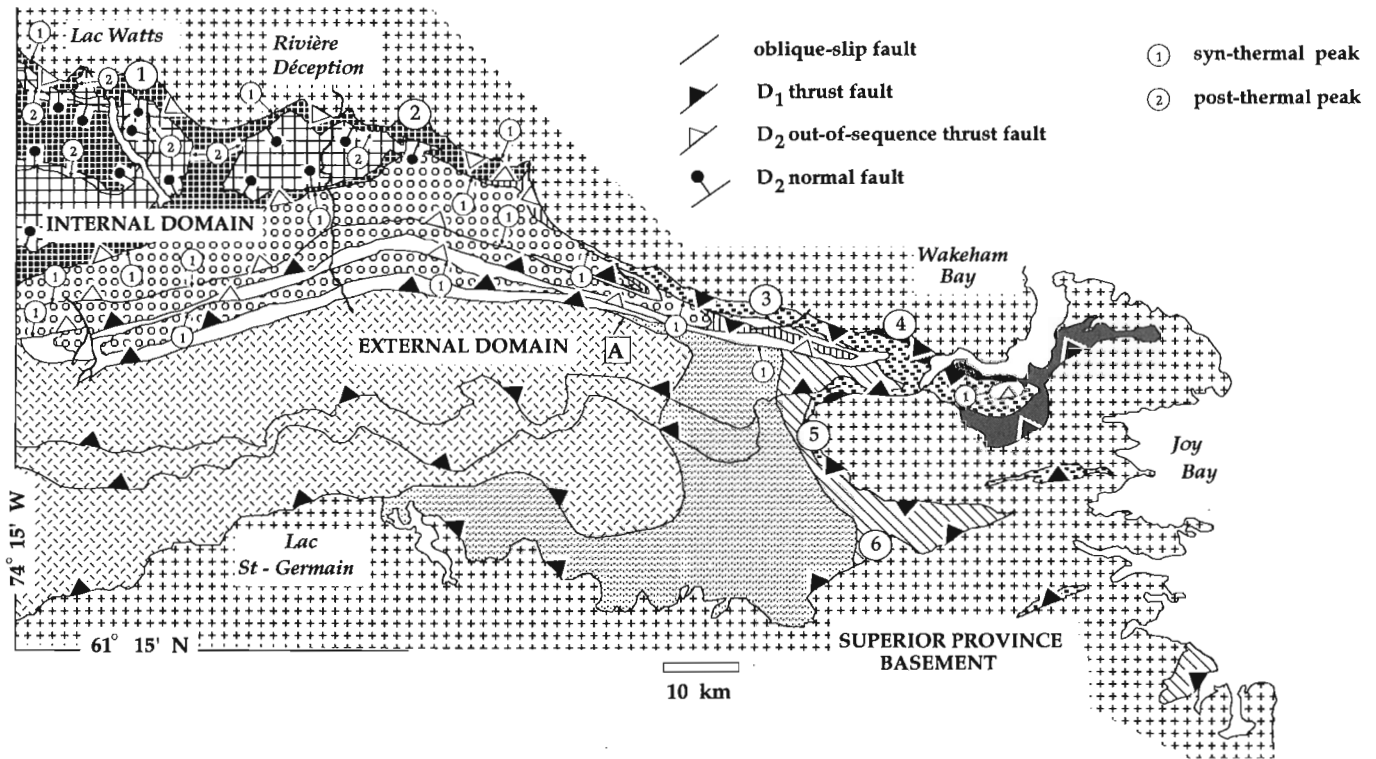


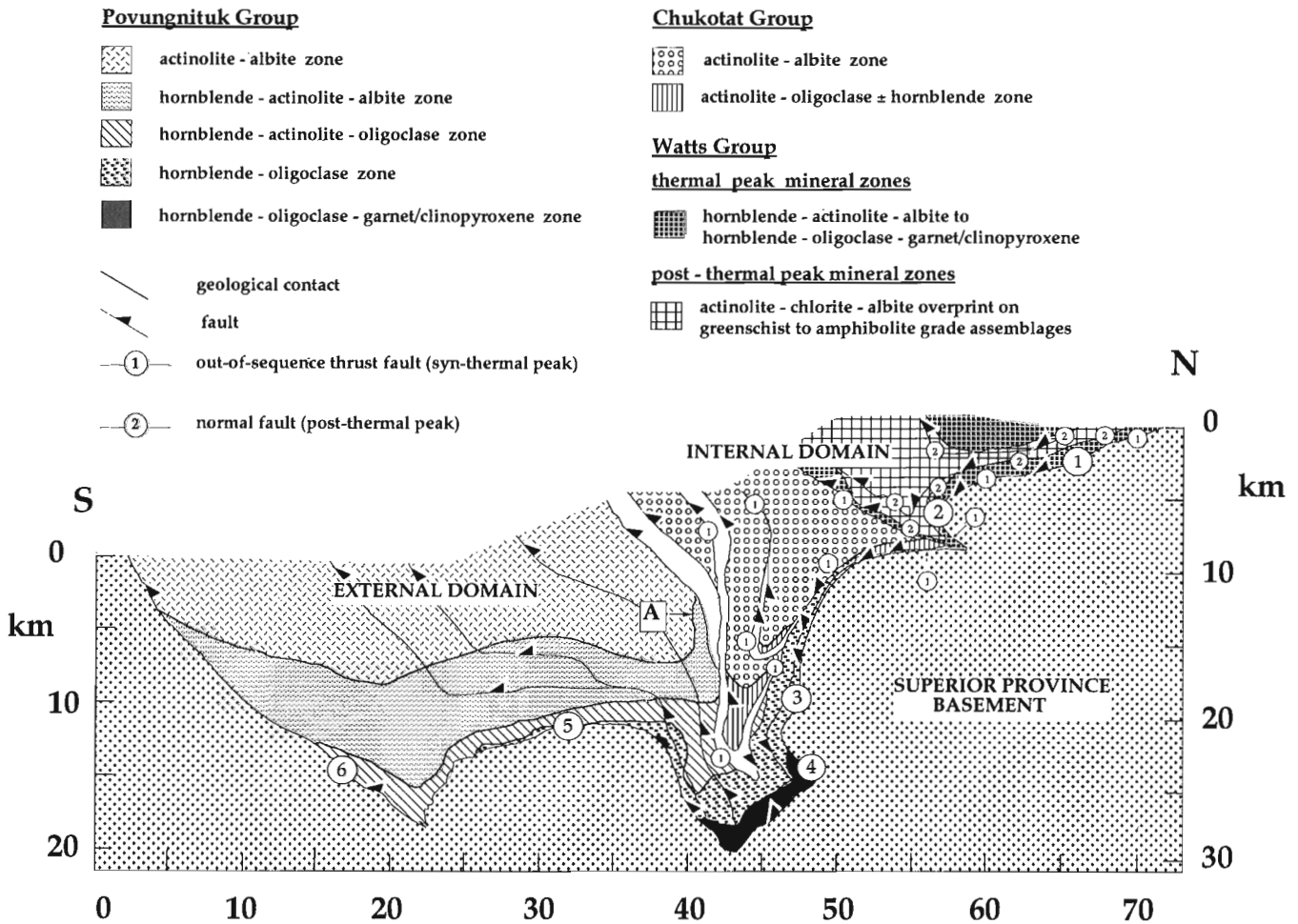
Figure 145. Metamorphic map of the eastern portion of the Cape Smith Belt, corresponding to the area shown in Figure 5. The distribution of the metamorphic mineral zones and isograds is after Bégin (1989a,b, 1992a). Thrust slices without a pattern lack sufficient mafic rocks to constrain the metamorphic mineral zones. Large circled numbers (1-6) refer to the locations of the samples of lower Povungnituk Group pelite used for the analytical P-T path determinations described in the text. "A" refers to the inverted isograd discussed in the text.

field work (Lucas and St-Onge, 1991) has documented the presence of mineral assemblages in reworked basement units that are equivalent to those found in the adjacent Cape Smith Belt.

The sequences of mineral isograds document an increase in metamorphic grade from lower greenschist facies to middle amphibolite facies conditions within the thrust belt (Fig. 145 and 147; Bégin, 1989a, b, 1992a). Two contrasting metamorphic field gradients (Spear et al., 1984) can be defined in the two tectonothermal domains of the thrust belt (Fig. 148). In the external domain a relatively higher-temperature gradient, characterized by hornblende-oligoclase and garnet-oligoclase assemblages, is exposed by the present erosion surface (Fig. 148; Bégin, 1992a). In contrast, the internal domain displays a relatively lower-temperature metamorphic field gradient, characterized by hornblende-albite (without actinolite) and garnet-albite mineral assemblages (Fig. 148; Bégin, 1992a).

External domain

In the external domain, a prograde suite of mineral isograds has been mapped in the metamorphosed basalts and mafic sills of the Povungnituk Group (Fig. 145). Four mineral isograds (hornblende, oligoclase, actinolite-out, and garnet or clinopyroxene) separate the following five regional metamorphic mineral zones in mafic rocks (Fig. 145; St-Onge et al., 1986; Bégin, 1989a, 1989b, 1992a): (1) actinolite-albite; (2) hornblende-actinolite-albite; (3) hornblende-actinolite-oligoclase; (4) hornblende-oligoclase (no actinolite); and (5) hornblende-oligoclase-garnet/clinopyroxene. Epidote, chlorite, calcite, quartz, sphene and/or ilmenite are common phases in most mineral zones (Bégin, 1989b). The mafic mineral zones are similar to those in the Barrow-Tilley zonal sequence of the Scottish Dalradians (Turner, 1981), the mineral zones mapped in



mafic rocks in Vermont (Laird & Albee, 1981), or those in the Haast Schist Group of Southern New Zealand (Cooper, 1972).

The distribution of mineral zones in the mafic rocks of the external domain indicates an increase in metamorphic grade from west to east. The increase in grade coincides with a gradual change from high structural levels preserved in the west to low structural levels exposed in the east. 'Structural level' refers to the plunge-corrected distance above a datum surface in the crust. The datum surface chosen for the Cape Smith Belt is the contact between the Superior Province basement and the Early Proterozoic cover units (see 'Structural sections of the Cape Smith Belt' above; Lucas, 1989a). The west-to-east change in structural levels is the result of the late, post-metamorphic D₄ cross-folding of the thrust belt about northwest axes (Lucas, 1989a; St-Onge and Lucas, 1990m).

The isograds mapped in the external domain were projected by Lucas (1989a) on a composite, down-plunge constrained cross-section of the thrust belt (Fig. 146). As

discussed in the 'Structural History of the Cape Smith Belt' section, the lines of projection used in the construction of the north-south cross-section were taken by Lucas (1989a) as being parallel to the local plunge directions of west-trending folds of basement and cover. Two observations support the assumption that the isograds plunge parallel to the major structures of the thrust belt and are thus predictable surfaces (and therefore projectable) at the regional scale. First, the isograds are approximately parallel to the underlying basal décollement (Fig. 145). Second, the isograds are folded by the west-trending folds of basement and cover (Fig. 145). As well, the complete absence of local heat sources in the Povungnituk Group (e.g. plutons), which may have generated or perturbed the isograds, supports the hypothesis that the isograds are predictable surfaces at the scale of the Cape Smith Belt. The cross-section shown in Figure 146 illustrates (1) the relation between the isograds and the structure of the thrust belt following D₃ west-trending folding but prior to D₄ cross-folding; and (2) the normal or 'hot-side-down' (St-Onge, 1981) nature of the prograde mineral zones in the Povungnituk Group.

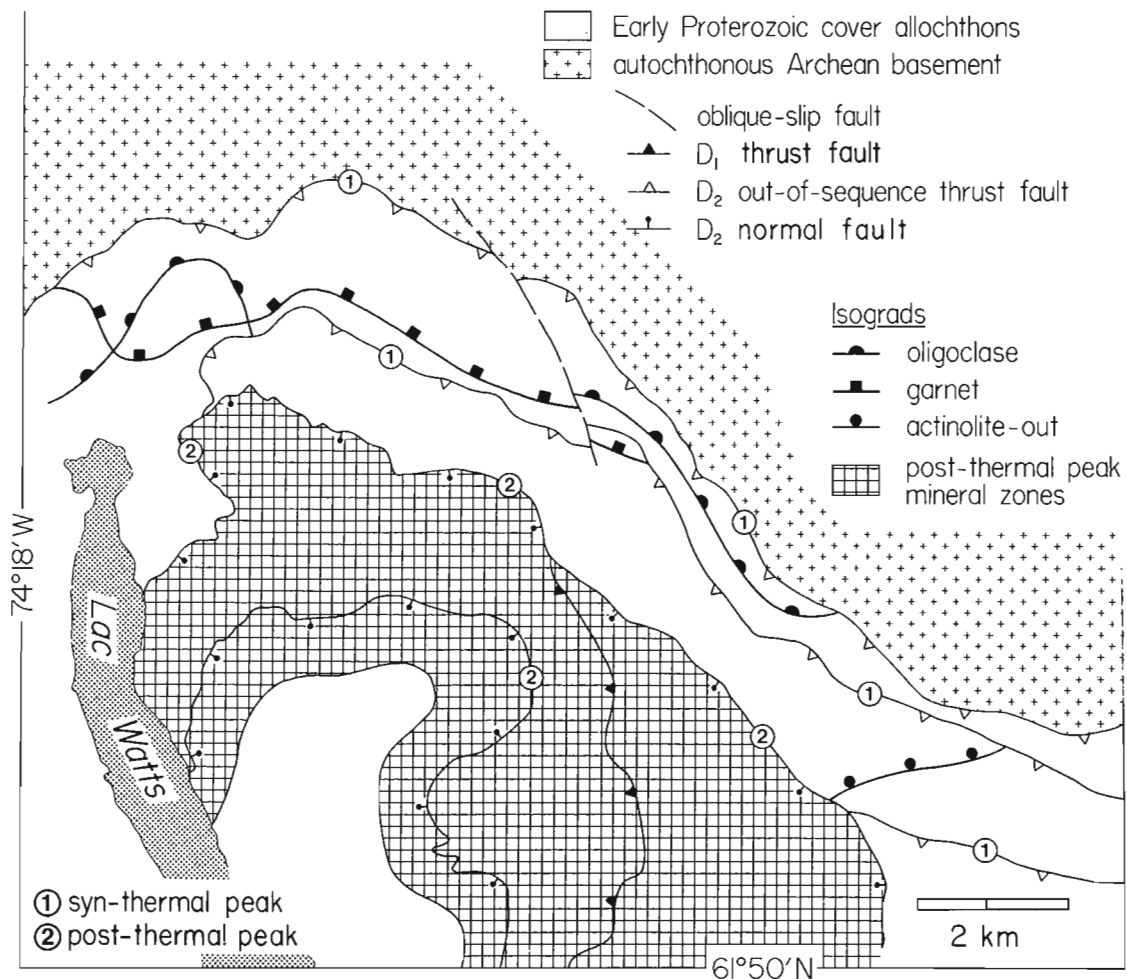


Figure 147. Detailed metamorphic map of the northern portion of the Cape Smith Belt at the northeast end of lac Watts (1721A). The distribution of the metamorphic mineral zones is after Bégin (1989a,b, 1992a).

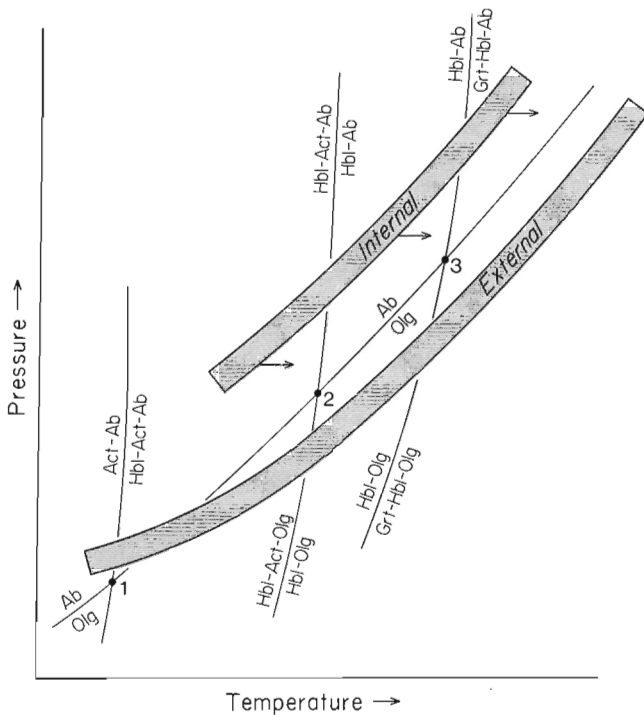


Figure 148. Schematic P-T diagram (after Bégin, 1989b, 1992a) showing the reaction curves corresponding to the hornblende, oligoclase, actinolite-out and garnet isograds. Constraints for the metamorphic field gradients of the external and internal domains are given in the text. Invariant points #1, 2, 3 are discussed in the text. Mineral abbreviations are: Ab - albite; Act - actinolite; Grt - garnet; Hbl - hornblende; Olg - oligoclase.

Bégin (1989b, 1992a) has shown that the relative sequence of mineral zones indicated by the assemblages hornblende-actinolite-albite and hornblende-actinolite-oligoclase (Fig. 145) constrains the lower temperature portion of the local metamorphic field gradient on a schematic P-T diagram for mafic rocks ('external' on Fig. 148). In detail, these assemblages bracket the field gradient to pass between two invariant points (#1 and #2; Fig. 148). Invariant point #1 is one of four bathograds (Carmichael, 1978) recently defined and calibrated for use in mafic rocks by Bégin (1989b, 1992a). The higher temperature segment of the metamorphic field gradient for the external domain (Fig. 148) was constrained by Bégin (1989b, 1992a) using pressure and temperature estimates based on: (1) Graham & Powell's (1984) geothermometer for garnet-hornblende-bearing rocks; and (2) Kohn & Spear's (1989) geobarometer for garnet-hornblende-plagioclase-quartz assemblages.

Internal domain

In the internal part of the thrust belt, two distinct suites of metamorphic mineral assemblages are preserved in the mafic rocks of the Watts Group (Fig. 145; Bégin, 1989b,

1992a; Lucas, 1989a, 1990; St-Onge and Lucas, 1990m, 1991). An early prograde suite is associated with thrusting (D₂) at thermal peak conditions. An overprinting retrograde suite is related to post-thermal peak normal faulting. The principal characteristics of the prograde metamorphic suite as documented by the mafic mineral isograds will be summarized in this section. Figures 145 to 147 document the extent to which retrograde chlorite-actinolite-albite assemblages are developed in the hanging walls of the post-thermal peak faults. The reader is referred to Bégin (1989b), Lucas (1990) and the 'Structural History' section above for descriptions of the retrograde mineral assemblages.

A prograde suite of mineral isograds was mapped in the metamorphosed mafic cumulates, basalts, and gabbroic sills of the Watts Group (Bégin, 1989a, b, 1992a). Three mineral isograds (actinolite-out, garnet/clinopyroxene and oligoclase) separate four mineral zones: (1) hornblende-actinolite-albite; (2) hornblende-albite (no actinolite); (3) garnet-hornblende-albite; and (4) garnet-hornblende-oligoclase. Epidote, chlorite, calcite, quartz, sphene, and/or ilmenite are common phases in most mineral zones (Bégin, 1989b). The prograde mineral zones in the mafic rocks of the internal domain are too narrow to illustrate on Figure 145. An example of the internal zone isograd suite is illustrated on a more detailed metamorphic map (Fig. 147) corresponding to the northeast end of lac Watts (1721A; Fig. 145). Bégin (1989b) has noted that the mineral assemblages (1) to (4) are similar to assemblages reported from the Sangabawa Belt in Japan (Enami, 1981; Maruyama et al., 1982).

The distribution of prograde mineral zones in the mafic rocks of the internal domain indicates an increase in metamorphic grade towards the northern contact between the Superior Province basement and the Early Proterozoic cover units (Fig. 147). The northward increase in thermal-peak temperature conditions generally coincides with a gradual change in exposed structural levels from shallower levels in the south to deeper levels in the north (with respect to the basement/cover contact datum surface). The change in structural levels is consistent with deeper structural levels being exposed as the basement/cover contact is approached, and is attributed to erosion following the two basement-involved folding episodes (D₃ and D₄; Lucas, 1989a; St-Onge and Lucas, 1990m).

On a schematic P-T diagram for mafic rocks, mineral assemblages (1) to (4) constrain the local metamorphic field gradient for the northern domain ('internal' on Fig. 148; Bégin, 1989b, 1992a) to lie on the low-temperature side of the albite-oligoclase reaction curve. This contrasts with the previously described metamorphic field gradient for the external domain (Fig. 148) which is generally restricted to the high-temperature side of the albite-oligoclase reaction curve. As shown on Fig. 148, assemblages (2) and (3) of the internal domain require that the local metamorphic field gradient pass above two invariant points (points #2 and #3). Invariant point

#3 is the garnet-albite bathograd defined and calibrated for use in mafic rocks by Bégin (1989b, 1992a). Combining the mapped isograd sequences with Bégin's (1989b, 1992a) bathograd grid for mafic rocks indicates that the external domain records a higher-temperature metamorphic field gradient than the internal domain (Fig. 148; Bégin, 1992a).

Locally, the oligoclase isograd mapped in the internal domain intersects the garnet and actinolite-out isograds (Fig. 147). The intersection of isograds in the field can be indicative of (1) changing paleopressure and/or paleo-temperature conditions across an area or (2) variation in the vapor phase composition (i.e., X_{CO_2}) during metamorphism (e.g. Carmichael, 1970). In the mafic rocks of the Cape Smith Belt, variations in the X_{CO_2} content of the vapour phase during metamorphism are constrained to a small range ($X_{CO_2} = 0.08$ to 0.12 ; Bégin, 1989b). Also, the change in the sequence of isograds occurs at more or less constant structural levels (i.e. equidistant from the northern basement/cover contact; Fig. 147), suggesting that a change in paleo-pressures is probably not the cause of the intersecting isograds. The intersection of the isograds may therefore principally reflect a shift in the local metamorphic field gradient to relatively higher-temperature conditions (indicated by horizontal arrows on Fig. 148). Because of this apparent strike-parallel variation in metamorphic conditions, the mineral isograds in the internal zone of the Cape Smith Belt were not projected by Lucas (1989a) onto the metamorphic cross-section (Fig. 146). Instead, the regional distribution of thermal peak and post-thermal peak metamorphic assemblages is qualitatively illustrated for Watts Group mafic rocks (Fig. 146; Lucas, 1989a).

RELATIONS BETWEEN MINERAL GROWTH AND DEFORMATION

Crosscutting relations between faults and the thermal peak mineral isograds highlight the chronology of deformation and metamorphism in the Cape Smith Belt. The isograds overprint the D_1 piggyback thrust structure and the basal shear zone in the external domain, but are truncated by D_2 syn- and post-thermal peak faults in the internal domain (Lucas, 1989a; St-Onge and Lucas, 1990m, 1991).

External domain

In the external part of the Cape Smith Belt, the map pattern of mineral isograds (Povungnituk Group; Fig. 145 and 146) clearly establishes the relative timing between regional metamorphism and deformation (Bégin, 1989b; St-Onge and Lucas, 1990m). The mafic isograds overprint the early D_1 thrust faults and the syn-metamorphic basal shear zone adjacent to the basal décollement. In turn, the thrust faults, basal shear zone, and mineral isograds are folded by the D_3 west-trending macroscopic folds. These map-scale observations document that regional metamorphism in the external domain postdates the early piggyback-sequence thrusting and predates the later basement-involved folding.

Thinsection observations also constrain the relative chronology of metamorphism and deformation in the external domain (Lucas, 1990; St-Onge and Lucas, 1991). At relatively high structural levels (above the basal shear zone, Fig. 82), low-temperature metamorphic minerals (e.g. biotite) have overgrown early D_1 fault zone foliations (Fig. 87). In contrast, prograde mineral assemblages within the basal shear zone are clearly syntectonic (Fig. 107). However, thermal peak mineral phases have consistently overgrown the shear zone foliation (Fig. 108, 111, 112, and 149), indicating that movement along the basal shear zone took place at or before the thermal peak of metamorphism.

Internal domain

Thermal peak mineral growth in the internal part of the Cape Smith Belt was synchronous with deformation in shear zones associated the D_2 thrust faults (Table 2; Lucas, 1989a, 1990; St-Onge and Lucas, 1990m, 1991). This relationship is illustrated in Figure 110: garnet grains in a semipelite contain sigmoidal inclusion trails of quartz and feldspar that are continuous with the tectonic fabric in the surrounding matrix. In contrast, the late D_2 normal fault zones are characterized by the development of retrograde mineral assemblages (Fig. 150 and 151; Lucas, 1990). Isograds in the internal domain are truncated by D_2 faults (Fig. 147; Bégin, 1989a, b, 1992a; Lucas, 1989a), further documenting that deformation must have continued past thermal peak equilibration in this

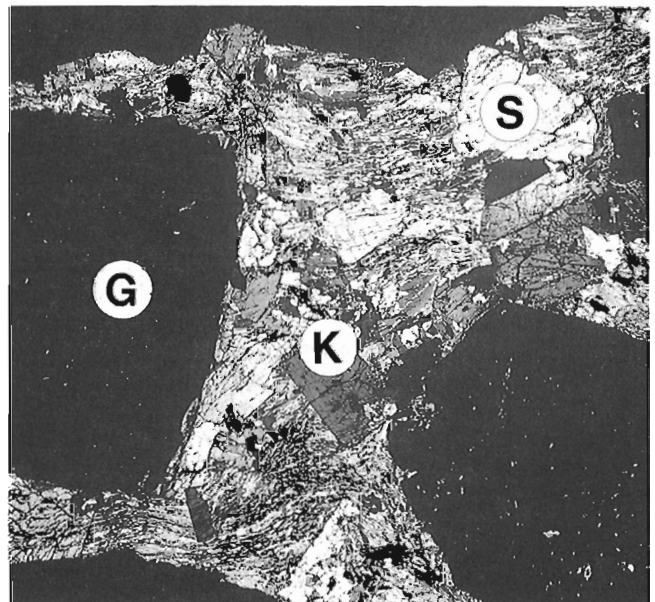


Figure 149. Photomicrograph of a garnet (G) - kyanite (K) - staurolite (S) pelite of the lower Povungnituk Group in the basal shear zone of the external domain, west shore of Wakeham Bay (Fig. 145). The shear zone fabric is defined by the alignment of muscovite, biotite, plaioclase, quartz, and graphite. Note that the thermal peak porphyroblasts of garnet, kyanite, and staurolite overgrow the tectonic fabric. Horizontal field of view is 48 mm. (GSC 205165-D)

domain. As in the external part of the thrust belt, the faults and metamorphic mineral zones were deformed by the west-trending folds of basement and cover (Fig. 145 and 146).

Relative timing of thermal peak metamorphism between domains

In order to use the timing of thermal peak metamorphism as a relative chronometer for deformation in the Cape Smith Belt, the assumption that thermal peak conditions were reached coevally at comparable structural levels within both the external and internal domains (Fig. 145) must be justified. Constraints on the relative timing of regional metamorphism between the two tectonothermal domains are indicated by: (1) the geometry of mineral isograds in the external domain; and (2) mineral growth/deformation relationships in both domains (Lucas, 1989a; St-Onge and Lucas, 1991). Syndeformation growth of thermal peak minerals in the internal part of the thrust belt indicate that it reached thermal peak conditions during deformation (D₂, Table 2). In the external domain, the hornblende isograd (Bégin, 1989a, b, 1992a) is locally steep to inverted (point 'A'; Fig. 145 and 146). Three causes for the inversion can be considered: (1) a structural inversion; (2) a thermal inversion related to plutonism; or (3) a thermal inversion due to the emplacement of hotter hanging wall rocks. Explanation (1) can be ruled out because pillow top directions indicate an upward-facing sequence. Explanation (2) can also be ruled out because of the complete absence of plutons within the external domain, and in the internal domain near the isograd. The most likely explanation is that the inversion is a thermal consequence of the emplacement of the immediately overlying thrust stack during out-of-sequence (D₂) thrusting (Table 2). However, unroofing of the external domain must have been rapid enough to preserve the overturned isograd.

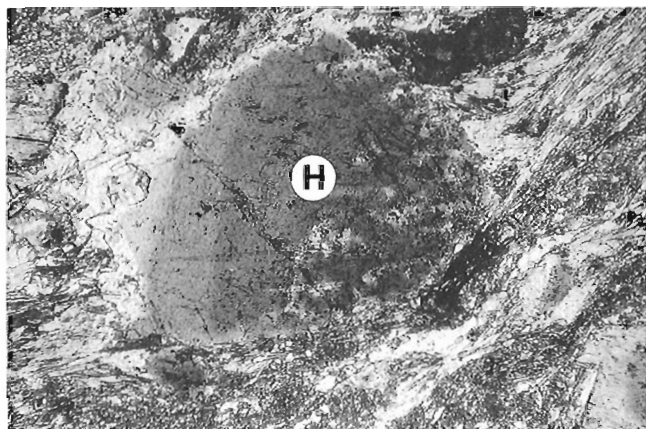


Figure 150. Photomicrograph of a hornblende porphyroblast (H) reacting to actinolite and epidote in a layered gabbro of the Watts Group. The sample is from a post-thermal peak mineral zone associated with D₂ normal faults 1 km east of lac Watts (Fig. 147). Horizontal field of view is 4 mm. (GSC 1992-106R)

These observations imply that thermal peak metamorphism in the external domain coincided with or immediately followed D₂ thrusting in the internal part of the thrust belt. In addition, these observations suggest that emplacement of the out-of-sequence (D₂) thrust stack (including Watts Group and Narsajuaq arc units; Fig. 1) onto the continental thrust belt may have precipitated thermal peak metamorphism of the external (footwall) domain (Lucas, 1989b; St-Onge and Lucas, 1990m, 1991; Lucas and St-Onge, 1992) leading to posttectonic mineral growth (Fig. 108, 111, 112, and 149). It therefore seems reasonable to conclude that the thermal peak of metamorphism in the two domains was broadly coeval at comparable structural levels (Lucas, 1989a).

ANALYTICALLY-DERIVED P-T PATHS IN PELITES

Pelitic layers of the lower Povungnituk Group with mineral assemblages appropriate for thermobarometric work were studied in both the external and internal tectonothermal domains of the Cape Smith Belt (St-Onge and Lucas, 1990m, 1991). All samples were collected within 200 m of the basement/cover contact in order to ensure that the samples shared a common structural position with respect to a regional datum surface (Fig. 145). This common structural basis for the samples allows the thermobarometric results to be compared on the basis of their domainal and transverse positions in the thrust belt. Pelites of the lower Povungnituk Group in the two domains contain the following mineral assemblage: *garne-muscovite-biotite-plagioclase-quartz-ilmenite-graphite±kyanite±staurolite±chlorite*. Of the pelite samples collected, six were selected for thermobarometric analysis (St-Onge and Lucas, 1990m, 1991): two samples

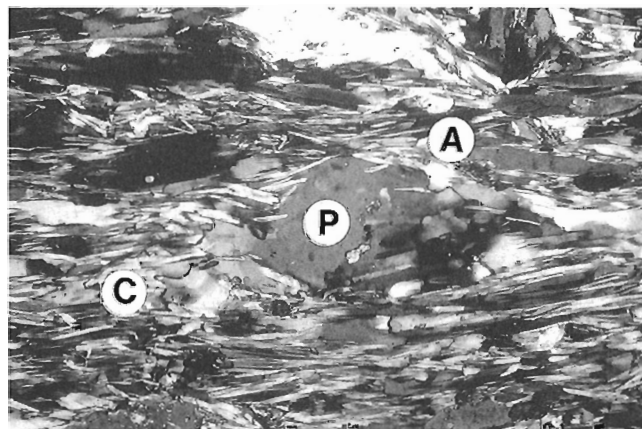


Figure 151. Photomicrograph of a retrograde mineral assemblage in a gabbro of the Watts Group east shore of lac Watts (Fig. 147). The mineral assemblage which is associated with a late D₂ normal fault comprises actinolite (A), plagioclase (P) and chlorite (C). Horizontal field of view is 2 mm. (GSC 205208-B)

Table 3. Representative garnet analyses

Spot no.	Garnet																							
	Rim							Core							Garnet							Rim		
	1	2	3	4	5	6	7	8	9	10	11	12	13	14	15	16	17	18	19	20	21			
SiO ₂	37.57	37.56	37.89	37.50	37.44	37.55	37.63	37.30	37.67	37.65	37.39	38.06	37.50	37.42	37.39	38.15	38.11	37.25	37.74	37.54	37.91			
Al ₂ O ₃	21.50	21.36	21.49	21.55	21.61	21.30	21.30	21.30	21.69	21.35	21.30	21.79	21.44	21.28	21.43	21.84	21.51	21.33	21.46	21.41	21.61			
FeO	32.32	32.45	31.96	32.08	31.56	31.01	30.71	30.27	30.29	30.07	29.93	30.91	31.01	31.41	31.66	31.86	32.26	32.52	32.59	32.57	32.51			
MgO	3.48	2.88	2.56	2.15	2.10	2.00	2.00	1.91	1.89	1.97	1.78	1.97	1.85	2.11	2.03	2.39	2.45	2.74	2.89	3.04	3.20			
MnO	0.07	0.08	0.14	0.55	1.42	1.78	2.17	2.40	2.53	2.81	2.76	2.23	2.01	1.38	0.86	0.38	0.22	0.06	0.05	0.06	0.01			
CaO	4.39	5.00	5.84	5.88	5.56	6.08	6.10	6.25	6.50	6.49	6.49	5.92	5.88	5.83	5.96	6.15	5.66	5.43	5.11	4.67	4.82			
Cr ₂ O ₃	0.14	0.05	0.09	0.06	0.11	0.04	0.01	0.06	0.08	0.05	0.10	0.06	0.09	0.06	0.09	0.11	0.08	0.09	0.08	0.07	0.10			
Total	99.47	99.38	99.97	99.77	99.80	99.76	99.92	99.49	100.65	100.39	99.75	100.94	99.78	99.49	99.42	100.88	100.29	99.42	99.92	99.36	100.16			
	Cations per 12 oxygens																							
Si	2.999	3.018	3.030	3.001	2.994	3.019	3.022	2.999	2.986	3.003	3.001	3.020	3.012	3.013	3.007	3.017	3.049	2.981	3.015	3.013	3.015			
Al	2.023	2.023	2.026	2.033	2.037	2.018	2.016	2.019	2.026	2.007	2.015	2.038	2.030	2.019	2.031	2.036	2.028	2.012	2.020	2.025	2.025			
Fe	2.158	2.180	2.138	2.147	2.111	2.085	2.063	2.036	2.008	2.006	2.009	2.051	2.083	2.115	2.129	2.107	2.158	2.177	2.177	2.186	2.162			
Mg	0.414	0.345	0.305	0.256	0.250	0.240	0.239	0.229	0.223	0.234	0.213	0.233	0.221	0.253	0.243	0.282	0.292	0.327	0.344	0.364	0.379			
Mn	0.005	0.005	0.009	0.037	0.096	0.121	0.148	0.163	0.170	0.190	0.188	0.150	0.137	0.094	0.059	0.025	0.015	0.004	0.003	0.004	0.001			
Ca	0.376	0.430	0.500	0.504	0.476	0.524	0.525	0.538	0.552	0.555	0.558	0.503	0.506	0.503	0.514	0.521	0.485	0.466	0.437	0.402	0.411			
Cr	0.009	0.003	0.006	0.004	0.007	0.003	0.001	0.004	0.005	0.003	0.006	0.004	0.006	0.004	0.006	0.007	0.005	0.006	0.005	0.004	0.006			
Total	7.984	8.005	8.015	7.983	7.973	8.009	8.014	7.988	7.970	7.998	7.990	8.000	7.995	8.001	7.989	7.996	8.032	7.973	8.002	7.998	7.999			
Mg/(Mg+Fe)	0.161	0.137	0.125	0.107	0.106	0.103	0.104	0.101	0.100	0.105	0.096	0.102	0.096	0.107	0.103	0.118	0.119	0.131	0.136	0.143	0.149			
Alm	0.731	0.736	0.724	0.729	0.719	0.702	0.693	0.686	0.680	0.672	0.677	0.698	0.707	0.713	0.723	0.718	0.731	0.732	0.735	0.740	0.732			
Prp	0.140	0.116	0.103	0.087	0.085	0.081	0.080	0.077	0.076	0.078	0.072	0.079	0.075	0.085	0.083	0.096	0.099	0.110	0.116	0.123	0.128			
Sps	0.002	0.002	0.003	0.013	0.033	0.041	0.050	0.055	0.058	0.064	0.063	0.051	0.046	0.032	0.020	0.009	0.005	0.001	0.001	0.001	0.001			
Crts	0.123	0.144	0.167	0.169	0.159	0.175	0.176	0.180	0.184	0.184	0.185	0.169	0.169	0.168	0.171	0.174	0.162	0.154	0.145	0.134	0.136			

from the internal domain (samples #1 and #2, Fig. 145 and 146) and four samples from the external domain (samples #3 to #6, Fig. 145 and 146).

Analytical procedure

Following serial slabbing, the garnet with the greatest diameter (between 10 and 22 mm) in each of the six pelitic samples was selected for analysis (St-Onge and Lucas, 1991). This procedure insures that chemical analyses are obtained as close as possible to the true centre of the zoned mineral phase and minimizes any potential 'sphere effect' (Indares and Martignole, 1985). The garnet porphyroblasts were analyzed along rim-core-rim traverses at regular intervals (0.4-0.9 mm depending on the size of the garnet) yielding an average of 25 spot-analyses per garnet. Matrix minerals were spot-analyzed three to five times and the analyses averaged. Larger matrix grains (2-3 mm) were analyzed along rim-core-rim traverses with 10 to 15 evenly spaced spot-analyses. Chemical zoning was detected only in garnet. Representative mineral analyses for sample #4 are given in Tables 3-5.

The spot-analyses were obtained using a Materials Analysis Corporation electron microprobe equipped with a Kevex energy dispersive spectrometer and automated to produce simultaneous multi-element analyses and data reduction (Plant and Lachance, 1973). Operating conditions were: 20 kV accelerating voltage, specimen current of 20 nA measured on standard kaersutite and a counting time of 100 s. Standards used are reported in Plant and Lachance (1973).

Microstructure and mineral chemistry

The analyzed pelitic samples display the same contrasting mineral growth/deformation relationships previously described for the two tectonothermal domains (St-Onge and Lucas, 1991). In samples #1 and #2 (internal domain; Fig. 145 and 146), the foliation related to D₂ thrusting is defined by the alignment of kyanite, muscovite, biotite, plagioclase, quartz, ilmenite, and graphite. As well, the foliation contains thermal peak porphyroblasts which clearly grew during deformation (e.g. Fig. 110). In samples #3 to #6 (external domain; Fig. 145 and 146), the basal shear zone fabric is defined by the alignment of muscovite, biotite, plagioclase,

Table 4. Representative biotite analyses

Grain no.	Biotite									
	1	2	3	4	5	6	7	8	9	10
SiO ₂	37.20	37.35	37.11	37.17	36.93	37.29	36.84	37.30	36.91	37.16
Al ₂ O ₃	18.72	18.97	18.61	18.69	18.85	18.87	18.76	18.63	18.61	18.64
TiO ₂	1.87	1.94	1.77	2.02	1.81	1.82	1.81	1.87	1.75	1.80
FeO	16.62	17.20	17.08	16.95	17.19	17.05	17.04	17.39	17.06	17.04
MgO	12.17	12.30	12.28	12.25	12.05	12.18	11.88	12.27	12.24	12.30
MnO		0.01			0.02		0.05	0.08		
Na ₂ O		0.09								
K ₂ O	9.21	9.16	8.91	9.00	9.04	8.92	8.97	9.16	9.12	8.92
Cr ₂ O ₃	0.05	0.07		0.05	0.03	0.07	0.05	0.05	0.05	0.03
Total	95.84	97.09	95.76	96.13	95.92	96.20	95.40	96.75	95.74	95.89
Cations per 11 oxygens										
Si	2.760	2.741	2.757	2.750	2.744	2.755	2.750	2.751	2.748	2.757
Al	2.200	1.641	1.630	1.630	1.650	1.644	1.651	1.619	1.633	1.629
Ti	0.104	0.107	0.099	0.112	0.101	0.101	0.102	0.104	0.098	0.100
Fe	1.031	1.056	1.061	1.049	1.068	1.054	1.064	1.073	1.062	1.057
Mg	1.346	1.345	1.360	1.351	1.334	1.341	1.322	1.349	1.358	1.360
Mn		0.001			0.001		0.003	0.005		
Na		0.013								
K	0.872	0.858	0.844	0.850	0.857	0.841	0.854	0.862	0.866	0.844
Cr	0.003	0.004		0.003	0.002	0.004	0.003	0.003	0.003	0.002
Total	7.752	7.765	7.751	7.745	7.758	7.740	7.749	7.765	7.769	7.750
Mg/(Mg+Fe)	0.566	0.560	0.562	0.563	0.555	0.560	0.554	0.557	0.561	0.563

quartz, ilmenite, graphite±chlorite. Thermal peak porphyroblasts overprint the external domain foliation (Fig. 149). A summary of the microstructural characteristics and chemistry of all phases in the analyzed samples is given below.

Garnet

Garnet grains display two morphological populations which correspond to the two tectonothermal domains of the Cape Smith Belt (St-Onge and Lucas, 1991). In the internal part of the thrust belt (samples #1 and #2; Fig. 145 and 146), the morphology of the garnet porphyroblasts ranges from subhedral grains with rotational (inclusion-defined) growth patterns (Fig. 110) to inequant grains whose long axes parallel the foliation. Garnet diameters vary from 3 to 20 mm. Inclusion trails are defined by tourmaline, muscovite, biotite, quartz, ilmenite, graphite, and rarely kyanite±staurolite, and are continuous from the garnet rims into the matrix foliation (Fig. 110). This continuity in fabric appears to rule out the

possibility that garnet rotation completely postdates growth. While the garnets may have fortuitously overgrown matrix microfolds and/or older foliations during subsequent deformation characterized by grain-scale strain partitioning (e.g., Bell, 1985, 1986; Bell and Johnson, 1989, 1990), such an explanation is difficult to prove and is not required to explain the microstructural observations. The P-T estimates derived from the garnet-bearing assemblages are interpreted to record the physical conditions during D₂ deformation.

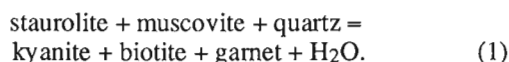
In the external part of the thrust belt (samples #3 to #6; Fig. 145 and 146), garnet porphyroblasts overgrow the basal shear zone foliation (Fig. 111 and 149; St-Onge and Lucas, 1991). Garnet in this domain is euhedral, poikiloblastic and ranges in diameter from 10 to 22 mm. The porphyroblasts contain inclusions of tourmaline, muscovite, quartz, ilmenite, graphite, and rarely staurolite. Inclusion trails are straight throughout the porphyroblasts and are continuous with the shear zone fabric in the pelitic matrix. Other higher-T minerals such as kyanite, staurolite and plagioclase also overgrow the D₁ matrix foliation (Fig. 111 and 149). It

Table 5. Representative plagioclase analyses

Grain no.	Plagioclase					
	1	2	3	4	5	6
SiO ₂	62.44	62.93	62.00	61.98	61.84	62.12
Al ₂ O ₃	23.98	24.07	24.42	24.10	23.82	24.00
FeO	0.08	0.06	0.12	0.10	0.04	0.05
CaO	5.13	4.96	5.55	5.24	5.12	5.09
Na ₂ O	8.56	8.41	8.27	8.40	8.51	8.40
K ₂ O	0.16	0.12	0.17	0.15	0.14	0.15
Total	100.35	100.55	100.53	99.97	99.47	99.81
Cations per 8 oxygens						
Si	2.756	2.766	2.735	2.747	2.754	2.755
Al	1.248	1.247	1.270	1.259	1.250	1.254
Fe	0.003	0.002	0.004	0.004	0.001	0.002
Ca	0.243	0.234	0.262	0.249	0.244	0.242
Na	0.733	0.717	0.707	0.722	0.735	0.722
K	0.009	0.007	0.010	0.008	0.008	0.008
Total	4.991	4.972	4.988	4.989	4.992	4.983
An	0.246	0.244	0.268	0.254	0.247	0.249
Ab	0.744	0.749	0.722	0.737	0.744	0.742
Or	0.009	0.007	0.010	0.009	0.008	0.009

should be noted that relations between garnet inclusion-trails and matrix foliations in all samples exclude the possibility that the porphyroblasts grew following microfolding associated with the west-trending folding event (e.g. Fig. 143). The P-T estimates derived by analyzing the garnet-bearing assemblages in the external domain therefore pertain to the physical conditions following basal shear zone deformation but prior to west-trending folding.

Concentric compositional zoning is well developed in all analyzed garnets (St-Onge and Lucas, 1990m, 1991). Representative garnet analyses are given in Table 3. Cores are notably enriched in grossular and spessartine components relative to the rims, and the zoning is approximately symmetrical with respect to the porphyroblast core (Fig. 152). Absence of breaks or gaps in the zoning trends (Fig. 152) and lack of distinct textural zones suggest that: (1) the porphyroblasts are not the result of polymetamorphism; and (2) individual garnet growth is consistent with a single reaction such as:



The garnet compositional zoning is further discussed below in the section on thermochemical modeling of garnet zonation.

Muscovite

Muscovite is found both as 0.25-0.5 mm laths in all sample matrices and as rare inclusions, less than 0.25 mm in length, in a number of garnet poikiloblasts. Within a given sample, the range in muscovite compositions is small and individual muscovite grains are homogeneous. Typical muscovite compositions range from $\text{Pg}_{(24)}\text{Ms}_{(76)}$ to $\text{Pg}_{(35)}\text{Ms}_{(65)}$. No compositional gradients were noted either parallel or perpendicular to the muscovite cleavage.

Biotite

In the internal domain, biotite is found as 0.25 to 0.5 mm laths defining the matrix foliation. In the external domain, biotite has two habits, although the compositions of the two types are indistinguishable. Small biotite laths (0.5 mm in length) are crystallographically and dimensionally aligned in the matrix foliation. Larger (3-4 mm) biotite grains overprint the shear zone fabric and are poikiloblastic, containing inclusion trails of muscovite, quartz, and tourmaline that are continuous with the matrix foliation. In both domains, the range in biotite compositions is small within a given sample with no evidence for compositional gradients either perpendicular or parallel to the biotite cleavage. Representative biotite analyses are given in Table 4.

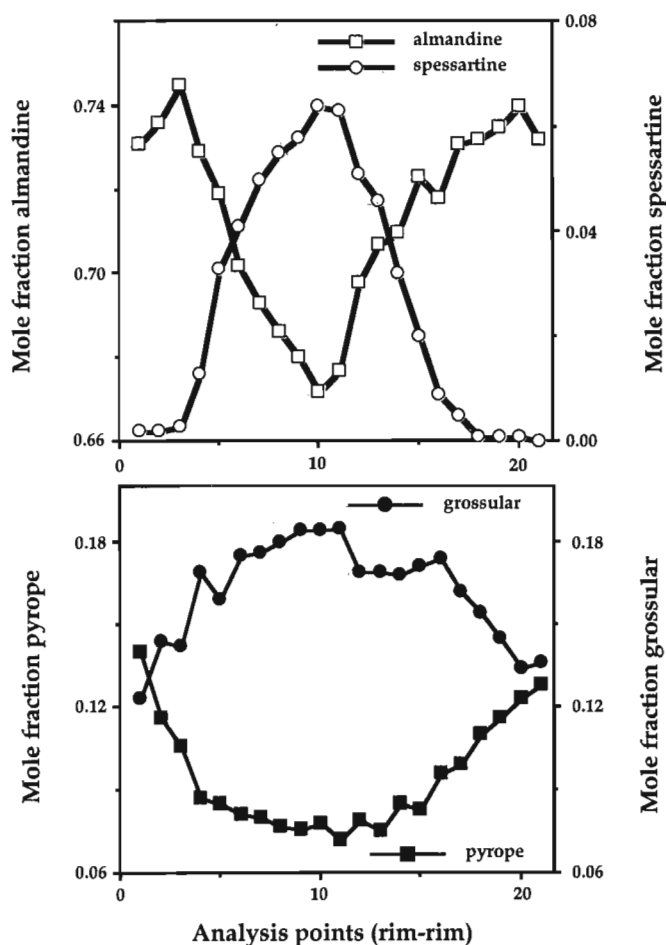


Figure 152. Garnet zoning profiles for pelite sample #4 (Fig. 145 and 146) discussed in the text. Numbers on vertical axes represent the mole fractions of the four garnet end-member components. Horizontal axis represents full diameter of garnet grain (21 analysis points spaced at 0.9 mm intervals).

Plagioclase

Plagioclase occurs as abundant small, anhedral grains in the matrices of all six samples. The grains are 0.5 to 1.0 mm in diameter and show no chemical zonation or significant compositional variation within a given sample. The range of the average plagioclase compositions between samples is from An_{19} (sample #6) to An_{27} (sample #3). Plagioclase and quartz grains define a granoblastic texture in the more siliceous layers of the pelite samples. Evidence of retrogression to sericite is rare. Representative plagioclase analyses are given in Table 5.

Quartz

Quartz is abundant in samples from both tectonothermal domains. It is found both as inclusions in the garnet porphyroblasts (0.25 to 0.75 mm in diameter) and as granoblastic grains in the matrices (0.5 to 1.0 mm in diameter). Quartz does not deviate from pure SiO_2 within the resolution of the electron microprobe.

Kyanite

In the internal domain, kyanite occurs as small subhedral to skeletal grains between 2 and 3 mm long. The grains are aligned parallel to the foliation related to the thermal peak (D₂) thrusts. The kyanite is poikiloblastic and contains numerous inclusions of tourmaline, biotite, quartz, graphite, and ilmenite.

In the external domain, kyanite forms euhedral to subhedral grains which range from 2 to 4 mm long and are often twinned and poikiloblastic. The kyanite porphyroblasts in the external domain overprint the basal shear zone fabric (Fig. 149) and contain straight inclusion trails of tourmaline, muscovite, biotite, quartz, ilmenite, and graphite that are continuous with the matrix foliation. In both domains, the kyanite is pure Al₂SiO₅ within the resolution of the electron microprobe.

Staurolite

Staurolite in the internal domain is poikiloblastic and contains many inclusions of tourmaline, muscovite, biotite, quartz, and graphite. The porphyroblasts are subhedral to anhedral, 2 to 3 mm long and are aligned parallel to the D₂ shear zone foliation. Embayed edges suggest that staurolite is a reactant phase in garnet-producing reactions such as (1) above.

In the external domain, staurolite porphyroblasts are also subhedral to anhedral with embayed edges and range from 2 to 4 mm in length. The staurolite grains overprint the basal shear zone fabric (Fig. 149) and contain inclusion trails of tourmaline, muscovite, biotite, quartz, and graphite that are continuous with the matrix foliation. The range in the Mg/(Mg+Fe) ratios for all analyzed staurolites is from 0.100 to 0.140.

Chlorite

Chlorite is part of the stable assemblage in samples #5 and #6. It occurs as 1 to 2 mm long flakes, and with biotite and muscovite grains, defines the basal shear zone foliation. Retrograde chlorite was not noted in any of the samples used for the thermobarometric study. The range in the Mg/(Mg+Fe) ratios for the analyzed chlorites is from 0.601 to 0.611.

Tourmaline, ilmenite and graphite

Tourmaline, ilmenite, and graphite are accessory phases in all the analyzed samples. These minerals occur both as matrix grains (<1 mm in length) and as inclusions in the higher-temperature porphyroblasts. Tourmaline is characterized by ubiquitous optical zoning. Ilmenite shows no evidence of oxidation or alteration.

Temperature and pressure determinations

Temperature estimates for thrust belt metamorphism were calculated from analyses of garnet porphyroblast rims and matrix biotites in the six selected samples (St-Onge and

Lucas, 1990m, 1991). Temperature determinations are based on the Fe-Mg exchange equilibrium between garnet and biotite, as experimentally calibrated by Ferry and Spear (1978) and modified by Hodges and Spear (1982). Garnet and biotite pairs were analyzed in thin section subdomains in which the two selected minerals were separated by a neutral (non-ferromagnesian) phase (e.g. quartz, muscovite, kyanite, tourmaline, etc.). This was done to avoid the potential effects of local retrograde diffusion between ferromagnesian minerals in contact (Hess, 1971; Tracy et al., 1976; Selverstone and Hollister, 1980).

Pressure determinations for the thermal peak of metamorphism were calculated from analyses of garnet porphyroblast rims and matrix plagioclase grains in the six samples (St-Onge and Lucas, 1990m, 1991). Pressure estimates are based on the grossular-kyanite-anorthite-quartz equilibrium (Kretz, 1959; Ghent, 1976), employing the calibration of Newton and Haselton (1981) as corrected by Ganguly and Saxena (1984), and using the modifications of Hodges and Spear (1982) and Hodges and Royden (1984). For each of the six samples, the thermobarometric calibrations yield P-T estimates which are interpreted to correspond to the conditions at equilibration between the garnet porphyroblast rim and the matrix assemblage. The P-T estimates are identified on Figures 153 and 154 as the 'rim determinations'.

Precision in thermobarometry is reflected in the scatter of P-T estimates that arise from errors in electron microprobe analyses. The precision of a temperature determination based on an Fe-Mg exchange geothermometer is generally $\pm 20\text{-}30^\circ\text{C}$ (Spear, 1989) at a given pressure. For a pressure determination based on the co-existence of garnet and plagioclase, the precision is generally $\pm 300\text{-}500$ bars at a given temperature (Spear, 1989).

The accuracy of a P-T determination is a function of uncertainties in (1) the activity-composition relationships employed, (2) the experimental calibrations of end-member reactions, and (3) the electron microprobe analyses. As an example, the recalibration of the grossular-kyanite-anorthite-quartz equilibrium by Koziol and Newton (1988) yields pressure estimates which are 0.8 to 1.0 kbar higher than the rim determinations shown in Figures 153 and 154. The composite accuracy error is difficult to quantify, but estimates of $\pm 150^\circ\text{C}$ on temperature and ± 5 kbar on pressure are reported by Hodges and McKenna (1987) for P-T determinations based on the thermobarometric calibrations used in the eastern Cape Smith Belt. Although such large accuracy error bars are discouraging, Spear (1989) suggests that for many applications the accuracy of thermobarometric determinations is of secondary importance to the precision. In the case of metamorphic P-T paths, the *absolute* locations of paths in P-T space will be more uncertain than their *relative* locations and shapes. However it is the relative locations and shapes which are often more important for tectonic interpretations (Spear, 1989).

Thermochemical modeling of garnet zoning

If H₂O is assumed to have been present as a phase during the metamorphism of the lower Povungnituk Group pelites, then seven-(mineral) phase subsets of the assemblage garnet-muscovite-biotite-plagioclase-quartz±kyanite±staurolite±chlorite have a chemical variance of three in the nine component system SiO₂-Al₂O₃-MgO-FeO-MnO-CaO-Na₂O-K₂O-H₂O. Physical variables such as pressure and temperature can therefore be expressed as functions of three independent compositional terms (e.g. X_{spessartine}, X_{grossular}). If minerals such as garnet are chemically zoned, the subset assemblages offer the potential to model changing pressure and temperature conditions as recorded during the growth of the zoned phase(s) (Spear and Selverstone, 1983; Spear, 1989). Given garnet rim/matrix P-T determinations, the calculated loci of modeled pressure and temperature increments can then be used to directly infer a metamorphic P-T path (St-Onge and Lucas, 1990m, 1991).

Two additional basic assumptions are inherent to this method (Spear, 1989). The first is that the chemical zoning observed in the zoned phase (e.g. garnet) is a product of growth by a continuous reaction. In the case of the pelitic samples from the Cape Smith Belt, this assumption is validated by three principal observations (St-Onge and Lucas, 1991). First, compositional trends in the analyzed garnet grains (Fig. 152) correspond to those predicted by a partial-equilibrium growth model (Tracy, 1982; Loomis,

1983). In this model, the slow rate of volume diffusion in garnet effectively isolates the interior of the growing crystal from the rest of the rock. This supports the notion that the garnet zoning records a set of equilibrium rim compositions for the growing porphyroblast. Second, the garnets lack any textural or compositional evidence for polymetamorphic growth. Third, careful examination of the entrapped inclusions (St-Onge and Lucas, 1991) suggests that the assemblages present during garnet growth were essentially the same as the assemblages now found in the matrices. The muscovite, biotite, quartz, kyanite and staurolite inclusions found in some of the analyzed garnet porphyroblasts are consistent with the matrix assemblage muscovite-biotite-plagioclase-quartz-ilmenite-graphite±kyanite±staurolite±chlorite, and thus with single continuous reactions such as (1) resulting in garnet growth.

The second assumption is that the partial-equilibrium zoning has not been modified by diffusional processes following growth of the zoned mineral. Microprobe analyses of the garnet rims in the Cape Smith Belt samples do not indicate any reversals in the compositional trends of Mn, Mg, and Ca (Fig. 152). Such reversals often indicate post-growth diffusion within garnet porphyroblasts (Tracy, 1982; Loomis, 1983; references therein). In fact, all the analyzed garnet grains are characterized by a continuous outward decrease in Mn, an increase in Ca, and an increase in the Mg/Fe ratio (Fig. 152). These trends, and the lack of textural evidence for

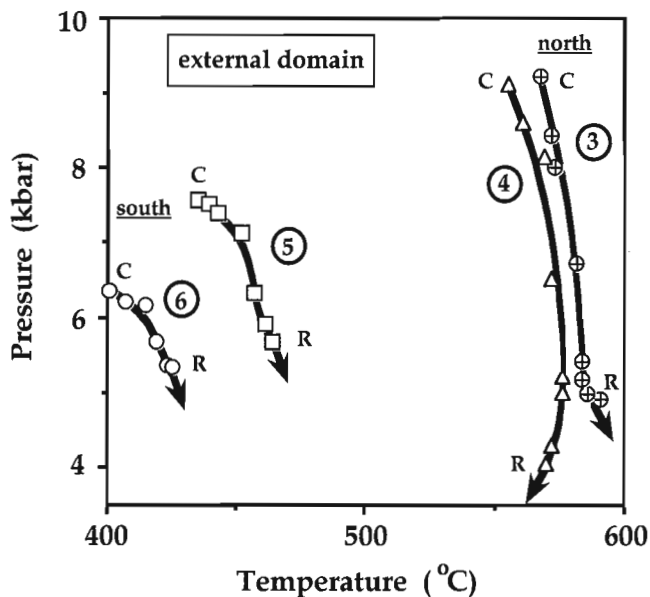


Figure 153. Analytically derived P-T paths for the four pelite samples (#3-#6) of the external domain (Figs 145 and 146). The paths record prograde decompression from garnet core to rim. For each path, 'R' refers to the P-T determination based on the analyses of the garnet rim / matrix mineral assemblage ('rim determination' discussed in the text). 'C' refers to the garnet core. All other points on the paths were calculated by thermochemical modelling of the garnet compositional zoning as discussed in the text.

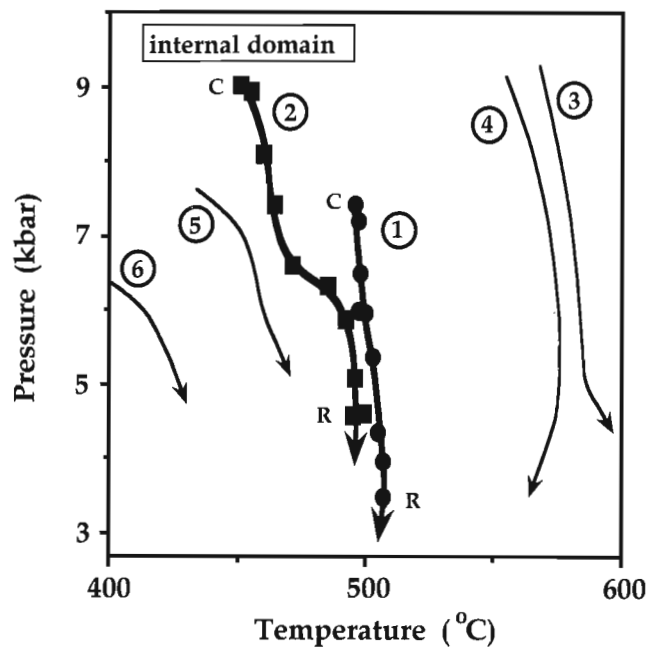


Figure 154. Analytically derived P-T paths for the two pelite samples (#1 and #2) from the internal domain (Fig. 145 and 146). The paths record prograde decompression from garnet core to rim. For each path, 'R' refers to the P-T determination based on the analyses of the garnet rim / matrix assemblage ('rim determination' discussed in the text). 'C' refers to the garnet core. All other points were calculated by thermochemical modelling of the garnet compositional zoning as discussed in the text. For comparison, paths from the external domains (Fig. 153) are shown as fine lines.

partial resorption of the garnet porphyroblasts suggest that: (1) the drop in the mole fraction of almandine near the garnet margins in sample #4 (Fig. 152) is a primary, growth-related phenomenon; and (2) post-growth volume diffusion was probably not significant (St-Onge and Lucas, 1991).

The preservation of growth-zoned garnets in muscovite-quartz-bearing schists is consistent with studies which indicate that thermally activated, intracrystalline diffusion in garnet is not significant at temperatures less than approximately 650°C (Tracy, 1982). More recently, Spear (1989) has argued that both the peak temperature experienced by the sample and the radius of the porphyroblast must be considered in evaluating the potential for post-growth diffusion in garnet. Spear's (1989) calculations show that for garnet grains with a radius of 10 mm, significant alteration of the zoning profile is not observed for temperatures less than approximately 600°C. For garnet grains with a 5 mm radius, the critical temperature is approximately 585°C. In this study, all analyzed garnet porphyroblasts have either (1) radii equal to or greater than 10 mm and peak temperatures less than 600°C, or (2) radii equal or greater than 5 mm and peak temperatures much less than 585°C (see below; Fig. 153 and 154). It is therefore unlikely that the compositional zoning in the analyzed garnets has been significantly affected by diffusional re-equilibration (Spear et al., 1990).

Utilizing the garnet rim/matrix P-T estimates, the thermodynamic modeling technique of Spear and Selverstone (1983; see also Spear, 1986) was used to calculate pressure and temperature increments from garnet rim to core based on the compositional zoning patterns (St-Onge and Lucas, 1989a, 1991). The six resulting P-T paths for the lower Povungnituk Group are plotted from the garnet rim (R) to core (C) in Figures 153 and 154. Each path indicates that decompression (i.e. exhumation) of the sample was concomitant with prograde metamorphism. The tectonic implications of the P-T paths for the two tectonothermal domains of the Cape Smith Belt are discussed in the next two sections (see also St-Onge and Lucas, 1990m, 1991).

P-T paths for external domain samples

P-T estimates based on the compositions of garnet rims and matrix minerals ('R' points in Fig. 153) indicate a progressive change in P-T conditions from south to north in the external domain. Progressively higher rim temperatures (430°C to 590°C) are recorded from southern (external) to more northern (internal) sample locations in the thrust belt (samples #6 to #3, Fig. 145). In addition, thermochemical modelling of the garnet zoning profiles indicates an increase in the recorded maximum pressures for the four samples ('C' points on Fig. 153), from 6.5 kbar for the most external sample along the southern margin of the belt (#6, Fig. 145) to over 9 kbar for the most internal sample of the external domain west of Wakeham Bay (#3, Fig. 145). Given the shapes of the paths on Figure 153, the recorded maximum pressures probably do not correspond to the actual maximum pressures experienced by the pelitic samples. The recorded maximum pressures likely correspond to the pressure at which individual samples crossed a garnet-producing

reaction (St-Onge and Lucas, 1991). However, it is interesting to note that the northward increases in the maximum temperatures and recorded maximum pressures are consistent with the interpretation of the Cape Smith Belt as a southward-tapering thrust wedge (Lucas, 1989a).

The four P-T paths are curvilinear and display a clockwise core-to-rim direction on a standard P-T diagram (Fig. 153). This is consistent with theoretical models relating metamorphism to heat conduction in thickened crust undergoing decompression due to erosional exhumation (e.g. England and Richardson, 1977; England and Thompson, 1984). The nested morphology of the four P-T paths suggests that the external domain samples may have experienced relatively similar decompression histories (cf. England and Thompson, 1984). The nested decompression histories may have resulted from isostatically-driven uplift in response to erosional unloading (Lucas, 1989b; St-Onge and Lucas, 1991).

P-T paths for internal domain samples

The two samples from the internal part of the Cape Smith Belt (samples #1 and #2, Fig. 145 and 146) yield P-T trajectories which distinct from those of the external domain (Fig. 154). Pressure temperature estimates for the internal domain samples, based on the analyses of garnet rims and matrix minerals ('R' points on Fig. 154), indicate that the two samples experienced lower peak temperatures (500-510°C) than samples #3 and #4 from the external domain even though the pressures were similar. The internal domain temperatures appear to be inconsistent with those of external domain samples #3 and #4 because, although all four samples are from comparable structural levels (i.e. adjacent to the basement-cover contact), the internal domain samples occur more internally (i.e. northward) within the thrust belt (Fig. 145 and 146). The P-T trajectories from the internal domain thus do not appear to fit the external domain pattern of a south-to-north increase in documented peak temperatures (Fig. 153).

While paths #1 and #2 are also decompression trajectories (from garnet core to rim), they are characterized by steeper dP/dT prograde segments than those for the external domain (samples #3 to #6, Fig. 153). The steeper dP/dT segments may reflect intervals of more rapid exhumation in the internal part of the thrust belt as compared to the external part (Lucas, 1989b; St-Onge and Lucas, 1991). This suggests that a different tectonic process may have controlled part of the P-T history of the internal domain. Potential explanations for the differences in P-T paths between the two domains include the thermal peak thrusting and post-thermal peak normal faulting which are unique to the internal domain (St-Onge and Lucas, 1991).

TECTONOTHERMAL EVOLUTION OF THE CAPE SMITH BELT

Contrasting metamorphic isograd sequences, mineral growth/deformation relations and P-T paths between the external and internal parts of the Cape Smith Belt document

the interaction of tectonic and thermal processes at the scale of the thrust belt. Initiation of regional metamorphism in the thrust belt is interpreted to result from crustal thickening by D₁ (piggyback-sequence) thrusting (Lucas, 1989b; St-Onge and Lucas, 1990m, 1991). The consequent rise of isotherms through the thrust belt promoted a brittle-to-ductile transition in deformation mechanisms at deeper structural levels and the development of a basal shear zone (Lucas, 1990). Later, the out-of-sequence thrusting and subsequent extensional faulting (D₂) had a fundamental effect on the thermal structure of the thrust belt, and appear to have generated the contrast in structural and metamorphic histories between the two domains (St-Onge and Lucas, 1990m, 1991). Emplacement of a >25 km thick thrust stack on the external domain seems to be responsible for the thermal peak metamorphic conditions generated in that domain and probably its principal exhumation episode (Fig. 146; Lucas, 1989b; St-Onge and Lucas, 1991). The overturned isograd in the external domain (footwall) below the D₂ thrust stack (Fig. 145 and 146) attests to the higher temperature footwall metamorphism being a consequence of hanging wall emplacement.

D₂ extensional faulting in the internal part of the Cape Smith Belt is thought to have resulted in the apparently arrested "heating" of samples #1 and #2 relative to the more external samples #3 and #4 (Fig. 154 ; St-Onge and Lucas, 1991). Samples #1 and #2 lie in the direct footwall of the extensional faults (Fig. 146), and may thus have experienced the exhumational effects of extensional faulting much sooner than structurally equivalent rocks to the south in the external domain. The near isothermal decompression indicated by all of the P-T paths (Fig. 153 and 154) may also be explained in part by exhumation due to the extensional faulting. Wedging of the large Narsajuaq arc thrust sheet into the base of the thrust belt (Fig. 1; see 'Post-thermal peak fault system' section) during D₂ deformation may have initiated the proposed extensional faulting (Table 2; Lucas and St-Onge, 1992).

One well-studied area with P-T paths similar to those of the Cape Smith Belt is the Tauern Window in the eastern Alps (Selverstone et al., 1984; Selverstone, 1985; Selverstone and Spear, 1985). The Tauern Window paths are characterized by relatively low temperatures (455-550°C), high pressures (5-10.5 kbar), and nearly isothermal decompression. The steep dP/dT segments of these paths have been interpreted to result from extensional faulting during the Alpine orogeny (Selverstone, 1988). Extension in the Tauern Window area is thought to have developed (1) simultaneously with compressional deformation at deeper structural levels and (2) as a direct consequence of the underplating of a large crystalline sheet, the 'Zentralgneis terrane' (Ratschbacher et al., 1989). Similar high-level normal faulting in a compressional mountain belt has also been reported in the high Himalayas (Burg et al., 1984; Burchfiel and Royden, 1985; Royden and Burchfiel, 1987).

METAMORPHIC CONDITIONS ASSOCIATED WITH BASEMENT-INVOLVED FOLDING

Study of the metamorphic conditions during basement-involved folding (Table 2) is hampered in many areas by a lack of new mineral growth during the deformation episodes. However, metamorphic phases which grew during D₃ west-trending folding and that are suitable for thermobarometric analysis are locally present southwest of Wakeham Bay (1728A; Fig. 5; St-Onge and Lucas, 1990m). The apparent absence of metamorphic assemblages associated with D₄ cross-folding makes it difficult to constrain the P-T conditions during that deformation episode. However, the presence of pressure solution cleavages associated with the cross-folds in sedimentary rocks at relatively deep structural levels (e.g., along the northern margin; Fig. 5) suggests that rocks were deformed at subgreenschist to greenschist facies conditions (Lucas, 1989b; St-Onge and Lucas, 1990m).

Thin section study of Povungnituk Group sedimentary rocks deformed during west-trending folding shows that biotite, muscovite, and chlorite commonly grew in association with the development of microfolds and crenulation cleavages (Fig. 144; St-Onge and Lucas, 1990m). In a few samples, garnet is also part of the syn-folding mineral assemblage (Fig. 155). The assemblage biotite-muscovite-chlorite-garnet is present immediately adjacent to a pelitic layer which contained one of the analyzed samples which yielded a quantitative D₁ P-T path (sample #5, Fig. 145 and 146; "A" on Fig. 58; St-Onge and Lucas, 1990m). The syn-folding mineral assemblage enables the P-T conditions for the folding episode to be determined and compared to the syn-D₂ P-T path for sample #5 (Fig. 153).

Estimates of the P-T conditions during west-trending folding have been derived through the application of geothermobarometry to the garnet-biotite-muscovite-chlorite assemblage (St-Onge and Lucas, 1990m). Temperature estimates were obtained from microprobe analyses of the (chemically unzoned) garnet and biotite based on the Fe-Mg exchange equilibrium (Ferry and Spear, 1978; Hodges and Spear, 1982). Pressure estimates were derived by applying microprobe analyses of biotite, muscovite, and chlorite to the calibration of the biotite-muscovite-chlorite-quartz equilibrium by Powell and Evans (1983). Simultaneous solution of the geothermometer and geobarometer equilibria yielded estimates of P and T for five domains of garnet, biotite, chlorite, and muscovite in the sample (St-Onge and Lucas, 1990m). The P-T determinations cluster at 5 kbar and 450°C and are interpreted as the ambient conditions during west-trending folding at this specific locality, subject to the uncertainties discussed above. This P-T estimate is consistent with the "thermal peak" P-T path derived for the adjacent pelitic layer (Fig. 153), suggesting that the D₃ folding episode followed soon after the thrusting event (St-Onge and Lucas, 1990m; Lucas and Byrne, 1992).

REGIONAL TECTONIC SETTING OF THE CAPE SMITH BELT

The geotectonic significance of the Cape Smith Belt has long been the subject of controversy (Dimroth et al., 1970; Gibb and Walcott, 1971; Dewey and Burke, 1973; Thomas and Gibb, 1977; Baer, 1977; Baragar and Scoates, 1981; Hoffman, 1985). The principal dispute has centered on whether the belt itself marks the site of: (1) a major collisional geosuture (e.g. Gibb and Walcott, 1971); (2) a geosuture marking the closure of a small, short-lived oceanic basin (e.g. Hynes and Francis, 1982; Picard et al., 1990); or (3) an ensialic fold belt (e.g. Baer, 1977). Hoffman (1985) proposed a new tectonic model for the belt based on the following two observations concerning the relationship between the Cape Smith Belt and the underlying basement: (1) basement gneisses along the northern margin record similar Rb-Sr whole rock ages (2.6-2.9 Ga; Doig, 1983) to the basement along the southern margin (Taylor and Loveridge, 1981); and (2) the basement at the east end of the belt is continuous around the belt from south to north margin (Taylor, 1982). To account for these observations, Hoffman (1985) suggested that the belt is essentially a klippe, isolated from its root zone (or geosuture) to the north by a post-thrusting basement antiform. In the Hoffman (1985) model, the geosuture would be located 50 to 100 km north of the belt at Sugluk Inlet (Fig. 2), where a major "break" was thought to occur in the gravity and magnetic fields (Thomas and Gibb, 1977; Geological Survey of Canada, 1983) as well as in metamorphic grade (Westra, 1978).

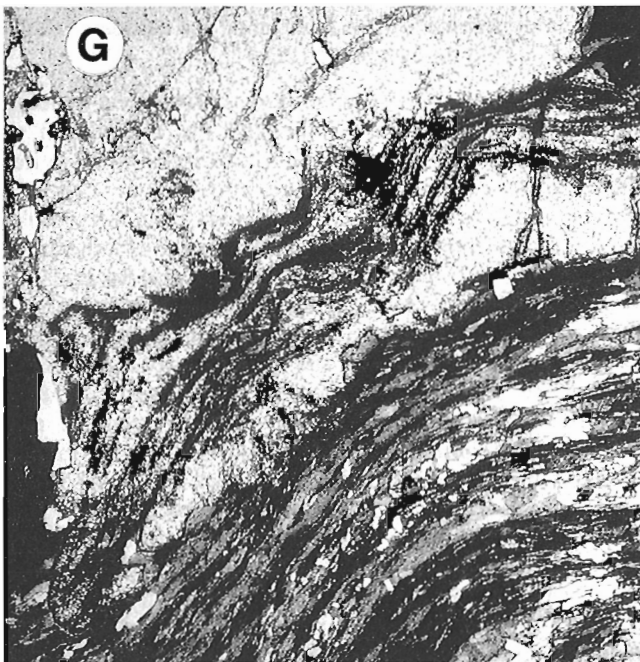


Figure 155. Photomicrograph of garnet porphyroblast (G) overgrowing D₃ microfolds of the basal shear zone fabric in a semipelite of the lower Povungnituk Group west of Wakeham Bay (Fig. 5). The garnet and associated late biotite (Fig. 144) are interpreted as D₃ in age (see text). Horizontal field of view is 2 mm. (GSC 204832)

As outlined above (see 'Previous and recent work' section), the western portion of the Cape Smith Belt was remapped at 1:50 000-scale by the MERQ (1983-89) and the eastern portion by the GSC (1985-87; St-Onge et al., 1986, 1987, 1988b). More recently, the entire northern hinterland to the Cape Smith Belt was remapped by the GSC (1989-91; St-Onge and Lucas, 1990n, 1992; Lucas and St-Onge, 1991). This recent work has shown that (1) the Cape Smith Belt was thrust southward over the Superior Province basement (Fig. 5 and 58); (2) autochthonous basement is exposed in two half-windows coring a large-scale antiform north of the belt (Fig. 1); (3) the belt contains a 2.00 Ga ophiolite, a ca. 1.86 Ga volcanic arc and possibly fore-arc sequence and a 2.04-1.92 Ga rift-to-drift sequence (Fig. 1); and (4) the hinterland is characterized by a 1.86-183 Ga magmatic arc terrane (Fig. 1) which collided with the Superior Province continental margin at ca. 1.82 Ga (Ungava orogeny).

Results from the recent work in the Ungava orogen clearly dispel two of the principal arguments against the operation of plate tectonics in the Precambrian: the apparent lack of evidence for mid-ocean ridge spreading (e.g. ophiolites) and for subduction (e.g. island arcs). The Ungava orogen also contains evidence for Phanerozoic-style convergent margin tectonics in its inferred A-type subduction of Superior Province continental crust (see 'Povungnituk and Chukotat groups (domain 2) deformation history' section above; Lucas, 1989a) and the relatively high-P/T metamorphism recorded in the Cape Smith Belt rocks (see 'Analytically-derived P-T paths in pelites' section above; St-Onge and Lucas, 1990m, 1991). As well many of the previous models for the geotectonic setting of the Cape Smith Belt can be at least partially eliminated because of inconsistencies with the current geoscientific database for the Ungava orogen (St-Onge and Lucas, 1990m; St-Onge et al., 1992).

By integrating the current multidisciplinary geoscientific information database, St-Onge et al. (1992) have developed a plate-tectonic model for the evolution of the northern rift-margin of the Superior Province and the adjacent 'suspect' assemblages in the Ungava orogen (see also Lucas and St-Onge, 1992; Lucas et al., 1992). In short, the model proposes that the Early Proterozoic Ungava orogen contains evidence for the development of a long-lived (>80 m.y.) and presumably wide ocean that was subsequently destroyed during plate convergence leading to arc-continent collision. Rifting of the Superior Province continental crust appears to have been underway by 2038 Ma (Fig. 8; N. Machado, pers. comm., 1992), the U/Pb age of a gabbro sill emplaced in the lower Povungnituk Group sedimentary rocks. Oceanic crust was being generated by 1998 Ma (Watts Group; Parrish, 1989), although significant oceanic crust age diachroneity is recorded in the orogen with 1958 Ma rhyolites near the top of the upper Povungnituk Group and 1918 komatiitic basalt magmatism at the base of the Chukotat Group (Parrish, 1989; St-Onge et al., 1992).

Picard et al. (1990) have suggested that the Parent Group in the western part of the Cape Smith Belt corresponds to the deposits of a subduction-related calc-alkaline volcanic arc. The only U-Pb zircon age for a Parent Group extrusive rock

at present is 1860 Ma, the age of a rhyodacite from the western part of the Cape Smith Belt (N. Machado, pers. comm., 1991). The fault-bound Spartan Group could represent a fore-arc clastic apron to the volcanic arc, given its similar structural position in the thrust belt to the Parent Group (Fig. 1; Lucas, 1989a). Alternatively the Spartan Group may represent distal deposits related to the Superior Province rift-margin. St-Onge et al. (1992) proposed that the Parent and Spartan groups represent deposits related to the establishment of a convergent plate boundary between the continental rift-margin deposits and the Watts Group oceanic crust. In this model, convergence between the two plates resulted in: (1) northward subduction of the (lower plate) Povungnituk-Chukotat groups oceanic basin (Picard et al., 1990); (2) accumulation of the Parent Group arc and related Spartan Group clastic apron on the (upper plate) oceanic crust of the Watts Group (Fig. 55); and (3) construction of the south-verging Cape Smith Thrust Belt. Development of the south-verging continental thrust belt containing units associated with prior rifting of the Archean Superior province basement probably records impingement of the upper plate against the underthrust continental margin ca. 1.87 Ga (Fig. 55; Lucas and St-Onge, 1992; St-Onge et al., 1992).

St-Onge et al. (1992) proposed that the Narsajuaq arc (Fig. 1) was built on the Watts Group oceanic crust, and that it represents the mid-crustal plutonic core to the Parent group magmatic arc (Fig. 55). The granitic to dioritic plutonic rocks in Narsajuaq arc range in age from 1863 to 1803 Ma (R. Parrish, 1989; St-Onge et al., 1992; Parrish, pers. comm., 1992), although the youngest units are interpreted to be collisional in origin (Dunphy and Ludden, 1992). Relatively small plutons intrude Watts (Fig. 5) and Parent group rocks (Taylor, 1982), and are broadly related in age (1898 to 1839 Ma; Fig. 8; R. Parrish, 1989, pers. comm., 1991; Machado et al., 1991) and composition to those in the Narsajuaq arc. Although the Watts and Parent groups are everywhere separated from the Narsajuaq arc by faults (Fig. 1), St-Onge et al. (1992) proposed that the plutons intruding the Watts and Parent Groups are genetically related to those in the Narsajuaq arc. In contrast, the Povungnituk and Chukotat groups and the Superior Province basement (lower-plate) are marked by a complete absence of intrusive rocks of 1.9-1.8 Ga age (Lucas and St-Onge, 1991; St-Onge et al., 1992). Given the apparent absence of Early Proterozoic plutons in these lower-plate rocks, the initial docking of the Watts and Parent groups is constrained to have occurred only after 1839 Ma, the age of the youngest arc-type pluton within these units (St-Onge et al., 1992; Dunphy and Ludden, 1992).

A distinct suite of younger plutonic rocks occurs in the Narsajuaq arc (Fig. 1), and is characterized by kilometre-scale bodies of quartz diorite, tonalite, monzonite, and monzogranite intruding older plutonic units. U/Pb zircon dating of younger suite plutons indicates that the suite spans the period ca. 1844 to 1826 Ma, with the bulk of the tonalitic and granitic magmatism occurring between about 1836 and 1830 Ma (Parrish, 1989; St-Onge et al., 1992). The northern part of the Narsajuaq arc is marked by an assemblage of sedimentary rocks (Sugluk Group, not shown in Fig. 1 because of scale; St-Onge et al., 1992) which is intruded by

1830 Ma plutonic units. Sugluk Group quartzites contain two distinct detrital zircon populations: one Archean and the other ranging in age from 1863 to 1830 Ma (Parrish, 1989). The data suggest that the sedimentary units were derived in part from rocks containing Archean zircons and in part from magmatic rocks of the active Narsajuaq arc. Lucas et al. (1992) have attributed the younger suite plutonism in Narsajuaq arc to a reversal in subduction polarity resulting in the initiation of south-dipping subduction on the north side of the Narsajuaq arc complex (Fig. 156). Northward subduction of the Superior Province continental crust is inferred to have led to the subduction polarity reversal.

Final accretion of the island-arc terrane and its oceanic basement is thought to have occurred after 1826 Ma (youngest dated unit in the Narsajuaq arc) and before 1758 Ma (syenogranite dykes which intrude units in all three tectonic domains of the orogen; Fig. 8; Parrish, 1989; St-Onge et al., 1992). The arc-continent collision resulted in a minimum of 65 km of tectonic overlap of the composite arc's plutonic core on the autochthonous footwall basement (Lucas and St-Onge, 1992).

The regional distribution and timing of Early Proterozoic deformation recorded at the margins of the Archean Superior craton has been the subject of recent discussion. Following the proposal of Gibb and Walcott (1971) that a Hudsonian-aged (1.8 Ga) suture marked the boundary between the Churchill and Superior provinces, Baragar and Scoates (1981) provided abundant stratigraphic and geochemical evidence of geosutures ringing the margins of the Superior craton. Using a compilation of precise U-Pb dates, Hoffman (1988, 1989) recognized that the period 2.0-1.7 Ga was fundamentally important in terms of the growth and amalgamation of the North American continent. Rocks of this age in the Canadian Shield, predominately found in the Trans-Hudson orogen and its eastern affiliates (e.g., Ungava, New Quebec, and Torngat orogens), contain evidence for continental rifting, oceanic spreading, generation of new crust in volcanic island arcs, and collisional tectonics that resulted in the welding of Archean continental fragments into the Laurentian protocontinent (see papers in Lewry and Stauffer, 1990). Hoffman (1988, 1989; see also Lewry and Stauffer, 1990) also developed testable plate tectonic models for the entire Trans-Hudson orogen, focusing on the timing of plate margin events and the kinematics of deformation and crustal accretion.

Hoffman (1990) further elaborated on the kinematics and timing of the Early Proterozoic (1.9-1.8 Ga) assembly of Laurentia in the northeast Canadian Shield and Greenland. He proposed a dynamic model, based on the Cenozoic evolution of Southeast Asia, in which large-scale crustal movements occur in response to the collisional indentation of the Superior Province into the Rae (Churchill) Province hinterland. The southeast arm of the Rae Province is suggested to have rotated clockwise in response to initial indentation of the Superior Province at its leading northern Ungava margin (Cape Smith Belt; Hoffman, 1990). A dextral pull-apart basin, analogous to the Andaman Sea basin of Southeast Asia, is envisaged to have formed along the leading edge of the rotating Rae Province block and lead to

the development of the large mafic sills now preserved in the Labrador Trough (New Quebec orogen). A similar collisional basin, this time analogous to the South China Sea, is predicted to have opened at the trailing edge of the rotating block (south-central Baffin Island; Hoffman, 1990). A critical aspect of the model is that collisional indentation was initiated by 1.88 Ga in northern Ungava. While the existing evidence suggests that thrusting in the Cape Smith Belt was underway by 1.87 Ga, the principal period of Narsajuaq arc magmatism was between 1.86 and 1.83 Ga, with arc-continent collision occurring after 1.83 Ga (Lucas and St-Onge, 1992; St-Onge et al., 1992). This new data does not refute Hoffman's (1990) model but it does necessitate revision of certain aspects.

Van Kranendonk (1992) has built on both the Hoffman (1990) model and a large number of new U-Pb ages to derive a new scenario for the assembly of northeastern Laurentia from 1.9-1.75 Ga. In addition to the timing of Narsajuaq arc growth between 1.86-1.83 Ga, the new model includes the detailed timing of collision (1.86 Ga) and subsequent intracratonic deformation and magmatism (1.84-1.74 Ga) in the Torngat orogen (Bertrand et al., in press). This data suggests that Nain-Rae suturing (Torngat orogen) preceded, as opposed to followed, Superior-Rae suturing (Ungava orogen). The central idea of the new model is that northwesterly wedging of the Archean Disko Province (Burwell terrane; Hoffman, 1990) into Rae Province, coeval with Slave-Rae collision to the west, led to the formation of the Cumberland batholith (continental arc) and the rift-margin sequences in the Foxe-Rinkian Belt, and isolation of the southeastern arm of the Rae Province (Van Kranendonk, 1992). The tectonic models offer an important regional framework for future studies in the northeastern Canadian Shield, including both geochronology (e.g., tighter age

bracket on D₁ thrusting in the Povungnituk and Chukotat groups) and field studies (e.g., evolution of the Dorset Belt, Baffin Island).

QUATERNARY GEOLOGY

General statement

The area of the eastern Cape Smith Belt described below represents approximately one quarter of the area covered by a more regional Quaternary study (Daigneault, 1990). The final report of that study will examine the regional late Quaternary paleogeography as well as the key aspects of glacial transport for the whole of the Ungava Peninsula north of 61°N.

Previous work

In 1897, Low (1899) was the first to recognize evidence of glaciation in the map area; he identified striae with a northeasterly orientation between Whitley Bay and Douglas Harbour (Fig. 157). Kretz (1960) established that transport of glacial debris in the central part of the Cape Smith Belt was essentially toward the north. In the area of the Cratère du Nouveau Québec, Currie (1965) recognized an older episode of ice flow toward the east-southeast which preceded a flow toward the northeast (Fig. 157) and deposited a few supracrustal erratics from the Cape Smith Belt in the area of the crater. The first episode of ice flow was named "Ungava" and the second one, "Payne" by Bouchard and Péloquin. (1989). Matthews (1967b) suggested that a late ice cap existed in the Purtuniqu area (1722A) and that postglacial sea level reached 136 m a.s.l. at lac Watts (1721A). In a country-wide study of the principal Quaternary features of Canada, Prest (1970) noted the presence of several

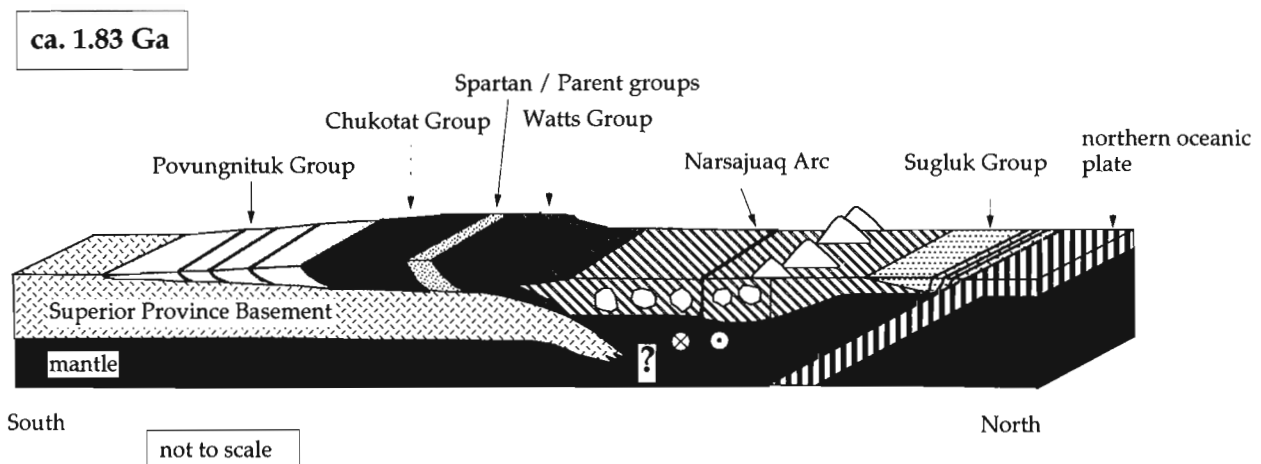


Figure 156. Schematic block diagram illustrating the proposed plate tectonic setting for the tectonostratigraphic units of the Ungava orogen at 1.83 Ga. Constraints for the plate tectonic model are given in the text and in St-Onge et al. (1992). The imbricated Povungnituk, Chukotat, Spartan, Parent, and Watts groups represent the advanced stage of formation of the Cape Smith Thrust Belt. The question mark refers to the unknown position of the northern termination of the lower plate at 1.87 Ga. The vertical plane drawn in the Narsajuaq arc symbolizes the component of transcurrent deformation documented in the arc rocks (Lucas and St-Onge, 1992). Circled 'X' indicates movement to the west. White blebs and triangular shapes in the Narsajuaq Arc represent respectively magma chambers and volcanoes (discussed in text).

glaciolacustrine phases that occurred as a result of glacial ice blocking the natural drainage of the rivière Povungnituk valley (Fig. 2); the highest phase is recorded at an elevation of 550 m. In contrast, St-Onge and Scott (1986) noted the absence of fine grained deposits and raised deltas and suggested there had been no widespread glaciolacustrine

phases in the study area. Gray and Lauriol (1985) identified several fluted landforms with a northeasterly trend and proposed a zonation of glacial features over the entire peninsula: the western part of the map area is located in a zone of featureless till while the eastern part is covered by thin till. Daigneault (1990) confirmed that ice flow in the western part

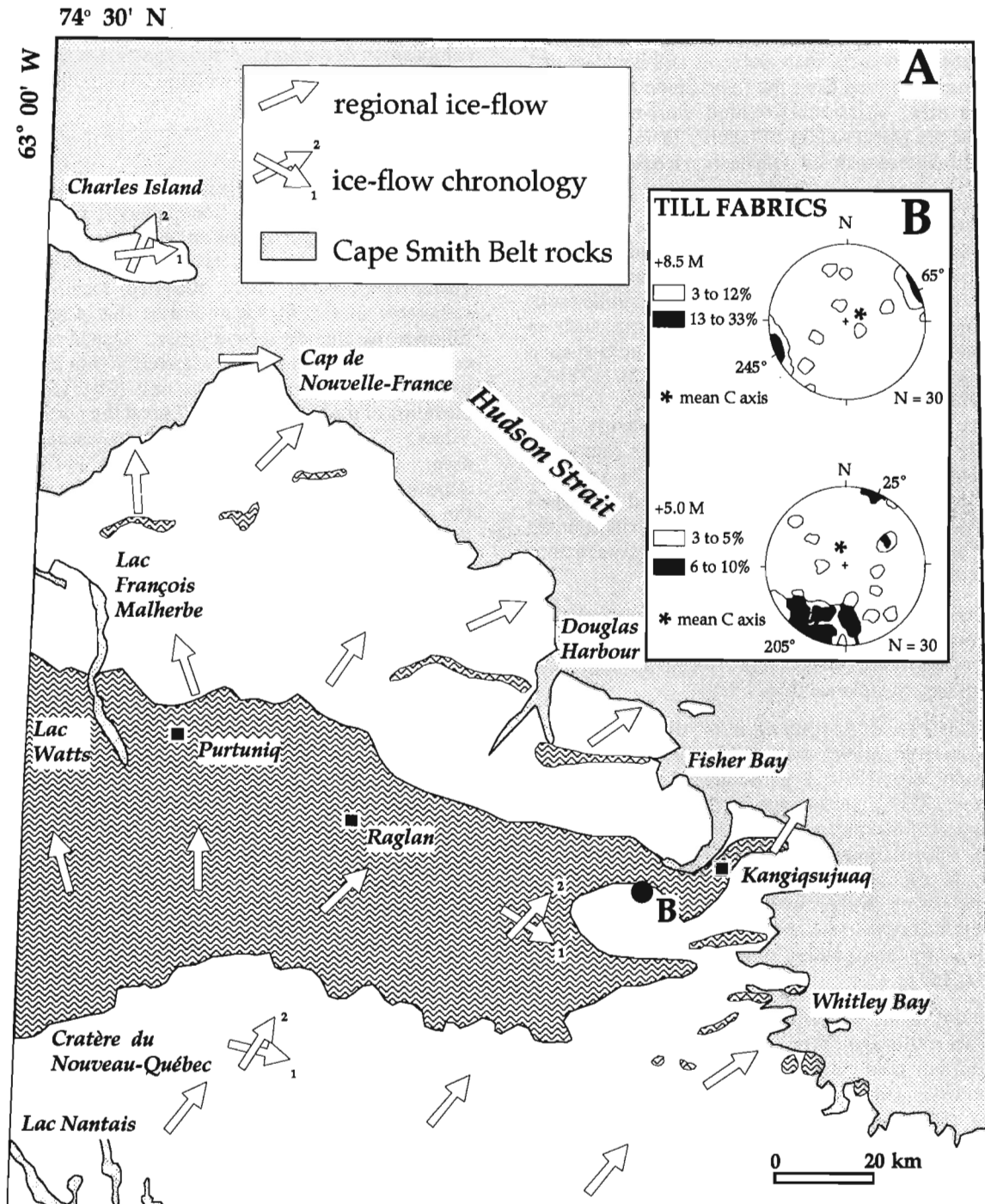


Figure 157. A. Ice flow directions from the record of striations, grooves, and drumlins. B. A-axis fabric of pebbles contained in till observed along the Wakeham River (1728A).

of the study area was predominantly toward the north and apparently transported dolomite boulders from the lower Povungnituk Group over a distance of more than 50 km.

Glacial features

Field evidence for the first ice flow (east-southeast) was found near the Cratère du Nouveau Québec (1731A) and about 10 km northeast of lac Vicenza (1733A). Near the Cratère du Nouveau-Québec it includes glacial grooves oriented west-northwest to east-southeast and boulders and granules of rocks derived from the Cape Smith Belt. In the lac Vicenza area, striations oriented west-northwest - east-southeast are preserved on an outcrop facing northeast. To date, no till sheet associated with the first ice flow has been found.

There are numerous features associated with the last episode of ice flow in the region. These include erosional microforms, mainly striae, that are better preserved on the mafic rocks of the Cape Smith Belt than on the granitic rocks of the Archean basement, as well as mesoforms such as 'roches moutonnées' in Fisher Bay (Fig. 158). The U-shaped valleys of Douglas Harbour (Fig. 157), lac Watts (1721A), and the rivières Wakeham, Laflau and Lataille (1728A, 1735A) are erosional macroforms that result from considerable overdeepening by glaciers; they cannot be attributed entirely to the last glacial phase. In addition, cirques observed between Douglas Harbour and Wakeham Bay (1729A) indicate that small local glaciers existed in the region over long periods of time following the disappearance of the regional ice sheet (inlandsis).

The record of ice-flow indicators shows regional flow toward the northeast in the eastern portion of the Cape Smith Belt; in the western part, flow diverged toward the north from the Purtunig-Raglan Uplands (Fig. 157).

Although it is generally featureless, the till sheet is locally streamlined in a direction parallel to the last ice flow (lac Saint-Germain area; 1732A), or hummocky as in the lac Vicenza area (1733A). Its average thickness exceeds 1 m in the western part of the map area, and it is thin, discontinuous, and strewn with perched boulders in the eastern sector (Fig. 157). It reaches its maximum observed thickness of 12 m in the rivière Wakeham valley (1728A), where till fabrics measured at two levels show that the till was deposited by a northeast-flowing glacier, probably during the Payne episode (Fig. 157).

The texture of the till matrix shows general control by local bedrock: tills overlying the Cape Smith Belt are generally siltier than those overlying granitic Archean basement rocks. However, a lithological analysis of the surface till sheet (boulders measuring over 20 cm and granules from 4 to 5.6 mm) indicates a variation in the composition of the till in the direction of ice movement. For example, in the Kangiqsuaq area (1729A), the amount of Proterozoic debris increases gradually downglacier (northeast) from the proximal contact with rocks of the Cape Smith Belt while upglacier (southwest) of the contact, the till is essentially composed of Archean rocks. It should be noted

that 50 km downglacier from the distal contact with Archean rocks, the Archean clasts make up almost 60% of the granules (4-5.6 mm) and 40% of the boulders (>20 cm). These numbers differ from those reported by Kretz (1960) for the central Cape Smith area (Fig. 1) where, at 13 km from the distal contact with Archean rocks, Archean erratics made up only 1% of the till lithology. North of the study area, the presence of massive peridotite boulders derived from the Cape Smith Belt suggests that glacial transport was effective over a distance of at least 60 km. The overall lithologic composition of the surface till suggests that glacial transport was essentially associated with the last ice-flow direction.

Deglaciation features

According to Dyke and Prest (1987), deglaciation began at about 8000 BP and the ice front generally retreated from the northeast toward the southwest, that is from the edge of the Ungava peninsula towards its centre. The presence of raised deltas composed of sandy, stratified, locally fossiliferous sediments in the fjords indicates that deglaciation was followed by marine submergence. Deltas are found at a maximum elevation of approximately 135 m in the upstream parts of valleys located to the east (Fig. 157). The low elevation of the highest delta (97 m) at the northern tip of lac Watts (1721A) suggest that ice retreat occurred later in this area. In the rivière Wakeham valley (1728A), marine deposits reach a thickness of 45 m. Along the Hudson Strait, the upper limits of wave-washing lie at 148 m near Cape Prince of Wales (1729A) and at 130 m west of pointe Akulivik (1729A). Outside the valleys, below the marine limit, the till is either reworked or absent and a veneer of beach sand and gravel commonly covers the bedrock.

In the interior of the Ungava peninsula, a series of eskers, meltwater channels and outwash plains indicates that the ice front retreated towards the southwest. Some of these meltwater landforms reach 40 km in length. However, in the eastern Cape Smith Belt, eskers are scarce and parallel to topographic depressions. In the Purtunig area (1722A), numerous ice-marginal and proglacial meltwater channels



Figure 158. Roche moutonnée indicating ice flow to the east-northeast at Fisher Bay (Fig. 2). (GSC 1992-148)

show that ice retreat was generally towards the south; no evidence was found to support the hypothesis of a late ice cap in this region.

Along the upper reaches of the rivièrè Povungnituk (1730A, 1731A, 1732A) glaciolacustrine shorelines (gravel beaches and zones of washed till) indicate the existence of a few lacustrine phases that were produced as normal drainage was blocked by the retreating glacier margin. This paleolake had a limited extent during its initial phase at an elevation of approximately 550 m. Water levels fell gradually as lower outlets were uncovered during deglaciation. Well-defined levels are found at 530, 460, and 411 m a.s.l. At the highest lake stage, drainage was probably eastward, from lac Itirviluarjuk (1733A) toward the rivièrè Laflau. The small size of the deltas associated with these bodies of water and the absence of fine grained deposits as noted by St-Onge and Scott (1986) are perhaps best explained by the short duration of the glaciolacustrine episodes. A ^{14}C date of 6920 ± 90 BP (To-1441; Richard et al., 1989) at the base of a lake sediment core from the area southwest of the Cratère du Nouveau Québec (1731A) indicates that the glacier ice had retreated from the study area before 7000 BP.

Modern geological processes

Since deglaciation, the evolution of the landscape in this area has been controlled mainly by periglacial processes. Stewart (1976) estimates that permafrost reaches a thickness of 540 m at Purtuniqu (1722A). According to Lévesque et al. (1990), the active layer in bedrock at the Kangiqsujuaq (1729A) airport is 3.4 m thick. In addition, temperature measurements in different materials at Salluit (Fig. 2), suggest that the active layer is 2 or 3 times thinner in Quaternary sediments than in bedrock.

Bedrock gelifraction is important and has led to the formation of large scree at the foot of rock cliffs along Hudson Strait. A few rock outcrops also show frost heave features. Sorted or unsorted mudboils occur throughout the till plain; they have undergone downslope stretching as a result of congelifluction. Congelifluction processes are also responsible for the partial or total obliteration of several marine or glaciolacustrine shorelines features. Polygonal networks are formed mainly on sandy-gravelly substrates (i.e., deltas and eskers). Finally, the 'rock pingos' reported south of Purtuniqu (1722A) by Seppälä (1988) are in fact partially frost-heaved bedrock outcrops of semipelite and quartzite. In these bedrock hills, where layering has not been disrupted by frost action, measurements of layering correspond both in strike and dip to those obtained from the surrounding bedrock plateau.

ECONOMIC GEOLOGY

History of mineral exploration

Geological observations by the Geological Survey of Canada on the northern Ungava Peninsula were first made during the coastal voyages of Bell (1885) and Low (1899, 1902). Low's (1902) recognition of "diabasic trap" rocks (Cape Smith Belt

basalts) was followed up by a consortium of mineral exploration companies in 1931-1932 who discovered sulphide bodies both along the coast and up to 100 km inland to the east (Gunning, 1934). The consortium included Cyril Knight Prospecting Co., Huronian Mining and Finance Co., Newmont Exploration Ltd., and Quebec Prospectors Ltd., and was represented in Ungava by a small field party led by W.B. Airth. One of the geologists on the exploration party in 1932 was Murray Watts, who in the course of that summer produced the first map of the inland geology of the Cape Smith Belt (Fig. 11 in Gunning, 1934), and who discovered asbestos at Purtuniqu (1722A) in 1957 (see below). The sulphide discoveries along the east coast of Hudson Bay were examined in detail by the Geological Survey of Canada in 1933 (Gunning, 1934).

Mineral exploration in the Cape Smith Belt during the 1950s resulted in the discovery of Ni-Cu deposits, culminating in 1957 with over 30 companies actively holding exploration permits covering almost the entire belt (Giovenazzo, 1986). The Québec Department of Mines (now Ministère de l'Énergie et des Ressources; MERQ) responded to the intense exploration activity and mapped approximately one-third of the Cape Smith Belt (Fig. 3; Bergeron, 1957a, 1959; Beall, 1959, 1960; DeMontigny, 1959; Stam, 1961; Gélinas, 1962; Gold, 1962). Detailed exploration and estimation of Ni-Cu deposits (see below) occurred through the 1960s and early 1970s until low base metal prices forced a halt to mine development at the Donaldson (Raglan) property (1726A) in 1972 (Taylor, 1982). The discovery of significant platinum-group element (PGE) reserves associated with Ni-Cu deposits (Giovenazzo, 1986; Giovenazzo et al., 1989), and multi-element occurrences with gold and silver values in the western Cape Smith Belt (Barrette, 1991), led to further exploration in the mid- to late-1980s. Re-mapping of the Cape Smith Belt at 1:50 000-scale by the MERQ and the Geological Survey of Canada occurred during this second period of mineral exploration activity. The local geology and tectonic setting of the principal ore deposits (asbestos, Ni-Cu-PGE sulphides) in the map area are reviewed in the following two sections.

Asbestos deposits

Chrysotile asbestos mineralization occurs in ultramafic cumulate rocks of the Watts Group at Purtuniqu (1722A; Fig. 2). Discovered in 1957 by Murray Watts during the course of an aerial reconnaissance survey, the Purtuniqu (Asbestos Hill) deposit was examined through detailed exploration and drilling in succeeding years (1958-62) and a 16 million ton (14.5 million tonnes) orebody defined (Stewart, 1976). The property was optioned to Hudson Strait Asbestos Corporation (a wholly-owned subsidiary of the Asbestos Corporation Ltd.) in 1962, and in 1964, the Asbestos Corporation bought the Purtuniqu property and the consolidated assets of Murray Watts' mining company. The orebody was mined between 1972 and 1984, principally as an open-pit operation which fed a 3000-ton-per-day (2721.6-tonnes-per-day) mill to produce 300 000 tons (272 155.4 tonnes) of concentrate annually (Taylor, 1982). The concentrate was trucked 67 km to Deception Bay (Fig. 2)

where it was stored for transport to Nordenham, West Germany, during the short summer shipping season. The mine slowed down and eventually closed in the early 1980s due to a collapse in the price of asbestos.

The deposit at Purtunig is located at the western end of the largest body of ultramafic rocks of the Watts Group ophiolite within the map area (1722A; Fig. 40). Scott (1990; see also Scott et al., 1991) has shown that the ultramafic rocks in this body are virtually plagioclase-free, and are compositionally-layered at centimetre to metre-scale (Fig. 42). The compositional layers are interpreted to reflect variations in the proportions of primary olivine and clinopyroxene, which are now partially pseudomorphed by metamorphic phases. The centimetre-scale modally-graded layers typically have dunitic bases which pass somewhat abruptly into wehrlitic-clinopyroxenitic tops (Scott, 1990), and are rhythmically repeated at the outcrop-scale. The ultramafic rocks also contain homogeneous, concordant layers of wehrlite and olivine-clinopyroxenite which have sharp contacts with the surrounding modally-graded layers.

Thin section study of samples from the modally-graded ultramafic rocks suggests a cumulate origin for the layering (Scott, 1990). Metamorphic (alteration) assemblages in dunitic layers include olivine, serpentine, magnetite, ferrichromite, chlorite, and calcite, and are consistent with the lower to middle amphibolite-facies regional metamorphism documented in nearby mafic and pelitic rocks (see above; Bégin, 1989b, 1992a; St-Onge and Lucas, 1991). The paragenesis of the alteration assemblages includes an early episode of serpentinization prior to regional metamorphism and deformation (Scott, 1990). Detailed studies of the asbestos ore by Stewart (1976) indicate that the economic chrysotile asbestos veins formed during the regional thermal peak metamorphism-deformation episode (D₂ for the Watts Group; Table 2). Whether the chrysotile mineralization developed during obduction of the ophiolite or subsequent deformation within the continental thrust belt is difficult to ascertain. Post-thermal peak metamorphism associated with late D₂ normal faulting (Table 2) in dunitic layers is principally characterized by talc-carbonate assemblages which in part replace the fibrous serpentinite in or adjacent to thermal peak shear zones (Stewart, 1976).

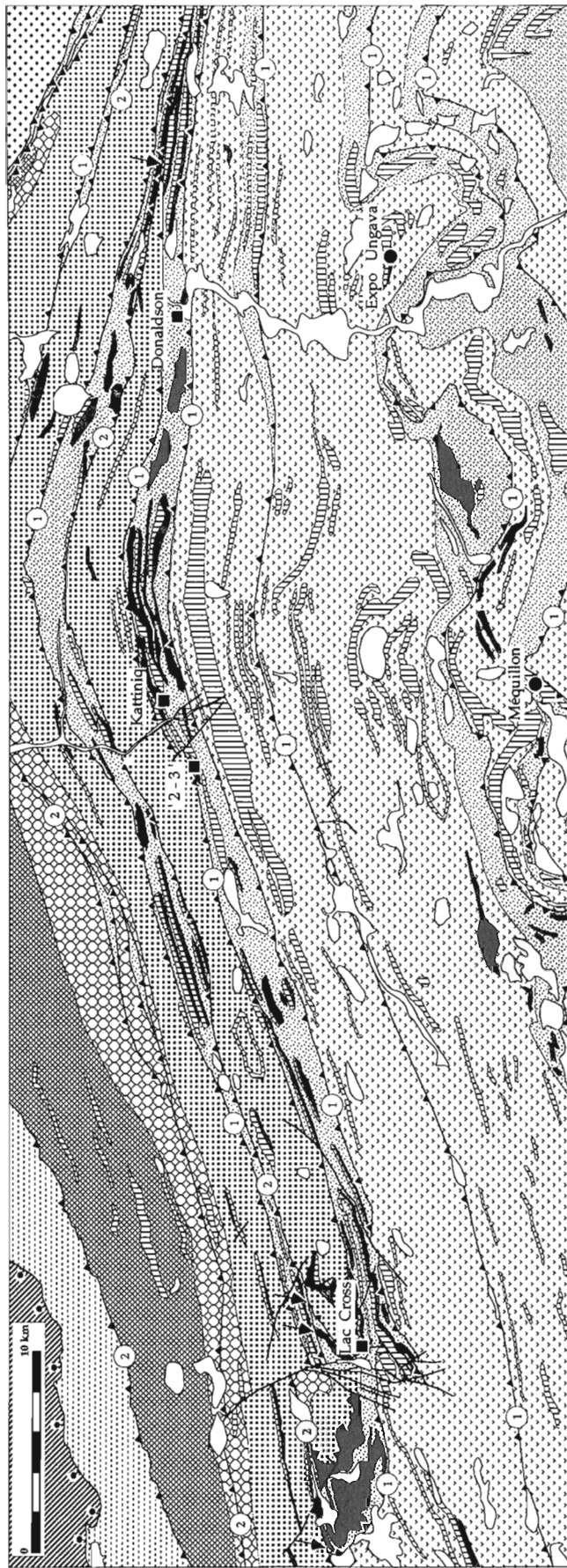
The actual orebody at Purtunig occurs in the ultramafic cumulate rocks on the overturned northern limb of a large west-trending synform (Fig. 40). The chrysotile asbestos mineralization occurs principally within serpentinitized dunite layers, and particularly where the dunite layers lie close (30-40 m) to major pyroxene-rich layers (Stewart, 1976). An open pit was developed to mine a serpentinitized dunite layer that is 150-180 m thick, with a lenticular shape in plan view (400 x 30-60 m; Taylor, 1982). The asbestos ore is considered to be a cross-fibre type, with extensional and shear veins (4.5-6 mm in width; centimetres to metres in length) generally parallel or perpendicular to primary compositional layering (Stewart, 1976).

Ni-Cu-PGE sulphide deposits

Numerous Ni-Cu-PGE sulphide deposits have been discovered in the eastern part of the Cape Smith Belt since the 1950s. The mineralization is associated with differentiated mafic-ultramafic bodies and more homogeneous ultramafic bodies (principally sills) which have been interpreted as co-magmatic with the MgO-rich komatiitic basalts (olivine-phyric) of the lower part of the Chukotat Group (Bédard et al., 1984; Giovenazzo et al., 1989; Thibert et al., 1989). The sills intrude all volcanic and sedimentary units of the Povungnituk Group and the predominantly olivine-phyric basalt sequence of the Chukotat Group (Fig. 159). The Ni-Cu-PGE mineralization occurs in two principal horizons in the map area. The most important deposits (subeconomic to economic) in the Cape Smith Belt occur in the Raglan horizon (thrust sheet M, Fig. 5; lac Cross, '2-3', Kattiniq, Donaldson deposits; Fig. 159), located at the tectonic boundary between the Povungnituk and Chukotat groups (Taylor, 1982; Giovenazzo et al., 1989). The second mineralized horizon (thrust sheets I, J and K, Fig. 5; Bravo, Delta, Méquillon and Expo-Ungava showings; Fig. 159, Barnes and Giovenazzo, 1990), termed the Delta horizon, occurs within the Povungnituk Group and is host to relatively small (sub- to noneconomic) Ni-Cu-PGE sulphide deposits (Giovenazzo et al., 1989). The local geology, mineralogy, and tectonic setting of these two mineralized horizons will be discussed in the following paragraphs.

The Raglan horizon was first staked in 1961 by Raglan Quebec Mines Ltd. (lac Cross area, Fig. 159) and Falconbridge Nickel Ltd. (Donaldson area, Fig. 159). Raglan Quebec Mines was purchased by Falconbridge Ltd. in 1966, and New Quebec Raglan Mines Ltd. (68.3% owned by Falconbridge) was established to further explore and develop the Raglan horizon (Taylor, 1982). Development between 1967 and 1972 included the sinking of a shaft at the Donaldson property and the construction of over 56 km of roads between the mineralized horizon and Douglas Harbour (Fig. 2) to the east (Taylor, 1982). After a shutdown due to the low price of Ni and Cu in 1972, Falconbridge Ltd. re-initiated exploration in 1989 and has since acquired 100% control of properties along the Raglan horizon and drilled extensively to update reserve estimates. Falconbridge Ltd.'s reserve estimates for six mineralized zones in the Raglan horizon, as of November 1991, are as follows (Cloutier and Dufresne, 1991): 17 million tonnes at 3.12% Ni and 0.88% Cu. The richest zone is at Kattiniq (Fig. 159), where proven reserves of 7.2 million tonnes at 3.16% Ni and 0.89% Cu and probable additional reserves of 4.6 million tonnes at 3.18% Ni are being evaluated for partial open pit recovery. Cloutier and Dufresne (1991) estimate that 800 000 tonnes of ore, resulting in 125 000 tonnes of Ni concentrate and 20 000 tonnes of refined Ni, will be processed annually at the proposed Kattiniq mine and concentrator facility.

The Raglan horizon (thrust sheet M, Fig. 5) is situated in relatively deep-water (distal) sedimentary units of the Povungnituk Group. The sedimentary rocks are characterized by black, graphitic and sulphidic pelites interlayered with minor semipelite and quartzite (Fig. 22, 23). The quartzite beds are relatively thin, laterally continuous, and have been interpreted as distal turbidites. Based on the



61° 30' N
74° 30' W

EARLY PROTEROZOIC

- domain 3**
- Spartan Group**
 - graphitic pelite, semipelite, quartzite
 - Watts Group**
 - basalt, gabbro sills and sheeted dykes

- domain 2**
- gabbro
 - peridotite
 - Chukotat Group**
 - dominantly plagioclase-phyric basalt, gabbro, peridotite
 - dominantly pyroxene-phyric basalt, gabbro, peridotite
 - dominantly olivine-phyric basalt, gabbro, peridotite
 - Upper Povungnituk Group**
 - basalt, gabbro, peridotite
 - Lower Povungnituk Group**
 - semipelite, quartzite, ironstone, basalt
 - volcaniclastic sedimentary rock, gabbro, peridotite

ARCHEAN

- domain 1**
- Superior Province**
 - tonalite, granite, amphibolite
 - oblique-slip fault
 - normal fault
 - D₂ thrust fault
 - D₁ thrust fault
 - geological boundary
 - Delta horizon showings
 - Raglan horizon deposits

Figure 159. Simplified geological map for the lac Cross (1724A) - Kattiniq (1725A) - Donaldson (Raglan) (1726A) area (Fig. 2). The map shows the distribution of the larger layered mafic-ultramafic and more homogeneous ultramafic sills which are associated with Cu-Ni-PGE mineralization in the lower Povungnituk Group (see text). The arrows point to cut-off structures in the footwall of a major D₂ out-of-sequence thrust fault (thrust fault O; Fig. 85).

sedimentology, the Raglan horizon (thrust sheet M) is interpreted as the most outboard (distal) deposits of the Povungnituk Group preserved in the Cape Smith Belt stratigraphy (St-Onge and Lucas, 1990m).

The Raglan horizon is structurally juxtaposed between footwall (south) Povungnituk Group basalts and hanging wall (north) Chukotat Group basalts (thrust sheet 'M'; Fig. 5). Detailed mapping has shown that the along-strike extent of the Raglan horizon is controlled by the structural geometry of a D₂ (out-of-sequence) thrust fault, which truncates both the hanging wall Chukotat Group basalts and the entire Raglan horizon (thrust fault O; Fig. 5; see arrows on Fig. 159). The detailed structural geometry of the lac Cross area was discussed above (see the discussion of D₂ structures in the 'Povungnituk and Chukotat groups (domain 2) deformation history').

At a regional scale, the Raglan horizon is situated in a broad D₄ cross-fold synform with the result that progressive structural truncation of the Raglan horizon occurs on both synformal flanks (western truncations are illustrated in Fig. 109 and 159; truncations of units in the eastern part of the thrust sheet are shown in Fig. 159). The same tectono-stratigraphic horizon appears to emerge again to the west of the map area on the eastern flank of the next cross-fold synform (at approximately 74° 45'; Lamothe et al., 1984).

The sulphide deposits occur in association with lenticular, concordant ultramafic sills which are in general thinner than 150 m but which often have significant strike-lengths (Fig. 159; see Miller, 1977; Giovenazzo et al., 1989; Barnes and Barnes, 1990). The sills are principally cored by olivine mesocumulate peridotite, which grades towards thin, orthocumulate-textured pyroxenitic margins (Barnes and Barnes, 1990). Hexagonal columnar jointing occurs in the lower third of the sills and quench features such as spinifex-textured olivine have been reported from the top of the Kattiniq ultramafic body (Barnes and Barnes, 1990). These and other observations by Barnes and Barnes (1990) have led to their re-interpretation of the Kattiniq ultramafic body as a lava lake which developed above a volcanic vent. However, baked margins in sedimentary rocks overlying some of the ultramafic bodies, partially-detached host rock enclaves (Fig. 39), and granophyric tops to some of the differentiated sills (Fig. 38; St-Onge et al., 1987; Thibert et al., 1989) suggest that at least some of the ultramafic bodies are best interpreted as sills emplaced in the distal Povungnituk Group pelites.

The sills were metamorphosed to lower greenschist facies conditions with the result that the olivine is largely replaced by antigorite, tremolite, talc, and/or carbonate (Giovenazzo et al., 1989). The peridotite mineral assemblage also includes poikilitic diopsidic clinopyroxene, chlorite, and antigorite in the matrix and sulphides.

The deposits themselves appear to occur in paleo-topographic depressions at the base of the ultramafic bodies (Miller, 1977; Giovenazzo et al., 1989; Barnes and Barnes, 1990). They are characterized by a thin basal horizon (<10 cm) of massive sulphides overlain by net-textured and disseminated sulphides (Giovenazzo et al., 1989). Sulphide

and oxide minerals associated with the deposits include pyrrhotite, pentlandite, chalcopyrite, magnetite, and ferrochromite, with rare pyrite and PGE minerals. The basal sulphide accumulations are interpreted as magmatic (Miller, 1977; Giovenazzo et al., 1989; Barnes and Barnes, 1990), forming when an immiscible sulphide liquid separated from the parent komatiitic magma due to sulphur saturation. Sulphur isotope studies have suggested that the sulphur is derived in part from assimilation of sulphidic sedimentary rocks and in part from a magmatic source (Giovenazzo et al., 1989; Tremblay and Barnes, 1989). The relatively high PGE content of the Raglan horizon sulphides suggests that either the immiscible sulphide liquid equilibrated with a large volume of silicate melt during its ascent, or that the parent komatiitic magma was exceptionally rich in PGE (Giovenazzo et al., 1989). Barnes and Barnes (1990) hypothesize that the proposed komatiitic lava lake at Kattiniq acted as a physical trap for droplets of immiscible sulphide liquid and that the sulphide liquid was turbulently mixed with a large enough volume of silicate liquid to generate the high PGE contents.

The Delta horizon is marked by Ni sulphide mineralization within differentiated mafic sills and ultramafic sills and dykes which intrude Povungnituk Group sedimentary and volcanic rocks (Giovenazzo et al., 1989). The horizon comprises the following showings: Echo, Bravo, Delta, Méquillon, and Expo-Ungava (Giovenazzo et al., 1989; Barnes and Giovenazzo, 1990). The differentiated sills generally contain layers of peridotite, pyroxenite, and gabbro, and locally display ferrogabbro, quartz ferrogabbro and/or anorthosite layers. While the intrusions themselves are typically poor in sulphides, localized deposits of Ni-Cu-PGE sulphides occur within thin (<1 m) pyroxene-rich pegmatoidal gabbro layers (e.g., Delta showing; Giovenazzo et al., 1989). The ultramafic bodies contain Ni-Cu-PGE mineralization near their bases (e.g. Méquillon dyke showing; Tremblay and Barnes, 1989) which is similar to that found in the Raglan horizon. The lithophile element chemistry of the sills and dykes suggests that they are comagmatic with the komatiitic (predominantly olivine-phyric) basalts of the Chukotat Group (Barnes and Giovenazzo, 1990). However, the sulphide compositions of some of these bodies appear to be out of equilibrium with the host intrusion and differ from those of the Raglan horizon. These differences have been attributed to a complex magmatic history and subsequent hydrothermal leaching of the sulphide ore (Barnes and Giovenazzo, 1990).

Several regional tectonostratigraphic considerations may explain the difference in deposit size between the Delta horizon and the Raglan horizon. The Delta horizon occurs in a more proximal facies of the Povungnituk Group than the Raglan horizon. The former is characterized by semipelite and quartzite interlayered with basalts, volcanoclastic rocks, and relatively minor pelite compared to the latter which is dominated by sulphidic pelite (St-Onge and Lucas, 1990m; see maps 1724A and 1730A). The Delta horizon probably had less opportunity to assimilate sulphidic pelite than the Raglan horizon, and thus had a lower potential for sulphur saturation during magma ascent and emplacement. The

second major tectonostratigraphic difference between the two horizons is the structural proximity to the Chukotat Group. The ultramafic bodies in the Raglan horizon have been interpreted as open-ended conduits feeding the komatiitic basalt flows of the Chukotat Group (Francis et al., 1983; Giovenazzo et al., 1989), as opposed to the sills and dykes in the Delta horizon which may represent intrusions away from the principal axis of volcanism. The volume of magma passing through the ultramafic bodies of the Raglan horizon was probably far greater than that for the Delta horizon intrusions, thus increasing its potential relative to the Delta horizon for accumulating sulphide liquid drops and scavenging PGEs from the erupting komatiitic magmas.

REFERENCES

- Ando, C.J., Czuchra, B.L., Klemperer, S.L., Brown, L.D., Cheadle, M.J., Cook, F.A., Oliver, J.E., Kaufman, S., Walsh, T., Thompson, J.B., Jr., Lyons, J.B. and Rosenfeld, J.L.**
1984: Crustal profile of mountain belt: COCORP deep seismic reflection profiling in New England Appalachians and implications for architecture of convergent mountain chains; *American Association of Petroleum Geology Bulletin*, v. 68, p. 819-837.
- Argand, E.**
1911: Les nappes de recouvrement des Alpes Pennines et leur prolongements structuraux; *Matière carte géologique de Suisse*, N.S. 31, Berne, 26 p.
- Avramtchev, L.**
1982: Cartes des gîtes minéraux du Québec, Région de la Fosse de l'Ungava; Ministère de l'Énergie et des Ressources du Québec, DPV-897, Maps M327 to M336, scale 1:250 000.
- Baer, A.J.**
1977: Gravity anomalies and deep structure of the Cape Smith Fold Belt, northern Ungava, Quebec, comment; *Geology*, v. 5, no. 11, p. 651.
- Baragar, W.R.A.**
1974: Volcanic studies in the Cape Smith-Wakeham Bay Belt, New Quebec; in Report of Activities, Part A, Geological Survey of Canada, Paper 74-1A, p. 155-157.
1983: The Circum-Ungava Belt of eastern Hudson Bay: Geology of the Cape Smith Region; in Current Research, Part A; Geological Survey of Canada, Paper 83-1A, p. 325-328.
1984: Pillow formation and layered flows in the Circum-Superior Belt of eastern Hudson Bay; *Canadian Journal of Earth Sciences*, v. 21, p. 781-792.
- Baragar, W.R.A. and Piché, M.**
1982: The Circum-Ungava Belt of eastern Hudson Bay: The geology of the Ottawa Islands and the Cape Smith region; in Current Research, Part A, Geological Survey of Canada, Paper 82-1A; p. 11-15.
- Baragar, W.R.A. and Scoates, R.F.J.**
1981: The Circum-Superior Belt: a Proterozoic plate margin?; in *Precambrian Plate Tectonics*, (ed.) A. Kroner; Elsevier, Amsterdam, p. 297-330.
- Baragar, W.R.A., Hervet, M. and Charland, M.**
1986: Structural character and plutonic setting at the western end of the Ungava Trough; dans *Exploration en Ungava: données récentes sur la géologie et la géologie*, (ed.) D. Lamothe, R. Gagnon et T. Clark; Ministère de l'Énergie et des Ressources du Québec, DV 86-16, p. 41-43.
- Barnes, S.-J. and Barnes, S.J.**
1990: A new interpretation of the Katiniq Nickel Deposit, Ungava, northern Quebec; *Economic Geology*, v. 85, p. 1269-1272.
- Barnes, S.-J. and Giovenazzo, D.**
1990: Platinum-group elements in the Bravo intrusion, Cape Smith Fold Belt, northern Quebec; *Canadian Mineralogist*, v. 28, p. 431-449.
- Barrette, J.-P.**
1990a: Géologie de la région du lac Bilson (Fosse de l'Ungava); Ministère de l'Énergie et des Ressources du Québec, ET 88-15. 28 p.
- Barrette, J.-P. (cont.)**
1990b: Géologie de la région du lac Bolduc (Fosse de l'Ungava); Ministère de l'Énergie et des Ressources du Québec, ET 89-03, 39 p.
1991: Étude géologique de la partie occidentale de la Fosse de l'Ungava, région des lacs Bilson, Bolduc, Vigneau et de la baie Korak; Ministère de l'Énergie et des Ressources du Québec, MB 91-22, 98 p.
- Bartley, J.M.**
1982: Limited basement involvement in Caledonian deformation, Hinnoy, north Norway, and tectonic implications; *Tectonophysics*, v. 83, p. 185-203.
- Beach, A.**
1979: Pressure solution as a metamorphic process in deformed terrigenous sedimentary rocks; *Lithos*, v. 12, p. 51-58.
- Beall, G.H.**
1959: Cross Lake area, New Quebec; Quebec Department of Mines, Preliminary Report 396, 9 p., and Preliminary Map 1267.
1960: Laflamme Lake area, New Quebec; Quebec Department of Mines, Preliminary Report 435, 10 p., and Preliminary Map 1351.
1962: Differentiation controls in subsiliceous gabbros; Ph.D. thesis, Massachusetts Institute of Technology, Boston, Massachusetts, 219 p.
1977: Final report on Cross Lake and Laflamme Lake areas; Ministère des Richesses Naturelles du Québec, DP-460, 79 p.
- Beall, G.H., Hurley, P.M., Fairbairn, H.W., and Pinson, W.H., Jr.**
1963: Comparison of K-Ar and whole-rock Rb-Sr dating in New Quebec and Labrador; *American Journal of Science*, v. 261, p. 571-580.
- Bédard, J.H., Francis, D.M., Hynes, A.J., and Nadeau, S.**
1984: Fractionation in the feeder system at a Proterozoic rifted margin; *Canadian Journal of Earth Sciences*, v. 21, p. 489-499.
- Bégin, N.J.**
1989a: P-T conditions of metamorphism inferred from the metabasites of the Cape Smith Belt, northern Quebec; *Geoscience Canada*, v. 16, p. 151-154.
1989b: Metamorphic zonation, mineral chemistry and thermobarometry in metabasites of the Cape Smith Thrust-Fold Belt, northern Quebec: Implications for its thermotectonic evolution; Ph.D. thesis, Queen's University, Kingston, Ontario, 313 p.
1992a: Contrasting mineral isograd sequences in metabasites of the Cape Smith Belt, northern Quebec, Canada: three new bathograds for mafic rocks; *Journal of Metamorphic Geology*, v. 10, p. 685-704.
1992b: Textural and compositional relationships of Ca-amphiboles in metabasites of the Cape Smith Belt, northern Quebec: implications for a miscibility gap at medium pressure; *Journal of Petrology*, v. 33, p. 1317-1343.
- Behrendt, J.C., Hutchinson, D.R., Lee, M., Thornber, C.R., Tréhu, A., Cannon, W., and Green, A.**
1990: GLIMPCE seismic reflection evidence of deep-crustal and upper-mantle intrusions and magmatic underplating associated with the Midcontinent Rift system of North America; *Tectonophysics*, v. 173, p. 595-615.
- Bell, R.**
1885: Observations on the geology, mineralogy, zoology and botany of the Labrador Coast, Hudson Strait and Bay; Geological Survey of Canada, Report of Progress, 1882-84.
- Bell, T.H.**
1981: Foliation development: the contribution, geometry and significance of progressive bulk inhomogeneous shortening; *Tectonophysics*, v. 75, p. 273-296.
1985: Deformation partitioning and porphyroblast rotation in metamorphic rocks: a radical reinterpretation; *Journal of Metamorphic Geology*, v. 3, p. 109-118.
1986: Foliation development and refraction in metamorphic rocks: reactivation of earlier foliations and decrenulation due to shifting patterns of deformation partitioning; *Journal of Metamorphic Geology*, v. 4, p. 421-444.
- Bell, T.H. and Johnson, S.E.**
1989: Porphyroblast inclusion trails: the key to orogenesis; *Journal of Metamorphic Geology*, v. 7, p. 279-310.
1990: Rotation of rigid objects during ductile deformation: well established fact or intuitive prejudice?; *Australian Journal of Earth Sciences*, v. 37, p. 441-446.

- Bergeron, R.**
 1957a: Cape Smith-Wakeham Bay Belt, New Quebec; Quebec Department of Mines, Preliminary Report 355, 8 p., and Preliminary Maps 1090 and 1196.
 1957b: Proterozoic rocks of the northern part of the Labrador Geosyncline, the Cape Smith Belt and the Richmond Gulf area; *in* The Proterozoic in Canada; Royal Society of Canada, Special Publication No. 2, p. 101-111.
 1958: The Cape Smith-Wakeham Bay Belt; Canadian Mining Journal, v. 79, no. 4, p. 115-117.
 1959: Povungnituk Range area, New Quebec; Quebec Department of Mines, Preliminary Report 392, 9 p., and Preliminary Map 1279.
- Bergeron, R., Bérard, J., and Gélinas, L.**
 1962: Tectonics of regions bordering the Ungava stable area; *in* The tectonics of the Canadian Shield; Royal Society of Canada, Special Publication No. 4, p. 144-148.
- Berthé, D., Choukroune, P., and Jegouzo, P.**
 1979: Orthogneiss, mylonite and non-coaxial deformation of granites: the example of the South Armorian Shear Zone; Journal of Structural Geology, v. 1, p. 31-42.
- Bertrand, J.-M., Roddick, J.C., Van Kranendonk, M.J., and Ermanovics, I.**
 in press: Geochronology of deformation and metamorphism in the Early Proterozoic Torngat Orogen, North River map area, Labrador; Canadian Journal of Earth Sciences.
- Bostock, H.S.**
 1970: Physiographic subdivisions of Canada; *in* Geology and economic minerals of Canada, 5th ed., Geological Survey of Canada, Economic Geology Report No. 1, p. 9-30.
- Bouchard, M.A.**
 1989: The Nouveau-Québec (Nunavik) crater: a possible site for a long range Cenozoic stratigraphic record beneath continental ice sheets; Geological Association of Canada, Program with Abstracts, v. 14, p. A61.
- Bouchard, M.A. and Péloquin, S.**
 1989: L'histoire naturelle du Cratère du Nouveau-Québec; Collection Environnement et Géologie, volume 7, Université de Montréal, 420 p.
- Boyer S.E. and Elliott, D.**
 1982: Thrust systems; Bulletin of the American Association of Petroleum Geologists, v. 66, p. 1196-1230.
- Brodie, K.H. and Rutter E.H.**
 1985: On the relationship between deformation and metamorphism, with special reference to the behaviour of basic rocks; *in* Metamorphic reactions: kinetics, textures and deformation, ed. A.B. Thompson and D.C. Rubie; Advances in Physical Geochemistry, Springer-Verlag, New York, v. 4, p. 138-179.
- Brown, R.J.E.**
 1967: Permafrost in Canada; Geological Survey of Canada, Map 1246A, scale 1:7 603 200.
- Bruneau, D. and Gray, J.T.**
 1991: Surficial geology, Salluit and Cap de Nouvelle-France area, Québec; Geological Survey of Canada, Map 11-1990, scale 1:250 000.
- Budkewitsch, P.**
 1986: Some preliminary observations on the structural style in a part of the Ungava Trough, New Quebec; dans Exploration en Ungava: données récentes sur la géologie et la géologie, (ed.) D. Lamothe, R. Gagnon et T. Clark; Ministère de l'Énergie et des Ressources du Québec, DV 86-16, p. 45-50.
- Burchfiel, B.C. and Royden, L.H.**
 1985: North-south extension within the convergent Himalayan region; Geology, v. 13, p. 679-682.
- Burg, J.P., Brunel, M., Gapais, D., Chen, G.M., and Liu, G.H.**
 1984: Deformation of leucogranites of the crystalline Main Central Thrust Sheet in southern Tibet (China); Journal of Structural Geology, v. 6, p. 535-542.
- Byrne, T. and Lucas, S.B.**
 1988: Rheological evolution of the decollement in A- and B-type subduction zones; Geological Society of America, Abstracts with Programs, v. 20, p. A270.
- Carmichael, D.M.**
 1970: Intersecting isograds in the Whetstone Lake area, Ontario; Journal of Petrology, v. 11, p. 147-181.
- Carmichael, D.M.(cont.)**
 1978: Metamorphic bathozones and bathograds: a measure of the depth of post-metamorphic uplift and erosion on the regional scale; American Journal of Science, v. 267, p. 259-272.
- Cloutier, J.-P. and Dufresne, M.**
 1991: Le gisement Raglan; dans Seminaire d'information 1991: Résumés des conférences, Ministère de l'Énergie et des Ressources du Québec, DV 91-26, p. 43-44.
- Cobbold, P.R. and Quinquis, H.**
 1980: Development of sheath folds in shear regimes; Journal of Structural Geology, v. 2, p. 119-126.
- Coney, P.J., Jones, D.L., and Monger, J.W.H.**
 1980: Cordilleran suspect terranes; Nature, v. 288, p. 329-333.
- Cooper, A.F.**
 1972: Progressive metamorphism of metabasic rocks from the Haast Schist Group of Southern New Zealand; Journal of Petrology, v. 13, p. 457-492.
- Currie, K.L.**
 1965: The geology of the New Quebec Crater; Canadian Journal of Earth Sciences, v. 2, p. 141-160.
 1966: Geology of the New Quebec Crater; Geological Survey of Canada, Bulletin 150, 36 p.
- Currie, K.L. and Dence, M.R.**
 1963: Rock deformation in the rim of the New Quebec Crater, Canada; Nature, v. 198, p. 80.
- Daigneault, R.-A.**
 1990: Résultats préliminaires sur les directions d'écoulement glaciaire dans la région de Salluit et des lacs Nuvilik, Nouveau-Québec; *in* Current Research, Part C; Geological Survey of Canada, Paper 90-1C, p. 25-29.
- Dell'Angelo, L.N. and Tullis, J.**
 1982: Textural strain softening in experimentally deformed aplite; EOS, Transactions of the American Geophysical Union, v. 63, p. 438.
- DeMontigny, P.A.**
 1959: Upper Deception River area, New Quebec; Quebec Department of Mines, Preliminary Report 398, 8 p., and Preliminary Map 1285.
- Dewey, J.F. and Burke, K.C.A.**
 1973: Tibetan, Variscan and Precambrian basement reactivation: products of continental collision; Journal of Geology, v. 81, p. 683-692.
- Dewey, J.F., Cande, S., and Pitman, W.C. III**
 1989: Tectonic evolution of the India/Eurasia collision zone; Eclogiae Helvetiae, v. 82, p. 717-734.
- Dimroth, E., Baragar, W.R.A., Bergeron, R., and Jackson, G.D.**
 1970: The filling of the Circum-Ungava geosyncline; *in* Symposium on basins and geosynclines of the Canadian Shield, (ed.) A.J. Baer; Geological Survey of Canada, Paper 70-40, p. 45-142.
- Dixon, J.M. and Summers, J.S.**
 1983: Patterns of total and incremental strain in subsiding troughs: experimental centrifuge models of interdiapir synclines; Canadian Journal of Earth Sciences, v. 20, p. 1843 - 1861.
- Doig, R.**
 1983: Rb-Sr isotopic study of Archean gneisses north of the Cape Smith Fold Belt, Ungava, Quebec; Canadian Journal of Earth Sciences, v. 20, p. 821-829.
 1987: Rb-Sr geochronology and metamorphic history of Proterozoic to early Archean rocks north of the Cape Smith Fold Belt, Quebec; Canadian Journal of Earth Sciences, v. 24, p. 813-825.
- Dorsey, R.J.**
 1992: Collapse of the Luzon volcanic arc during onset of arc-continent collision: evidence from a Miocene-Pliocene unconformity, eastern Taiwan; Tectonics, v. 11, p. 177-191.
- Drinnan, R.H. and Prior, L.**
 1955: Physical characteristics of the Ungava Bay area; Geographical Bulletin of Canada, no. 7, p. 17-37.
- Dugas, J.**
 1971: Mineralization in the Cape Smith-Wakeham Bay area; Ministère des Richesses Naturelles du Québec, Special Paper 9.
- Dunphy, J.M. and Ludden, J.N.**
 1992: The Narsajuaq Terrane, northern Quebec: A mid-crustal section of an Early Proterozoic magmatic arc; EOS. Transactions American Geophysical Union, v. 73 (supplement), p. 318.
- Dyke, A.S. and Prest, V.K.**
 1987: Late Wisconsinian and Holocene retreat of the Laurentide Ice Sheet; Geological Survey of Canada, Map 1702A, scale 1:5 000 000.

Earth Physics Branch

- 1980: Gravity Map of Canada; Energy, Mines and Resources, Canada, Gravity Map Series 80-1, scale 1:5 000 000.
- Elliott, D. and Johnson, M.R.W.**
1980: Structural evolution in the northern part of the Moine thrust belt, NW Scotland; Transactions of the Royal Society of Edinburgh, v. 71, p. 69-96.
- Enami, M.**
1981: On sodic plagioclase in some rocks of the Sanbagawa metamorphic belt in the Bessi district, Shikoku, Japan; Proceedings of the Japanese Academy, v. 57, p. 188-193.
- England, P.C. and Richardson, S.W.**
1977: The influence of erosion upon the mineral facies of rocks from different metamorphic environment; Journal of the Geological Society of London, v. 134, p. 201-213.
- England, P.C. and Thompson, A.B.**
1984: Pressure-temperature-time paths of regional metamorphism I. Heat transfer during the evolution of regions of thickened continental crust; Journal of Petrology, v. 25, p. 894-928.
- Fahrig, W.F., Irving, E. and Jackson, G.D.**
1971: Paleomagnetism of the Franklin diabases; Canadian Journal of Earth Sciences, v. 8, p. 455-467.
- Feininger, T.**
1986: An unusual alaskite located 40 km west of Asbestos Hill; dans Exploration en Ungava: données récentes sur la géologie et la gîtologie, (ed.) D. Lamothe, R. Gagnon et T. Clark; Ministère de l'Énergie et des Ressources du Québec, DV 86-16, p. 51-56.
- Feininger, T., Lamothe, D., St-Onge, M.R., and Losier, L.**
1985: Interprétation gravimétrique de la Fosse de l'Ungava; Ministère de l'Énergie et des Ressources du Québec, DV 85-12.
- Ferry, J.M. and Spear, F.S.**
1978: Experimental calibration of the partitioning of Fe and Mg between biotite and garnet; Contributions to Mineralogy and Petrology, v. 66, p. 113-117.
- Fletcher, R.C.**
1972: Application of a mathematical model to the emplacement of mantled gneiss domes; American Journal of Science, v. 272, p. 197-216.
1974: Wavelength selection in the folding of a single layer with power-law rheology; American Journal of Science, v. 274, p. 1029-1043.
- Francis, D.M. and Hynes, A.J.**
1979: Komatiite-derived tholeiites in the Proterozoic of New Quebec; Earth and Planetary Science Letters, v. 44, p. 473-481.
- Francis, D.M., Hynes, A.J., Ludden, J.N., and Bédard, J.**
1981: Crystal fractionation and partial melting in the petrogenesis of a Proterozoic high-MgO volcanic suite, Ungava Quebec; Contributions to Mineralogy and Petrology, v. 78, p. 27-36.
- Francis, D.M., Ludden, J. and Hynes, A.J.**
1983: Magma evolution in a Proterozoic rifting environment; Journal of Petrology, v. 24, p. 556-582.
- Ganguly, J. and Saxena, S.K.**
1984: Mixing properties of aluminosilicate garnets: constraints from natural and experimental data, and applications to geothermobarometry; American Mineralogist, v. 69, p. 88-97.
- Gaonac'h, H., Ludden, J.N., Picard, C., and Francis, D.M.**
1992: Highly alkaline lavas in a Proterozoic rift zone: Implications for Precambrian mantle metasomatic processes; Geology, v. 20, p. 247-250.
- Gaonac'h, H., Picard, C., Ludden, J.N. and Francis, D.M.**
1989: Alkaline rocks from a Proterozoic volcanic island in the Cape Smith Thrust Belt, New Quebec; Geoscience Canada, v. 16, p. 137-139.
- Gélinas, L.**
1962: Watts Lake area, New Quebec; Quebec Department of Natural Resources, Preliminary Report 471, 11 p., and Preliminary Map 1414.
- Geological Survey of Canada**
1983: Rivière Kovic, Quebec and Northwest Territories; Geological Survey of Canada, Magnetic Anomaly Map NP 17-17-AM, scale 1: 1 000 000.
- Ghent, E.D.**
1976: Plagioclase-garnet-Al₂SiO₅-quartz: A potential geobarometer-geothermometer; American Mineralogist, v. 61, p. 710-714.
- Gibb R.A.**
1983: Model of suturing of Superior and Churchill plates; An example of double indentation tectonics, v. 11, p. 413-417.
- Gibb R.A. and Walcott, R.I.**
1971: A Precambrian suture in the Canadian Shield; Earth and Planetary Science Letters, v. 10, p. 417-422.
- Gibb, R.A., Thomas, M.D., Lapointe, P.L. and Mukhopadhyay, M.**
1983: Geophysics of proposed Proterozoic sutures in Canada; Precambrian Research, v. 19, p. 349-384.
- Giovenazzo, D.**
1986: La Fosse de l'Ungava: une province métallogénique enrichie en éléments du groupe de platine; dans Exploration en Ungava: données récentes sur la géologie et la gîtologie, (ed.) D. Lamothe, R. Gagnon et T. Clark; Ministère de l'Énergie et des Ressources du Québec, DV 86-16, p. 75-81.
- Giovenazzo, D. and Lefebvre, C.**
1986: Classification des indices minéralisés de la Fosse de l'Ungava; dans Exploration en Ungava: données récentes sur la géologie et la gîtologie, (ed.) D. Lamothe, R. Gagnon et T. Clark; Ministère de l'Énergie et des Ressources du Québec, DV 86-16, p. 73-6.
- Giovenazzo, D., Picard, C., and Guha, J.**
1989: Tectonic setting of Ni-Cu-PGE deposits in the central part of the Cape Smith Belt; Geoscience Canada, v. 16, p. 134-136.
- Gold, D. P.**
1962: Brisebois Lake area, New Quebec; Quebec Department of Natural Resources, Preliminary Report 470, 11 p., and Preliminary Map 1413.
- Graham, C.M. and Powell, R.**
1984: A garnet-hornblende geothermometer: calibration, testing, and application to the Pelona Schist, southern California; Journal of Metamorphic Petrology, v. 2, p. 13-31.
- Gray, J.T. and Lauriol, B.**
1985: Dynamics of the Late Wisconsin ice sheet in the Ungava Peninsula interpreted from geomorphological evidence; Arctic and Alpine Research, v.17, p. 289-310.
- Gunning, H.C.**
1934: Sulphide deposits at Cape Smith, east coast of Hudson Bay; Geological Survey of Canada, Summary Report 1933, Part D, p. 139-154.
- Hanmer, S.**
1986: Asymmetrical pull-aparts and foliation fish as kinematic indicators; Journal of Structural Geology, v. 8, p. 111-122.
- Harris, C.W., Gibson, R.G., Simpson, C., and Eriksson, K.A.**
1987: Proterozoic cusped basement-cover structure, Needle Mountains, Colorado; Geology, v. 15, p. 950-953.
- Harris, L.B. and Cobbold, P.R.**
1985: Development of conjugate shear bands during bulk simple shearing; Journal of Structural Geology, v. 7, p. 37-44.
- Harrison, J.M.**
1954: Ungava (Chubb) crater and glaciation; Journal of Royal Astronomical Society of Canada, v. 48, p. 16-20.
- Hashimoto T.**
1962: Iron silicate equilibria in the Cape Smith belt, New Quebec; unpublished M.Sc. thesis, McGill University, Montreal, Quebec, 124 p.
- Hashimoto T. and Béland, R.**
1968: Low- to medium-grade metamorphism in silicate iron-formations of the Cape Smith Belt, New Quebec; Canadian Journal of Earth Sciences, v. 4, p. 881-893.
- Hegner, E. and Bevier, M.L.**
1989: Geochemical constraints on the origin of mafic rocks from the Cape Smith Belt; Geoscience Canada, v. 16, p. 148-151.
1991: Nd and Pb isotopic constraints on the origin of the Purtuniqu ophiolite and Early Proterozoic Cape Smith Belt, northern Quebec, Canada; Chemical Geology, v. 91, p. 357-371.
- Hervet, M.**
1986: Géologie de la région de la vallée de Narsajuaq, Fosse de l'Ungava; dans Exploration en Ungava: données récentes sur la géologie et la gîtologie, (ed.) D. Lamothe, R. Gagnon et T. Clark; Ministère de l'Énergie et des Ressources du Québec, DV 86-16, p. 21-29.
- Hess, P.C.**
1971: Prograde and retrograde equilibrium in garnet-cordierite gneisses in south-central Massachusetts; Contributions to Mineralogy and Petrology, v. 30, p. 177-195.
- Hodges, K.V. and McKenna, L.W.**
1987: Realistic propagation of uncertainties in geologic thermobarometry; American Mineralogist, v. 72, p. 702-709.

- Hodges, K.V. and Royden, L.**
1984: Geologic thermobarometry of retrograded metamorphic rocks: an indication of the uplift trajectory of a portion of the northern Scandinavian Caledonides; *Journal of Geophysical Research*, v. 89, p. 7077-7090.
- Hodges, K.V. and Spear, F.S.**
1982: Geothermometry, geobarometry and the Al_2SiO_5 triple point at Mt. Moosilauke, New Hampshire; *American Mineralogist*, v. 67, p. 1118-1134.
- Hoffman, P.F.**
1985: Is the Cape Smith Belt (northern Quebec) a klippe?; *Canadian Journal of Earth Sciences*, v. 22, p. 1361-1369.
1988: United plates of America, the birth of a craton: Early Proterozoic assembly and growth of Laurentia; *Annual Review of Earth and Planetary Science*, v. 16, p. 543-603.
1989: Precambrian geology and tectonic history of North America; in *The geology of North America - An overview*, (ed.) A.W. Bally, and A.R. Palmer; Geological Society of America, *The Geology of North America*, v. A, p. 447-512.
1990: Dynamics of the tectonic assembly of northeast Laurentia in geon 18 (1.9 - 1.8 Ga); *Geoscience Canada*, v. 17, p. 222-226.
- Hoffman, P.F., Tirrul, R., King, J.E., St-Onge, M.R., and Lucas, S.B.**
1988: Axial projections and modes of crustal thickening, eastern Wopmay orogen, northwest Canadian Shield; in *Processes of continental lithospheric deformation*, (ed.) S.P. Clark; Geological Society of America, *Special Paper 213*, p. 1-29.
- Hunt, P.A. and Roddick, J.C.**
1991: A compilation of K-Ar ages: Report 21; in *Radiogenic age and isotopic studies: Report 5*, Geological Survey of Canada, Paper 91-2, p. 207-261.
- Hynes, A.J. and Francis, D.M.**
1982: A transect of the Early Proterozoic Cape Smith foldbelt, New Quebec; *Tectonophysics*, v. 88, p. 23-59.
- Indares, A. and Martignole, J.**
1985: Biotite-garnet geothermometry in granulite-facies rocks: evaluation of equilibrium criteria; *Canadian Mineralogist*, v. 70, p. 272-278.
- Innes, M.J.S., Goodacre, A.K., Weston A.A. and McConnell, R.K.**
1967: Structural implications of the gravity field in Hudson Bay and vicinity; *Canadian Journal of Earth Sciences*, v. 4, p. 881-893.
- Innes, M.J.S., Goodacre, A.K., Weston, A.A., and Weber, J.R.**
1968: Gravity and isostasy in the Hudson Bay region; in *Science, History and Hudson Bay*, vol. 2, (ed.) C.S. Beals and S.A. Shentone; Department of Energy, Mines and Resources, Canada, p. 703-728.
- Jacob, R.E., Snowden, P.A. and Bunting, F.J.L.**
1983: Geology and structural development of the Tumas basement dome and its cover rocks; in *Evolution of the Damara Orogen*, (ed.) R. McMiller; Geological Society of South Africa, p. 157-172.
- Jamieson, R.A. and Beaumont, C.**
1988: Orogeny and metamorphism: a model for deformation and pressure-temperature-time paths with applications to the central and southern Appalachians; *Tectonics*, v. 7, p. 417-445.
- Johnson, A.M.**
1980: Folding and faulting of strain-hardening sedimentary rocks; *Tectonophysics*, v. 62, p. 251-278.
- Jordan, P.G.**
1987: The deformational behaviour of bimineralic limestone-halite aggregates; *Tectonophysics*, v. 135, p. 185-197.
- King, J.E.**
1986: The metamorphic internal zone of Wopmay Orogen (Early Proterozoic), Canada: 30 km of structural relief in a composite section based on plunge projection; *Tectonics*, v. 5, p. 973-994.
- Kohn, M.J. and Spear, F.S.**
1989: Empirical calibration of geobarometers for the assemblage garnet+hornblende+plagioclase+quartz; *American Mineralogist*, v. 74, p. 77-84.
- Koziol, A.M. and Newton, R.C.**
1988: Redetermination of the anorthite breakdown reaction and improvement of the plagioclase-garnet- Al_2SiO_5 -quartz geobarometer; *American Mineralogist*, v. 73, p. 216-223.
- Kretz, R.**
1959: A chemical study of garnet, biotite and hornblende from gneisses of southwestern Quebec with emphasis on the distribution of elements in coexisting minerals; *Journal of Geology*, v. 67, p. 371-402.
- Kretz, R. (cont.)**
1960: Geological observations in northern New Quebec; Geological Survey of Canada, Paper 60-12, 17 p.
- Laird, J. and Albee, L.**
1981: Pressure, temperature and time indicators in mafic schist: their application to reconstructing the polymetamorphic history of Vermont; *American Journal of Science*, v. 281, p. 127-175.
- Lamothe, D.**
1986: Développements récents dans la Fosse de l'Ungava; dans *Exploration en Ungava: données récentes sur la géologie et la géologie*, (ed.) D. Lamothe, R. Gagnon et T. Clark; Ministère de l'Énergie et des Ressources du Québec, DV 86-16, p. 1-6.
- Lamothe, D., Picard, C., and Moorhead, J.**
1984: Région du lac Beauport, bande de Cap Smith-Maricourt, Nouveau-Québec; Ministère de l'Énergie et des Ressources du Québec, DP 84-39, 2 sheets, scale 1:50 000.
- Laubach, S.E. and Jackson, M.L.W.**
1990: Origin of arches in the northwestern Gulf of Mexico basin; *Geology*, v. 18, p. 595-598.
- Lévesque, R., Allard, M., Seguin, M.K., and Pilon, J.A.**
1990: Données préliminaires sur le régime thermique du pergélisol dans quelques localités du Nunavik, Québec; Actes de la Cinquième conférence canadienne sur le pergélisol, collection Nordicana, v. 54, p. 207-213.
- Lewry, J.F. and Stauffer, M.R.**
1990: The Early Proterozoic Trans-Hudson orogen of North America; Geological Association of Canada Special Paper, v. 37, 505 p.
- Loomis, T.P.**
1983: Compositional zoning of crystals: a record of growth and reaction history; in *Kinetics and equilibrium in mineral reactions*, (ed.) S.K. Saxena; Springer-Verlag, New York, p. 1-60.
- Low, A.P.**
1899: Report on an exploration of part of the south shore of Hudson Strait and Ungava Bay; Geological Survey of Canada, Annual Report, Vo. XI, pt L, 47 p.
1902: Report on an exploration of the east coast of Hudson Bay from Cape Wolstenholme to the south end of James Bay; Geological Survey of Canada, Annual Report, vol. XIII, pt D, 84 p.
- Lucas, S.B.**
1989a: Structural evolution of the Cape Smith Thrust Belt and the role of out-of-sequence faulting in the thickening of mountain belts; *Tectonics*, v. 8, p. 655-676.
1989b: Geometrical, rheological and mechanical evolution of continental thrust belts: examples from the Cape Smith Belt, northern Quebec, Canada; Ph.D. thesis, Brown University, Providence, Rhode Island, 253 p.
1990: Relations between thrust belt evolution, grain-scale deformation, and metamorphic processes: Cape Smith Belt, northern Canada; *Tectonophysics*, v. 178, p. 151-182.
- Lucas, S.B. and Byrne, T.**
1992: Footwall involvement during arc-continent collision in the Ungava orogen, Canada; *Journal of the Geological Society, London*, v. 149, p. 237-248.
- Lucas S.B. and St-Onge, M.R.**
1989a: Structural evolution of the Cape Smith Belt from initial thrusting to basement-involved folding; *Geoscience Canada*, v. 16, p. 122-126.
1989b: Shear zone softening at the base of the Cape Smith Belt: implications for the rheological evolution of thrust belts; *Geoscience Canada*, v. 16, p. 158-163.
1991: Evolution of Archean and Early Proterozoic magmatic arcs in the northeastern Ungava Peninsula, Quebec; in *Current Research, Part C*; Geological Survey of Canada, Paper 91-1C, p. 109-119.
1992: Terrane accretion in the internal zone of the Ungava orogen, northern Quebec. Part 2: Structural and metamorphic history; *Canadian Journal of Earth Sciences*, v. 29, p. 765-782.
- Lucas, S.B., St-Onge, M.R., Parrish, R.R., and Dunphy, J.M.**
1992: Long-lived continent-ocean interaction in the Early Proterozoic Ungava orogen, northern Quebec, Canada; *Geology*, v. 20, p. 113-116.
- Machado, N., Gariépy, C., Philippe, S., and David, J.**
1991: Géochronologie U-Pb du territoire québécois: Fosses du Labrador et de l'Ungava et sous-province de Pontiac; Ministère de l'Énergie et des Ressources du Québec, MB 91-07, p. 19-29.

- Mackin, J.H.**
1950: The down-structure method of viewing geologic maps; *Journal of Geology*, v. 58, p. 55-72.
- Maruyama, S., Liou, J.G. and Suzuki, L.**
1982: The peristerite gap in low-grade metamorphic rocks; *Contribution to Mineralogy and Petrology*, v. 81, p. 268-276.
- Marvin, U.B., Kring, D.A. and Boulger, J.D.**
1988: Petrography of impactite from the New Quebec Crater (abstract); *Meteoritics*, v. 23, p. 287-288.
- Mattauer, M.**
1986: Intracontinental subduction, crust-mantle decollement and crustal-stacking wedge in the Himalayas and other collision belts; in *Collision tectonics*, (ed.) M.P. Coward and A.C. Ries; Geological Society of London, Special Publication 19, p. 37-50.
- Matthews, B.**
1962: Glacial and postglacial geomorphology of the Sugluk - Wolstenholme area, northern Ungava; McGill Sub-Arctic Research Paper, no. 12, Annual Report 1960-61, p. 17-46.
1966: Radiocarbon dated postglacial land uplift in northern Ungava, Canada; *Nature*, v. 211, p. 1164-1166.
1967a: Late Quaternary land emergence in northern Ungava, Quebec; *Arctic*, v. 20, p. 176-202.
1967b: Late Quaternary events in northern Ungava; Ph.D. thesis, McGill University, Montreal, Quebec, 283 p.
- McAdoo, D.C. and Sandwell, D.T.**
1985: Folding of the oceanic lithosphere; *Journal of Geophysical Research*, v. 90, p. 8563-8569.
- McKenzie, D. and Bickle, M.J.**
1988: The volume and composition of melt generated by extension of the lithosphere; *Journal of Petrology*, v. 29, p. 625-679.
- Meen, V.B.**
1950: Chubb Crater, Ungava, Quebec; *Journal of the Royal Astronomical Society of Canada*, v. 44, p. 169-180.
1951a: The Canadian meteor crater; *Scientific American*, v. 184, p. 64-69.
1951b: Chubb Crater, Ungava, Quebec; *Proceedings of the Geological Association of Canada*, v. 4, p. 49-59.
1952: Solving the riddle of Chubb Crater; *National Geographic*, v. 101, p. 1-32.
1957: Chubb Crater - a meteor crater; *Journal of the Royal Astronomical Society of Canada*, v. 51, p. 137-154.
- Miller, A.R.**
1977: Petrology and geochemistry of the 2-3 ultramafic sill and related rocks, Cape Smith-Wakeham Bay Fold Belt, Quebec; Ph.D. thesis, University of Western Ontario, London, Ontario, 219 p.
- Millman, P.M.**
1956: A profile study of the New Quebec crater; *Publication of the Dominion Observatory, Ottawa*, v. 18, no. 4, p. 59-82.
- Moore, J.M.**
1977: Orogenic volcanism in the Proterozoic of Canada; in *Volcanic regimes in Canada*, (ed.) W.R.A. Baragar, L.C. Coleman, and J.M. Hall; Geological Association of Canada, Special Paper 16, p. 127-148.
- Moore, E.M.**
1982: Origin and emplacement of ophiolites; *Reviews of Geophysics and Space Physics*, v. 20, p. 735-760.
- Moorhead, J.**
1986: Géologie de la région des lacs Chukotat et Hubert, Fosse de l'Ungava; dans *Exploration en Ungava: données récentes sur la géologie et la géologie*, (ed.) D. Lamothe, R. Gagnon, et T. Clark; Ministère de l'Énergie et des Ressources du Québec, DV 86-16, p. 7-14.
1989: Géologie de la région du lac Chukotat (Fosse de l'Ungava); Ministère de l'Énergie et des Ressources du Québec, ET87-10, 56 p.
- Neurath, C. and Smith, R.B.**
1982: The effect of material properties on growth rates of folding and boudinage: experiments with wax models; *Journal of Structural Geology*, v. 4, p. 215-229.
- Newton, R.C. and Haselton, H.T.**
1981: Thermodynamics of the garnet-plagioclase- Al_2SiO_5 -quartz geobarometer; in *Thermodynamics of Minerals and Melts*, (ed.) R.C. Newton, A. Navrotsky, and B.J. Wood.; Springer-Verlag, New York, p. 131-147.
- O'Hara, K.**
1988: Fluid flow and volume loss during mylonitization: an origin for phyllonite in an overthrust setting, North Carolina, U.S.A.; *Tectonophysics*, v. 156, p. 21-36.
- Parrish, R.R.**
1989: U-Pb geochronology of the Cape Smith Belt and Sugluk block, northern Quebec; *Geoscience Canada*, v. 16, p. 126-130.
- Picard, C.**
1986: Lithogéochimie de la partie centrale de la Fosse de l'Ungava; dans *Exploration en Ungava: données récentes sur la géologie et la géologie*, (ed.) D. Lamothe, R. Gagnon and T. Clark; Ministère de l'Énergie et des Ressources du Québec, DV 86-16, p. 57-72.
1989a: Pétrologie et volcanologie des roches volcaniques de la partie centrale de la Fosse de l'Ungava; Ministère de l'Énergie et des Ressources du Québec, ET 87-07, 88 p.
1989b: Lithochimie des roches volcaniques protérozoïques de la partie occidentale de la Fosse de l'Ungava (région au sud du lac Lanyan); Ministère de l'Énergie et des Ressources du Québec, ET 87-14, 73 p.
- Picard, C., Giovenazzo, D. and Lamothe, D.**
1989: Geotectonic evolution by asymmetric rifting of the Proterozoic Cape Smith Belt, New Quebec; *Geoscience Canada*, v. 16, p. 130-134.
- Picard, C., Lamothe, D., Piboule, M., and Olivier, R.**
1990: Magmatic and geotectonic evolution of a Proterozoic oceanic basin system: the Cape Smith Thrust-Fold Belt (New Quebec); *Precambrian Research*, v. 47, p. 223-249.
- Plant A.G. and Lachance, G.R.**
1973: Quantitative electron microprobe analysis using an energy dispersive spectrometer; *Proceedings of the Eighth National Conference on Electron Probe Analysis*, v. 8, paper 13, 5 p.
- Platt, J.P. and Vissers, R.L.M.**
1980: Extensional structures in anisotropic rocks; *Journal of Structural Geology*, v. 2, p. 397-410.
- Powell, R. and Evans, J.A.**
1983: A new geobarometer for the assemblage biotite-muscovite-chlorite-quartz; *Journal of Metamorphic Geology*, v. 1, p. 331-336.
- Prest, V.K.**
1970: Quaternary geology of Canada; in *Geology and economic minerals of Canada*, 5th ed., Geological Survey of Canada, Economic Geology Report No. 1, p. 675-764.
- Prest, V.K., Grant, D.R. and Rampton, V.N.**
1968: Glacial map of Canada; Geological Survey of Canada, Map 1253A, scale 1:5 000 000.
- Price, R.A.**
1986: The southeastern Canadian Cordillera: thrust faulting, tectonic wedging, and delamination of the lithosphere; *Journal of Structural Geology*, v. 8, p. 239-254.
- Ramberg, H.**
1966: The Scandinavian Caledonides as studied by centrifuged dynamic models; *Geological Institute of the University of Uppsala Bulletin*, v. 43, p. 1-45.
- Ramsay, J.G., Casey, M., and Kligfield, R.**
1983: Role of shear in development of the Helvetic fold-thrust belt of Switzerland; *Geology*, v. 11, p. 439-442.
- Ratschbacher, L., Frisch, W., Neubauer, F., Schmid, S.M., and Neugebauer, J.**
1989: Extension in compressional orogenic belts: the eastern Alps; *Geology*, v. 17, p. 404-407.
- Richard, P.J.H., Larouche, A.C. and Morasse, N.**
1989: Etudes floristiques et paléophytogéographiques au Cratère du Nouveau-Québec; dans *L'histoire naturelle du Cratère du Nouveau Québec*; Collection Environnement et Géologie, volume 7, Université de Montréal, p. 315-342.
- Richards, M.A., Duncan, R.A. and Courtillot, V.E.**
1989: Flood basalts and hot-spot tracks: plume heads and tails; *Science*, v. 246, p. 103-107.
- Robin, P.-Y.F.**
1979: Theory of metamorphic segregation and related processes; *Geochimica et Cosmochimica Acta*, v. 43, p. 1587-1600.
- Roddick, J.C.**
1990: ^{40}Ar - ^{39}Ar evidence for the age of the New Quebec Crater, northern Quebec; in *Radiogenic Age and Isotopic Studies: Report 3*, Geological Survey of Canada, Paper 89-2, p. 7-16.

- Roy, C.**
1989: Géologie de la région du lac Bélanger, Fosse de l'Ungava; Ministère de l'Énergie et des Ressources du Québec, MB 89-13, 102 p.
- Royden, L.H. and Burchfiel, B.C.**
1987: Thin-skinned N-S extension within the convergent Himalayan region: gravitational collapse of a Miocene topographic front; in Continental extensional tectonics, (ed.) M.P. Coward, J.F. Dewey, and P.L. Hancock; Geological Society of London Special Publication, v. 15, p. 611-619.
- Sawyer, E.W. and Robin, P.-Y.F.**
1986: The subsolidus segregation of layer-parallel quartz-feldspar veins in greenschist to upper amphibolite facies metasediments; Journal of Metamorphic Geology, v. 4, p. 237 - 260.
- Schimann, K.**
1978a: Geology of the Wakeham Bay area, eastern end of the Cape Smith Belt, New Quebec; Ph.D. thesis, University of Alberta, Edmonton, Alberta, 271 p.
1978b: On regional metamorphism in the Wakeham Bay area, New Quebec; in Metamorphism in the Canadian Shield, eds. J.A. Fraser and W.W. Heywood; Geological Survey of Canada, Paper 78-10, p. 245-248.
- Schwarz, E.J. and Fujiwara, Y.**
1977: Komatiitic basalts from the Proterozoic Cape Smith Range in northern Quebec, Canada; in Volcanic regimes in Canada, (ed.) W.R. A. Baragar, L.C. Coleman, and J.M. Hall; Geological Association of Canada, Special Paper 16, p. 193-201.
- Sclar, C.B.**
1965: Layered mylonites and the processes of metamorphic differentiation; Geological Society of America Bulletin, v. 76, p. 611-612.
- Scott, D.J.**
1986: Metamorphism, structure, and tectonics of the eastern Cape Smith Belt, northern Quebec; B.Sc. thesis, McMaster University, Hamilton, Ontario, 176 p.
1990: Geology and geochemistry of the Early Proterozoic Purtuniqu ophiolite, Cape Smith Belt, northern Quebec, Canada; Ph.D. thesis, Queen's University, Kingston, Ontario, 289 p.
- Scott, D.J. and Bickle, M.J.**
1991: Field relationships in the Early Proterozoic Purtuniqu ophiolite, Lac Watts and Purtuniqu map areas, Quebec; in Current Research, Part C; Geological Survey of Canada, Paper 91-1C, p. 179-188.
- Scott, D.J. and Hegner, E.**
1990: Two mantle sources for the two-billion year-old Purtuniqu ophiolite, Cape Smith Belt, northern Quebec; in Program with Abstracts, Geological Association of Canada, v. 15, p. A118.
- Scott, D.J., Helmstaedt, H., and Bickle, M.J.**
1992: Purtuniqu ophiolite, Cape Smith Belt, northern Quebec, Canada: a reconstructed section of Early Proterozoic oceanic crust; Geology, v. 20, p. 173-176.
- Scott, D.J., St-Onge, M.R., Lucas, S.B., and Helmstaedt, H.**
1989: The 1998 Ma Purtuniqu ophiolite: imbricated and metamorphosed oceanic crust in the Cape Smith Thrust Belt, northern Quebec; Geoscience Canada, v. 16, p. 144-147.
1991: Geology and chemistry of the Early Proterozoic Purtuniqu ophiolite, Cape Smith Belt, northern Quebec, Canada; in Ophiolite genesis and evolution of the oceanic lithosphere, (ed.) T. Peters; Kluwer Academic Publishers, Amsterdam, p. 825-857.
- Searle, M.P.**
1985: Sequence of thrusting and origin of culminations in the northern and central Oman Mountains; Journal of Structural Geology, v. 7, p. 129-143.
- Selverstone, J.**
1985: Petrologic constraints on imbrication, metamorphism, and uplift in the SW Tauern Window, eastern Alps; Tectonics, v. 4, p. 687-704.
1988: Evidence for east-west crustal extension in the eastern Alps: Implications for the unroofing history of the Tauern Window; Tectonics, v. 7, p. 87-105.
- Selverstone, J. and Hollister, L.S.**
1980: Cordierite-bearing granulites from the Coast Ranges, British Columbia: P-T conditions of metamorphism; Canadian Mineralogist, v. 18, p. 119-129.
- Selverstone, J. and Spear, F.S.**
1985: Metamorphic P-T paths from pelitic schists and greenstones from the south-west Tauern Window, Eastern Alps; Journal of Metamorphic Geology, v. 3, p. 439-465.
- Selverstone, J., Spear, F.S., Franz, G., and Morteani, G.,**
1984: High-pressure metamorphism in the SW Tauern Window, Austria: P-T paths from hornblende-kyanite-staurolite schists; Journal of Petrology, v. 84, p. 501-531.
- Seppälä, M.**
1988: Rock pingos in northern Ungava Peninsula, Quebec, Canada; Canadian Journal of Earth Sciences, v. 25, p. 629-634.
- Shelley, D.**
1974: Mechanical production of metamorphic banding, a critical appraisal; Geological Magazine, v. 3, p. 287-292.
- Sheperd, N.**
1960: The petrography and mineralogy of the Cross Lake area, Ungava, New Quebec; Ph.D. thesis, University of Toronto, Toronto, Ontario, 176 p.
- Smith, R.B.**
1975: Unified theory of the onset of folding, boudinage and mullion structure; Geological Society of America Bulletin, v. 86, p. 1601-1609.
- Spear, F.S.**
1986: PTPATH: A fortran program to calculate pressure-temperature paths from zoned metamorphic garnets; Computers and Geosciences, v. 12, p. 247-266.
1989: Petrologic determinations of metamorphic pressure-temperature-time paths; in Metamorphic pressure-temperature-time paths, (ed.) F.S. Spear, and S.M. Peacock; American Geophysical Union Short Course in Geology, v. 7, p. 1-56.
- Spear, F.S. and Selverstone, J.**
1983: Quantitative P-T paths from zoned minerals: Theory and tectonic applications; Contributions to Mineralogy and Petrology, v. 83, p. 348-357.
- Spear, F.S., Kohn, M.J., Florence, F.P., and Menard, T.**
1990: A model for garnet and plagioclase growth in pelitic schists: implications for thermobarometry and P-T path determinations; Journal of Metamorphic Geology, v. 8, p. 683-696.
- Spear, F.S., Selverstone, J., Hickmott, D., Crowley, P., and Hodges, K.V.**
1984: P-T paths from garnet zoning: a new technique for deciphering tectonic processes in crystalline terranes; Geology, v. 12, p. 87-90.
- Stam, J.C.**
1961: On the geology and petrology of the Cape Smith-Wakeham Bay Belt, Ungava, New Quebec; Geologie en Mijnbouw, v. 40, p. 412-421.
- Steltenpohl, M.G. and Bartley, J.M.**
1988: Cross folds and back folds in the Ofoten-Tysfjord area, north Norway, and their significance for Caledonian tectonics; Geological Society of America Bulletin, v. 100 p. 140-151.
- Stephenson, R.A., Richetts, B.D., Cloetingh, S.A., and Beekman, F.**
1990: Lithosphere folds in the Eurekan orogeny, Arctic Canada?; Geology, v. 18, p. 603-606.
- Stewart, R.V.**
1976: Geology of the Asbestos Hill area; Canadian Institute of Mining and Metallurgy Bulletin, v. 69, no. 77, p. 62-69.
- Stockwell, C.H.**
1950: The use of plunge in the construction of cross-sections of folds; Proceedings of the Geological Association of Canada, v. 3, p. 97-121.
- St-Onge, D.A. and Scott, J.S.**
1986: Notes on the geomorphology and Quaternary geology of northeastern Ungava Peninsula, Nouveau Quebec; in Current Research, Part A; Geological Survey of Canada, Paper 86-1A, p. 783-785.
- St-Onge, M.R.**
1981: 'Normal' and 'inverted' metamorphic isograds and their relation to syntectonic Proterozoic batholiths in the Wopmay Orogen, Northwest Territories, Canada; Tectonophysics, v. 76, p. 295-316.
- St-Onge, M.R. and King, J.E.**
1987: Evolution of regional metamorphism during back-arc stretching and subsequent crustal shortening in the 1.9 Ga Wopmay Orogen, Canada; in Tectonic settings of regional metamorphism, (ed.) E.R. Oxburgh, B.W.D. Yardley, and P.C. England; Philosophical Transactions of the Royal Society of London, ser. A, v. 321, p. 199-218.

- St-Onge, M.R. and Lucas, S.B.**
1986: Structural and metamorphic evolution of an Early Proterozoic thrust-fold belt, eastern Cape Smith belt (Ungava Trough), Quebec; dans *Exploration en Ungava: données récentes sur la géologie et la géologie*, (ed.) D. Lamothe, R. Gagnon et T. Clark; Ministère de l'Énergie et des Ressources du Québec, DV 86-16, p. 31-39.
- 1989a: Geology, Lac Watts, Quebec; Geological Survey of Canada, Map 1721A, scale 1:50 000.
- 1989b: Geology, Purtuniqu, Quebec; Geological Survey of Canada, Map 1722A, scale 1:50 000.
- 1989c: Geology, Lac Lecorre, Quebec; Geological Survey of Canada, Map 1723A, scale 1:50 000.
- 1989d: Tectonic controls on the thermal evolution of the Cape Smith Belt, northern Québec; *Geoscience Canada*, v. 16, p. 154-158.
- 1990a: Geology, Lac des Deux-Îles, Quebec; Geological Survey of Canada, Map 1724A, scale 1:50 000.
- 1990b: Geology, Lac Fleury, Quebec; Geological Survey of Canada, Map 1725A, scale 1:50 000.
- 1990c: Geology, Lac Rinfret, Quebec; Geological Survey of Canada, Map 1726A, scale 1:50 000.
- 1990d: Geology, Lac Wakeham, Quebec; Geological Survey of Canada, Map 1727A, scale 1:50 000.
- 1990e: Geology, Mont Albert-Low, Quebec; Geological Survey of Canada, Map 1728A, scale 1:50 000.
- 1990f: Geology, Wakeham Bay, Quebec; Geological Survey of Canada, Map 1729A, scale 1:50 000.
- 1990g: Geology, Lac Forcier, Quebec; Geological Survey of Canada, Map 1730A, scale 1:50 000.
- 1990h: Geology, Cratère du Nouveau-Québec, Québec; Geological Survey of Canada, Map 1731A, scale 1:50 000.
- 1990i: Geology, Lac Courmoyer, Québec; Geological Survey of Canada, Map 1732A, scale 1:50 000.
- 1990j: Geology, Lac Vicenza, Québec; Geological Survey of Canada, Map 1733A, scale 1:50 000.
- 1990k: Geology, Lac Samandré-Lac Charlery, Québec; Geological Survey of Canada, Map 1734A, scale 1:50 000.
- 1990l: Geology, Joy Bay-Burhoine Bay, Québec; Geological Survey of Canada, Map 1735A, scale 1:50 000.
- 1990m: Evolution of the Cape Smith Belt: Early Proterozoic continental underthrusting, ophiolite obduction and thick-skinned folding; *in* The Early Proterozoic Trans-Hudson Orogen of North America, (ed.) J.F. Lewry and M.R. Stauffer; Geological Association of Canada, Special Paper 37, p. 313-351.
- 1990n: Early Proterozoic collisional tectonics in the internal zone of the Ungava (Trans-Hudson) orogen: Lac Nuvilik and Sugluk map areas, Québec; *in* Current Research, Part C; Geological Survey of Canada, Paper 90-1C, p. 119-132.
- 1991: Evolution of regional metamorphism in the Cape Smith Thrust Belt (northern Quebec, Canada): interaction of tectonic and thermal processes; *Journal of Metamorphic Geology*, v. 9, p. 515-534.
- 1992: New insight on the crustal structure and tectonic history of the Ungava Orogen, Kovik Bay and Cap Wolstenholme, Quebec; *in* Current Research, Part C; Geological Survey of Canada, Paper 92-1C, p. 31-41.
- St-Onge, M.R., Lucas, S.B. and Parrish, R.**
1992: Terrane accretion in the internal zone of the Ungava orogen, northern Quebec. Part I: Tectonostratigraphic assemblages and their tectonic implications; *Canadian Journal of Earth Sciences*, v. 29, p. 746-764.
- St-Onge, M.R., Lucas, S.B., Scott, D.J., and Bégin, N.J.**
1986: Eastern Cape Smith Belt: an Early Proterozoic thrust-fold belt and basal shear zone exposed in oblique section, Wakeham Bay and Cratère du Nouveau-Québec map areas, northern Quebec; *in* Current Research, Part A; Geological Survey of Canada, Paper 86-1A, p. 1-14.
- 1987: Tectonostratigraphy and structure of the lac Watts-lac Cross-rivière Déception area, central Cape Smith Belt, northern Quebec; *in* Current Research, Part A; Geological Survey of Canada, Paper 87-1A, p. 619-632.
- 1988a: Geology, eastern portion of the Cape Smith Thrust-Fold Belt, parts of the Wakeham Bay, Cratère du Nouveau-Québec and Nuvilik Lake map areas, northern Quebec; Geological Survey of Canada, Open File Maps 1730a to 1730p, scale 1:50 000.
- 1989: Evidence for the development of oceanic crust and for continental rifting in the tectonostratigraphy of the Early Proterozoic Cape Smith Belt; *Geoscience Canada*, v. 16, p. 119-122.
- St-Onge, M.R., Lucas, S.B., Scott, D.J., Bégin, N.J., Helmstaedt, H., and Carmichael, D.M.**
1988b: Thin-skinned imbrication and subsequent thick-skinned folding of rift-fill, transitional-crust and ophiolite suites in the 1.9 Ga Cape Smith Belt, northern Quebec; *in* Current Research, Part C; Geological Survey of Canada, Paper 88-1C, p. 1-18.
- Suppe, J.**
1983: Geometry and kinematics of fault-bend folding; *American Journal of Science*, v. 283, p. 684-721.
- Tanner, J.G. and McConnell, R.K.**
1964: The gravity anomaly field in the Ungava region of northern Quebec, with maps; *Dominion Observatory, Gravity Map Series*, 21 p.
- Taylor, F.C.**
1974: Reconnaissance geology of a part of the Precambrian Shield, northern Quebec and Northwest Territories; Geological Survey of Canada, Paper 74-21, 10 p.
- 1982: Reconnaissance geology of a part of the Canadian Shield, northern Quebec and Northwest Territories; Geological Survey of Canada, Memoir 399, 32 p.
- Taylor, F.C. and Loveridge, W.D.**
1981: A Rb-Sr study of a New Quebec Archean granodiorite; *in* Rb-Sr and U-Pb Isotopic Age Studies, Report 4, *in* Current Research, Part C; Geological Survey of Canada, Paper 81-1C, p. 105-106.
- 1985: A Rb-Sr study of granitoid intrusive rocks of the Cape Smith Belt, northern Quebec; *in* Current Research, Part A; Geological Survey of Canada, Paper 85-1A, p. 65-67.
- Thibert, F., Picard, C., and Trzciencki, W.**
1989: Pétrologie des filons-couches différenciés Roméo 1 et 2 dans la partie centrale de la bande du Cap Smith; *Geoscience Canada*, v. 16, p. 140-144.
- Thomas, M.D. and Gibb, R.A.**
1977: Gravity anomalies and deep structure of the Cape Smith Fold Belt, northern Ungava, Quebec; *Geology*, v. 5, no. 3, p. 169-172.
- Tracy, R.J.**
1982: Compositional zoning and inclusions in metamorphic minerals; *in* Characterization of metamorphism through mineral equilibria, (ed.) J.M. Ferry; Mineralogical Society of America, *Reviews in Mineralogy*, v. 10, p. 355-397.
- Tracy, R.J., Robinson, P. and Thompson, A.B.**
1976: Garnet composition and zoning in the determination of temperature and pressure of metamorphism, central Massachusetts; *American Mineralogist*, v. 61, p. 762-775.
- Tremblay, C. and Barnes, S.-J.**
1989: Platinum-group elements in Mequillon dyke, Ungava Trough, New Quebec; Geological Association of Canada, Program with Abstracts, v. 14, p. A79.
- Tremblay, G.**
1986: Géologie de la région des lacs Vanasse et Lessard, Fosse de l'Ungava, Nouveau-Québec; dans *Exploration en Ungava: données récentes sur la géologie et la géologie*, (ed.) D. Lamothe, R. Gagnon et T. Clark; Ministère de l'Énergie et des Ressources du Québec, DV 86-16, p. 15-20.
- 1989: Géologie de la région du lac Vanasse (Fosse de l'Ungava); Ministère de l'Énergie et des Ressources du Québec, ET 87-08, 21 p.
- 1991: Géologie de la région du lac Lessard (Fosse de l'Ungava); Ministère de l'Énergie et des Ressources du Québec, ET 88-09, 24p.
- Tullis, J.**
1983: Deformation of feldspars; *in* Feldspar Mineralogy, (ed.) P.H. Ribbe; Mineralogical Society of America, *Reviews in Mineralogy*, v. 2, p. 297-323.
- Tullis, J. and Mardon, D.**
1984: Effect of muscovite content on deformation of quartz aggregates; Geological Society of America, *Abstracts with Programs*, v. 16, p. 678.
- Tullis, J. and Yund, R.A.**
1980: Hydrolitic weakening of experimentally deformed Westerly granite and Hale albite rock; *Journal of Structural Geology*, v. 2, p. 439-451.
- 1985: Dynamic recrystallization of feldspar: a mechanism for ductile shear zone formation; *Geology*, v. 13, p. 238-241.
- Turner, F.J.,**
1981: *Metamorphic Petrology*; 2nd edition, McGraw & Hill, New York, 524 p.

Van Kranendonk, M.J.

1992: New insights on the tectonic assembly of northeastern Laurentia from 1.9 - 1.75 Ga; EOS, Transactions American Geophysical Union, v. 73 (supplement), p. 333.

Van Staal, C.R., Ravenhurst, C.E., Winchester, J.A., Roddick, J.C., and Langton, J.P.

1990: Post-Taconic blueschist suture in the northern Appalachians of northern New Brunswick, Canada; Geology, v. 18, p. 1073-1077.

Westra, L.

1978: Metamorphism in the Cape Smith-Wakeham Bay area north of 61°N, New Quebec; in Metamorphism in the Canadian Shield, (ed.) J.A. Fraser and W.W. Heywood; Geological Survey of Canada, Paper 78-10, p. 237-244.

White, J.C. and Mawer, C.K.

1986: Extreme ductility of feldspars from a mylonite, Parry Sound, Canada; Journal of Structural Geology, v. 8, p. 133-143.

White, R.S.

1987: When continents rift; Nature, v. 327, p. 191.

White, R.S., Spence, G.D., Fowler, S.R., McKenzie, D.P., Westbrook, G.K., and Bowen, A.N.

1987: Magmatism at rifted continental margins; Nature, v. 330, p. 439-444.

White, S.H., Burrows, S.E., Carreras, J., Shaw, N.D., and Humphreys, F.J.

1980: On mylonites in ductile shear zones; Journal of Structural Geology, v. 2, p. 175-187.

Zuber, M.T.

1987: Compression of oceanic lithosphere: an analysis of intraplate deformation in the Central Indian Basin; Journal of Geophysical Research, v. 92, p. 4817-4825.

